Molecular Precursor Routes to Transition Metal Sulfides

Christopher Walter Dinnage

Supervised by Dr. C. J. Carmalt and Prof. I. P. Parkin

Christopher Ingold Laboratories, University College London

This thesis is submitted in partial fulfilment of the requirements for the degree of Doctor of Philosophy (Chemistry)

ProQuest Number: U642790

All rights reserved

INFORMATION TO ALL USERS
The quality of this reproduction is dependent upon the quality of the copy submitted.

In the unlikely event that the author did not send a complete manuscript
and there are missing pages, these will be noted. Also, if material had to be removed,
a note will indicate the deletion.

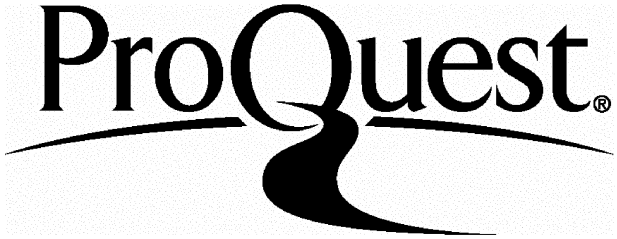

ProQuest U642790

Published by ProQuest LLC(2016). Copyright of the Dissertation is held by the Author.

All rights reserved.
This work is protected against unauthorized copying under Title 17, United States Code.
Microform Edition © ProQuest LLC.

ProQuest LLC
789 East Eisenhower Parkway
P.O. Box 1346
Ann Arbor, MI 48106-1346

Abstract

This thesis is primarily concerned with the synthesis of homoleptic early transition metal thiolates and the subsequent preparation of bulk and thin-film metal disulfides from these compounds. **Chapter 1** gives an introduction into the properties, preparation procedures and uses of bulk and thin-film transition metal disulfides as well as giving an overview of early transition metal thiolates synthesied so far in the literature (for titanium, zirconium, tantalum and niobium). **Chapter 2** is concerned with the synthesis of a number of ionic and neutral transition metal thiolates. The main synthetic methodologies discussed in this chapter include substitution reactions of transition metal amides and alkyls with thiols, salt metathesis reactions of transition metal chlorides with alkali metal thiolates or with a base / thiol and the use of Grignard reagents. **Chapter 3** discusses the preparation of bulk transition metal disulfides using the thiolates prepared in the previous chapter *via* a thio "sol-gel" route. The preparation of a range of bulk metal and mixed-metal disulfides using transition metal chlorides and hexamethyldisilathiane is also discussed in this chapter. Finally, **chapter 4** is concerned with the attempted preparation of thin-films of some transition metal disulfides. Decomposition studies of some of the thiolates prepared in **chapter 2** are discussed using thermal gravimetric analysis. Vapour-phase deposition studies are also explored in order to test the potential of the transition metal thiolates as precursors to the disulfides. Experiments using low-pressure chemical vapour deposition and aerosol-assisted chemical vapour deposition are also described.

Index

Chapter 4 Transition metal thiolates as precursors to metal sulfides

List of Figures **Page**

Chapter 1

Chapter 2

Chapter 3

Chapter 4

List of Tables **Page**

Chapter 2

Chapter 3

List of abbreviations

Å	Angstrom
AACVD	Aerosol-assisted chemical vapour deposition
APCVD	Atmospheric pressure chemical vapour deposition
Bu	Butyl
Cp	Cyclopentadienyl
Cp*	Pentamethylcyclopentadienyl
CVD	Chemical vapour deposition
δ	Chemical shift (NMR)
d	Doublet
EDXA	Energy dispersive analysis by X-rays
Et	Ethyl
g	Gram
HMDST	Hexamethyldisilathiane
^{i}Pr	Isopropyl
IR	Infra-red
L	Ligand
LPCVD	Low pressure chemical vapour deposition
m	Multiplet
mg	Milligram
mmol	Millimol
Me	Methyl
Mes	Mesityl
MS_2	Transition metal disulfide

NMR	Nuclear magnetic resonance
Ph	Phenyl
ppm	Parts per million
R	Organyl
s	Singlet
SEM	Scanning electron microscopy
t	Triplet
^{t}Bu	Tertiary butyl
TGA	Thermal gravimetric analysis
THF	Tetrahydrofuran
UV - vis	Ultra-violet - visible
XRD	X-ray diffraction
XPS	X-ray photoelectron spectroscopy

Acknowledgements

I would like to thank Dr. C. J. Carmalt and Prof. I. P. Parkin for their invaluable assistance and advice during the course of my PhD.

I am also very grateful for the assistance of numerous technicians - Alan Stones, Jill Maxwell, Kevin Reeves, Dave Knapp, Dave Morphett, Joe Nolan, Steve Firth, Marianne Odlyha (Birkbeck), Dr. Andrew White (IC), Prof. David Williams (IC) and Dr. Jon Steed (KCL) - in making equipment and analysing chemicals.

I would also like to thank all the people who have worked in Lab. 301 over the years and made it an enjoyable place to work and socialise.

Finally I would like to thank members of my family and friends from outside the department for their encouragement over the past three years.

Chapter 1 Introduction

1.1 Transition metal disulfides

Transition metal dichalcogenides are extremely versatile compounds that exhibit a wide range of electronic and optical properties.[1] For example, titanium disulfide (TiS_2) and molybdenum disulfide (MoS_2) are semiconducting materials, titanium and tungsten diselenides ($TiSe_2$ and WSe_2) are semi-metals and tantalum disulfide (TaS_2) is a superconductor.[2] The disulfides of titanium, zirconium, hafnium, vanadium, niobium and tantalum have layer structures. These structures comprise of two adjacent close-packed layers of sulfur atoms with the transition metal atoms in octahedral interstices. These are then stacked so that there are adjacent layers of sulfur atoms (Figure 1.1).[3] Lithium can be intercalated into these layers of the lattice making it a viable cathode material for both bulk and thin-film rechargeable lithium batteries.[4] The layers are held together by weak van der Waals forces. These layers can easily slide over each other and therefore make the disulfides useful solid lubricant materials.[5-7] Molybdenum disulfide, which also has a layered structure, is used as a solid lubricant for high-precision space-borne applications such as satellite bearings, gears and gimbals.[8] Transition metal disulfides have also found uses as hydrogenation catalysts.[5-7]

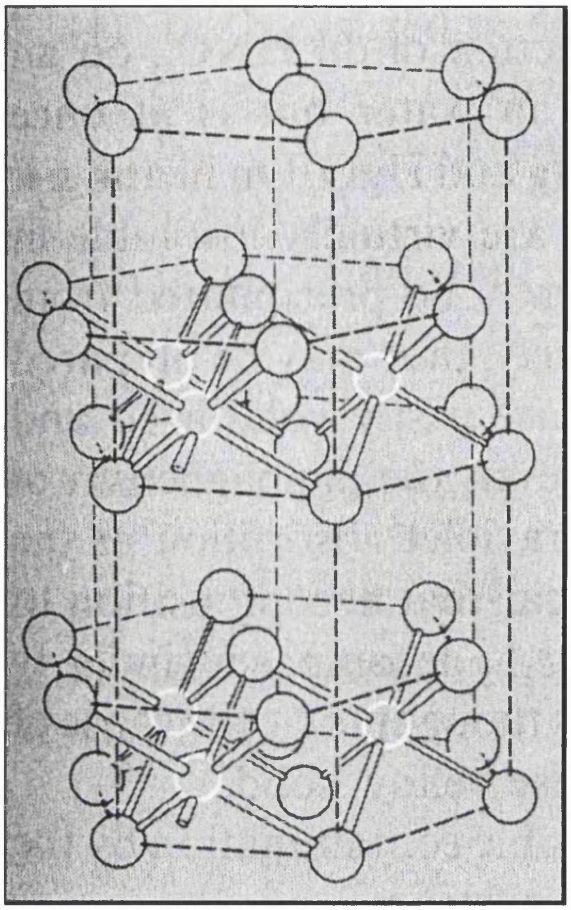

Figure 1.1 Layered structure of TiS_2 (titanium - white; sulfur - black)[3]

The optical and electronic properties of semiconducting metal disulfide materials are strongly affected by inhomogenities and impurities in the structure that may be caused by the preparation procedure. The conventional synthesis of these compounds involves direct combination of the materials in evacuated silica tubes.[9] This method requires high temperatures of around 1000 °C for prolonged periods of time, with repeated grinding and reheating of the constituent elements. It is believed that this could lead to the incorporation of impurities into the sulfides produced,

together with undesirable microstructure. The preparation procedure is also energy and time-consuming. It would therefore be preferable to develop a rapid, low-temperature preparation of transition metal sulfides with improved purity and greater control of microstructure. In addition, for some of the applications outlined above thin-films of the metal sulfides are required.

1.2 Physical deposition methods

Physical deposition techniques involve vaporising a substance from one place and transporting it to another to produce a thin-film on a substrate. This can be achieved using a beam of ions where the kinetic energy of the ions converts the substance to the gas phase in a process called sputtering. This technique has been used for the production of thin-films of TiS_2.[10] Several physical deposition processes for NbS_2 have also been reported.[11] Thin-films of TiS_2 have also been made by evaporation.[12] This is a similar technique to sputtering, except that the precursor is converted into the gas phase *via* thermal energy. Heating is achieved using either a resistive heater, or an electron gun. Both methods use low-pressure systems to transport the vapour produced onto a substrate where the film is deposited. For the purposes of this project, however, attempts to produce thin-films of transition metal sulfides will involve the use of chemical vapour deposition.

1.3 Chemical vapour deposition

Chemical vapour deposition (CVD) involves the preparation of a thin solid film deposited onto a substrate *via* a gas phase reaction.[13] In conventional CVD the precursors react in the gas phase and thermal decomposition of these precursors promotes film growth (Figure 1.2). These depositions can be carried out at atmospheric pressure (APCVD) where a carrier gas (e.g. nitrogen or argon) is used, or at low pressure (LPCVD) where the precursors are transported to the substrate under a vacuum.

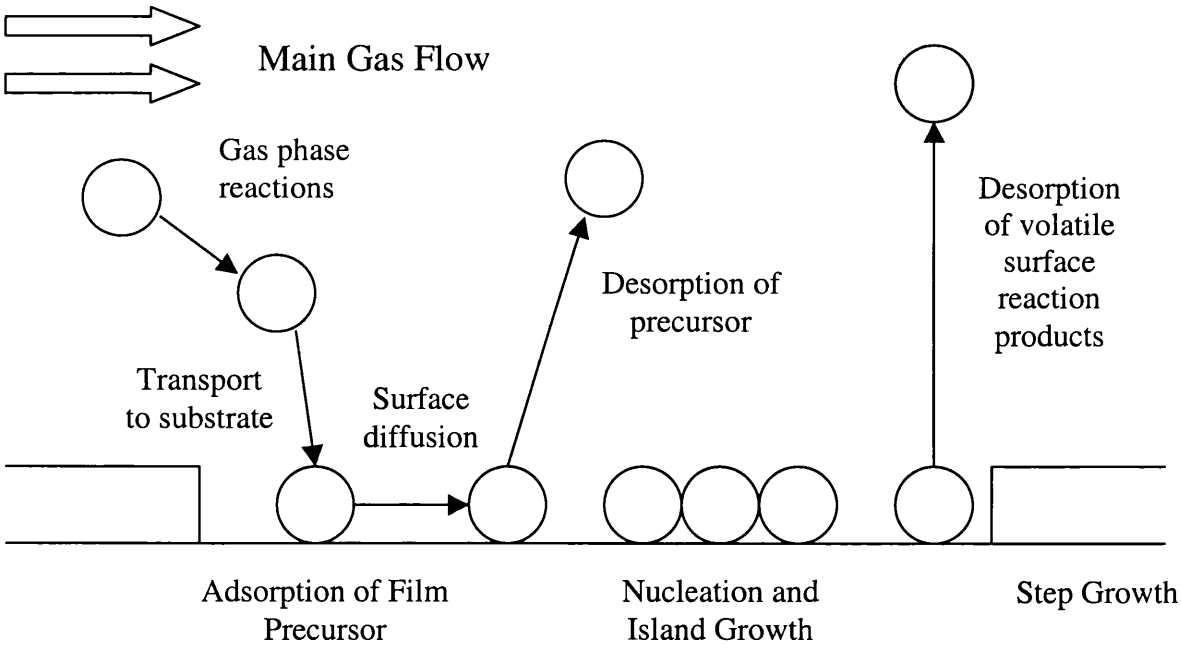

Figure 1.2 Gas transport and reaction processes of CVD

Another method of transporting the precursors can be achieved using a mist. The precursors are dissolved in a suitable solvent and the mist is produced using a nebulizer. This technique is called aerosol-assisted CVD (AACVD).[14,15]

Plasma-assisted chemical vapour deposition has also been successfully used in the production of TiS_2 films but this technique was not explored in this project.[16] The synthesis of titanium sulfides using APCVD reactions has been previously reported.[5] The reaction of $TiCl_4$ with H_2S in the temperature range 450-540 °C, results in the formation of TiS_2, as shown in equation (1.1). $TiCl_4$ is a volatile liquid that is easily heated into the gas phase.

$$TiCl_4 + 2\,H_2S \longrightarrow TiS_2 + 4\,HCl \qquad (1.1)$$

APCVD of TiS_2 was also reported by using $TiCl_4$ with organothiols (e.g. *tert*-butylthiol and hexamethyldisilathiane) in a hot-walled reactor in the temperature range 200-600 °C.[17] The TiS_2 produced from this method contained no carbon or chlorine contamination from XPS analysis (< 2% detection limit). Some of the disadvantages involved in using these dual-source systems, however, include the use of malodorous and extremely toxic reagents (thiols) coupled with the corrosive nature of $TiCl_4$ and HCl.[5] This could be a particular problem when using metal substrates due to the Ti-Cl bonds being potentially corrosive to the substrate at the temperatures used for these CVD processes.[18] Furthermore, the mixing of two chemical species in the gas phase also makes the precise stoichiometry in the final product difficult to control.[5] One way of potentially overcoming this problem is to

use a single-source precursor instead of the dual-source system.[19,20] This approach could also reduce the toxicity and waste produced by the reaction, which would be a significant factor when the process is scaled up.[5]

1.4 Single-source precursors to transition metal sulfides

Ideally, single-source precursors should contain all the atoms present in the target material, preferably in the right stoichiometry, should be volatile and should decompose cleanly to the required material.[5] Some of the advantages and disadvantages of using a single-source system compared to a dual-source system are described below.[21]

Advantages of single-source precursors

1. Reduced toxicity – no H_2S gas required
2. Pre-reaction is limited – there is only a single-source in the supply stream.
3. Low temperature growth is often possible.

Disadvantages of single-source precursors

1. Single-source precursors tend to have a lower volatility, which makes them difficult to use in conventional CVD equipment.
2. Control of stoichiometry can be difficult.

3. Polynuclear decomposition fragments may have a lower surface mobility, inhibiting epitaxial growth.

The potential use of neutral homoleptic titanium(IV) thiolate compounds as single-source molecular precursors for the formation of titanium sulfide thin films was demonstrated in 1988 using LPCVD.[22] In this case, $[Ti(S^tBu)_4]$ was used as the precursor. Initial investigations suggested that a purple film of TiS was deposited *via* this method, with a 3-5% carbon contamination (analysed by EDAX and SEM). Subsequent studies using the same precursor, however, showed that grey-blue films of TiS_2 were formed with 4% oxygen and < 3% carbon contamination (analysed by XPS).[23] In the latter study, the precursor decomposes at temperatures as low as 130 °C to give TiS_2, according to reaction (1.2). The gaseous byproducts of the reaction were analysed by g.c.m.s (gas chromatography mass spectrometry).

$$Ti(S^tBu)_4 \longrightarrow TiS_2 + {}^tBuSH + H_2S + 3CH_2{=}CMe_2 \qquad (1.2)$$

Although a solid, $[Ti(S^tBu)_4]$ is volatile and the vapour can be easily obtained by heating under a vacuum. Another single-source precursor to TiS_2 reported recently is $[TiCl_4(HSR_2)]$ (where R = C_6H_{11}, C_5H_9), prepared from the direct reaction between $TiCl_4$ and the thiol in hexane at room temperature. These precursors deposited bronze-coloured films of TiS_2 using LPCVD in the temperature range 200-400 °C.[18] XPS analysis of the TiS_2 films obtained showed no carbon or chlorine contamination to within a 2% detection limit. Thin-films of MoS_2 have

been prepared from $[Mo(S^tBu)_4]$ at temperatures above 110 °C.[23] The MoS_2 thin-films were dark-brown in colour and showed no carbon, chlorine, MoO_2 or MoO_3 contamination from XPS. Complexes of the general formula $[NbCl_4(S_2R_2)_2][NbCl_6]$ (where R = CH_3, $CH(CH_3)_2$) were prepared by direct reaction between $NbCl_5$ and the disulfides (R_2S_2) in dichloromethane. Deposition studies conducted at 500 °C resulted in dark-gold, specular, thin-films that consisted of a mixture of NbS_2 and Nb_2O_5 (analysed by XPS).[11] To our knowledge, no other examples of preparing thin-films of early transition metal sulfides exist in the literature using a single-source precursor. Nonetheless, the use of homoleptic transition metal thiolates as precursors to metal disulfides could theoretically be extended to other transition metals (e.g. zirconium, tantalum and niobium). The synthesis of potential single-source precursors to metal sulfides also represents a challenge. The preparation of homoleptic thiolates of early transition metals has so far received little attention in the literature.[24] These complexes would make ideal precursors to sulfides and would also be of interest to the synthetic chemist in general. It was therefore decided to attempt the synthesis of a range of homoleptic transition metal thiolates in the hope of using these compounds to grow films of transition metal disulfides by LPCVD. Any transition metal thiolates synthesised could also be tested as precursors to sulfides using AACVD as this method also does not require a dual-source approach. This would enable a single-source precursor to be used at atmospheric pressure as well as low pressure.

One of the difficulties encountered in synthesising thiolates of early transition metal centres occurs because of thiolates being "soft" ligands. The early

transition metals have "hard" centres and the orbitals used in bonding do not readily overlap with the *p* orbitals of the sulfur atom. This creates a challenge to the synthetic chemistry. A brief description of the thiolates of titanium, zirconium, tantalum and niobium synthesised is described below.

1.5 Early transition metal thiolates

1.5.1 *Titanium*

The chemistry of homoleptic thiolate compounds of titanium is an undeveloped area with only a few well characterised examples. Early preparative routes to thiolates of titanium involved the reactions of titanium amides, $[Ti(NR_2)_4]$ (where R = Me, Et), with thiols (R'SH where R' = Me, Et or ^{i}Pr).[25] These reactions resulted in the formation of species of the general formula $[Ti(SR')_4(R'SH)_x(RNH)_y]$ (where (x + y) vary from 0.8 to 1.33 from elemental analysis). Further studies using $[Ti(NMe_2)_4]$ and controlled addition of the thiol eventually yielded the partially substituted products of general formula $[Ti(NMe_2)_{4-x}(SR')_x]$ (where x = 1 or 2 and R' = Et, ^{i}Pr). These compounds, consisting of thiolate and amide ligands only, demonstrated the possibility of attaching thiolate ligands to a transition metal centre.

The first report of a homoleptic titanium thiolate was the thermally unstable complex $[Ti(SC_6F_5)_4]$ prepared from the reaction of $TiCl_4$ and C_6F_5SH.[26] This structure has not been fully characterised and only infra-red analysis was presented. Therefore, the true nature of this compound has not been established. A related homoleptic thiolate, $[Ti(S^{t}Bu)_4]$, has been prepared from the reaction of $[Ti(NEt_2)_4]$

or $[Ti(NMe_2)_4]$ with an excess of ^tBuSH.[22,23] The compound, $[Ti(S^tBu)_4]$ was characterised by NMR spectroscopy and elemental analysis and has also been used as a precursor to TiS_2 using LPCVD as described earlier.

The first structurally characterised monomeric homoleptic titanium thiolate was the dianion $[Ti(SCH_2CH_2S)_3]^{2-}$, which was reported in 1985 (Figure 1.3).[27] The crystal structure of $[Ti(SCH_2CH_2S)_3]^{2-}$ shows that the geometry around the titanium centre is a distorted octahedron with Ti-S bond distances in the range 2.334(4) to 2.419(1) Å. A Ti(III) homoleptic anion, $[Ti(SC_6H_2\text{-}2,4,6\text{-}i\text{-}Pr_3)_4]^-$,[28] was stabilised using a bulky thiolate ligand. The structure of the anion shows that the titanium centre adopts a pseudo-tetrahedral arrangement with an average Ti-S bond length of 2.361(2) Å. However, it was not until 1995 that the first structurally characterised example of a neutral monomeric homoleptic thiolate compound, namely $[Ti(S\text{-}2,3,5,6\text{-}Me_4C_6H)_4]$ was reported (Figure 1.4).[29] The compound, $[Ti(S\text{-}2,3,5,6\text{-}Me_4C_6H)_4]$ was prepared from the reaction of the potassium salt of the thiolate and $TiCl_4$. The geometry at the titanium centre is approximately tetrahedral with average Ti-S bond distances of 2.292(6) Å. Neutral compounds are advantageous as CVD precursors when compared to ionic compounds as they are generally more volatile.

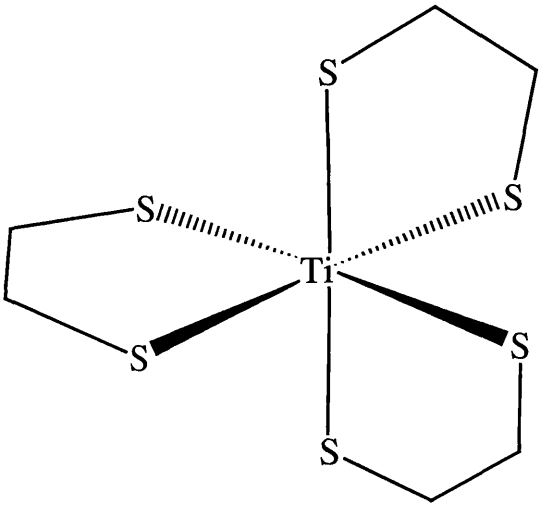

Figure 1.3 Structure of the dianion $[Ti(SCH_2CH_2S)_3]^{2-}$

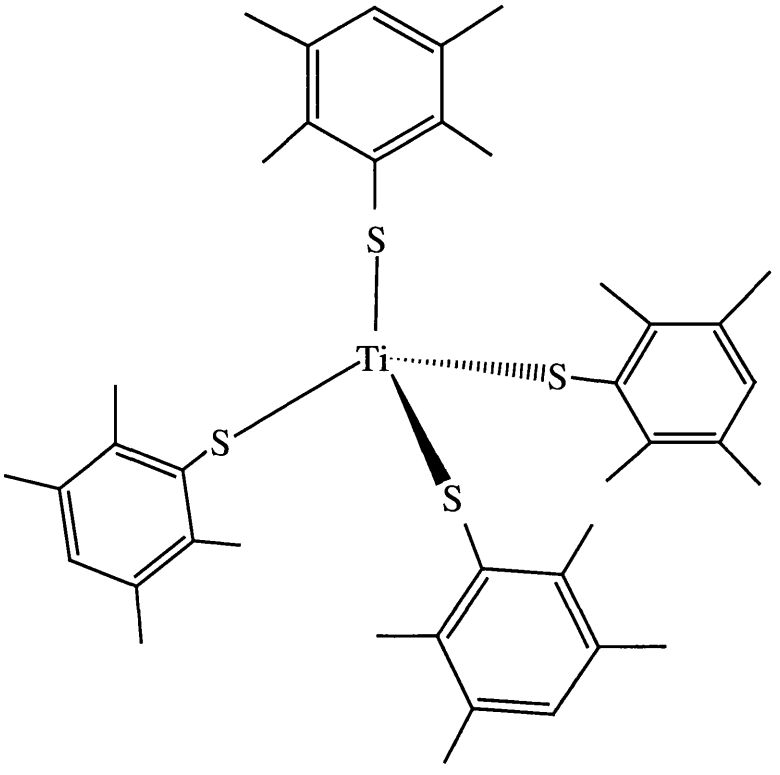

Figure 1.4 Structure of the compound $[Ti(S\text{-}2,3,5,6\text{-}Me_4C_6H)_4]$

The formation of titanium thiolates from amides has also been utilised in the preparation of the interesting ionic species $[Me_2NH_2][Ti_2(\mu\text{-}SMe)_3(SMe)_6]$ and the neutral complex $[Ti_3(\mu\text{-}SMe)_6(SMe)_6]$ (Figures 1.5 and 1.6 respectively).[30] The compound, $[Me_2NH_2][Ti_2(\mu\text{-}SMe)_3(SMe)_6]$ was made from the reaction of $[Ti(NEt_2)_4]$ and seven equivalents of MeSH whereas the compound, $[Ti_3(\mu\text{-}SMe)_6(SMe)_6]$ was prepared using four equivalents of MeSH and $[Ti(NEt_2)_4]$. The anion, $[Me_2NH_2][Ti_2(\mu\text{-}SMe)_3(SMe)_6]$ contains two titanium atoms each coordinated by three terminal and three bridging ligands and adopts a distorted face-sharing bioctahedal arrangement. The neutral complex consists of three titanium atoms, the two outer titanium atoms are coordinated by three terminal and three bridging MeS ligands while the central titanium atom is coordinated by six bridging MeS ligands. The Ti_3S_{12} framework is described as a trigonal-prismatic centre with a face-sharing octahedron on both trigonal faces.[30] More recent examples of titanium thiolate compounds include $[Li(thf)_4][Ti_2(SPh)_9]$[31] and $[Et_4N]_2[Ti(SPh)_6]$.[32] A range of titanium thiolate complexes of the type $[Cp_2Ti(SR)_2]$ have been reported and are of interest mainly as potential catalysts.[33]

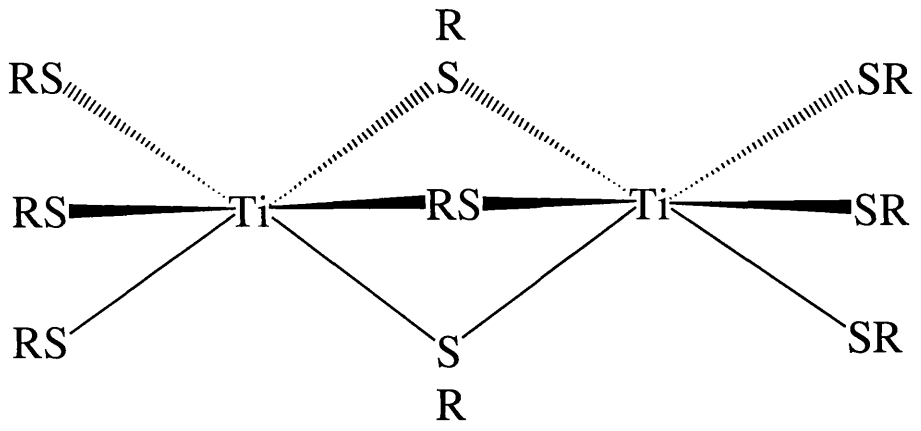

Where R = Me

Figure 1.5 Structure of the anion in $[Me_2NH_2][Ti_2(\mu\text{-}SMe)_3(SMe)_6]$

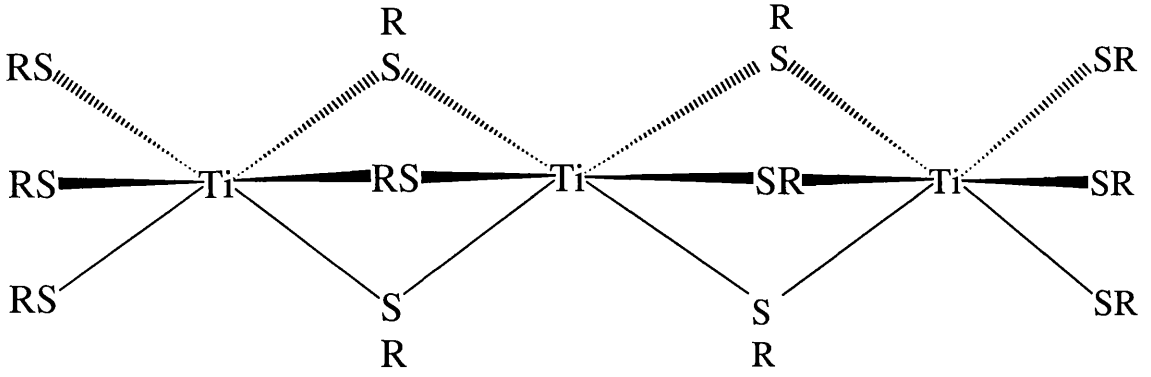

Where R = Me

Figure 1.6 Structure of the compound $[Me_2NH_2][Ti_2(\mu\text{-}SMe)_3(SMe)_6]$

1.5.2 *Zirconium*

The chemistry of zirconium thiolate compounds is largely unexplored. In fact, no neutral monomeric homoleptic zirconium thiolates have been reported in the literature except for a report of $[Zr(SPh)_4]$.[34] The compound $[Zr(SPh)_4]$ was not analytically characterised. However, zirconium-sulfur chemistry has been explored in an attempt to make a Zr=S chromophore, resulting in the synthesis and characterisation of several Zr-S containing compounds, including $[Zr_3(S)(S^tBu)_{10}]$ (Figure 1.7).[35] The only fully characterised homoleptic complex was reported in 1976 and this was the ionic species $[NMe_4]_2[Zr(S_2C_6H_4)_3]$.[36] Five and six coordinate 2-methyl 2-propanethiolato complexes, of the type $[Li(DME)_3][Zr(SCMe_3)_5]$ have also been prepared.[37] More research has been carried out using zirconium-chalcogenate complexes, specifically the tellurolates and selenolates. Such compounds have been prepared from the precursor $[Zr(CH_2Ph)_4]$, for example the reaction of $[Zr(CH_2Ph)_4]$ with four equivalents of $[(THF)_2LiSeSi(SiMe_3)_3]$ produced $[Zr(SeSi(SiMe_3)_3)_4]$.[38]

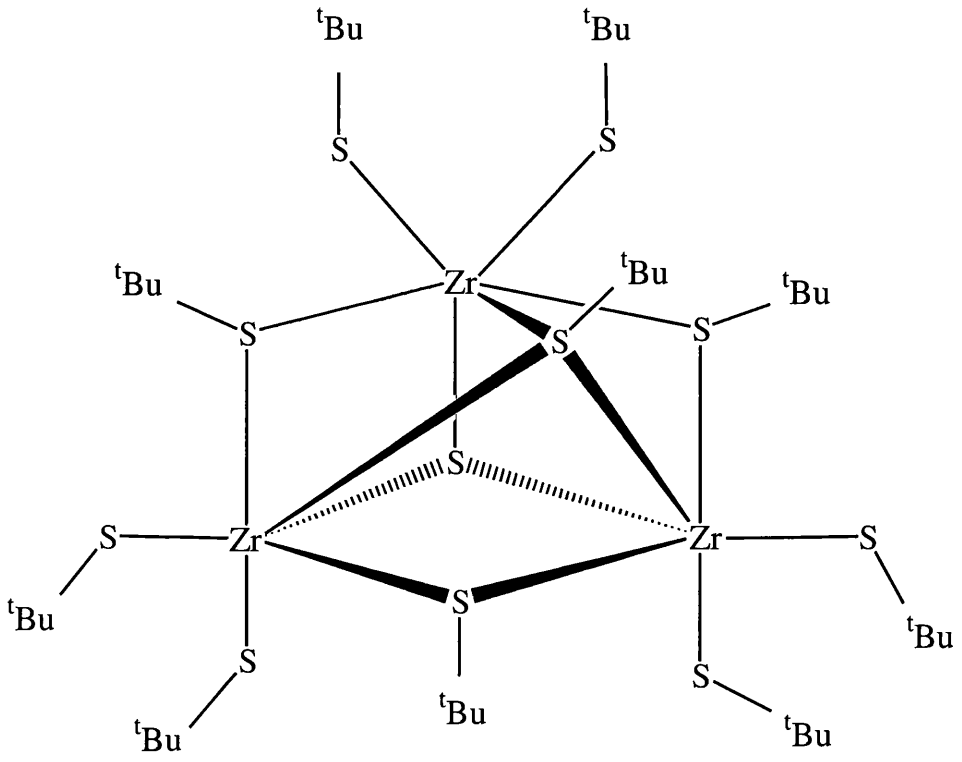

Figure 1.7 Structure of $[Zr_3(S)(S^tBu)_{10}]$

1.5.3 *Tantalum*

The chemistry of tantalum thiolate compounds is also an undeveloped area of research with few fully characterised examples. Initial attempts to prepare the homoleptic thiolate $[Ta(SC_6F_5)_5]$ resulted in the formation of $[TaCl_3(SC_6F_5)_2]$.[26] The compound, $[TaCl_3(SC_6F_5)_2]$ was prepared from the reaction of $TaCl_5$ and five equivalents of C_6F_5SH and the product was analysed by IR spectroscopy. The homoleptic anions $[Ta(SCH_2CH_2S)_3]^-$ and $[Ta(SCH_2CH_2CH_2S)_3]^-$ were prepared using the lithium salt of the thiolate and $TaCl_5$ and analysed by NMR and UV-vis.[39,40] Another homoleptic anion, $[Ta(SPh)_6]^-$ was prepared in 1990 from the

reaction of six stoichiometric equivalents of NaSPh and $TaCl_5$ and fully characterised.[41]

The first structurally characterised example of a neutral monomeric homoleptic thiolate compound of tantalum with exclusively monodentate ligands was prepared in 1995.[29] The compound, namely [Ta(S-2,3,5,6-$Me_4C_6H)_5$], was isolated from the reaction of five equivalents of the potassium salt of the thiolate with $TaCl_5$ (Figure 1.8).[29] The geometry of the Ta centre is a distorted five-coordinate geometry. It is intermediate between the structures of a trigonal bipyramid and a square-based pyramid (axial S-Ta-S angle of 156.7 °) with average Ta-S bond lengths of 2.373 Å.

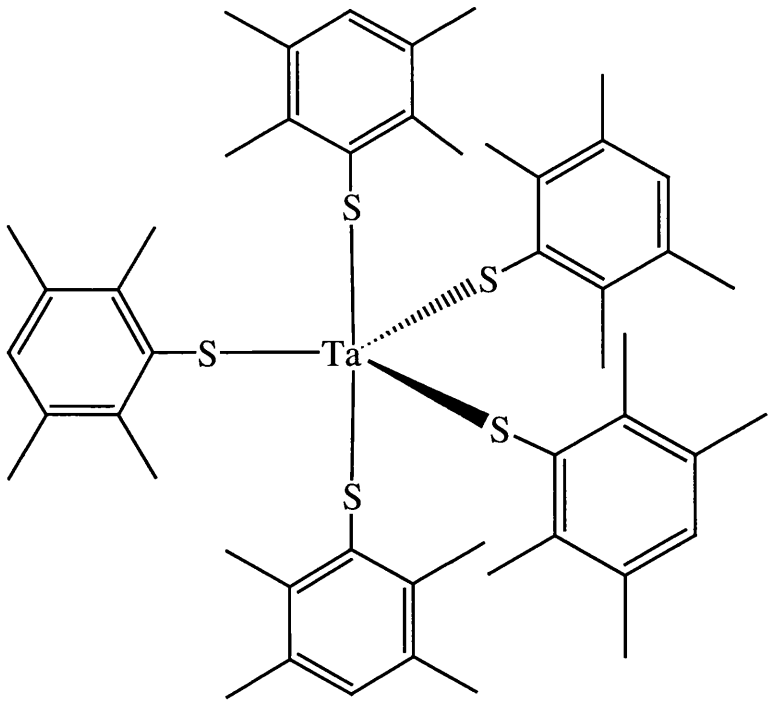

Figure 1.8 Structure of the compound [Ta(S-2,3,5,6-$Me_4C_6H)_5$]

Other tantalum thiolate compounds which have been synthesised include organometallic species of the type $[Cp^*TaCl_2(SCH_2CH_2S)_2]$.[42] These compounds were prepared from the reaction between $[Cp^*TaCl_4]$, two equivalents of $HSCH_2CH_2SH$ and two equivalents of triethylamine (Et_3N). Triethyl ammonium chloride, Et_3NHCl, is formed during the reaction. The compound $[CpTa(SPh)_4]$ was also synthesised in 1991.[43]

1.5.4 *Niobium*

The first report of a homoleptic niobium thiolate was $[Nb(SC_6F_5)_5]$,[26] although this compound was only characterised by IR spectroscopy. The first structurally characterised homoleptic niobium thiolate was the anion $[Nb(SCH_2SCH_2S)_3]^-$, prepared from the reaction of $NbCl_5$ and three equivalents of $LiSCH_2CH_2SLi$.[44] The anion, $[Nb(SCH_2SCH_2S)_3]^-$ has C_3 symmetry with the geometry at the Nb centre midway between trigonal prismatic and octahedral. The compounds $[Nb(SPh)_6]^-$ and $[Nb(SPh\text{-}p\text{Me})_6]^-$ were prepared in 1990 from the reaction of $NbCl_5$ and six equivalents of NaSPh (Figure 1.9) and NaSPh-*p*Me respectively.[41] The crystal structures of these two compounds show that the geometries around the niobium centres in both anions are approximately octahedral. The average Nb-S bond lengths of these species are 2.541(3) and 2.488(3) Å respectively.

Recently, a niobium adduct was prepared and evaluated as a single-source precursor to NbS_2 films as described earlier.[11] The compound prepared was $[NbCl_4(S_2(^iPr)_2][NbCl_6]$ and depositions were carried out at 500 °C. Subsequent

analysis, however, suggested the formation of a mixture of niobium oxide and sulfide phases.[11]

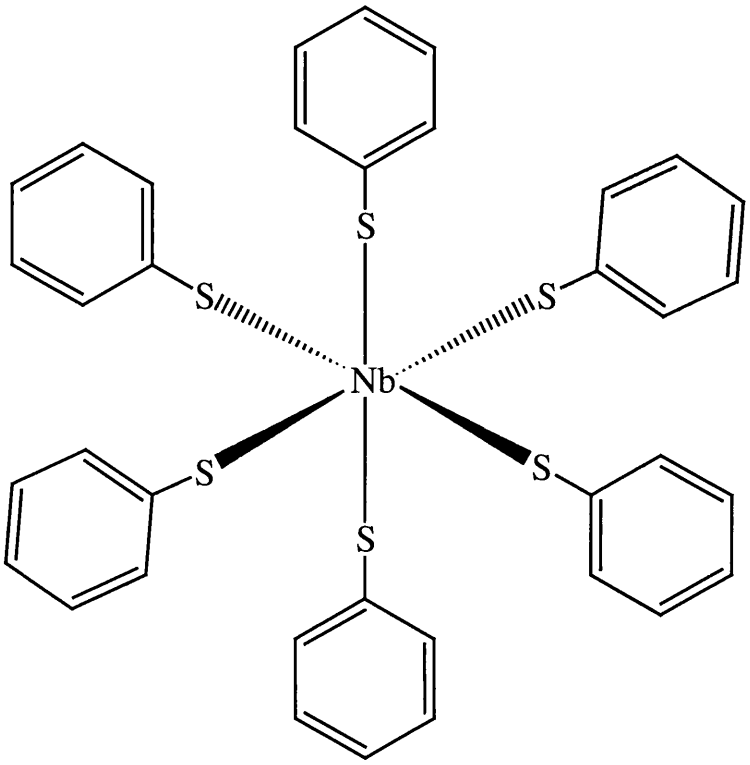

Figure 1.9 Structure of the anion $[Nb(SPh)_6]^-$

1.6 Bulk metal disulfides

Bulk metal disulfides (MS_2) have been prepared by direct reaction of the elements,[9] solid-state metathesis reactions[45] and chemical vapour transport using iodine as a transport agent (TiS_2).[46] Amorphous MS_2 has also been prepared *via* the solution phase metathetical reaction of MCl_x (x = 4, M = Ti, Mo; x = 5, M = Nb) with Li_2S.[47] Recently, solution based approaches to MoS_2 have been reported. The hydrothermal reaction between $Na_2S_2O_3$ and Na_2MoO_4 resulted in the formation of amorphous MoS_2.[48,49] After annealing the amorphous product at 350 °C crystalline MoS_2 was

produced.[48] For this project it was decided to attempt the preparation of bulk solids of the disulfides using a modified thio "sol-gel" process and using hexamethyldisilathiane.

1.7 Sol-gel techniques

Sol-gel techniques have been used for the synthesis of metal oxides for many years by using metal alkoxides as the precursors.[50,51] These metal alkoxides are of the form $[M(OR)_x]$, where M is a metal of valency x and the R group is either alkyl or aryl. The preparation of oxide materials *via* this conventional sol-gel route using organometallic or inorganic precursors generally involves hydrolysis/condensation reactions. This method has not been extensively used for the formation of non-oxide materials,[52] although a sol-gel type of process has been investigated for the formation of sulfides (e.g. TiS_2 and GeS_2) where alkoxides and H_2S gas were used as precursors.[53,54] Recently, the formation of TiS_2 and NbS_2 have been investigated applying this principle.[55] Bubbling H_2S gas through a solution of $[Ti(O^iPr)_4]$ resulted in the formation of a dark brown precipitate believed to be the result of HS^- substituting for alkoxide groups and a subsequent condensation reaction according to equations (1.3) and (1.4).[55]

$$[Ti(O^iPr)_4] + n\ H_2S \longrightarrow [Ti(O^iPr)_{4-n}(SH)_n] + n\ {}^iPrOH \qquad (1.3)$$

$$2m\ [Ti(O^iPr)_{4-n}(SH)_n] \longrightarrow [(^iPrO)_{4-n}(SH)_{n-1}Ti\text{-}S\text{-}Ti(SH)_{n-1}(^iPrO)_{4-n}]_m + m\ H_2S \qquad (1.4)$$

Reactions (1.3) and (1.4) have produced products that contain a mixture of metal-oxygen and metal-sulfur bonds. An additional reaction has to be used in order to eliminate the oxide component and purify the metal sulfide product.[55,56] This is achieved by heating the product in the presence of H_2S to high temperatures. At around 700 °C the alkoxy groups react with sulfur formed from the decomposition of H_2S gas, forming a crystalline disulfide (TiS_2 and NbS_2). At temperatures below 700 °C oxide impurities occur in the final material. This is due to the favoured high temperature condensation of the unreacted alkoxy groups. It is therefore hoped that a thio "sol-gel" process could be developed using a metal thiolate as the starting material, in place of the alkoxide, and reacting the thiolate with H_2S gas. This could provide a homogeneous product with a low level of impurities. It is also hoped that pure crystalline TiS_2 can be prepared at temperatures below 700 °C.

The formation of metal sulfides from homoleptic transition metal thiolates synthesised is reported in this thesis using the thio "sol-gel" process.

1.8 Use of hexamethyldisilathiane as a sulfur source

Another potential low temperature route to bulk MS_2 (where M = transition metal) involves the reaction of hexamethyldisilathiane (HMDST, $S(SiMe_3)_2$) with metal chlorides. A report in 1979 showed that the equimolar reaction between $TiCl_4$ and HMDST resulted in the formation of $TiSCl_2$.[57] This procedure involved the loss of two stoichiometric equivalents of Me_3SiCl leaving the product behind. Theoretically, the reaction of $TiSCl_2$ with a further molar equivalent of HMDST should produce the

desired disulfide as well as two further equivalents of Me_3SiCl. Subsequent studies showed that when metal chlorides (e.g. $TiCl_4$, $NbCl_5$, $MoCl_4$ and VCl_4) were reacted with excess HMDST amorphous precipitates were isolated.[58-62] The composition of these initial precipitates was not fully analysed. Annealing of these precipitates afforded the metal disulfide for titanium and niobium (analysed by XRD). In some cases, however, these were contaminated with a large percentage of oxide or resulted in the formation of non-stoichiometric sulfides (by powder XRD) e.g. VS_4. Nevertheless, these reports indicate that this procedure could be an excellent route to metal sulfides and warrants further investigation. It is anticipated that this type of procedure could be applied to the chlorides of other transition metals (tantalum and niobium). Investigations of this type are reported in chapter 3.

1.9 Heterobimetallic disulfides

By analogy with the alkoxides, it would be of interest to investigate the synthesis of mixed-metal sulfides from heterobimetallic thiolate compounds. It is known that binary alkoxides have the ability to form mixed-metal species of the type $[MM'(OR)_m(OR')_n]$.[63,64] There are a number of these heterobimetallic alkoxides characterised in the literature[64] and such compounds are potential precursors to mixed-metal oxides. One example of this is the heterobimetallic complex $[LiNb(OEt)_6]$, which can be easily prepared by refluxing an ethanol solution of lithium ethoxide and niobium ethoxide, $[Nb(OEt)_5]$ in the correct ratio. The compound, $[LiNb(OEt)_6]$ has subsequently been used to form high quality $LiNbO_3$ films.[63] Heterobimetallic thiolate complexes of the early and late transition metals

tend to be organometallic derivatives with bridging thiolate ligands of the type $[Cp_2M(\mu\text{-}SR)_2ML_n]$.[65] It would therefore be worth investigating the synthesis of heterobimetallic thiolates according to equation (1.5).

$$M(SR)_m + M'(SR')_n \longrightarrow MM'(SR)_m(SR')_n \qquad (1.5)$$

The reaction shown in equation (1.5), relies on the acid-base behaviour of the thiolates. Heterobimetallic thiolate compounds could potentially be used as precursors to mixed-metal sulfides. An example of this would be thiospinels of the type AB_2X_4 (where A and B are transition metals and X is sulfur). Thiospinels have interesting magnetic properties, for example, $MnCr_2S_4$ and $CoCr_2S_4$ are ferromagnetic.[1]

It would also be of interest to prepare bulk mixed-metal sulfides. This could be achieved using HMDST or thio "sol-gel" techniques. To our knowledge, there are no known mixed-metal sulfides containing only the early transition metals.

Chapter 2 Synthesis of homoleptic early transition metal thiolates

2.1 Synthetic strategies for transition metal thiolates

Five main synthetic methodologies were attempted in order to synthesise homoleptic thiolates of early transition metals. Two routes involved salt metathesis reactions between alkaline metal thiolate salts and a metal chloride or by direct reaction of a thiol and a metal chloride in the presence of a base. Two other procedures involved substitution reactions of the thiol with transition metal amides (e.g. $[Ti(NEt_2)_4]$) or alkyls (e.g. $[Zr(CH_2Ph)_4]$). The final method involved the use of Grignard reagents. The five reaction schemes investigated in this thesis are described below.

(1) Salt metathesis using alkali metal (eg. sodium) salts of the thiol and the transition metal chloride (eg. $TiCl_4$) as shown in equation (2.1).

$$4\,NaSR + TiCl_4 \longrightarrow 4\,NaCl + Ti(SR)_4 \qquad (2.1)$$

The driving force for this reaction is the high lattice energy of the co-formed alkali metal chloride.

(2) Direct reaction of a thiol and a metal chloride in the presence of a base (e.g. Et_3N) as shown in equation (2.2).

$$4\,RSH + TiCl_4 + 4\,Et_3N \longrightarrow 4\,Et_3NHCl + Ti(SR)_4 \qquad (2.2)$$

This reaction is promoted by the formation of an ammonium salt.

(3) Substitution reaction between transition metal amides (eg. $[Ti(NEt_2)_4]$) and a thiol as shown in equation (2.3).

$$Ti(NEt_2)_4 + RSH_{(xs)} \longrightarrow Ti(SR)_4 + 4\,Et_2NH \qquad (2.3)$$

In this instance, it was anticipated that the reaction will proceed due to the formation of Et_2NH. The S-H bond is more acidic than the N-H bond, which should result in the formation of the amine Et_2NH. This amine is a volatile liquid and is easily removed from the desired product.

(4) Substitution reaction between transition metal alkyl (eg. $Ti(CH_2Ph)_4$) and thiol as shown in equation (2.4).

$$Ti(CH_2Ph)_4 + RSH_{(xs)} \longrightarrow Ti(SR)_4 + 4\,C_6H_5CH_3 \qquad (2.4)$$

Similarly, it was anticipated that the thiolate anion would substitute the alkyl one in an acid / base reaction.

(5) Preparation of thiolates using a Grignard reagent and inserting sulfur into the material by reaction with elemental sulfur as shown in equation (2.5).

$$MesMgBr + 1/8\ S_8 \longrightarrow MesSMgBr \quad (2.5)$$

(where Mes = mesityl, 2,4,6-$Me_3C_6H_2$)

Further reaction with a transition metal chloride is then carried out in order to produce the desired product as shown in equation (2.6).

$$4\ MesSMgBr + TiCl_4 \longrightarrow Ti(SMes)_4 + MgBrCl \quad (2.6)$$

2.2 Synthesis of transition metal thiolates by substitution reactions

One of the earliest titanium thiolates characterised was [Ti(S^tBu)$_4$] as described earlier (see Introduction).[22,23] This compound was prepared from the reaction of [Ti(NEt_2)$_4$] and an excess of the thiol, ^{t}BuSH. For the purpose of synthesising novel homoleptic early transition metal thiolates, it was decided to begin with this methodology. Consequently, [Ti(NEt_2)$_4$] was prepared according to literature methods[66] and subsequently reacted with a range of thiols (e.g. benzyl mercaptan and pentafluorothiophenol). These thiols were chosen on account of their steric size in an attempt to stabilise the metal centre giving a neutral homoleptic compound.

2.3 Reaction of [Ti(NEt_2)$_4$] and $PhCH_2SH$

The reaction between [Ti(NEt_2)$_4$] and an excess of benzyl mercaptan ($PhCH_2SH$) was carried out in toluene at room temperature. The solution immediately changed colour from orange to dark red on addition of the thiol. The solvent was pumped off *in vacuo* affording a dark red oil. Single crystals suitable

for X-ray analysis were obtained by dissolving the oil in the minimum amount of CH_2Cl_2 and overlaying with hexane. Solvent diffusion at -20 °C overnight gave dark red crystals in a 65% yield. Analytical and spectroscopic data showed the crystals to be $[Et_2NH_2][Ti_2(\mu\text{-}SCH_2Ph)_3(SCH_2Ph)_6]$ (compound **1**) as shown in equation (2.7) below.

$$Ti(NEt_2)_4 + \text{xs } PhCH_2SH \longrightarrow [Et_2NH_2][Ti_2(\mu\text{-}SCH_2Ph)_3(SCH_2Ph)_6] \quad (2.7)$$

Other species produced during the reaction were Et_2NH and $PhCH_2SH$, however these are volatile and easily removed during work-up of the reaction. The anticipated product, $[Ti(SCH_2Ph)_4]$, was not formed. Both titanium atoms in the anion of compound **1** have a coordination number of six (see structural description below). This is probably due to the thiolate ligand being too small to saturate the titanium centre with just four ligands. The $[Et_2NH_2]^+$ cation is a result of protonation of diethylamine formed as a result of the thiol substituting an amide ligand on $[Ti(NEt_2)_4]$. Therefore a salt is produced and not the neutral compound, $[Ti(SCH_2Ph)_4]$. Compound **1** has a similar structure to $[Me_2NH_2][Ti_2(\mu\text{-}SMe)_3(SMe)_6]$, as described in chapter 1.[30] The melting point (103-105 °C) of compound **1** is higher than the neutral titanium thiolate complex, $[Ti(S^tBu)_4]$ (melting point, 45 °C) due to these intermolecular ionic bonds. Ideally, for CVD precursors, neutral compounds are preferable as these tend to have a lower melting point and higher vapour pressure.

2.4 Spectroscopic data for compound 1

The behaviour of $[Ti_2(\mu\text{-}SMe)_3(SMe)_6]^-$ in solution (at room temperature) was described as being complicated and it was suggested that it dissolves to afford $[Ti_3(\mu\text{-}SMe)_6(SMe)_6]$ and at least one other compound.[30] At lower temperatures (-25 °C, -60 °C and -85 °C), the ^1H NMR spectra of $[Ti_2(\mu\text{-}SMe)_3(SMe)_6]^-$ undergoes a series of changes which were tentatively assigned to the presence of $[Ti_3(\mu\text{-}SMe)_6(SMe)_6]$ and a complex of the type $[Ti(SMe)_4(HSMe)_x(NHMe_2)_y]$.[30] In contrast, the room temperature ^1H NMR spectrum of **1** contains only peaks which can be assigned directly to the compound, therefore suggesting that it does not undergo comparable reactions. Two singlets in the room temperature ^1H NMR of compound **1** are observed at 4.90 and 5.30 ppm corresponding to the CH_2 group of the benzyl ligand. Integration for these two peaks show a 1:2 ratio corresponding to bridging and terminal thiolates respectively. The aromatic protons occur between 7.00 and 7.50 ppm. Peaks corresponding to the diethyl ammonium cation occur as a triplet at 0.85 ppm (NCH_2CH_3) and a quartet at 2.40 ppm (NCH_2CH_3) (*cf.* 1.06 and 3.48 ppm for $[Ti(NEt_2)_4]$). The peak corresponding to the Et_2NH_2 protons was not observed. At lower temperatures (0 to -90 °C; spectra obtained at 10 °C intervals) the ^1H NMR spectra also undergoes a series of changes and it is clear that the behaviour of compound **1** in solution at low temperatures is complicated. At -50 °C the peak at 5.3 ppm (CH_2 groups of the terminal ligands) splits into two doublets in a 1:1 ratio (see Figure 2.1). This suggests that the CH_2 groups of the six terminal $PhCH_2S^-$ ligands are no longer equivalent. It is also possible that

another species has formed at lower temperatures. At temperatures lower than -50 °C the peaks become broad, due to the compound crystallising in solution.

An infra-red spectrum was taken of compound **1** and also the starting thiolate, $PhCH_2SH$, for comparison. A peak at 2570 cm^{-1}, corresponding to an SH group is present in the spectrum of $PhCH_2SH$ and not the spectrum of **1** as would be expected for a thiolate complex. Mass spectroscopy proved to be inconclusive for the thiolate compounds prepared in this chapter. A peak at 74, corresponding to the diethylamine ion, $Et_2NH_2^+$ was found for compound **1** and a peak at 91 was present due to the $PhCH_2^+$ ion but no other identifiable peaks were present.

Figure 2.1 VT-NMR of compound 1 at (a) Room temperature, (b) -30 °C and (c) -50 °C

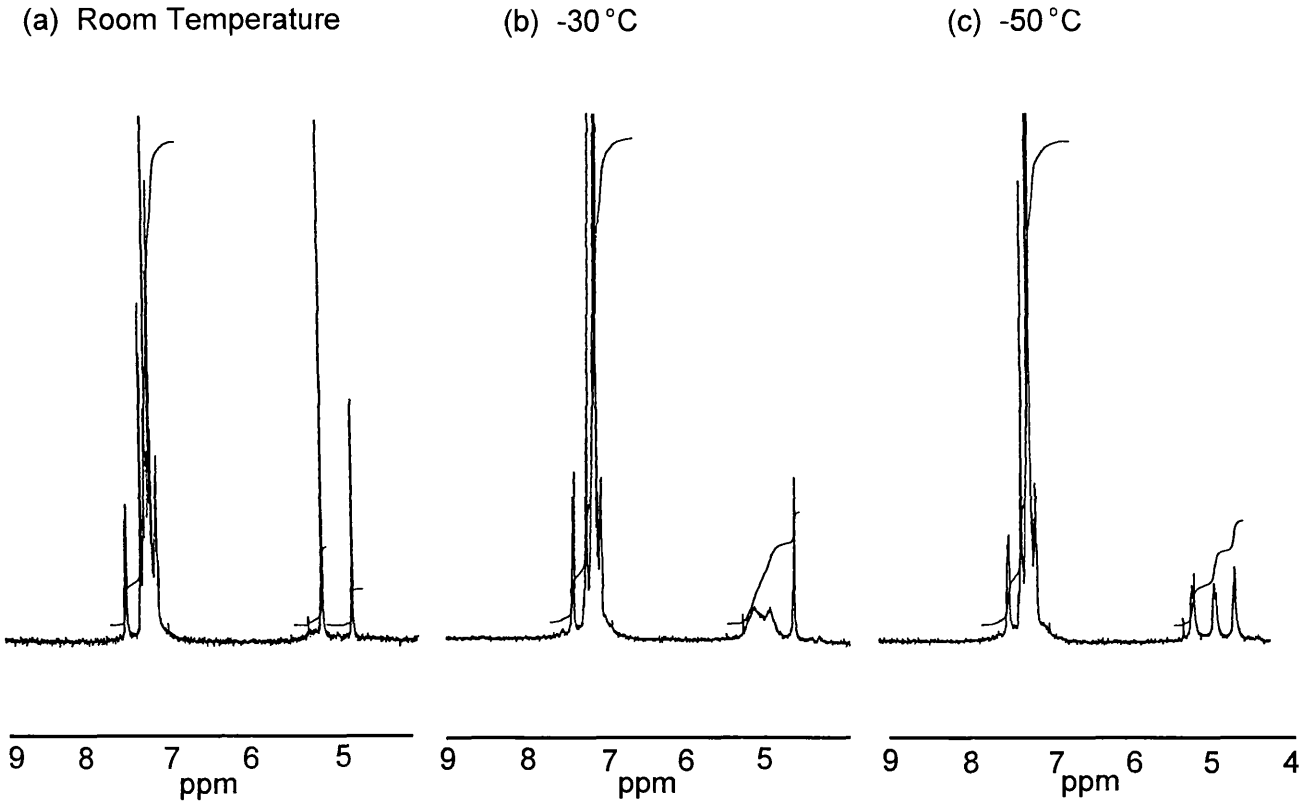

2.5 X-ray structure of compound 1

The structure of compound **1** was confirmed by X-ray crystallography, the results of which are shown in Fig. 2.2; selected bond lengths and angles are shown in Table 2.1. Tables of all the bond lengths, angles and crystallographic data for **1** and all subsequent structures presented in this thesis are shown in the appendix. The compound crystallises in the monoclinic space group $P2_1/c$. The structure is ionic and consists of $[Et_2NH_2]^+$ cations and $[Ti_2(\mu\text{-}SCH_2Ph)_3(SCH_2Ph)_6]^-$ anions with no close interionic contacts. In the anion, the two titanium atoms are each coordinated by three terminal (Ti-S bond lengths range from 2.3183(9) - 2.4090(10) Å) and three bridging (Ti-S bond lengths range from 2.5364(9) - 2.5609(9) Å) $PhCH_2S^-$ ligands. Therefore, the coordination number at each titanium centre is six and the geometry is approximately octahedral (*trans* S-Ti-S 158.75(3) - 172.34(3)° and *cis* S-Ti-S 75.53(3) - 102.35(3)°). The structure of compound **1** is similar to that of the anion $[Ti_2(\mu\text{-}SMe)_3(SMe)_6]^-$ in which the Ti_2S_9 framework also has a face-sharing bioctahedral arrangement (terminal Ti-S bond lengths range from 2.321(1) - 2.362(1) Å, bridging Ti-S bond lengths range from 2.513(1) - 2.561(1) Å).[30]

Figure 2.2 Molecular structure of the anion in compound 1

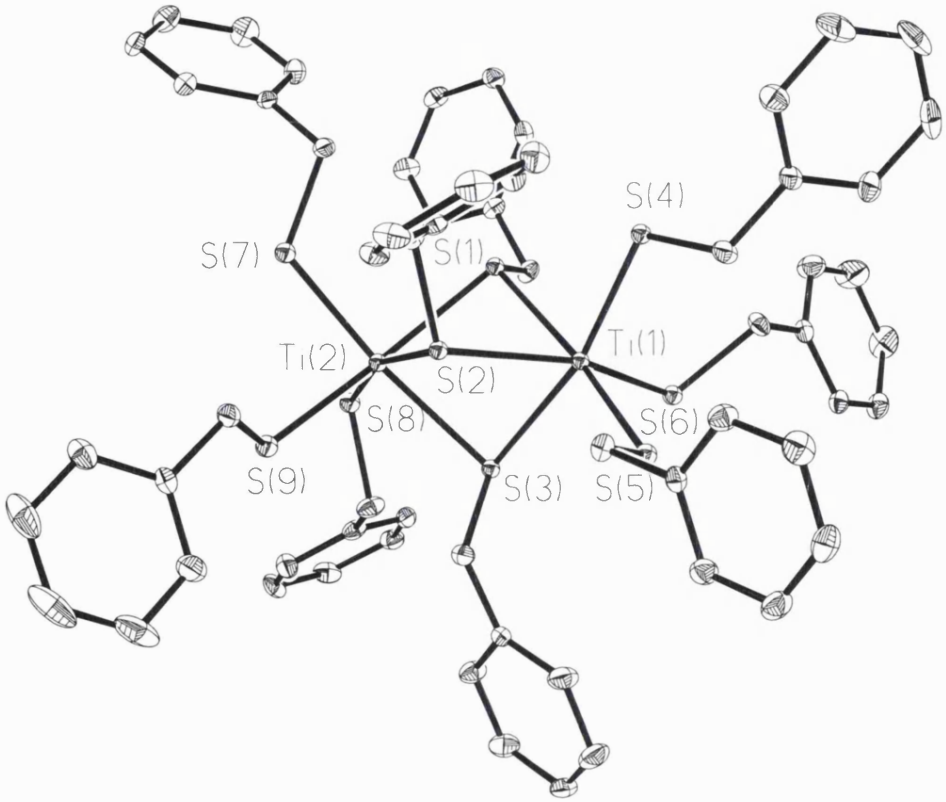

Table 2.1 Selected Bond Distances (Å) and Angles (°) for compound 1

Ti(1)–S(1)	2.5609(9)	Ti(1)–S(2)	2.5395(10)
Ti(1)–S(4)	2.3308(9)	Ti(1)–S(5)	2.3183(9)
Ti(2)–S(1)	2.5132(10)	Ti(2)–S(2)	2.5249(9)
Ti(2)–S(7)	2.3366(11)	Ti(2)–S(8)	2.4090(10)
Ti(1)–S(3)	2.5364(9)	Ti(2)–S(3)	2.5295(10)
Ti(1)–S(6)	2.3582(10)	Ti(2)–S(9)	2.3484(11)

S(5)–Ti(1)–S(4)	98.64(3)	S(8)–Ti(2)–S(1)	102.35(3)
S(5)–Ti(1)–S(6)	92.27(4)	S(9)–Ti(2)–S(8)	88.96(3)
S(4)–Ti(1)–S(6)	99.54(4)	S(7)–Ti(2)–S(8)	98.20(3)
S(5)–Ti(1)–S(3)	95.66(3)	S(9)–Ti(2)–S(3)	98.68(3)
S(4)–Ti(1)–S(3)	165.02(3)	S(7)–Ti(2)–S(3)	171.75(3)
S(6)–Ti(1)–S(3)	84.26(3)	S(8)–Ti(2)–S(3)	88.53(3)
S(5)–Ti(1)–S(2)	96.14(4)	S(9)–Ti(2)–S(2)	92.05(3)
S(4)–Ti(1)–S(2)	98.44(3)	S(7)–Ti(2)–S(2)	97.41(3)
S(6)–Ti(1)–S(2)	158.75(3)	S(8)–Ti(2)–S(2)	164.39(3)
S(3)–Ti(1)–S(2)	75.53(3)	S(2)–Ti(2)–S(3)	75.91(3)
S(5)–Ti(1)–S(1)	172.34(3)	S(9)–Ti(2)–S(1)	168.63(3)
S(4)–Ti(1)–S(1)	83.45(3)	S(7)–Ti(2)–S(9)	86.26(3)
S(6)–Ti(1)–S(1)	94.65(3)	S(7)–Ti(2)–S(1)	91.00(3)
S(3)–Ti(1)–S(1)	81.79(3)	S(1)–Ti(2)–S(3)	82.87(3)
S(2)–Ti(1)–S(1)	76.23(3)	S(1)–Ti(2)–S(2)	77.35(3)
Ti(2)–S(1)–Ti(1)	86.14(3)	Ti(2)–S(2)–Ti(1)	86.35(3)
Ti(2)–S(3)–Ti(1)	86.32(3)		

2.6 Further reactions with $PhCH_2SH$

Attempts to react $[Ti(NEt_2)_4]$ with four equivalents of benzyl mercaptan, and not an excess as described previously, resulted in the formation of a red/brown solid. ^1H NMR (CD_2Cl_2) studies of this solid suggested that more than one species was present in solution (Figure 2.3). Peaks corresponding to the thiolate ligands $PhCH_2S^-$, occur as a singlet at 3.62 ppm (-CH_2 groups) and at 7.15-7.32 ppm (-Ph groups). These peaks have shifted considerably from compound **1** and shows that the benzyl ligand is present in a different environment, e.g. $[Ti(SCH_2Ph)_4]$. However, peaks corresponding to coordinated

amide groups are also present in the spectrum as a quartet at 1.17 ppm ($-CH_3$ groups) and a triplet at 3.43 ppm ($-CH_2$ groups). Furthermore, peaks corresponding to free thiol were observed as a doublet at 3.74 ppm ($-CH_2$ groups), a triplet at 1.82 ppm (-SH group) and a multiplet from 7.15-7.32 ppm (-Ph groups), suggesting that hydrolysis/decomposition of the product had occurred. This was confirmed by the gradual formation of an insoluble brown solid in the samples analysed.

The ^1H NMR (CD_2Cl_2) was subsequently repeated and showed only the presence of $PhCH_2S^-$ ligands at 3.63 ppm and 7.25-7.35 ppm (Figure 2.4). Elemental analysis showed the presence of nitrogen in the final product (2.29 %). It is possible, therefore, that the final product is a mixture of $[Ti(SCH_2Ph)_4]$ and an amido species, for example $[Ti(NEt_2)_4]$ or compounds of the type, $[Ti(NEt_2)_{4-x}(SCH_2Ph)_x]$.

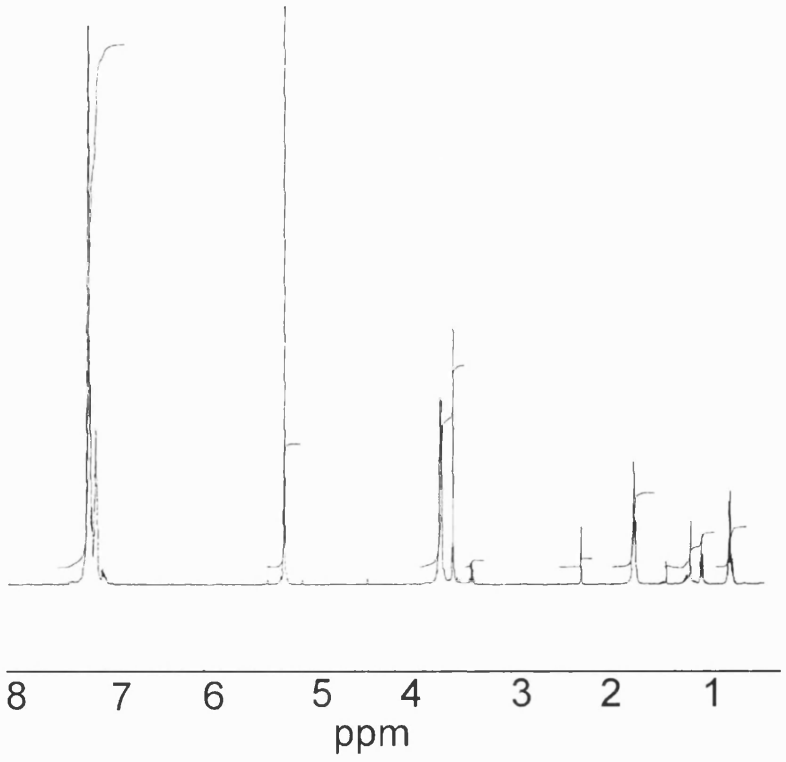

Figure 2.3 ^1H NMR spectrum for reaction of $[Ti(NEt_2)_4]$ with four equivalents of benzyl mercaptan

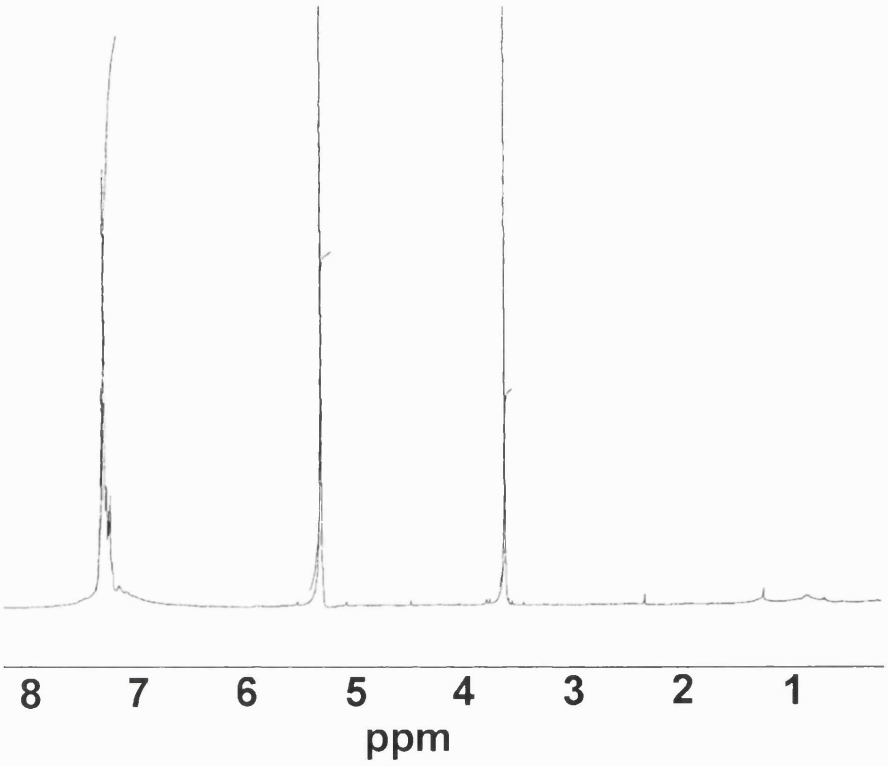

Figure 2.4 Repeated ^{1}H NMR spectrum for reaction of $[Ti(NEt_2)_4]$ with four equivalents of benzyl mercaptan

It was decided to repeat the reaction but with the further addition of two equivalents of a two-electron donor ligand in the hope of crystallising a monomeric species, of the type shown in Scheme 1.

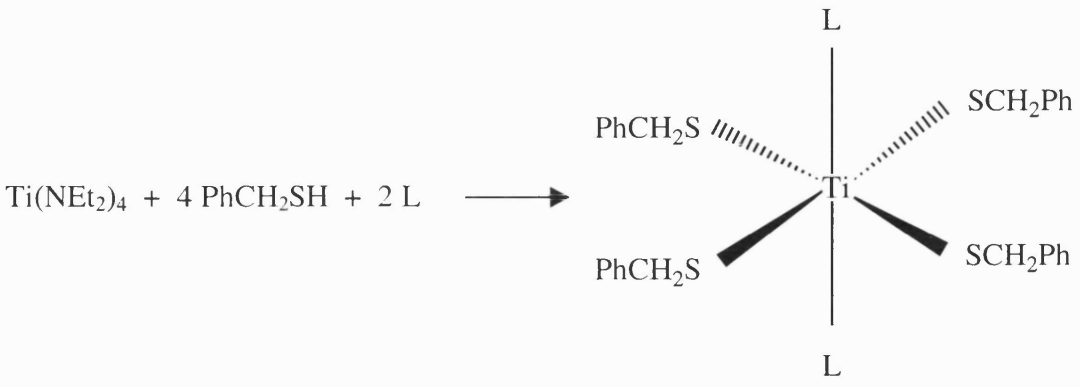

Scheme 1

The ligand chosen was tetrahydrothiophene (C_4H_8S), in order to retain an all-sulfur coordination sphere around the titanium centre. ^1H NMR data of the red solid obtained from the reaction was complicated with peaks observed in the region of 0.8-2.66 ppm that were very broad. The spectrum did not match the proposed compound, $[Ti(SCH_2Ph)_4(SC_4H_8)_2]$, and no evidence of tetrahydrothiophene was present in the final compound. Peaks were observed at 7.15-7.28 ppm and at 3.59 ppm suggesting that a similar species had been made as in the previous reaction, i.e. $[Ti(SCH_2Ph)_4]$. Peaks corresponding to coordinated amide groups were not observed in this instance, but broad signals at 1.10 ppm and 2.66 ppm suggested the presence of ethyl groups, e.g. from diethylamide in the final product. Decomposition or hydrolysis has again occurred. A subsequent ^1H NMR spectrum showed the presence of coordinated thiolate groups at 3.62 ppm ($-CH_2$ groups) and 7.14-7.34 ppm (Ph groups) but very little impurities. Analytical data again showed the presence of nitrogen in the final product (1.46 %), however, suggesting that contamination has occurred. It was decided not to proceed further with this approach to making thiolate compounds, but to choose a different thiol to react with $[Ti(NEt_2)_4]$. A more suitable thiolate ligand would have to have a greater steric bulk in order to prevent the titanium metal centre from adopting a coordination number greater than four.

2.7 Reaction of $[Ti(NEt_2)_4]$ and excess C_6F_5SH

Pentafluorothiophenol (C_6F_5SH) was chosen next as a ligand. A study into the formation of $[Ti(SC_6F_5)_4]$ was reported in the literature, as described earlier, although it was not fully characterised.[26] The fluorine atoms give the thiol more steric bulk than $PhCH_2SH$ and it was hoped that this would prevent the formation of a salt. Pentafluorothiophenol is also more Lewis acidic than $PhCH_2SH$. This could result in the thiolates bridging, e.g. in $[Bi(SC_6F_5)_3]_2$ which is dimeric *via* thiolate bridges.[67] The reaction between $[Ti(NEt_2)_4]$ and excess C_6F_5SH was carried out in toluene and a dark red solution formed immediately on addition of the thiol. After work up a dark red solid resulted. Crystals suitable for X-ray analysis were formed by dissolving the red solid in a minimal amount of CH_2Cl_2, overlaying with hexane and leaving to diffuse at room temperature over a period of five days. Analytical and spectroscopic data were consistent with the formation of $[Et_2NH_2]_3[Ti(SC_6F_5)_5][SC_6F_5]_2$ (compound **2**). This is in contrast to the previous report that suggested $[Ti(SC_6F_5)_4]$ had been made from the reaction of $TiCl_4$ and C_6F_5SH, although this compound was only characterised from an IR spectrum.[26]

The formation of **2** is interesting in comparison with compound **1**, that was prepared *via* the similar reaction between $[Ti(NEt_2)_4]$ and ten equivalents of $PhCH_2SH$. It is assumed that $C_6F_5S^-$, because of its bulkiness, could not form a similar face-sharing bioctahedral arrangement as observed for the anion in **1**.[68] The titanium centre has a coordination number of five. However, the $C_6F_5S^-$ group is not large enough to saturate the titanium centre with four ligands, hence producing the salt.

2.8 Analytical data of compound 2

The ^{1}H NMR spectrum of compound **2** contained peaks at 1.49 and 3.29 ppm corresponding to the ethyl groups of the $[Et_2NH_2]^+$ cation and a singlet at 8.33 ppm due to the $-NH_2$ group of the ammonium cation. The chemical shifts in the ^{19}F NMR spectrum were similar to those reported for the $-SC_6F_5$ group in other perfluorophenyl thiolate derivatives consisting of three multiplets at -132.9, -160.9 and -165.3 ppm (*cf.* $[Ti(\eta^5\text{-}C_5H_4SiMe_3)_2(SC_6F_5)_2]$ where the *ortho* F is a doublet at -131.0, the *meta* F a triplet at -163.5 and the *para* F a triplet at -157.9 ppm).[71] This suggests that the compound in solution exhibits fluctional exchange between the $[Ti(SC_6F_5)_5]^-$ anion and the $[SC_6F_5]^-$ anions as no separate peaks are observed for $[SC_6F_5]^-$.

2.9 X-ray structure of compound 2

An X-ray analysis of crystals of **2** shows that the structure consists of the homoleptic $[Ti(SC_6F_5)_5]^-$ complex anion shown in Figure 2.5, together with two $[SC_6F_5]^-$ monoanions and three $[Et_2NH_2]^+$ cations; selected bond lengths and angles are shown in Table 2.2. The geometry at the titanium centre is distorted trigonal bipyramidal, with S(3), S(4) and S(5) forming the equatorial plane. The angles at the metal centre produced by the equatorial atoms range from 115.5(1) - 126.5(1)°, and the two axial sulfur atoms subtend an angle of 172.7(1)° at the metal centre (Table 2.2). The Ti-S bond lengths of the equatorial groups (2.350(2) - 2.357(2) Å) are shorter than the axial ones (2.386(1) and 2.406(1) Å) as expected. The Ti-S bond lengths observed in the present structure are similar

to those in, for example, [Ti(S-2,3,5,6-$Me_4C_6H)_4$] (average Ti-S bond length 2.361(2) Å)[29] and [$TiCl_2(S^tBu)$(Diars)] (where Diars is *o*-phenylene bis(dimethylarsine)) (average Ti-S bond length 2.332(3) Å);[69] and to the terminal Ti-S bond lengths in [Me_2NH_2][$Ti_2(\mu$-$SMe)_3(SMe)_6$] (Ti-S bond lengths 2.321(1) - 2.362(1) Å),[30] [$Ti_3(\mu$-$SMe)_6(SMe)_6$] (Ti-S 2.3134(7) - 2.3177(7) Å),[30] and compound **1** (Ti-S 2.3308(9) - 2.4090(10) Å).[70] However, as expected, the Ti-S bond distances are shorter than those reported for bridging thiolate ligands, e.g. in **1** (Ti–S bond lengths 2.513(1) - 2.561(1) Å).[70] The Ti-S bond distances in compound **2** are also shorter than those observed in [$Ti(\eta^5$-$C_5H_4SiMe_3)_2(SC_6F_5)_2$] (Ti-S bond lengths 2.431(2) and 2.438(2) Å) as a result of the trimethylsilylcyclopentadienyl groups.[71] There is also a weak C-F···π interaction[72] from one of the *ortho* fluorine atoms of the S(1) based C_6F_5 ring to the S(5) ring (interaction **a** in Figure 2.5).

The anion, [$Ti(SC_6F_5)_5$]$^-$ has a "paddle-wheel-like" structure, as all of the Ti-S-Ar bends are in the same direction. This paddle-wheel structure produces the linking of adjacent complexes. There are π-π stacking interactions between the S(1) ring in one complex and the S(2) ring in the next (interaction **b** in Figure 2.6) and also between the S(3) and S(5) rings in neighbouring complexes (interaction **c** in Figure 2.6). These interactions combine to form an extended two-dimensional sheet of complex anions. There is also a C-F···π interaction between one of the fluorine atoms of an S(3) ring and the opposite face of a π-stacked S(2) ring (interaction **d** in Figure 2.6).

The spaces between these parallel anionic two-dimensional sheets are occupied by the three [Et_2NH_2]$^+$ cations and the two [SC_6F_5]$^-$ anions. These are

linked *via* N-H···S hydrogen bonds using all six of the available donor N-H hydrogen atoms (interactions **e** to **j** in Figure 2.7).

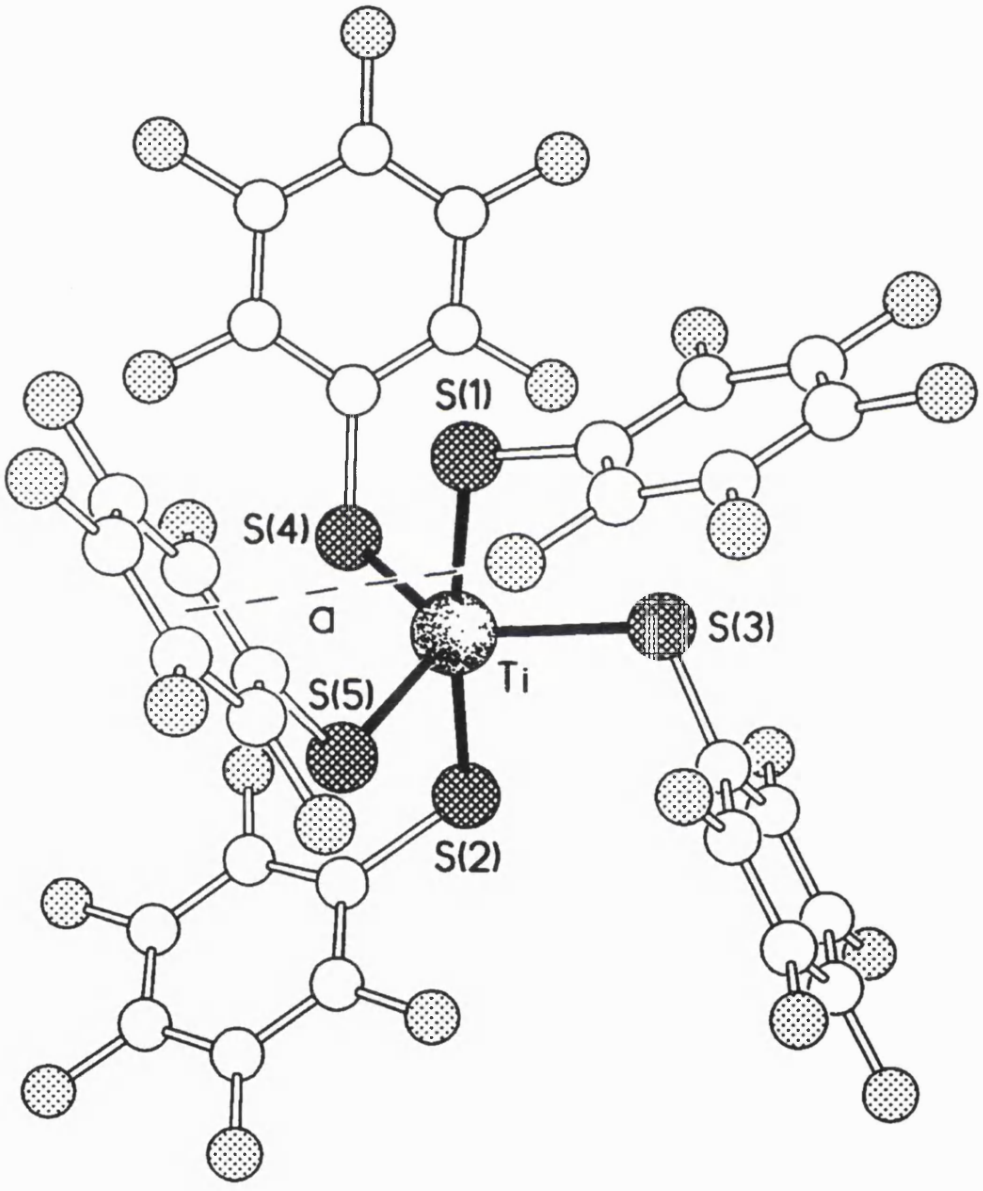

Figure 2.5 The homoleptic anion in compound 2

Figure 2.6 View of the packing of the complex anions in compound 2

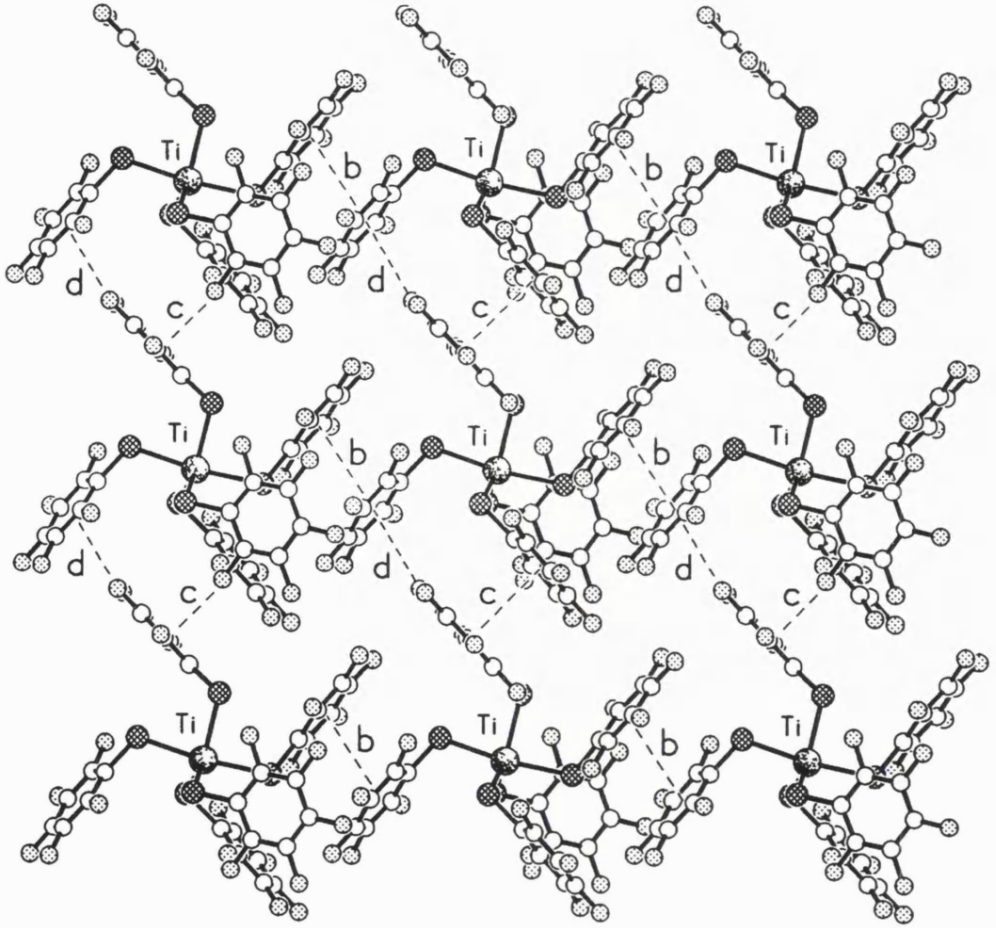

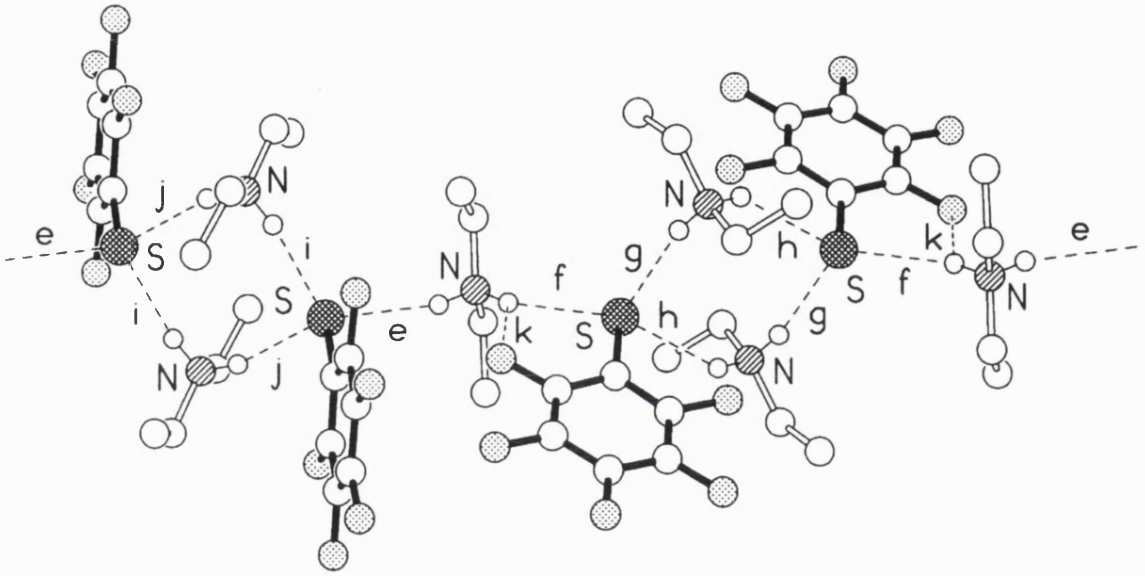

Figure 2.7 Part of one of the N–H···S linked anion/cation hydrogen bonded chains in compound 2

Table 2.2 Selected bond distances (Å) and angles (°) for compound 2

Ti-S(1)	2.386(1)
Ti-S(2)	2.406(1)
Ti-S(3)	2.350(2)
Ti-S(4)	2.356(2)
Ti-S(5)	2.357(2)
S(3)-Ti-S(4)	115.52(7)
S(3)-Ti-S(5)	126.47(7)
S(4)-Ti-S(5)	117.14(6)
S(3)-Ti-S(1)	88.22(5)
S(4)-Ti-S(1)	92.24(5)
S(5)-Ti-S(1)	98.65(5)
S(3)-Ti-S(2)	84.76(5)
S(4)-Ti-S(2)	89.10(5)
S(5)-Ti-S(2)	87.07(5)
S(1)-Ti-S(2)	172.73(6)

2.10 Reaction of $[Ti(NEt_2)_4]$, four equivalents of C_6F_5SH and tetrahydrothiophene

In an attempt to satisfy the coordination requirements of the titanium metal centre and produce a neutral monomeric compound of the type $[Ti(SC_6F_5)_4(L_2)]$, the reaction between $[Ti(NEt_2)_4]$, four equivalents of C_6F_5SH and two equivalents of a two-electron donor ligand was carried out. Two ligands, tetrahydrothiophene (C_4H_4S) and 2,6-dimethylpyridine, were used as the donor ligands. The reaction of $[Ti(NEt_2)_4]$, four equivalents of C_6F_5SH and two equivalents of tetrahydrothiophene afforded a dark red solution. Work-up and crystallisation from saturated CH_2Cl_2/hexanes at room temperature for five days produced dark red crystals suitable for X-ray analysis. Analytical and spectroscopic data showed that $[Et_2NH_2][Ti(SC_6F_5)_4(NEt_2)]$ (compound **3**) had formed and not $[Ti(SC_6F_5)_4(L)_2]$ as expected. An overall reaction scheme is shown in scheme 2.

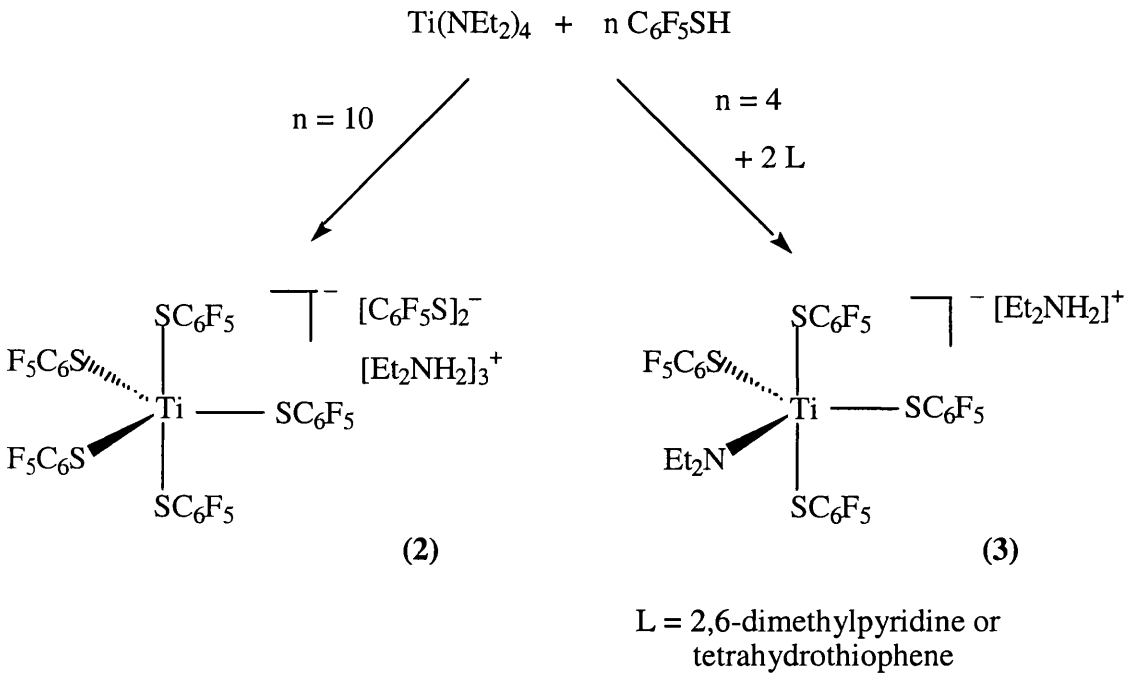

Scheme 2 Summary of the two reactions using $[Ti(NEt_2)_4]$ and C_6F_5SH

2.11 Spectroscopic data for compound 3

The ^1H NMR (CD_2Cl_2) spectrum of **3** shows peaks for the ethyl groups of the amide ligand occurring at 1.05 and 4.34 ppm as well as those for the ammonium cation at 1.50 and 3.45. A singlet also occurs at 7.30 ppm due to the NH_2 groups of the ammonium cation (Figure 2.8). The ^{19}F NMR was very similar to that obtained for compound **2** with peaks at -132.5, -160.5 and -164.9 ppm. It is worth noting that no peaks due to tetrahydrothiophene were observed in the ^1H NMR of the product.

When $[Ti(NEt_2)_4]$ was reacted with only four equivalents of C_6F_5SH, however, compound **3** was not produced. The ^1H NMR spectrum of the reaction

product was consistent with the formation of **2** suggesting that the presence of the donor ligands in the reaction mixture does influence the final product.

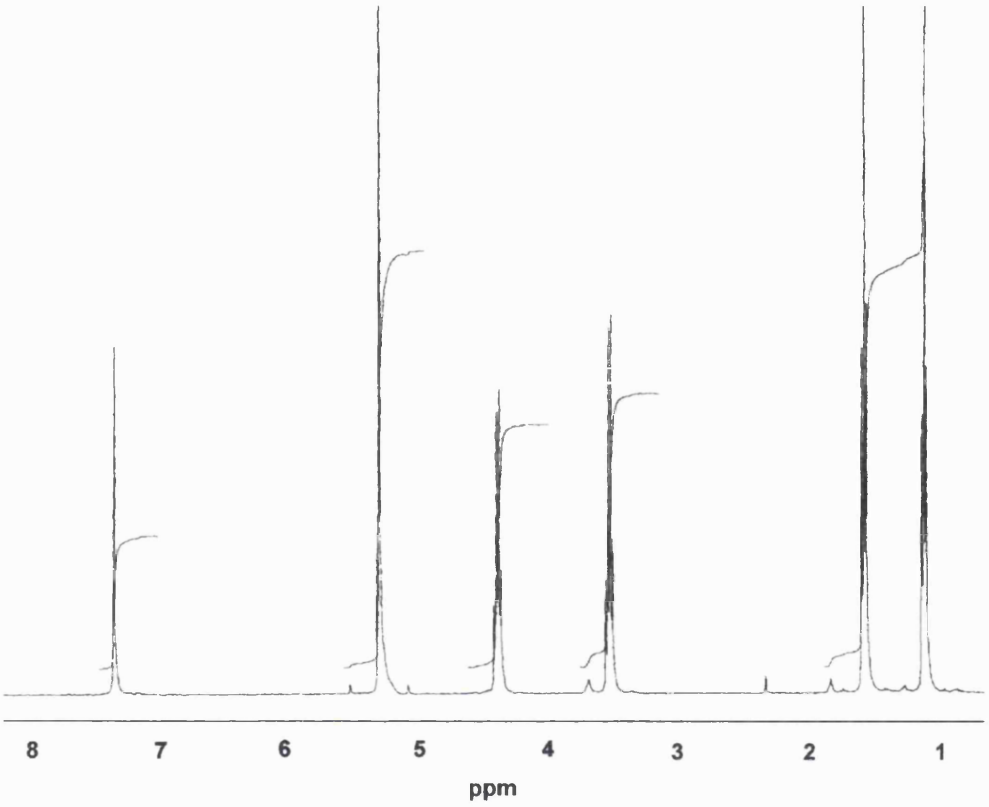

Figure 2.8 ^{1}H NMR spectrum for the reaction of $[Ti(NEt_2)_4]$ with four equivalents of pentafluorothiophenol and two equivalents of tetrahydrothiophene

2.12 X-ray structure of compound 3

The single crystal X-ray structure determination of **3** reveals a structure that is very similar to that of the complex anion in compound **2** but with one of the pentafluorothiophenolate ligands replaced by a diethylamino group to give the C_2 symmetric diethylammonium salt of $[Ti(SC_6F_5)_4(NEt_2)]^-$ (Figure 2.9). Selected bond lengths and angles are given in Table 2.3. The geometry at the titanium

centre is again a distorted trigonal bipyramid with S(1), S(1A) and N occupying the equatorial sites. The angles at the titanium centre within this plane are 119.9(1), 105.9(1) and 120.3(1)° (Table 2.3). The axial sulfur atoms subtend an angle of 148.2(1)° at the metal centre. This produces a greater distortion in the coordination geometry than is observed in compound **2** (where this angle is 172.7(1)°). The geometry observed in **3** can therefore be considered as intermediate between trigonal bipyramidal and square pyramidal. The Ti-S bond lengths for the axial and equatorial sulfur atoms (2.427(1) Å for Ti-S(2) and 2.417(1) Å for Ti-S(1) respectively) are longer than the analogous Ti-S bonds in compound **2**. The Ti-N bond length is 1.849(4) Å, indicating a degree of partial double bond character. The Ti–N bond distance is similar to those found in related amido complexes such as $[Ti(NEt_2)_2(PhNNNPh)_2]$ (Ti–N 1.883 Å).[73]

The rotations about the Ti-S bonds are again of interest, with all of the $C_6F_5S^-$ ligands being bent towards the diethylamino ligand. This geometry results in the creation of a cleft within the structure where the diethylammonium cation is located. This structure also adopts a paddle-wheel-like conformation where the Ti-S-Ar bends are all in the same direction. This conformation again forms a two-dimensional sheet, as can be seen in Figure 2.10. This arrangement is stabilised by a combination of π-π (**a**), C-F···π (**b** and **c**) and F···π (**d**) interactions.

The reaction with $[Ti(NEt_2)_4]$, four equivalents of C_6F_5SH and two equivalents of 2,6-lutidine also gave compound **3**.

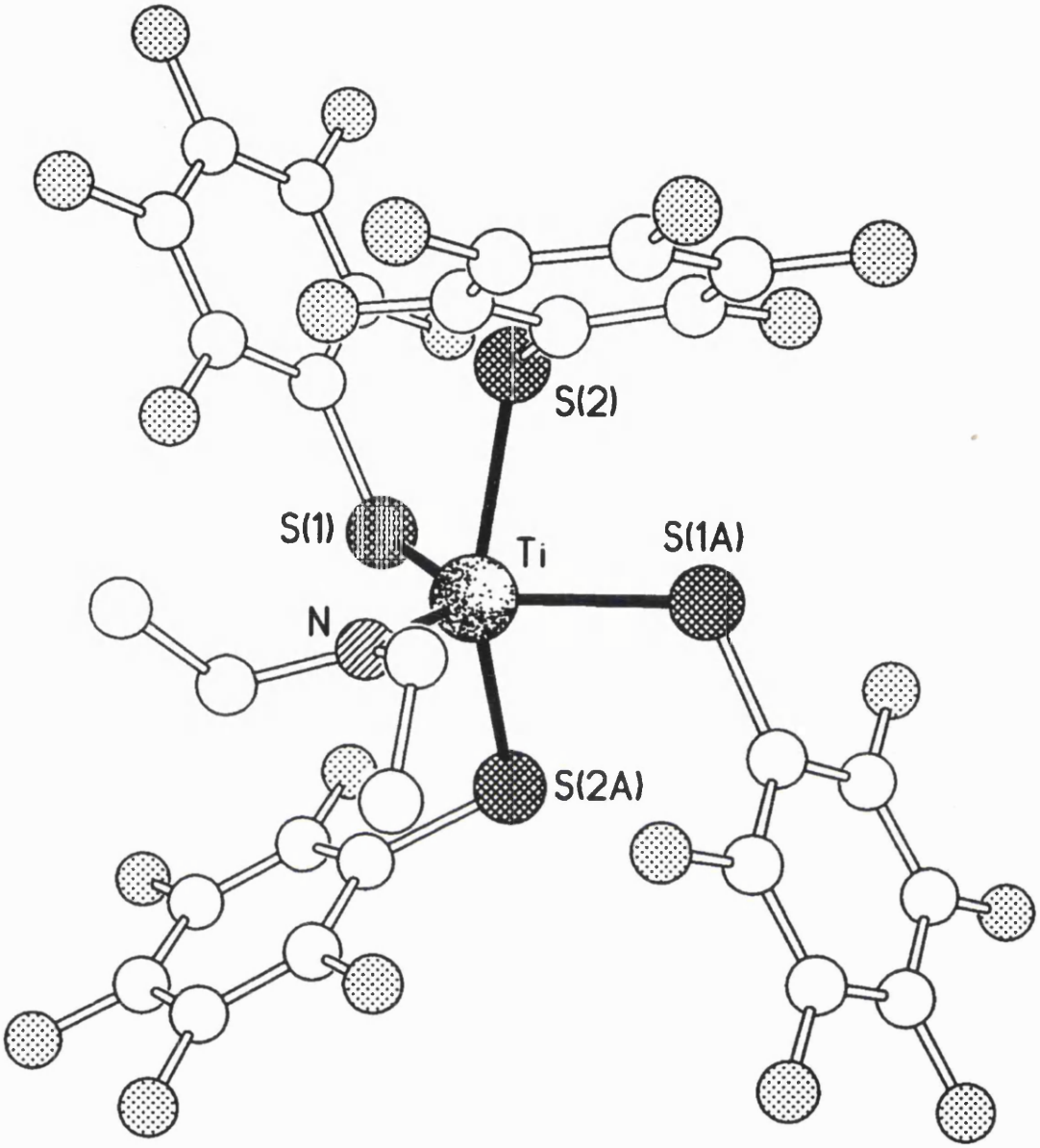

Figure 2.9 The molecular structure of the complex anion in compound 3

Figure 2.10 View of part of one of the anionic two-dimensional sheets of π-π, C–F···π and F···π linked complexes in compound 3

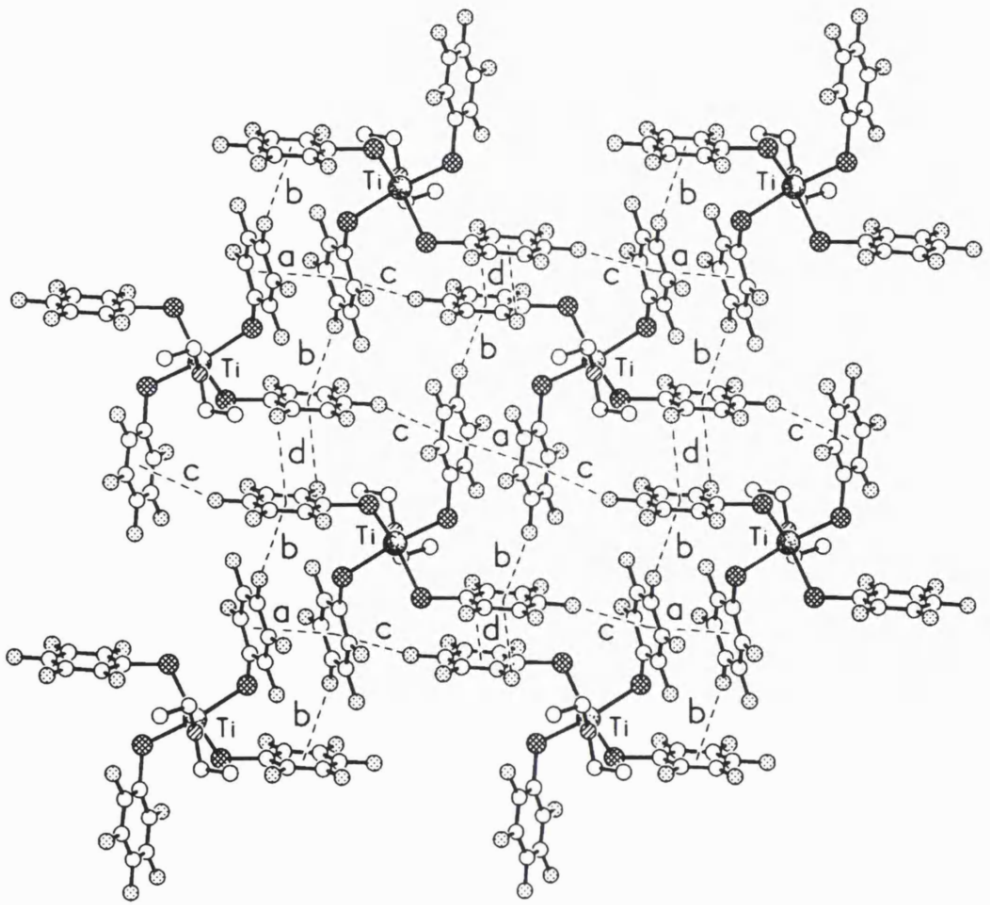

Table 2.3 Selected bond distances (Å) and angles (°) for compound 3

Ti-S(1)	2.417(1)
Ti-S(2)	2.427(1)
Ti-N	1.849(4)
N-Ti-S(1)	119.86(3)
N-Ti-S(2)	105.90(3)
S(1)-Ti-S(1A)	120.27(6)
S(1)-Ti-S(2)	83.39(3)
S(1)-Ti-S(2A)	80.92(3)
S(2A)-Ti-S(2)	148.20(5)

2.13 Further reactions with C_6F_5SH

The reaction between $[Ti(NEt_2)_4]$, four equivalents of C_6F_5SH and one equivalent of the chelating ligand, bipyridine, was carried out in order to investigate the influence of this ligand on the product. A red solid resulted, after work-up of the reaction mixture. X-ray quality crystals were not obtained even after numerous recrystallisation attempts. ^1H NMR studies of the red solid showed that the positions of the ethyl groups are noticeably different to those observed for compound **3**, with the two CH_3 peaks at 1.32 and 1.48 ppm (*cf.* 1.05 and 1.50 ppm for **3** and the two CH_2 peaks at 3.07 and 4.96 ppm (*cf.* 3.45 and 4.34 ppm). These results suggest that the final product contains an ammonium cation $[Et_2NH_2]^+$ (peaks at 1.48 and 4.96 ppm) and free amine (peaks at 1.05 and 3.07 ppm) and, therefore, that the species $[Ti(SC_6F_5)_4(NEt_2)]^-$ has not formed. A singlet at 2.34 ppm is also present in the NMR, which could correspond to the thiol C_6F_5SH. It is clear that the environments of the ethyl groups have changed due to the presence of the bipyridyl ligand. Peaks corresponding to bipyridine occur from 7.11-8.42 ppm. From analytical data, it is proposed that the species

$[Et_2NH_2][Ti(SC_6F_5)_5]$ has formed and co-crystallised with bipyridine and other amine impurities. More analysis would be required to determine the true nature of this compound, for example ^{19}F NMR and single crystal studies.

In a final attempt to isolate the neutral homoleptic species $[Ti(SC_6F_5)_4]_n$, compound **2** was heated in vacuo (100 °C, 10^{-3} mmHg). It was expected that **2** would lose amine and thiol as has been observed in some related metal thiolate salts to give the desired product.[74] However, prolonged heating resulted in a brown insoluble solid that contained nitrogen from elemental analysis, suggesting that the amine had not been lost.

The reactions involving C_6F_5SH, described above, did not result in neutral compounds but ionic ones (*cf.* $PhCH_2SH$ reactions). These products have high melting points and low volatility (108 °C for compound **2** and 148 °C for compound **3**). It was therefore decided to repeat the synthesis of $[Ti(S^tBu)_4]$ in order to see if a neutral compound could be isolated.[23] The compound $[Ti(S^tBu)_4]$ had not been crystallographically characterised in the literature but was analysed by ^1H NMR spectroscopy and elemental analysis (%C and %H).

2.14 Reaction of $[Ti(NEt_2)_4]$ and ^{t}BuSH

The addition of excess ^{t}BuSH to a solution of $[Ti(NEt_2)_4]$ in toluene resulted in an immediate colour change from orange to dark red. Work-up of the reaction mixture and crystallisation from a saturated hexane solution resulted in the formation of dark red needles in a 65% yield. Analytical and spectroscopic data showed this product to be a mixture of $[Ti(S^tBu)_4]$ and $[Ti(S^tBu)_3(NEt_2)]$ (compounds **4** and **5** respectively). This is in contrast to the earlier report that

suggested only $[Ti(S^tBu)_4]$ had been formed,[23] although this product was only analysed from microanalytical data. From elemental analysis carried out on the product, 2.78% nitrogen was obtained (% N calculated for compound **5** = 3.62%) suggesting that although this crystallises more readily there is some $[Ti(S^tBu)_4]$ present in the product. The reaction between $[Ti(NEt_2)_4]$ and excess ^{t}BuSH was repeated a number of times. Analytical data on subsequent samples of the red crystalline material isolated revealed that the % N varies from 0.71 to 2.78. Thus, even after repeated recrystallisations a small amount of nitrogen was always present in the material.[75]

The formation of compound **5** is obviously a result of incomplete substitution of all the amide ligands by the thiol. This is surprising since an excess of thiol is present in the reaction mixture. Earlier work by Bradley (see chapter1) indicated that the reaction of excess thiol R'SH (R' = Me, Et or ^{i}Pr) with $[Ti(NR_2)_4]$ (R = Me or Et) resulted in the formation of complexes of the type $[Ti(SR')_4(R'SH)_x(R_2NH)_y]$ (where x + y varied from 0.8 to 1.33).[25] However, controlled addition of R'SH to $[Ti(NMe_2)_4]$ afforded the partially substituted compounds $[Ti(NMe_2)_{4-x}(SR')_x]$ (where x = 1 or 2; R' = Et or ^{i}Pr).[21] This product appears to confirm this early hypothesis. The ^{1}H NMR data of the mixture of compounds **4** and **5** showed the presence of Ti-NEt_2 ligands in the mixture at 1.21 and 4.12 ppm and so supports the formation of compound **5**. The reaction product obtained (**4** and **5**), a neutral species, had a much lower melting point, at 51 °C, than the ionic compounds previously synthesised. This is likely to make the solid a more volatile species, and therefore a more desirable precursor to metal sulfides *via* CVD routes. An attempt to react only three stoichiometric equivalents with $[Ti(NEt_2)_4]$ did not produce the compound **5**, but a red oil. Integration of the ^{1}H

NMR peaks of the red oil showed that between one and two thiols had attached to the titanium centre (Figure 2.11).

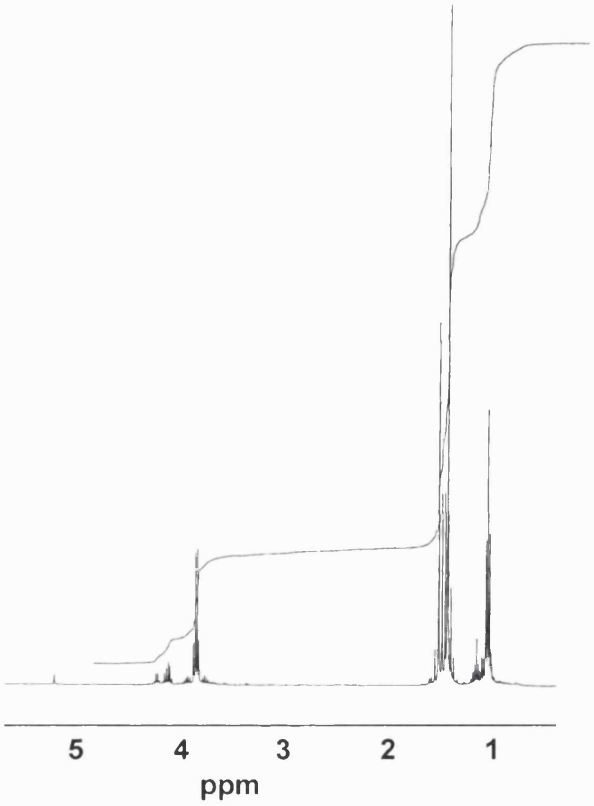

Figure 2.11 ^{1}H NMR spectrum for reaction of $[Ti(NEt_2)_4]$ with three equivalents of ^{t}BuSH

2.15 X-ray structure of compound 5

A single crystal structure determination revealed compound **5** to be a partially substituted thiolate species (Figure 2.12). Selected bond lengths and angles are shown in Table 2.4. The geometry at the titanium centre is a distorted tetrahedral structure with angles in the range of 101.16(7) - 115.5(2)° (Table 2.4). The Ti-S bond lengths range from 2.283(2) to 2.302(2) Å. These values are

similar to those found in analogous compounds e.g. $[Ti(\eta^5\text{-}NC_4Me_4)(SPh)_3]$,[76] where the Ti-S distances range from 2.285 to 2.314 Å. The Ti-S-C bond angles at sulfur are 112.7(2), 114.6(2) and 121.2(2)° for S(1), S(2) and S(3) respectively. The larger size of the angle at S(3) is possibly due to a steric conflict between its *tert*-butyl group and the diethylamido ligand. The geometry at the nitrogen centre is trigonal planar, and the Ti–N bond length is 1.856(5) Å which indicates a degree of double bond character. This bond is similar in length to those between titanium and the dimethylamido ligands in $[Ti(NMe_2)_2(OC_6H_2Bu^t_3\text{-}2,4,6)_2]$[77] (1.865 and 1.897 Å). The outer surface of compound **5** consists of hydrophobic *tert*-butyl and ethyl groups, and as such there are no intermolecular packing interactions of interest.

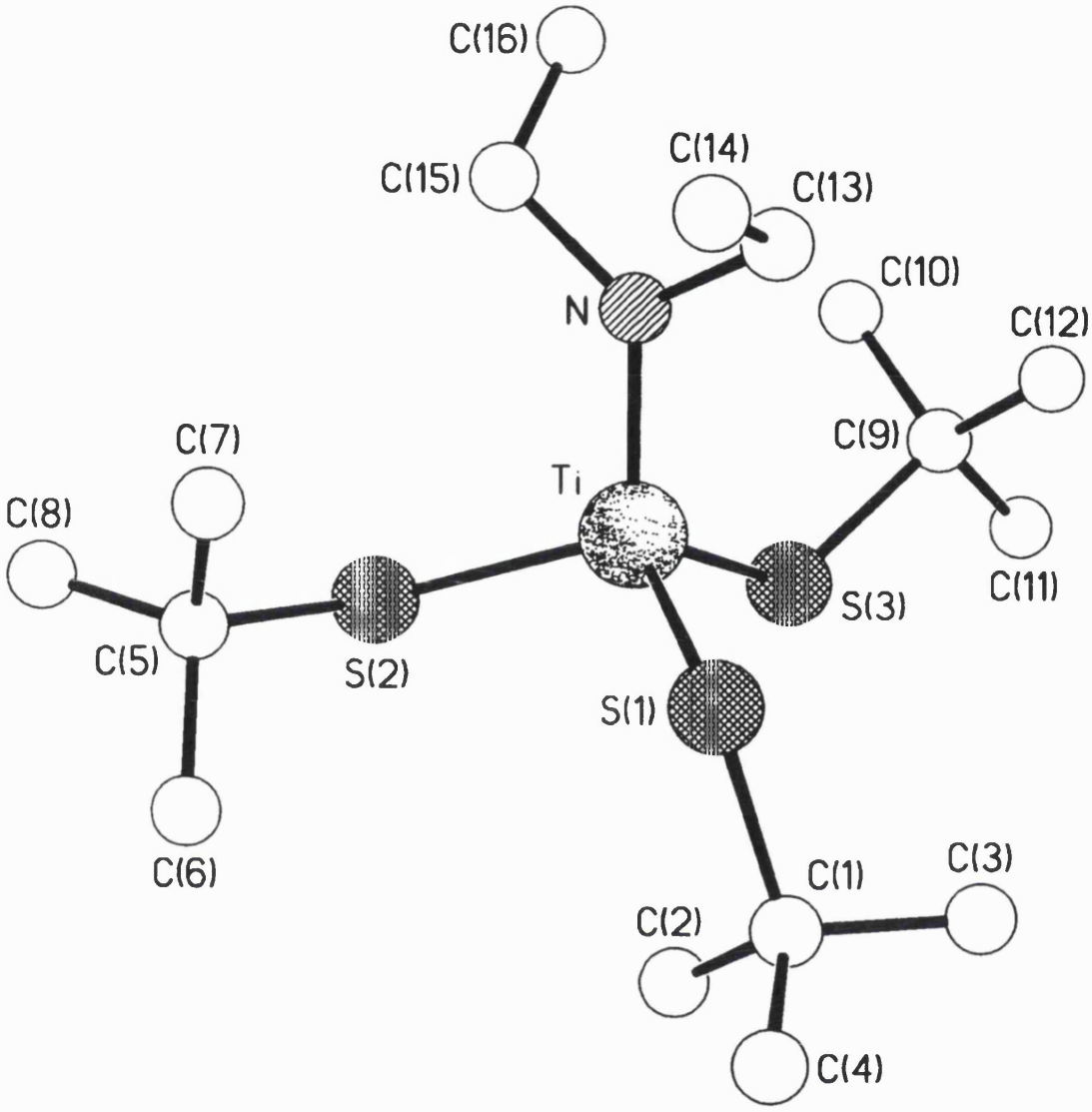

Figure 2.12 The molecular structure of compound 5

Table 2.4 Selected bond distances (Å) and angles (°) for compound 5

Ti-S(1)	2.295(2)
Ti-S(2)	2.302(2)
Ti-S(3)	2.283(2)
Ti-N	1.856(5)
N-Ti-S(1)	105.2(2)
N-Ti-S(2)	110.06(14)
N-Ti-S(3)	115.5(2)
S(1)-Ti-S(2)	112.62(7)
S(3)-Ti-S(1)	112.52(7)
S(3)-Ti-S(2)	101.16(7)
C(1)-S(1)-Ti	112.7(2)
C(9)-S(3)-Ti	121.2(2)
C(5)-S(2)-Ti	114.6(2)
C(15)-N-C(13)	113.5(4)
C(15)-N-Ti	127.0(4)
C(13)-N-Ti	119.2(3)

2.16 Reaction of $[Ti(NEt_2)_4]$ and 2,6 dimethylthiophenol

The reaction of $[Ti(NEt_2)_4]$ and an excess of 2,6-dimethylthiophenol produced a red solution on addition of the thiol. This solution darkened after stirring for two hours. After work-up of the reaction, red crystals were obtained from a solution of toluene at room temperature. Unfortunately it was not possible to obtain a single crystal structure of the product. ^1H NMR of the red crystals did not show the presence of an -SH group from the starting thiol in the product suggesting a reaction of some type had occurred. Peaks corresponding to the methyl and phenyl groups of the thiol were present in the spectrum (2.20 and 6.8-7.2 ppm respectively) as were peaks for the ethyl groups of an amine species (at 0.8 and 2.3 ppm). A significant peak occurred within the spectrum at 1.1 ppm that could not be accounted for. Elemental analysis showed nitrogen to be present

in the final product (2.03%). These results suggest that this reaction is incomplete with only partial substitution of the amide ligands by the thiol. This is surprising given the steric bulk of the ligand and the fact that [Ti(S-2,3,5,6-Me_4C_6H)$_4$] has been successfully synthesised,[29] albeit by a salt elimination method. It was then decided to react the compound **4/5** mixture obtained previously with an excess of 2,6-dimethylthiophenol in the hope that this synthetic method could yield the desired neutral product [Ti(S-2,6-$Me_2C_6H_3$)$_4$].

2.17 Reaction of compounds 4/5 and 2,6-$Me_2C_6H_3SH$

The reaction described in section 2.14 ([Ti(NEt_2)$_4$] and excess ^{t}BuSH) was repeated. The product (compound **4/5**) was then dissolved in toluene to give a dark red solution and an excess of 2,6 dimethylthiophenol was added. A colour change was not observed, but a dark insoluble precipitate was formed indicating that a reaction had occurred. The remaining dark red solution was filtered and the solvent removed *in vacuo*. This resulted in a dark red oil that was dissolved in hexane. Dark red needles were produced from this solution in a 50% yield. ^{1}H NMR and elemental analysis of these needles were consistent with the formation of [Ti(S-2,6-$Me_2C_6H_3$)$_4$] (compound **6**) although peaks corresponding to 2,6-$Me_2C_6H_3SH$ were observed at 2.26 ppm (-C*H*$_3$ groups) and 3.24 ppm (-S*H*) as well as in the aromatic region. The peak corresponding to the methyl groups of the thiolate ligand occurred as a singlet at 2.16 ppm. Peaks corresponding to the *tert*-butyl groups of compounds **4/5** and those of -NEt_2 were not observed in the spectrum, indicating that complete substitution of the amide and thiolate ligands of the starting product had occurred. A crystal structure was not obtained,

however, despite numerous attempts to repeat the reaction and using a variety of different solvent systems. The reaction proved to be difficult to repeat but it does indicate that a neutral monomeric thiolate can be produced without amide ligands being attached to the titanium centre. This offers a new route to making transition metal thiolates that, to our knowledge, has not been previously explored. It is interesting that compound **6** was not obtained from $[Ti(NEt_2)_4]$ and an excess of $Me_2C_6H_3SH$ despite repeated attempts.

2.18 Reactions with other transition metal amides

Given the success of obtaining a neutral monomeric titanium thiolate from the titanium amide precursor, it was decided to extend this route to zirconium, tantalum and niobium. Consequently the amides $[Zr(NEt_2)_4]$,[66] $[Ta(NMe_2)_5]$[78] and $[Nb(NMe_2)_5]$[79] were prepared according to literature procedures. The diethylamides of tantalum and niobium were not prepared on account of their tendency to form metal centres in the +4 oxidation state and not the +5 as required.[79] The bulky thiol 2,6-$Me_2C_6H_3SH$, was chosen to react with the metal amide.

2.19 Reaction of $[Ta(NMe_2)_5]$ and 2,6-$Me_2C_6H_3SH$

The reaction of $[Ta(NMe_2)_5]$ with an excess of 2,6-$Me_2C_6H_3SH$ produced an immediate colour change from pale yellow to dark red-orange. Filtration of the solution and removal of the solvent *in vacuo* resulted in a dark red/orange solid. Bright red crystals were obtained in a 50% yield by diffusion of an

overlayer of hexane to a saturated CH_2Cl_2 solution of the solid produced. Analytical and spectroscopic data were consistent with the formation of the neutral species [Ta(S-2,6-$Me_2C_6H_3$)$_4$(NMe_2)] (compound **7**). As with compound **5**, an amide group is attached to the metal centre despite an excess of 2,6-$Me_2C_6H_3SH$ present in the reaction mixture. This is unexpected, given the existence of the compound [Ta(S-2,3,5,6-Me_4C_6H)$_5$] and the similarity of the two thiolate ligands.[29] However, [Ta(S-2,3,5,6-Me_4C_6H)$_5$] was prepared from a salt elimination route. The protons of the -NMe_2 group in compound **7** occur as a singlet at 2.76 ppm in the ^{1}H NMR and those of the methyl groups of the thiolate ligand at 2.45 ppm. Aromatic protons in **7** were found from 6.78 - 7.04 ppm. The melting point of **7** (200 °C) is also surprisingly high given that the product is neutral. Nonetheless, it is hoped that compound **7** can be used as a precursor to making tantalum disulfide *via* a "thio" sol-gel route or from deposition studies.

2.20 X-ray structure of compound 7

A single crystal structure determination showed compound **7** to be the incompletely thiolate-substituted complex shown in Figure 2.13. The complex has molecular C_2 symmetry about the N-Ta bond direction. The geometry at tantalum is distorted trigonal bipyramidal. The equatorial plane consists of the Ta, N, S(3) and S(4) atoms. The angles within the equatorial plane range from 119.04(6) to 121.6(2)° and the axial substituents subtend the tantalum centre at an angle of 164.37(5)° (Table 2.5). As expected, the Ta–S bond lengths of the axial ligands (Ta-S(1) 2.427(2) Å and Ta-S(2) 2.428(2)Å) are longer than the equatorial ones (Ta-S(3) 2.398(2) Å and Ta-S(4) 2.389(2) Å). This is not observed in the

homoleptic complex [Ta(SC_6HMe_4-2,3,5,6)$_5$].[29] In this complex, the geometry is distorted slightly more towards square pyramidal and the axial S-Ta-S angle is 156.7° and the Ta-S distances range from 2.330 to 2.402 Å. In [Ta(CH^{t}Bu)($SC_6H_2{}^i Pr_3$-2,4,6)$_3$(SEt_2)],[80] which has a distorted trigonal bipyramidal geometry similar to that of **7** (the axial ligands subtend an angle of 162.2° at the tantalum centre), the three equatorial Ta–S distances only range between 2.390 and 2.394 Å. These values are similar to those observed in **7**. The Ta-N bond length is 1.921(5) Å which suggests a degree of multiple bond character. This bond distance compares with a Ta=N double bond length of 1.894 Å in [{Ta($SC_6H_3Pr^i_2$-2,6)$_3$(THF)}$_2$(η-N_2)],[81] and Ta-N single bonds of, for example, 1.949 Å in [TaCl($NSiMe_3$){$N(SiMe_3)_2$}(η-Cl)]$_2$[82] and 2.024 Å in [Ta(OMe)($NSiMe_3$){$N(SiMe_3)_2$}(η-OMe)]$_2$.[82] The exterior of compound **7** consists of the hydrophobic -CH_3 groups of both the thiolate ligand and the amide. This prevents any significant intermolecular packing interactions.

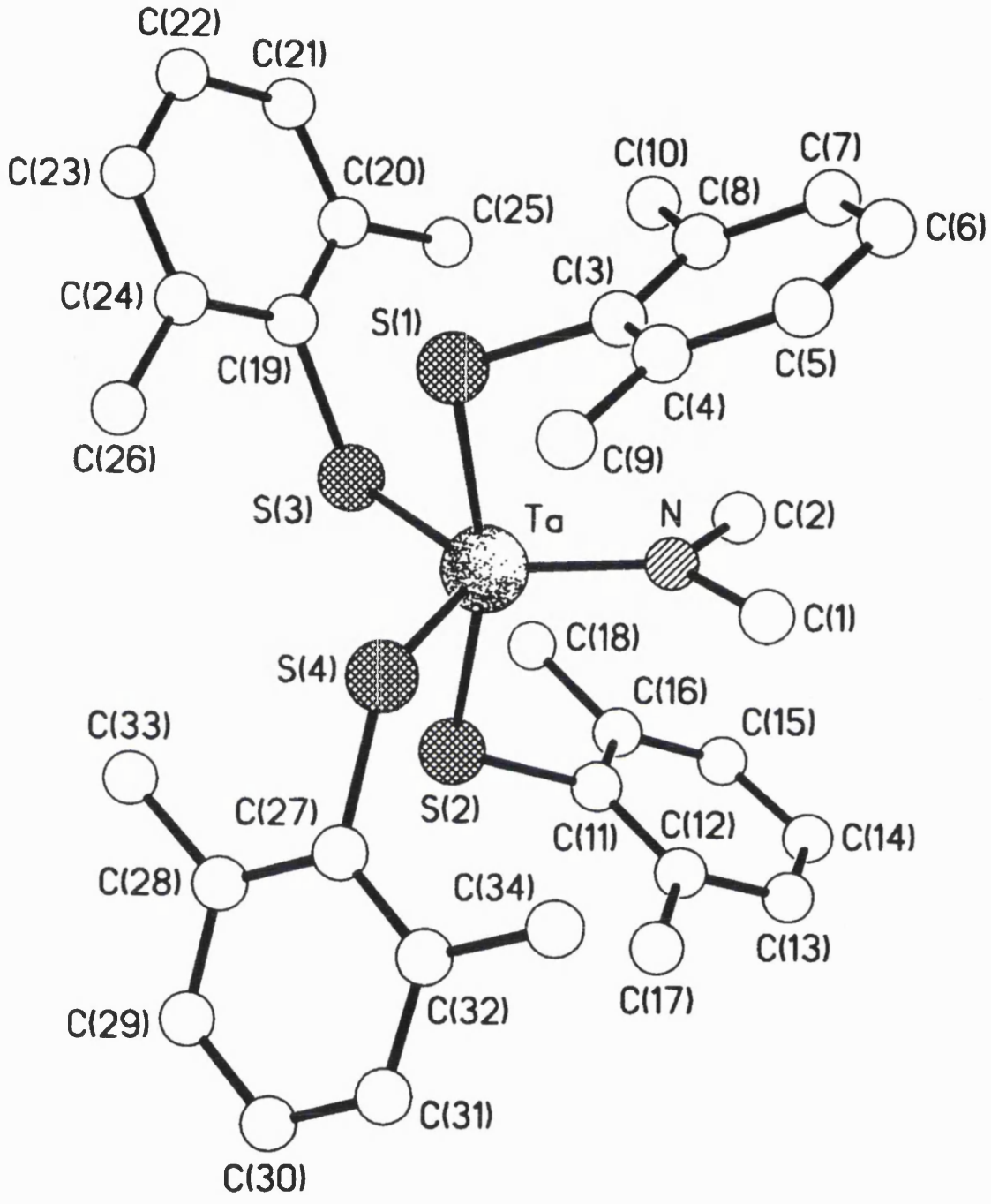

Figure 2.13 The molecular structure of compound 7

Table 2.5. Selected bond distances (Å) and angles (°) for compound 7

Ta-S(1)	2.427(2)
Ta-S(2)	2.428(2)
Ta-S(3)	2.398(2)
Ta-S(4)	2.389(2)
Ta-N	1.921(5)
S(4)-Ta-S(2)	93.49(6)
S(4)-Ta-S(1)	81.40(6)
S(4)-Ta-S(3)	119.04(6)
S(1)-Ta-S(2)	164.37(5)
S(3)-Ta-S(1)	89.17(6)
S(3)-Ta-S(2)	80.37(6)
C(19)-S(3)-Ta	115.7(2)
C(27)-S(4)-Ta	116.1(2)
C(1)-N-Ta	122.1(5)
C(2)-N-Ta	125.9(5)
C(2)-N-C(1)	111.9(6)
C(3)-S(1)-Ta	106.9(2)
C(11)-S(2)-Ta	109.2(2)
N-Ta-S(1)	98.5(2)
N-Ta-S(2)	96.9(2)
N-Ta-S(3)	121.6(2)
N-Ta-S(4)	119.4(2)

This reaction was subsequently repeated using the niobium amide, $[Nb(NMe_2)_5]$, where it was expected that a similar reaction product would result.

2.21 Reaction of $[Nb(NMe_2)_5]$ and 2,6-$Me_2C_6H_3SH$

On addition of an excess of 2,6-$Me_2C_6H_3SH$ to $[Nb(NMe_2)_5]$ an immediate colour change was observed from pale yellow to dark red. Removal of the solvent and crystallisation from a saturated CH_2Cl_2 solution gave dark red single crystals. Analytical and spectroscopic data for the crystals were consistent

with the formation of [Nb(S-2,6-$Me_2C_6H_3$)$_5$] (compound **8**) in a 50% yield. The ^{1}H NMR of compound **8** shows peaks characteristic of 2,6-$Me_2C_6H_3S^-$ thiolate ligands at 2.35 ppm and in the aromatic region from 6.85-7.05 ppm. Impurities due to -NMe_2 groups are present at 2.62 ppm in the ^{1}H NMR spectrum of compound **8** and in the elemental analysis (where the % N is 0.47) but this is due to the difficulty in isolating the crystals from the viscous saturated CH_2Cl_2 solution. To our knowledge, this structure represents the first fully characterised neutral monomeric homoleptic thiolate of niobium. It is interesting that this structure is different to that obtained with tantalum. The two atoms have a very similar size and it would be expected that the chemistries would be very similar. However, complete substitution of the amide has occurred in this instance. The melting point of compound **8** was 138 °C, which is lower than the value obtained for compound **7** but still quite high for CVD purposes (*cf.* compound **5**). Nonetheless, it is hoped that this compound can act as a precursor to niobium disulfide.

2.23 X-ray structure of compound 8

A single crystal structure determination of **8** revealed the compound to be the fully substituted neutral homoleptic thiolate species (Figure 2.14). Selected bond lengths and angles are shown in Table 2.6. The geometry at the niobium centre is a distorted trigonal bipyramidal structure. The equatorial plane is made up of the thiolate ligands of S(3), S(4) and S(5) respectively with angles at the niobium centre in the range 107.57(3) - 127.11(3)° (Table 2.6). The S(1)-Nb-S(2) angle is 155.18(3)° and suggests a distortion of the structure towards a square

pyramid (*cf.* compound **3** where this angle is 148.2(1)°). This is probably due to the steric demands of attaching five large 2,6-$Me_2C_6H_3S^-$ ligands to the niobium centre. The Nb-S bond lengths range from 2.3609(9) to 2.4289(8) Å. These values are shorter than those found in ionic niobium thiolate compounds e.g. $[(PPh_4)_2][Nb(SPh)_6]$ where the Nb-S bond lengths range from 2.476(3) - 2.500(3) Å.[41] To our knowledge, there are no analogous neutral homoleptic thiolates of niobium with which to compare bond lengths, angles etc. The outer surface of the compound consists of the hydrophobic methyl groups and, as such, there are no significant intermolecular interactions.

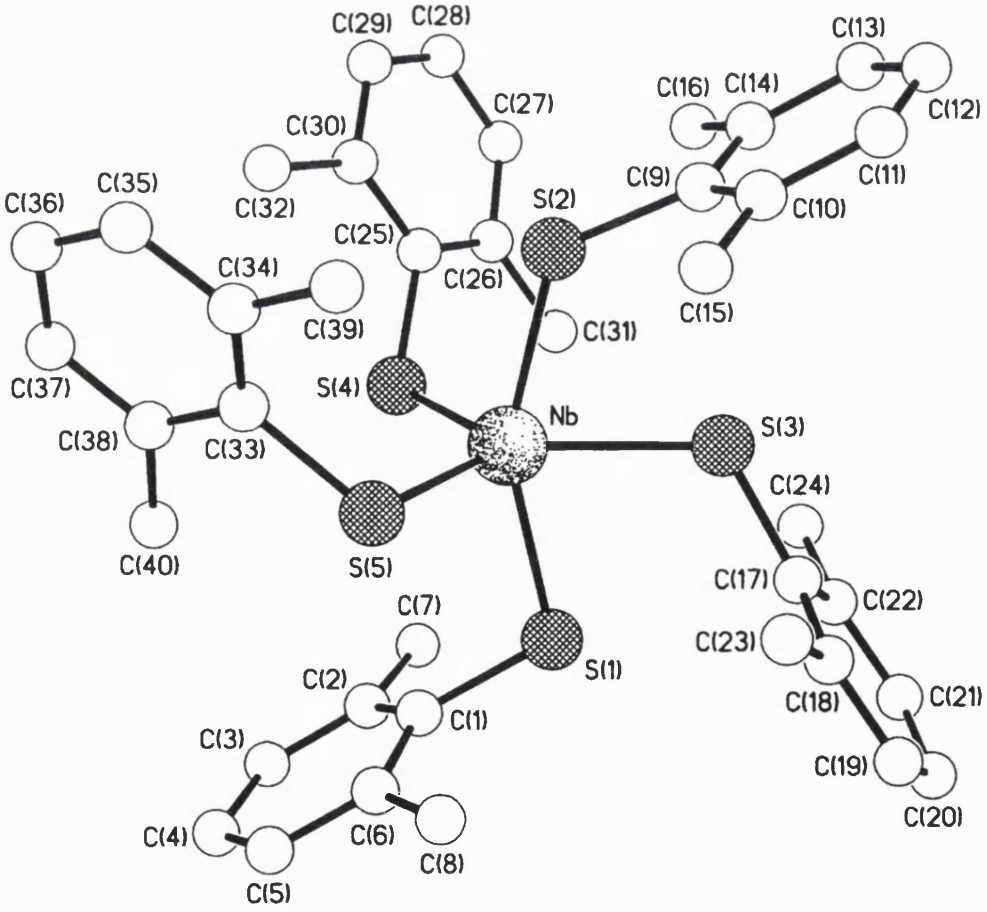

Figure 2.14 Structure of compound 8

Table 2.6 Selected bond distances (Å) and angles (°) for compound 8

Nb-S(1)	2.3961(8)
Nb-S(2)	2.3708(9)
Nb-S(3)	2.4289(8)
Nb-S(4)	2.3609(9)
Nb-S(5)	2.3707(8)
S(5)-Nb-S(2)	101.87(3)
S(1)-Nb-S(2)	155.18(3)
S(5)-Nb-S(1)	92.31(3)
S(3)-Nb-S(1)	78.12(3)
S(5)-Nb-S(3)	127.11(3)
S(3)-Nb-S(2)	77.08(3)
S(4)-Nb-S(5)	107.57(3)
S(4)-Nb-S(3)	125.32(3)
S(4)-Nb-S(2)	93.91(3)
S(4)-Nb-S(1)	101.16(3)

2.23 Reactions using $[Zr(NEt_2)_4]$

Given the success obtained with the previous metal amides, it was decided to prepare a zirconium amide starting material. However, reactions with $[Zr(NEt_2)_4]$ proved more problematic than the other metal amides used and it was difficult to isolate any significant species. The reaction of $[Zr(NEt_2)_4]$ with an excess of 2,6-dimethylthiophenol produced an insoluble bright yellow solid. ^1H NMR studies were not possible as the solid was not even sparingly soluble in any solvents. Elemental analysis performed on the solid did show a good match to the compound $[Et_2NH_2][Zr(S\text{-}2,6\text{-}Me_2C_6H_3)_5]$ but it is more likely that some form of extended polymerisation has occurred producing the insoluble species. To our knowledge no neutral monomeric thiolate compounds of zirconium exist except for a poorly characterised report of $[Zr(SPh)_4]$.[34] The cluster compound

$[Zr_3(S)(S^tBu)_{10}]$ has been reported to be made from the reaction of $[Zr(CH_2Ph)_4]$ and ^tBuSH with each zirconium atom having a coordination number of six.[35] The reaction of $[Zr(NEt)_2]$ and ^tBuSH was also performed. An orange solid was isolated from the reaction. The ^1H NMR spectra of the product showed a mixture of species in solution. Five singlets of different intensities were observed from 1.58-1.87 ppm corresponding to *tert*-butyl thiolate groups and numerous peaks occurred throughout the spectrum which were difficult to assign. This is in contrast to the ^1H NMR spectrum obtained for $[Zr_3(S)(S^tBu)_{10}]$, where four singlets were observed at 1.81, 1.93, 2.01 and 2.32 ppm with an intensity ratio of 3:3:3:1.[35] Evidence of a $[Et_2NH_2]^+$ cation did occur as a triplet at 0.96 ppm (CH_3 groups), a quartet at 2.47 ppm (CH_2 groups) and a broad singlet at 7.67 ppm (NH_2 groups) but these peaks were much smaller than those of the butyl groups. The elemental analysis was difficult to interpret. Nitrogen was found in the sample (1.52%) showing that an amide or ammonium cation was present. The carbon content was only 35.56% (*cf.* $[Et_2NH_2][Zr(S^tBu)_5]$ has 39.3% carbon) and so any further estimates as to what had been made were not possible. Bulkier thiols would probably have to be used in order to isolate a neutral monomeric product from this route, eg. 2,4,6-$^tBu_3C_6H_2SH$. The starting amide was also quite difficult to synthesise and so extensive studies were not carried out. It was therefore decided to attempt an alternative synthetic route to zirconium thiolate compounds.

2.24 Substitution reactions using metal alkyl complexes

The use of a metal amide starting material created difficulties in either the production of an ammonium cation, or incomplete substitution of the amide ligands. Therefore, using an alkyl transition metal starting material could eliminate these problems. It was therefore decided to synthesise $[Zr(CH_2Ph)_4]$[83] and $[Ti(CH_2Ph)_4]$[83] according to literature preparations and react these complexes with different thiols.

2.25 Reactions using $[Zr(CH_2Ph)_4]$

A reaction of $[Zr(CH_2Ph)_4]$ with pentafluorothiophenol did not yield any reaction (e.g. no colour change or heat produced) and so it was decided to attempt a reaction with the much larger thiol, Ph_3CSH. The reaction of $[Zr(CH_2Ph)_4]$ with four equivalents of Ph_3CSH resulted in a colour change from yellow to orange. An orange solid was isolated, which was insoluble in all solvents except THF. The elemental analysis for this orange solid gave a carbon content of only 62.7% which is lower than the calculated % carbon in $[Zr(CH_2Ph)_4]$ (73.8%) and the theoretical product $[Zr(SCPh_3)_4]$ (76.2%). X-ray crystal diffraction of orange crystals obtained from a THF solution showed only the presence of the starting thiol, Ph_3CSH. Elemental analysis for Ph_3CSH would give a carbon content of 82.6% and so clearly there are other species being produced in this reaction.

Finally, the addition of elemental sulfur to a solution of $[Zr(CH_2Ph)_4]$ was carried out in the hope of inserting sulfur into the Zr-C bond. A brown insoluble

product resulted suggesting decomposition had occurred and no analysis of the brown solid was performed.

2.26 Reactions using $[Ti(CH_2Ph)_4]$

Reaction of $[Ti(CH_2Ph)_4]$ with an excess of 2,6-dimethylthiophenol resulted in the formation of a small amount of an insoluble yellow precipitate and a dark red liquid. ^1H NMR of the red liquid (CD_2Cl_2) showed peaks corresponding to 2,6-dimethylthiophenol only and not of the thiolate ligands. This reaction route is in contrast to the reaction with $[Ti(NEt_2)_4]$ where a substitution reaction clearly occurred. Peaks corresponding to benzyl groups of $[Ti(CH_2Ph)_4]$ were not present in the final product, however, indicating that some form of reaction had occurred.

Reaction of $[Ti(CH_2Ph)_4]$ with an excess of $CF_3(CF_2)_5CH_2CH_2SH$ yielded an insoluble brown solid, suggesting that decomposition or polymerisation had occurred. It is surprising that this method proved so unsuccessful. It was hoped that the starting material would prevent the formation of any cationic species and so encourage the thiolate ligands to bond to the metal centre. Another major problem encountered with this route was the making of the starting materials. The synthesis was time consuming and the final product extremely sensitive ($[Zr(CH_2Ph)_4]$ being light sensitive as well as air and moisture sensitive). For practical purposes, it was decided to investigate alternative routes rather than prepare other metal alkyl species.

2.27 Synthesis of metal thiolates *via* salt elimination routes

A series of reactions were carried out using the transition metal chlorides $TiCl_4$, $TaCl_5$ and $NbCl_5$ and an alkali metal salt of the thiol, MSR (where M = Li, Na or K and R = alkyl/aryl group). The alkali metal salt was easily synthesised *via* reduction of the thiol by the alkali metal (for Na and K) or BuLi in THF followed by removal of the solvent *in vacuo*. This salt was then reacted directly with the metal chloride in a suitable solvent using the correct stoichiometry. This procedure was based on that used for the preparation of $[Ti(S\text{-}2,3,5,6Me_4C_6H)_4]$ and $[Ta(S\text{-}2,3,5,6Me_4C_6H)_5]$.[29] It was decided to begin with the thiol 2,6-dimethylthiophenol due to its similarity to $2,3,5,6\text{-}Me_4C_6HSH$.

2.28 Reactions of $TiCl_4$, $TaCl_5$ and $NbCl_5$ with 2,6-dimethylthiophenol

The alkali metal salt of the thiol was synthesised as a white solid as described above. Reaction of four equivalents of $NaS\text{-}2,6\text{-}Me_2C_6H_3$ with $TiCl_4$ in hexane resulted in a dark red solution. A grey solid precipitate was also formed in the reaction that was assumed to be sodium chloride. Filtration of the solution gave a dark red oil that was soluble in hexane. Work-up of the resulting red solution resulted in a dark red solid. ^1H NMR of the dark red solid showed the presence of $2,6\text{-}Me_2C_6H_3S^-$ ligands (2.37 ppm for CH_3 groups; 6.95-7.10 ppm for the aromatic protons). Peaks due to small amounts of free thiol, $2,6\text{-}Me_2C_6H_3SH$ and hexane were also observed. Two broad singlet peaks were also observed at 1.99 and 4.33 ppm due to THF (used in the initial alkali metal salt preparation) coordinated to the titanium centre. An elemental analysis of the

red solid showed a close match to the formation of [TiCl(S-2,6-$Me_2C_6H_3)_3$.THF] and not the fully substituted thiolate [Ti(S-2,6-$Me_2C_6H_3)_4$]. Unfortunately, X-ray quality crystals were not obtained from this method.

The addition of $TaCl_5$ to five equivalents of NaS-2,6-$Me_2C_6H_3$ in hexane resulted in a red/orange solution being produced. After work-up of this red/orange solution, a small amount of a red/orange solid resulted (yield 7%). ^1H NMR of the red/orange solid showed peaks in the aromatic region and a singlet at 2.35 ppm corresponding to the methyl groups of the thiolate. Elemental analysis was taken on the red/orange solid to see if full substitution had occurred. These results suggest that the partially substituted species [$TaCl_2$(S-2,6-$Me_2C_6H_3)_3$] had been formed.

The reaction between $NbCl_5$ and five equivalents of NaS-2,6-$Me_2C_6H_3$ in hexane resulted in a dark red solution on refluxing. The dark red solution was then filtered through Celite. Increasing the concentration of the dark red solution by removal of solvent resulted in the formation of caramel crystals (*cf.* dark red for compound **8**). An X-ray analysis of these crystals revealed the structure to be the disulfide (2,6-$Me_2C_6H_3S)_2$. Therefore, decomposition or oxidation of the metal centre has occurred. The starting thiol was also observed in the ^1H NMR and, despite repeated attempts at this reaction, the same caramel coloured product was always obtained.

2.29 Further reactions using salt metathesis

Further reactions with a variety of different thiols, for example, $PhCH_2SH$, ^tBuSH, C_6F_5SH and Ph_3CSH resulted in decomposition of the products. One of the main problems encountered with this synthetic method appeared to be the highly sensitive nature of the compounds produced to air and moisture. Any promising reaction species obtained (usually indicated by a red or red/orange colour) soon decomposed during refluxing or even at room temperature to a brown precipitate. Isolation of any reaction products proved very difficult. Although successful with $2,6\text{-}Me_2C_6H_3SH$ it proved difficult to stabilise the metal centre with any other thiols used. It is likely that decomposition products or mixed products are being formed by this route. A final reaction of $TiCl_4$ with four equivalents of $NaSC_6F_5$ and two equivalents of 2,6-lutidine only resulted in a sparingly soluble yellow solid. The ^1H NMR spectrum of this solid did give a singlet at 2.84 ppm that could be assigned to the methyl groups of 2,6-lutidine, as well as the aromatic protons at 7.31 and 7.96 ppm. Elemental analysis of the yellow solid proved difficult to assign. Evidence of chlorine present in the final material (3.67%) suggested that full substitution had not occurred. The closest match to any theoretical product was $[TiCl(SC_6F_5)_3.2,6\text{-lutidine}]$. The relative insolubility of the product indicates that a more complicated, extended structure may have occurred

2.30 Synthesis using triethylamine

An initial reaction using four equivalents of C_6F_5SH, $TiCl_4$ and an excess of Et_3N was attempted but, as with the salt metathesis approach described earlier, decomposition occurred. It was decided not to proceed with any of the thiols used previously but to attempt a reaction with 2-dimethylaminoethane thiol ($Me_2NCH_2CH_2SH$) instead, where additional dative bonding of the nitrogen atom to the metal centre is possible. Reaction of $TiCl_4$, four equivalents of $Me_2NCH_2CH_2SH.HCl$ and excess Et_3N in toluene resulted in the formation of a dark red solution. Work-up of the reaction mixture afforded a dark red solid that was only sparingly soluble in CH_2Cl_2 and insoluble in all other solvents. The ^1H NMR spectra of the red solid showed a number of peaks that were difficult to assign. Broad peaks occurred from 2.20-4.06 ppm and a broad singlet was also found at around 10.2 ppm. Elemental analysis of the red solid suggested the product $[TiCl_2(SCH_2CH_2NMe_2)_2]$ had been made although impurities are likely to be present. Again complete substitution of the chloride ligands by thiolate groups has not occurred. The analogous reaction with $TaCl_5$ produced an orange solid that did not appear to contain any thiolate at all from ^1H NMR studies. Peaks corresponding to the ethyl protons of triethylamine occurred at 1.24 and 2.95 ppm. The analogous reaction with $NbCl_5$ decomposed to give a dark brown insoluble product.

This method also proved difficult and did not result in the desired products. Giolando *et al.* also described the lack of success using this methodology when attempting to synthesise titanium thiolates, suggesting the formation of mixtures of compounds of the type $[TiCl_{4-x}(SR)_x]$ (where x varies

from 1-4) to be responsible.[30] Finally a Grignard methodology was attempted to see if this would produce interesting results.

2.31 Synthesis using Grignard reagents

In this instance, the Grignard reagent mesityl magnesium bromide (MesMgBr) was reacted with elemental sulfur in toluene giving a yellow solution that was assumed to be MesSMgBr. Addition of $TiCl_4$ to four equivalents of MesSMgBr gave a dark red solution that was extremely sensitive and could not be isolated without decomposition occurring. The reaction of five equivalents of MesSMgBr with $NbCl_5$, however, gave a dark red solution that yielded a dark red solid after work-up. ^1H NMR of the red solid showed a singlet at 6.90 ppm corresponding to the two aromatic protons of the ligand, the *para*-methyl group of the aryl species occurred as a singlet at 2.26 ppm and the two *ortho*-methyl groups at 2.22 ppm. It was hoped that the product $[Nb(SMes)_5]$ had formed. Elemental analysis of the red solid did not correspond to this product as the percentage carbon and hydrogen were too high (66.4% and 6.32% *cf.* 63.7% and 6.49% for $[Nb(SMes)_5]$). If incomplete substitution of the chloride ions had occurred then the carbon and hydrogen contents of the product would have been lower than $[Nb(SMes)_5]$. One possibility for the observed results would be if the disulfide, $(MesS)_2$, had been produced during the reaction due to oxidation of the thiolate. Small contamination of this would account for the increase in carbon and hydrogen in the final product. The yield for this reaction was less than 10% and as such was not particularly useful as a precursor for materials analysis.

The reaction of five equivalents of MesSMgBr and $TaCl_5$ was also carried out and a dark red solid was isolated from the reaction. Elemental analysis on this red solid showed a carbon and hydrogen content higher than that expected for the fully substituted compound, $[Ta(SMes)_5]$ suggesting that the disulfide may have been produced and contaminated the final product. The ^1H NMR of the red solid showed three singlets in the methyl region at 2.20, 2.28 and 2.34 ppm and not just two as in the case with the niobium analogue. This does give further indication of impurities being present in the final product. Crystals suitable for X-ray crystallography could not be grown and the yield was also low. It was decided to use the six compounds characterised by single crystal X-ray crystallography as precursors to the chalcogenides using the thio "sol-gel" method and chemical vapour deposition studies.

2.32 Conclusions

Studies performed on the synthesis of homoleptic early transition metal thiolates proved successful in the preparation and characterisation of three ionic compounds, (**1**, **2** and **3**) and three neutral species (**4/5**, **7** and **8**). These were prepared from the reactions between the transition metal amides and an excess of the thiols. The neutral compounds were prepared from the bulkier thiols, ^tBuSH and 2,6-$Me_2C_6H_3SH$ whereas the ionic complexes were synthesised using the smaller thiols, $PhCH_2SH$ and C_6F_5SH.

The compound $[Ti(S\text{-}2,6\text{-}Me_2C_6H_3)_4]$ (**6**) was prepared from the reaction between the mixed thiolate, $[Ti(S^tBu)_4]/[Ti(S^tBu)_3(NEt_2)]$ (**4/5**) and an excess of ^tBuSH, although this compound was not crystallographically characterised.

Synthesis of thiolate compounds using transition metal alkyl starting materials did not yield significant products and synthetic studies of thiolates using the salt elimination route and NEt_3 produced partially substituted thiols.

The synthetic route using Grignard reagents produced compounds of general formula $[M(SMes)_5]$ (where M = Nb or Ta), although some contamination from $(SMes)_2$ is likely to have occurred and the yields for the reactions were less than 10%. Nonetheless, given more time this is a synthetic route that would be worth exploring further.

2.33 Experimental

General Procedures. All manipulations were performed under a dry, oxygen-free dinitrogen atmosphere using standard Schlenk techniques or in a MBraun Unilab glove box. All solvents were distilled from appropriate drying agents prior to use (sodium / benzophenone for toluene, hexanes and THF; CaH_2 for CH_2Cl_2). $[Ti(NEt_2)_4]$,[66] $[Zr(NEt_2)_4]$,[66] $[Ta(NMe_2)_5]$,[78] $[Nb(NMe_2)_5]$,[79] $[Ti(CH_2Ph)_4]$[83] and $[Zr(CH_2Ph)_4]$[83] were prepared according to literature procedures. All other reagents were procured commercially from Aldrich and used without further purification. Microanalytical data were obtained at University College London.

Physical Measurements. NMR spectra were recorded on Brüker AMX300 or DRX400 spectrometers at UCL. The NMR spectra are referenced to CD_2Cl_2 or $CDCl_3$ which were degassed and dried over molecular sieves prior to use; ^1H and ^{13}C chemical shifts are reported relative to $SiMe_4$ (0.00 ppm). ^{19}F chemical shifts are relative to $CFCl_3$. Mass spectra (CI) were run on a micromass ZABSE

instrument, and IR spectra on a Nicolet 205 instrument. Melting points were obtained in sealed glass capillaries under nitrogen and are uncorrected.

2.34 Preparation of $[Ti(NEt_2)_4]$

This reaction was carried out using a similar procedure to the literature,[66] although the quantities of reagents used differ slightly. Butyllithium (70 cm^3, 1.6 M solution in hexanes) and diethylamine (11.5 cm^3, 21 mmol) were added to ether (30 cm^3) at -20 °C and stirred for 30 minutes resulting in a viscous creamy solution. $TiCl_4$ (27.7 cm^3, 1M solution in toluene) was then added dropwise to this solution and an exothermic reaction resulted producing a dark brown solution with some brown precipitate forming after 10 minutes. The mixture was slowly warmed to room temperature and refluxed for 2 hours. After cooling to room temperature the solvent was removed *in vacuo* and replaced with an equal volume of toluene, in which the product was soluble. After filtering through Celite the mixture was pumped down to dryness under vacuum resulting in a dark brown oil. This oil was distilled under vacuum resulting in a red/orange viscous liquid (bp 108 °C, yield 52 %). ^1H NMR ($CDCl_3$): δ 1.06 (t, 24H, CH_2CH_3), 3.48 (q, 16H, CH_2CH_3).

2.35 Preparation of compound 1

Benzyl mercaptan (2.1 cm^3, 17.8 mmol) was added dropwise to an orange solution of $[Ti(NEt_2)_4]$ (0.6 cm^3, 1.66 mmol) in toluene (20 cm^3) at room temperature with stirring. The solution turned dark red immediately on addition of the thiol. The mixture was stirred for 2 hours at room temperature and then the solvent was removed *in vacuo*. The resulting dark red oil was dissolved in toluene

(20 cm^3) and filtered through Celite. The solution was reduced in volume to approximately 10 cm^3 under vacuum and cooled to -20 °C which over a period of days resulted in the formation of a dark red solid. This solid was redissolved in CH_2Cl_2 (4 cm^3) and an overlayer of hexanes (20 cm^3) was added carefully. Solvent diffusion over a period of days at -20 °C afforded X-ray quality dark red crystals of **1** (0.518 g, 60% yield), mp 103-105 °C. Anal. Calc. for $C_{68}H_{75}N_1S_9Ti_2$: C, 59.57; H, 5.60; N, 1.04. Found C, 60.07; H, 5.63; N, 1.59. Mass Spec. *m/z* 74 (diethylamine), 91 ($PhCH_2$). ^{1}H NMR δ/ppm (CD_2Cl_2): δ 0.85 (t, 6H, NCH_2CH_3), 2.40 (q, 4H, NCH_2CH_3), 4.90 (s, 6H, μ-$SCH_2C_6H_5$), 5.32 (s, 12H, t-$SCH_2C_6H_5$), 7.26 - 7.65 (m, 45H, $SCH_2C_6H_5$). $^{13}C\{^1H\}$NMR (CD_2Cl_2) δ 13.1 (NCH_2CH_3), 43.7 (NCH_2CH_3), 51.6 ($SCH_2C_6H_5$), 128.8 (*o*-$SCH_2C_6H_5$), 130.7 (*m*-$SCH_2C_6H_5$), 131.0 (*m*-$SCH_2C_6H_5$), 145.8 (*i*-$SCH_2C_6H_5$). IR (KBr, cm^{-1}): 698 s, 758 s, 1073 s, 1453 s, 1495 s, 2920 s, 3029 s, 3062 s, 3085 s.

2.36 Attempted preparation of [$Ti(SCH_2Ph)_4$]

The same procedure described above (section 2.35) was used but with 0.78 cm^3 (6.6 mmol) of benzyl mercaptan. A red/brown solid was formed (0.154 g). Elemental Analysis Found: C, 56.26; H, 6.05; N, 2.29. ^{1}H NMR δ/ppm (CD_2Cl_2): δ 1.17 (t, NCH_2CH_3), 1.82 (t, $PhCH_2SH$), 3.43 (q, NCH_2CH_3), 3.62 (s, SCH_2Ph), 3.74 $PhCH_2SH$), 7.15-7.32 (m, $SCH_2C_6H_5$ and $C_6H_5CH_2SH$). Repeated ^{1}H NMR (CD_2Cl_2): δ 3.62 (s, SCH_2Ph) and 7.25-7.38 (m, $SCH_2C_6H_5$).

2.37 Attempted preparation of $[Ti(SCH_2Ph)_4(L)_2]$

The same procedure as above (section 2.35) was adopted using 0.78 cm^3 (6.6 mmol) of benzyl mercaptan to yield a red solution. 0.29 cm^3 of tetrahydrothiophene (3.32 mmol) was then added to this red solution. A red/brown insoluble solid was formed (0.502 g). Anal. Calc. Found C, 58.21; H, 5.82; N, 1.46. ^1H NMR δ/ppm ($CDCl_3$): δ 1.10 (NCH_3CH_2), 2.66 (NCH_3CH_2), 3.58 (SCH_2Ph), 7.15-7.28 (m, $SCH_2C_6H_5$). Mass Spec. *m/z*: 74 (diethylamine), 91 ($PhCH_2$), 215 ($(PhCH_2)_2SH$). ^1H NMR (CD_2Cl_2): δ 3.61 (s, SCH_2Ph), 7.14-7.34 (m, $SCH_2C_6H_5$).

2.38 Preparation of compound 2

Pentafluorothiophenol (2.25 cm^3, 16.90 mmol) was added dropwise to an orange solution of $[Ti(NEt_2)_4]$ (0.6 cm^3, 1.66 mmol) in toluene (20 cm^3) at room temperature with stirring. The solution turned dark red immediately on addition of the thiol. The mixture was stirred for 2 hours at room temperature and then the solvent was removed *in vacuo*. The resulting dark red oil was dissolved in toluene (20 cm^3) and filtered through Celite to give a dark red solution. Cooling of this solution to -20 °C overnight afforded a 75% yield of red crystalline solid (1.240 g). Single crystals suitable for crystallography were obtained by dissolving the red solid in CH_2Cl_2 (4 cm^3) and overlaying this solution with hexanes (20 cm^3). Solvent diffusion at room temperature over a period of days afforded dark red needles of compound **2** (m.p. 108-112 °C). Anal. Calc. for $C_{54}H_{36}N_3F_{35}S_7Ti$: C, 38.9; H, 2.16; N, 2.52. Found C, 40.06; H, 2.28; N, 2.84. Mass Spec. *m/z*: 200 (pentafluorothiophenol). ^1H NMR δ/ppm (CD_2Cl_2): δ 1.49 (t, 6H, NCH_2CH_3), 3.29 (q, 4H, NCH_2CH_3), 8.33 (s, 2H, $H_2NCH_2CH_3$). $^{13}C\{^1H\}$

NMR (CD_2Cl_2): δ 11.2 (NCH_2CH_3), 42.0 (NCH_2CH_3), 125.3 (*p*-SC_6F_5), 128.2 (*o*-SC_6F_5), 129.0 (*m*-SC_6F_5). $^{19}F\{^1H\}$ NMR (CD_2Cl_2, reference $CFCl_3$): δ -132.9 (m, 10F, $F^{2,6}$ of C_6F_5), -160.9 (m, 5F, F^4 of C_6F_5), -165.3 (m, 10F, $F^{3,5}$ of C_6F_5). IR (KBr, cm^{-1}): 668 s, 861 s, 974 s, 1081 s, 1480 s, 1512 s, 2342 s, 2357 s, 2927 s, 2956 s.

2.39 Preparation of compound 3

2,6-dimethylpyridine (0.39 cm^3, 3.34 mmol) was added to an orange solution of [$Ti(NEt_2)_4$] (0.6 cm^3, 1.66 mmol) in toluene (20 cm^3) at room temperature. Pentafluorothiophenol (0.88 cm^3, 6.60 mmol) was added dropwise and the solution turned dark red immediately. After stirring for 2 hours at room temperature, the solvent was removed *in vacuo*. The resulting dark red oil was dissolved in toluene (20 cm^3) and filtered through Celite to give a dark red solution. Cooling of this solution to -20 °C overnight resulted in the formation of a crystalline red solid. Single crystals suitable for crystallography were obtained by dissolving the solid in CH_2Cl_2 (4 cm^3) and overlaying this solution with hexanes (20 cm^3). Solvent diffusion over a period of days at room temperature afforded dark red crystals of compound **3** (1.068 g, yield = 65%; m.p. 148 - 150 °C). Anal. Calc. for $C_{32}H_{22}N_2F_{20}S_4Ti$: C, 38.79; H, 2.22; N, 2.83. Found C, 38.83; H, 2.10; N, 3.17. ^1H NMR (CD_2Cl_2): δ 1.05 (t, 6H, NCH_2CH_3), 1.50 (t, 6H, $H_2NCH_2CH_3$), 3.45 (q, 4H, $H_2NCH_2CH_3$), 4.34 (q, 4H, NCH_2CH_3), 7.30 (s, 2H, $H_2NCH_2CH_3$). $^{13}C\{^1H\}$ NMR (CD_2Cl_2): δ 11.6 (NCH_2CH_3), 12.7 ($H_2NCH_2CH_3$), 43.4 ($H_2NCH_2CH_3$), 49.7 (NCH_2CH_3), 120.6 (*p*-C of SC_6F_5), 137.7 (*o*-SC_6F_5) 146.5 (*m*-SC_6F_5). $^{19}F\{^1H\}$ NMR (CD_2Cl_2, reference $CFCl_3$): δ -

132.5 (m, 8F, $F^{2,6}$ of C_6F_5), -160.5 (m, 4F, F^4 of C_6F_5) and -164.9 (m, 8F, $F^{3,5}$ of C_6F_5).

2.40 Attempted preparation of $[Ti(SC_6F_5)_4.bipy]$

Bipyridine (0.26 g, 1.66 mmol) was added to an orange solution of $[Ti(NEt_2)_4]$ (0.6 cm^3, 1.66 mmol) in toluene (20 cm^3) at room temperature. Pentafluorothiophenol (0.88 cm^3, 6.60 mmol) was added dropwise and the solution turned dark red immediately. After stirring for 2 hours at room temperature, the solvent was removed *in vacuo*. Dissolving the resulting red oil in 5 cm^3 of CH_2Cl_2 and cooling overnight at -20 °C gave a red solid. Elemental Analysis Found C, 43.48; H, 2.68; N, 4.74. ^1H NMR (CD_2Cl_2): δ 1.32 (t, 6H, NCH_2CH_3), 1.48 (t, 6H, $H_2NCH_2CH_3$), 3.07 (q, 4H, $H_2NCH_2CH_3$), 4.96 (q, 4H, $H_2NCH_2CH_3$), 7.11–8.42 ppm (m, 14H, $N_2C_{10}H_8$).

2.41 Preparation of compound 4/5

^{t}BuSH (1.9 cm^3, 16.9 mmol) was added dropwise to an orange solution of $[Ti(NEt_2)_4]$ (0.6 cm^3, 1.66 mmol) in toluene (20 cm^3) at room temperature with stirring. The solution turned to a dark red colour during a period of 30 minutes and the solution was allowed to stir for a further two hours. The solvent was then removed *in vacuo* resulting in a dark red oil. This oil was dissolved in hexane (15 cm^3) and filtered through Celite to give a dark red solution. The solution was finally concentrated to 2 cm^3 and cooled overnight at -20 °C to give a 65% yield of the mixture of compounds **4** and **5** (m.p. 51-53 °C). Single crystals of **4**, suitable for crystallography, were produced from this method. Anal. Calc. for $C_{16}H_{36}S_4Ti$: C, 46.70; H, 8.82; N, 0. Anal. Calc. for $C_{16}H_{37}NS_3Ti$: C, 49.6; H,

9.56; N, 3.62. Found C, 47.7; H, 9.73; N, 2.78 and C, 47.3; H, 9.01; N, 0.71. ^{1}H NMR (CD_2Cl_2): δ 1.21 (t, H, NCH_2CH_3), 1.53 (s, H $SC(CH_3)_3$) 4.12 (q, H, NCH_2CH_3). $^{13}C\{^{1}H\}$ NMR (CD_2Cl_2): δ 13.9 (NCH_2CH_3), 30.7 (NCH_2CH_3), 36.4 ($SC(CH_3)_3$), 59.2 ($SC(CH_3)_3$).

2.42 Attempted preparation of [Ti(S-2,6-$Me_2C_6H_3)_4$]

2,6-$Me_2C_6H_3SH$ (2.1 cm^3, 16.9 mmol) was added dropwise to an orange solution solution of [$Ti(NEt_2)_4$] (0.6 cm^3, 1.66 mmol) in toluene (20 cm^3) at room temperature with stirring. The solution turned to a dark red colour during a period of 30 minutes and was allowed to stir for a further two hours. The solvent was then removed *in vacuo* resulting in a dark red oil. This oil was dissolved in 20 cm^3 of toluene. Reducing the volume to 5 cm^3 and leaving for 2-3 days at room temperature resulted in the formation of a dark red microcrystalline solid. Anal. Calc. for $C_{32}H_{36}S_4Ti$: C, 64.0; H, 6.00; N, 0.00. Found C, 59.43; H, 6.58; N, 2.03. ^{1}H NMR ($CDCl_3$): δ 0.80 (q, NCH_2CH_3), 1.25 (s), 2.15 (s, 2,6-$(CH_3)_2SC_6H_3$), 2.30 (t, NCH_2CH_3), 6.83-7.10 (m, 3H, 2,6-$(CH_3)_2SC_6H_3$).

2.43 Preparation of compound 6

The mixture of compunds **4/5** (0.17 g) was prepared as described previously (section 2.41) and dissolved in toluene giving a dark red solution. 2,6-$Me_2C_6H_3SH$ (0.17 cm^3, 1.32 mmol) was added to this solution producing an insoluble dark red solid in a dark red solution. The reaction mixture was filtered and the solvent was removed *in vacuo*. Dissolving the resulting red solid in hexane (5 cm^3) and cooling overnight at -20 °C gave dark red crystals. Anal. Calc. for $C_{32}H_{36}S_4Ti$: C, 64.0; H, 6.00; N, 0.00. Found C, 64.69; H, 6.58; N, 0.63.

^{1}H NMR (CD_2Cl_2): δ 2.16 (s, 24H, S 2,6-(CH_3)$_2$C$_6$H$_3$), 2.26 (s, HS-2,6-(CH_3)$_2$C$_6$H$_3$), 3.23 (s, *H*S-2,6-(CH_3)$_2$C$_6$H$_3$), 6.78-7.18 (m, 12H, 2,6-(CH_3)$_2$SC$_6$*H*$_3$).

2.44 Preparation of [Ta(NMe$_2$)$_5$]

This reaction was carried out using a similar procedure to the literature,[78] although the quantities of reagents used differ slightly. $TaCl_5$ (2 g, 5.58 mmol) and $LiNMe_2$ (1.42 g, 27.89 mmol) were added to hexane (70 cm^3) and stirred at room temperature for 24 hrs. A yellow solution and a brown precipitate were produced. The mixture was filtered and the solvent removed *in vacuo* giving a dark yellow oil. Sublimation at 100 °C for 4 hours at reduced pressure (10^{-1} mmHg) produced 1 g of [Ta(NMe$_2$)$_5$], a light yellow solid. Anal. Calc. for $C_{10}H_{30}N_5Ta$: C, 29.9; H, 7.48; N, 17.46. Found C, 31.65; H, 7.86; N, 17.22. ^{1}H NMR ($CDCl_3$): δ 3.06 (s, N(CH_3)$_2$), 3.23 (s, N(CH_3)$_2$).

2.45 Preparation of [Nb(NMe$_2$)$_5$]

This reaction was carried out using a similar procedure to the literature,[79] although the quantities of reagents used differ slightly. $NbCl_5$ (3.17 g, 11.7 mmol) and $LiNMe_2$ (3 g, 58.8 mmol) were added to hexane (70 cm^3) and stirred at room temperature for 24 hrs. A yellow solution and a brown precipitate were produced. The mixture was filtered and the solvent removed *in vacuo* giving a dark yellow oil. Sublimation of the oil at 100 °C for 4 hours at reduced pressure produced 1 g of [Nb(NMe$_2$)$_5$], a light yellow solid. Anal. Calc. for $C_{10}H_{30}N_5Nb$: C, 38.4; H, 9.59; N, 22.4. Found C, 38.6; H, 10.4; N, 23.0. ^{1}H NMR ($CDCl_3$): δ 3.08 (s, N(CH_3)$_2$).

2.46 Preparation of $Zr[(NEt_2)_4]$

This reaction was carried out using a similar procedure to the literature,[66] although the quantities of reagents used differ slightly. Butyllithium (33 cm^3, 1.6 M solution in hexanes) and diethylamine (5.46 cm^3, 52.8 mmol) were added to ether (30 cm^3) at -20 °C and stirred for 30 minutes resulting in a viscous creamy solution. $ZrCl_4$ (3.076 g, 13.2 mmol) was then added to this solution and an exothermic reaction resulted producing a dark yellow solution and a white precipitate. The mixture was slowly warmed to room temperature and refluxed for 2 hours. After cooling to room temperature the solvent was removed *in vacuo* and replaced with an equal volume of toluene, in which the product was soluble. After filtering through Celite the mixture was pumped down to dryness under vacuum resulting in a dark green/yellow oil. The oil was distilled under vacuum resulting in 3 cm^3 of a light green/yellow liquid.

2.47 Preparation of compound 7

The dropwise addition of 2,6-$Me_2C_6H_3SH$ (0.66 cm^3, 4.98 mmol) to a pale yellow solution of $[Ta(NMe_2)_5]$ (0.20 g, 0.499 mmol) in toluene (20 cm^3) at room temperature resulted in a colour change to dark orange-red. The reaction mixture was allowed to stir for 2 hours, after which the solvent was removed *in vacuo*. The resulting dark red-orange oil was redissolved in CH_2Cl_2 (1.5 cm^3) and filtered. A dark orange-red solution resulted and an hexanes overlayer (7 cm^3). was added carefully. Solvent diffusion at room temperature over a period of days produced bright red crystals of **7** in a 50% yield. Anal. Calc. for $C_{34}H_{42}NS_4Ta$: C, 52.8; H, 5.47; N, 1.81. Found C, 52.0; H, 5.82; N, 2.15. ^1H NMR (CD_2Cl_2): δ 2.45 (s, 24H, S 2,6-(CH_3)$_2C_6H_3$), 2.76 (s, 6H, NCH_3), 6.78 - 7.18 (m, 12H, 2,6-

$(CH_3)_2SC_6H_3$). $^{13}C\{^1H\}$ NMR (CD_2Cl_2): δ 22.4 (S 2,6-$(CH_3)_2C_6H_3$), 39.7 (NCH_3), 125.9 (*p*-C of (S 2,6-$(CH_3)_2C_6H_3$)), 137.9 (*o*-(S 2,6-$(CH_3)_2C_6H_3$) 143.8 (*m*-(S 2,6-$(CH_3)_2C_6H_3$)).

2.48 Preparation of compound 8

The dropwise addition of 2,6-$Me_2C_6H_3SH$ (0.66 cm^3, 4.98 mmol) to a yellow solution of [$Nb(NMe_2)_5$] (0.16 g, 0.511 mmol) in toluene (20 cm^3) at room temperature resulted in a colour change to dark red. The reaction mixture was allowed to stir for 2 hours, after which the solvent was removed *in vacuo*. The resulting dark red oil was redissolved in CH_2Cl_2 (15 cm^3) and filtered through Celite. Concentrating this solution to 2 cm^3 and cooling to -20 °C for 24 hours resulted in the formation of **8** in a 50% yield. Anal. Calc. for $C_{34}H_{42}NS_4Nb$: C, 61.6; H, 5.77; N, 0.00. Found C, 63.8; H, 6.84; N, 0.47. ^1H NMR (CD_2Cl_2): δ 2.37 (s, 24H, S 2,6-$(CH_3)_2C_6H_3$), 2.69 (s, NCH_3), 6.80 - 7.01 (m, 12H, 2,6-$(CH_3)_2SC_6H_3$).

2.49 Attempted preparation of [Zr(S-2,6-$Me_2C_6H_3)_4$]

On addition of 2,6-$Me_2C_6H_3SH$ (1.80 cm^3, 13.5 mmol) to a yellow/green solution of [$Zr(NEt_2)_4$] (0.5 cm^3, 1.35 mmol) in toluene (20 cm^3) 1.2 g of an insoluble bright yellow solid was immediately produced. The light yellow/green solution was filtered off and the solid bright yellow solid was dried *in vacuo*. Anal. Calc. for $C_{44}H_{57}NS_5Zr$: C, 61.7; H, 6.43; N, 1.64. Found C, 62.0; H, 6.82; N, 1.55.

2.50 Attempted preparation of $[Zr(S^tBu)_4]$

The same procedure was adopted as above (section 2.49), except that ^tBuSH (1.52 cm^3, 13.5 mmol) was added to the amide, $[Zr(NEt_2)_4]$. A colour change from yellow/green to orange was observed after stirring at room temperature for 24 hours. Removal of the solvent and cooling to -20 °C resulted in orange needles. Elemental Analysis Found C, 35.6; H, 6.85; N, 1.52. ^1H NMR (CD_2Cl_2): δ 0.96 (t, NCH_2CH_3), 1.58, 1.59, 1.73, 1.75, 1.87 (five singlets due to $SC(CH_3)_3$ in a 2:2:2:1:1 ratio), 2.47 (q, NCH_2CH_3), 7.67 (s, $H_2NCH_2CH_3$).

2.51 Preparation of $[Zr(CH_2Ph)_4]$

This reaction was carried out using a similar procedure to the literature,[83] although the quantities of reagents used differ slightly. $ZrCl_4$ (1.17 g, 5 mmol) was added to a solution of $PhCH_2MgCl$ (20 cm^3, 1M solution in diethyl ether) in diethyl ether (20 cm^3) at -15 °C. The mixture was stirred for 8 hours resulting in a yellow solution that was filtered at 0 °C. Removal of the solvent *in vacuo* gave a yellow oil. Recrystallising the yellow oil twice from toluene (40 cm^3) afforded bright yellow crystals of $[Zr(CH_2Ph)_4]$ (0.330 g). Anal. Calc. for $C_{28}H_{28}Zr$: C, 73.9; H, 6.15; N, 0. Found C, 72.0; H, 6.27; N, 0. ^1H NMR (CD_2Cl_2): δ 1.35 (s, 8H, $CH_2C_6H_5$), 6.35 - 7.26 (m, 20H, $CH_2C_6H_5$).

2.52 Preparation of $[Ti(CH_2Ph)_4]$

This reaction was carried out using a similar procedure to the literature,[83] although the quantities of reagents used differ slightly. $TiCl_4$ (12.5 cm^3, 1M solution in toluene) was added slowly to a solution of $PhCH_2MgCl$ (50 cm^3, 1M solution in diethyl ether) in diethyl ether (20 cm^3) at -15 °C. The mixture was

stirred for 8 hours resulting in a red solution that was filtered at 0 °C. Removal of the solvent *in vacuo* gave a dark red oil. Addition of 30 cm^3 of hexane to the red oil, followed by cooling to -20 °C gave a dark red solid (0.403 g). The solid was isolated by filtering the red solution and dried *in vacuo*. ^1H NMR (CD_2Cl_2): δ 1.26 (s, 8H, $CH_2C_6H_5$), 6.55 - 7.49 (m, 20H, $CH_2C_6H_5$).

2.53 Attempted preparation of [$Zr(SCPh_3)_4$]

Ph_3CSH (0.97 g, 3.50 mmol) was added to a yellow solution of [$Zr(CH_2Ph)_4$] (0.4 g, 0.88 mmol) in toluene (20 cm^3). The reaction mixture was stirred at room temperature for 2 hours giving a gelatinous orange solution. Removal of the solvent *in vacuo*, followed by addition of hexane (10 cm^3) resulted in an orange solid and a light orange solution. The orange solid was isolated by removing the light orange solution and dried *in vacuo*. Elemental Analysis Found C, 62.7; H, 5.24.

2.54 Attempted preparation of [$Ti(S\text{-}2,6\text{-}Me_2C_6H_3)_4$] using [$Ti(CH_2Ph)_4$]

2,6-$Me_2C_6H_3SH$ (0.6 cm^3, 4.90 mmol) was added dropwise to a red solution solution of [$Ti(CH_2Ph)_4$] (0.2 g, 0.49 mmol) in toluene (15 cm^3) at room temperature with stirring. Removal of the solvent *in vacuo*, followed by addition of hexane (20 cm^3) resulted in a red solution with a pale yellow precipitate. The red solution was filtered through Celite. Removal of this solvent yielded a dark red liquid. ^1H NMR (CD_2Cl_2): δ 2.22 (s, HS-2,6-$(CH_3)_2C_6H_3$), 3.17 (s, *H*S-2,6-$(CH_3)_2C_6H_3$), 6.90 (m, HS-2,6-$(CH_3)_2C_6H_3$).

2.55 Attempted preparation of [Ti(S-2,6-$Me_2C_6H_3$)$_4$] using salt elimination

$TiCl_4$ (2.5 cm^3, 1M solution in toluene) was added directly to KS-2,6-$Me_2C_6H_3$ (10 mmol) giving a dark red solid. Addition of hexane (70 cm^3) resulted in a dark red solution. After stirring for 3 hours at room temperature, the solution was filtered and the solvent concentrated to 10 cm^3. Cooling of this solution overnight at -20 °C gave a dark red solid (0.342 g). Anal. Calc. for $C_{24}H_{27}S_3ClTi$.THF: C, 59.3; H, 6.17; N, 0.00. Found C, 58.9; H, 6.35; N, 0.00. ^{1}H NMR (CD_2Cl_2): δ 2.37 (s, 6H, S-2,6-(CH_3)$_2C_6H_3$), 6.83 - 7.24 (m, 3H, 2,6-(CH_3)$_2SC_6H_3$). Peaks for THF observed at 1.99 and 4.33 ppm in a 1:1 ratio and for free thiol (2,6-$Me_2C_6H_3SH$) at 3.32 ppm and 6.83 - 7.24 ppm.

2.56 Attempted preparation of [Ta(S-2,6-$Me_2C_6H_3$)$_5$] using salt elimination

$TaCl_5$ (0.354 g, 30 mmol) was added directly to LiS-2,6-$Me_2C_6H_3$ (6 mmol) giving a dark red/orange solid. Addition of hexane (70 cm^3) resulted in a dark red/orange solution after stirring for 1 hour at room temperature. The solution was then refluxed for a further 5 hours producing a darker red/orange solution. The solvent was then removed *in vacuo* and the resulting oil dissolved in 50 cm^3 of hot hexanes. The solution was then filtered and the solvent concentrated to 10 cm^3. Cooling of this solution overnight at -20 °C gave a dark red/orange solid (0.030 g). Anal. Calc. for $C_{24}H_{27}S_3Cl_2Ta$: C, 43.4; H, 5.01; N, 0.00. Found C, 42.5; H, 5.01; N, 0.00. ^{1}H NMR (CD_2Cl_2): δ 2.35 (s, S-2,6-(CH_3)$_2C_6H_3$), 6.83 - 7.07 (m, 2,6-(CH_3)$_2SC_6H_3$).

2.57 Attempted preparation of [Nb(S-2,6-$Me_2C_6H_3$)$_5$] using salt elimination

A similar procedure was adopted as above (section 2.56) except using $NbCl_5$ (0.167 g, 6mmol) in place of $TaCl_5$. The solution initially turned dark red but, after work-up, caramel crystals of the disulfide, $(Me_2C_6H_3S)_2$ were obtained. ^1H NMR ($CDCl_3$): δ 2.27 (s, 6H, HS-2,6-(CH_3)$_2C_6H_3$), 2.40 (s, 6H, S-2,6-(CH_3)$_2C_6H_3$), 3.26 (s, 1H, *H*S-2,6-$(CH_3)_2C_6H_3$), 6.83 - 7.07 (m, 12H, 2,6-$(CH_3)_2SC_6H_3$).

2.58 Attempted preparation of [Ti(SC_6F_5)$_4$(L)$_2$]

$TiCl_4$ (2.5 cm^3, 1M solution in toluene) and 2,6-lutidine (0.58 cm^3, 5 mmol) were added directly to NaS-2,6-$Me_2C_6H_3$ (10 mmol) giving a dark red solution. Addition of toluene (20 cm^3) resulted in a dark red solution. Work-up from CH_2Cl_2 resulted in a yellow solid (0.221 g). Anal. Calc. for $C_{18}S_3ClF_{15}Ti$.2,6-lutidine: C, 37.9; H, 1.13; N, 1.77; Cl, 4.48. Found C, 39.5; H, 1.41; N, 0.94; Cl, 3.67. ^1H NMR (CD_2Cl_2): δ 2.83 (s, 6H, 2,6-(CH_3)$_2C_5H_3N$), 7.31 and 7.96 (s, 3H, 2,6-$(CH_3)_2C_5H_3N$).

2.59 Reaction of $TiCl_4$, NEt_3 and $Me_2NCH_2CH_2SH$

NEt_3 (2.79 cm^3, 10 mmol) and $Me_2NCH_2CH_2SH$.HCl (1.417 g, 10 mmol) were added in CH_2Cl_2 (70 cm^3) giving a clear solution. $TiCl_4$ (2.5 cm^3, 1M solution in toluene) was than added to give a dark red solution. Work-up of the solution and layering a saturated CH_2Cl_2 solution with hexanes afforded dark red crystals (0.124 g). Anal. Calc. for $C_8H_{20}N_2S_2Cl_2Ti$: C, 29.4; H, 6.12; N, 8.56; Cl, 21.7. Found C, 30.0; H, 6.49; N, 7.47; Cl, 24.4. ^1H NMR (CD_2Cl_2): δ 2.20 - 4.06

ppm gave a number of broad peaks that are difficult to assign, 10.2 ppm (broad singlet).

2.60 Reaction of $TaCl_5$, NEt_3 and $Me_2NCH_2CH_2SH$

The same procedure as described above (section 2.59) except using $TaCl_5$ (0.716 g, 2 mmol) to give an orange solid. ^1H NMR (CD_2Cl_2): δ 1.24 (t, ($CH_3CH_2)_3N$)), 2.95 (q, ($CH_3CH_2)_3N$)).

2.61 Reaction of MesSMgBr and $NbCl_5$

$NbCl_5$ (0.675 g, 2.5 mmol) was added to a solution of MesSMgCl (12.5 cm^3) in toluene (20 cm^3). The solution immediately changed colour from yellow to a dark red colour. Filtering through Celite and concentrating the solution to 5 cm^3 resulted in a dark red solid. Anal. Calc.for $C_{45}H_{55}S_5Nb$: C, 63.7; H, 6.49; N, 0.00. Found C, 66.4; H, 7.32; N, 0.00. ^1H NMR (CD_2Cl_2): δ 2.22 (s, 6H, S-2,4,6-*ortho*-($CH_3)_3C_6H_2$), 2.26 (s, 3H S-2,4,6-*para*-($CH_3)_3C_6H_2$), 6.90 (s, 2H, S-2,4,6-$(CH_3)_3C_6H_2$).

2.62 Reaction of MesSMgBr and $TaCl_5$

$TaCl_5$ (0.895 g, 2.5 mmol) was added to a solution of MesSMgCl (12.5 cm^3) in toluene (20 cm^3). The solution immediately changed colour from yellow to a dark red colour. Filtering through Celite and concentrating the solution to 5 cm^3 resulted in a dark red solid. Anal. Calc.for $C_{45}H_{55}S_5Ta$: C, 57.7; H, 5.88; N, 0.00. Found C, 59.3; H, 6.47; N, 0.38. ^1H NMR (CD_2Cl_2): δ 2.20 (s, 6H, S-2,4,6-*ortho*-($CH_3)_3C_6H_2$), 2.28 (s, 3H, S-2,4,6-*para*-($CH_3)_3C_6H_2$), 2.34 (s), 6.86 (s, 2H, S-2,4,6-$(CH_3)_3C_6H_2$).

Chapter 3 Preparation of bulk transition metal sulfides

In this chapter, attempts at preparing bulk early transition metal disulfides are described. This involved two methods, the thio "sol-gel" process and using hexamethyldisilathiane (HMDST) as a source of sulfur. The latter method was also employed in making bulk mixed-metal disulfides.

3.1 Thio "sol-gel" routes to early transition metal disulfides

The potential of transition metal thiolate compounds to act as precursors to metal disulfides using a novel thio "sol-gel" route was investigated. Crystalline metal disulfides (MS_2) have previously been prepared from metal alkoxides by bubbling H_2S gas through a solution of the metal alkoxide and then annealing the precipitates under a stream of H_2S gas at 800 °C for 6 hours (see chapter 1).[55] This method resulted in the formation of a mixture of TiS_2 and TiO_2 at temperatures below 800 °C. It was decided to adopt this method using some of the thiolates synthesised in chapter 2 as precursors. Initial investigations focussed on the formation of TiS_2 using the titanium precursors, $[Et_2NH_2][Ti_2(\mu\text{-}SCH_2Ph)_3(SCH_2Ph)_6]$, $[Et_2NH_2]_3[Ti(SC_6F_5)_5][SC_6F_5]_2$, $[Et_2NH_2][Ti(SC_6F_5)_4(NEt_2)]$ and $[Ti(S^tBu)_4]/[Ti(S^tBu)_3(NEt_2)]$ synthesised as described in chapter 2. The general preparation procedure is described at the end of this chapter.

3.2 Results and Discussion

3.2.1 Thio "sol-gel" reaction

Initial attempts to prepare TiS_2 involved the thio "sol-gel" reaction of the titanium thiolates with H_2S gas in toluene at room temperature (Scheme 3). In all cases, an insoluble black/brown precipitate formed immediately when H_2S was bubbled through the toluene solution of the titanium thiolate. A ^1H NMR spectrum of the toluene solution, that was filtered after the completion of the reaction, was taken in order to analyse the byproducts formed during the reaction. The spectrum showed the presence of R_2S_2 (where R = ^{t}Bu or CH_2Ph) and $[Et_2NH_2][SC_6F_5]$ (where R = C_6F_5) in the washings. This suggests that SH^- groups from the H_2S are replacing -SR and -NEt_2 ligands during the thio "sol-gel" reaction. The substitution of the thiolate and amide groups of the titanium thiolate precursor by H_2S forms the basis of the modified thio "sol-gel" reaction.[84] This is very similar to the hydrolysis/condensation reactions described previously in sol-gel processes.[55] An example of the overall reaction proposed for the thio "sol-gel" process between $[Ti(S^tBu)_4]$ and H_2S is shown in equations (3.1) and (3.2).

$$[Ti(S^tBu)_4] + n\ H_2S \longrightarrow [Ti(S^tBu)_{4-n}(SH)_n] + n\ ^tBuSH \qquad (3.1)$$

$$2p\ [Ti(S^tBu)_{4-n}(SH)_n] \longrightarrow [(^tBuS)_{4-n}(SH)_{n-1}Ti\text{-}S\text{-}Ti(SH)_{n-1}(S^tBu)_{4-n}]_p + p\ H_2S \qquad (3.2)$$

Further evidence for the replacement of -SR and -NEt_2 ligands by -SH groups in the thio "sol-gel" step was obtained from elemental analysis (C, H and N) taken for the precipitates. The analytical results can be seen in Table 3.1. The carbon content of the precipitates was lower than in the titanium thiolate precursors themselves. This is expected if -SR groups are replaced by -SH groups. The % carbon obtained from the precipitates is still high (17.53 - 32.24%), suggesting that complete substitution of the thiolate/amide ligands does not occur. Although the thio "sol-gel" step is analogous to that used previously with alkoxide precursors,[55] the final product in this instance does not contain any Ti-O bonds. It is anticipated that this will prevent the formation of TiO_2 at temperatures lower than 800 °C.

Table 3.1 Elemental analytical data for the thiolate precursors and the precipitates obtained after H_2S treatment

	Thiolate precursor			**Precipitate**		
Thiolate Precursor	%C	%H	%N	%C	%H	%N
$[Ti(S^tBu)_4]/[Ti(SBu^t)_3(NEt_2)]$	47.25	9.01	0.71	21.06	4.08	3.85
$[Et_2NH_2]_3[Ti(SC_6F_5)_5][(SC_6F_5)_2]$	40.06	2.28	2.84	32.24	4.06	4.05
$[Et_2NH_2][Ti(SC_6F_5)_4(NEt_2)]$	38.83	2.10	3.17	17.53	2.28	2.80
$[Et_2NH_2][Ti_2(\mu\text{-}SCH_2Ph)_3(SCH_2Ph)_6]$	60.07	5.60	1.04	24.01	4.97	2.68

Powder XRD of the precipitates obtained[85] showed that they were all X-ray amorphous. It was therefore decided to anneal these amorphous precipitates under a variety of conditions, in an attempt to convert the precipitates to

crystalline TiS_2. The procedures used and the results obtained are summarised in Scheme 3.

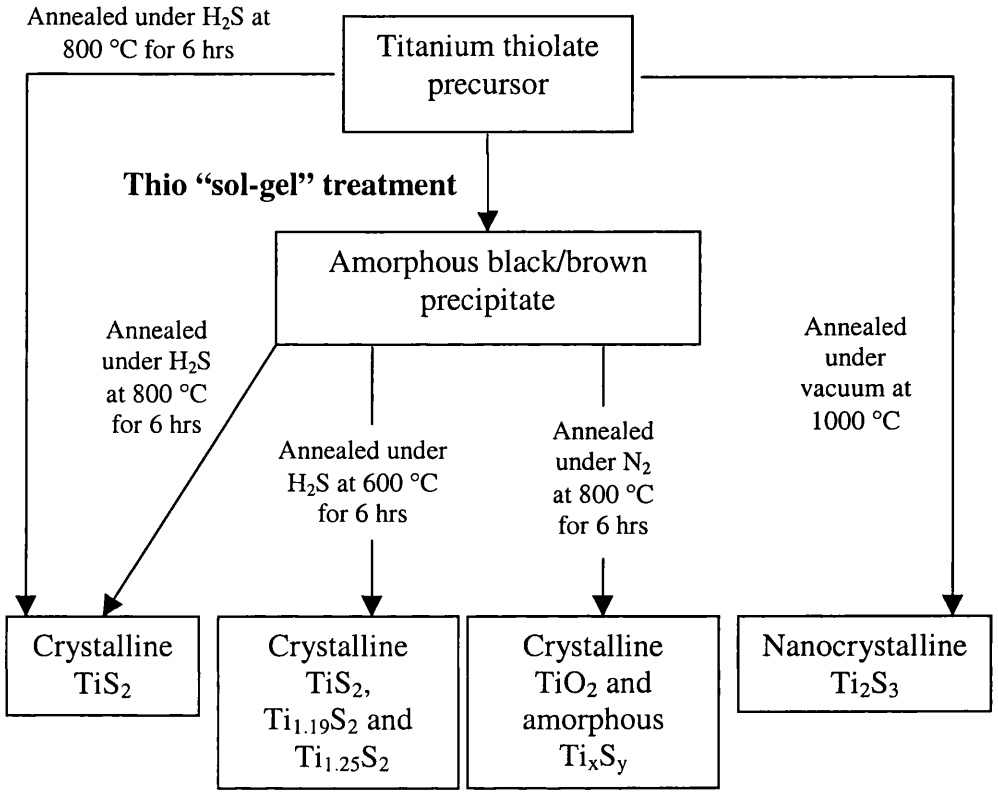

Scheme 3. Experimental procedure for the thio "sol-gel" method

3.2.2 Annealing precipitates under H_2S gas at 800 °C

Initial attempts to convert the amorphous precipitates to crystalline TiS_2 involved heating the precipitates under an atmosphere of H_2S gas at 800 °C for 6 hours. A temperature of 800 °C was initially chosen based on the previous conversions of the amorphous precipitates formed from the thio "sol-gel" reaction of $[Ti(O^iPr)_4]$ with H_2S to crystalline TiS_2.[55] In all cases a black precipitate formed after the annealing process, except when

$[Et_2NH_2][Ti_2(\mu\text{-}SCH_2Ph)_3(SCH_2Ph)_6]$ was used as the initial thiolate precursor. In this instance, a black precipitate with a gold surface resulted. Powder XRD of the materials[85] showed that a single phase of hexagonal TiS_2 had formed (Table 3.2) with a typical crystallite size from the X-ray broadening of 800 Å. Figure 3.1 shows the powder XRD pattern of TiS_2 prepared from this route using $[Et_2NH_2][Ti(SC_6F_5)_4(NEt_2)]$.

The X-ray powder pattern of the TiS_2 obtained was indexed and gave exact matches to literature measurements. Cell parameter values of a = 3.4049 Å and c = 5.6912 Å from the literature[86] compared well with a = 3.4174(3) Å and c = 5.724(2) Å for the sample shown above. The other TiS_2 samples obtained from the three other starting thiolates were also indexed and gave values for a and c ranging from 3.4094(2) - 3.415(1) Å and 5.699(3) - 5.710(1) Å respectively (Table 3.2). The EDXA data (Energy Dispersive Analysis by X-rays) also showed a 1:2 ratio of Ti:S over a number of spots for all of the samples analysed. This is in good agreement with TiS_2.

Figure 3.1 X-ray diffraction pattern for product of annealing precipitate from $[Et_2NH_2][Ti(SC_6F_5)_4(NEt_2)]$ under H_2S (top) and standard TiS_2 (bottom)

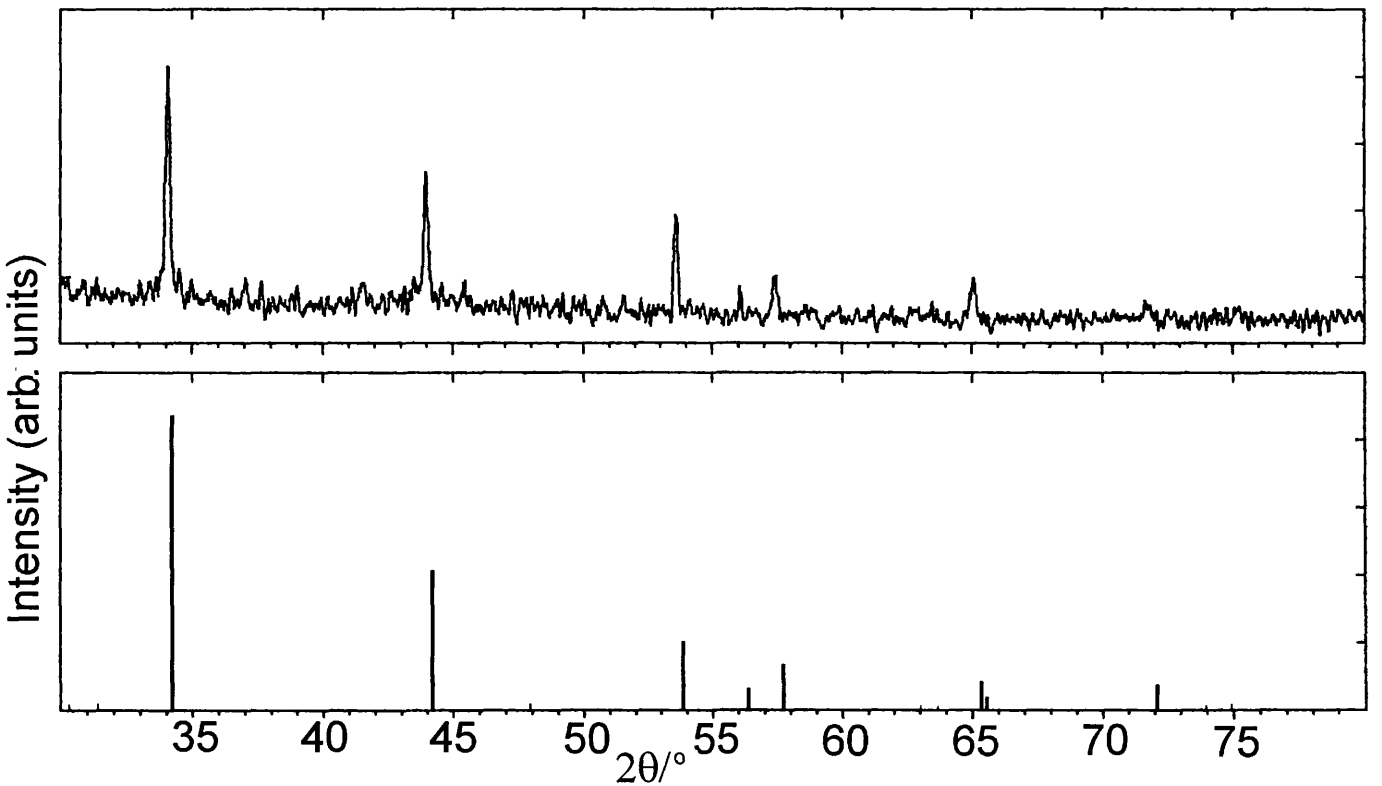

Table 3.2 X-ray powder diffraction data for TiS_2 obtained after annealing thio "sol-gel" precipitates and thiolates themselves to 800 °C under H_2S

	Lattice parametres of TiS_2[a,b] obtained			
	Thio "sol-gel" step		No thio "sol-gel" step	
Thiolate Precursor	*a*	*c*	*a*	*c*
$[Ti(S^tBu)_4]/[Ti(S^tBu)_3(NEt_2)]$	3.415	5.705		
$[Et_2NH_2]_3[Ti(SC_6F_5)_5][(SC_6F_5)_2]$	3.409	5.699		
$[Et_2NH_2][Ti(SC_6F_5)_4(NEt_2)]$	3.417	5.724	3.400	5.692
$[Et_2NH_2][Ti_2(\mu\text{-}SCH_2Ph)_3(SCH_2Ph)_6]$	3.409	5.710	3.405	5.706

[a]Unit cell dimensions *a*, *c* in Å (±0.005 Å)

[b]Literature values for TiS_2: $a = 3.4049$; $c = 5.6912$[86]

A Raman spectrum was also taken for all of the samples prepared. Figure 3.2(a) shows the Raman spectrum of the TiS_2 prepared after the annealing stage using the starting thiolate, $[Ti(S^tBu)_4]/[Ti(S^tBu)_3(NEt_2)]$. This shows a good agreement to the Raman spectrum of a sample of TiS_2 purchased from Aldrich (Figure 3.2(b)). The results obtained are similar to those reported from the heat treatment of the precipitates formed from the thio "sol-gel" reaction of $[Ti(O^iPr)_4]$ and H_2S at 800 °C.[55] In these reactions, the formation of single phase TiS_2 was also observed. At lower temperatures (600 °C), however, a mixture of TiS_2 and rutile and anatase phases of TiO_2 were formed.[55]

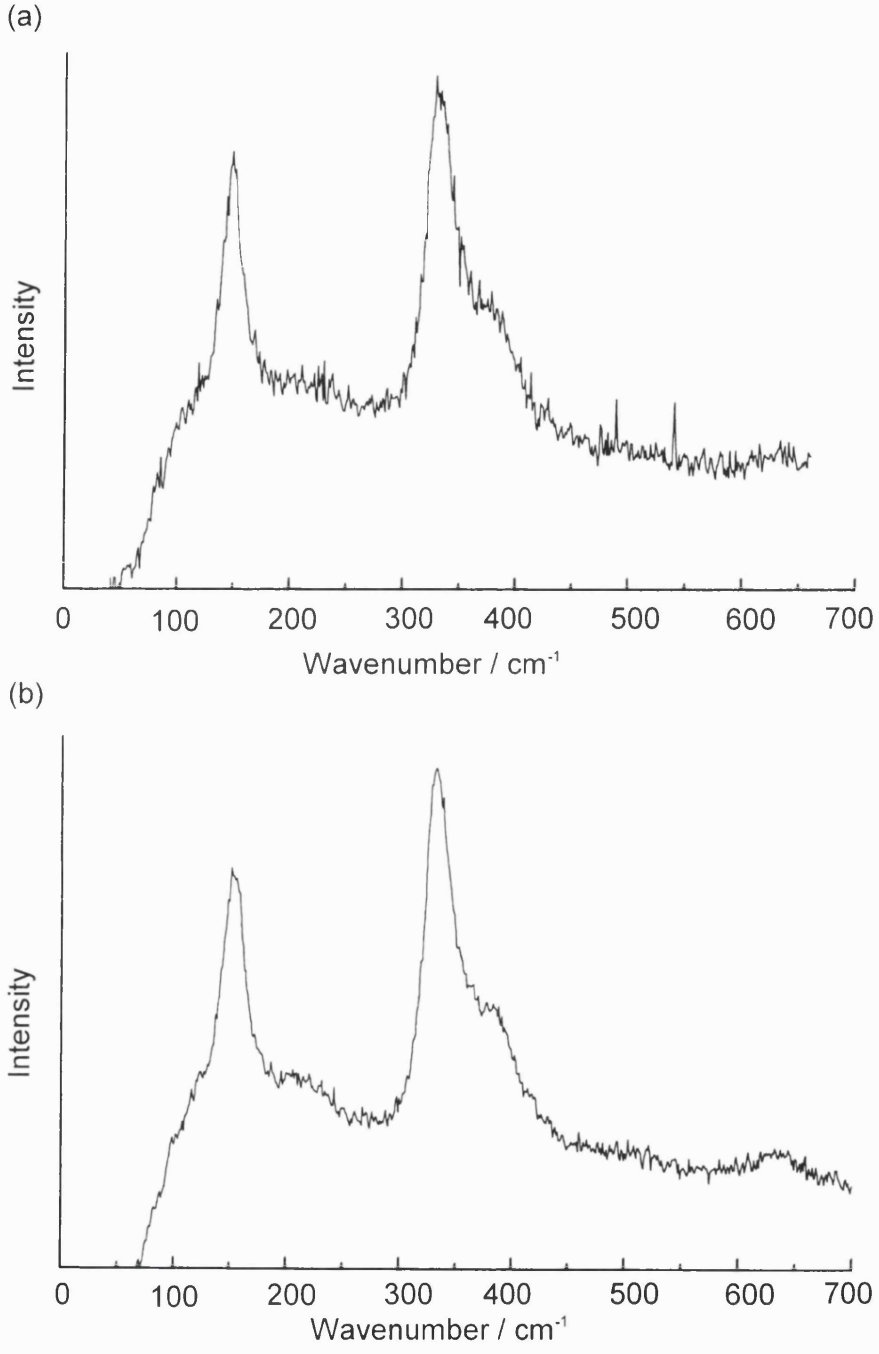

Figure 3.2(a) Raman spectrum of TiS_2 obtained from the thio "sol-gel" method using $[Ti(S^tBu)_4]/[Ti(S^tBu)_3(NEt_2)]$ (top) and (b) Standard TiS_2 obtained from Aldrich (bottom)

3.2.3 Annealing the precipitates under H_2S gas at 600 °C

The precipitate formed from the modified thio "sol-gel" process of $[Et_2NH_2][Ti(SC_6F_5)_4(NEt_2)]$ was annealed at 600 °C under H_2S gas, in order to see if crystalline TiS_2 could be made at lower temperatures. Powder XRD of the resulting black solid[85] showed it to consist of crystalline TiS_2, crystalline $Ti_{1.19}S_2$ and crystalline $Ti_{1.25}S_2$ (Figure 3.3). No evidence of TiO_2 was observed from the XRD pattern. EDXA data showed a 1:2 ratio of Ti:S over a number of spots, suggesting the formation of TiS_2. However, a temperature greater than 600 °C is probably required to form purely crystalline TiS_2. The formation of a mixture of crystalline titanium sulfides at this temperature without any TiO_2 impurities suggests an advantage of using a titanium thiolate precursor over a titanium alkoxide precursor.

Figure 3.3 X-ray diffraction pattern for product of annealing $[Et_2NH_2][Ti(SC_6F_5)_4(NEt_2)]$ under H_2S at 600 °C (top) and standard TiS_2 (blue), $Ti_{1.19}S_2$ (red) and $Ti_{1.25}S_2$ (green)

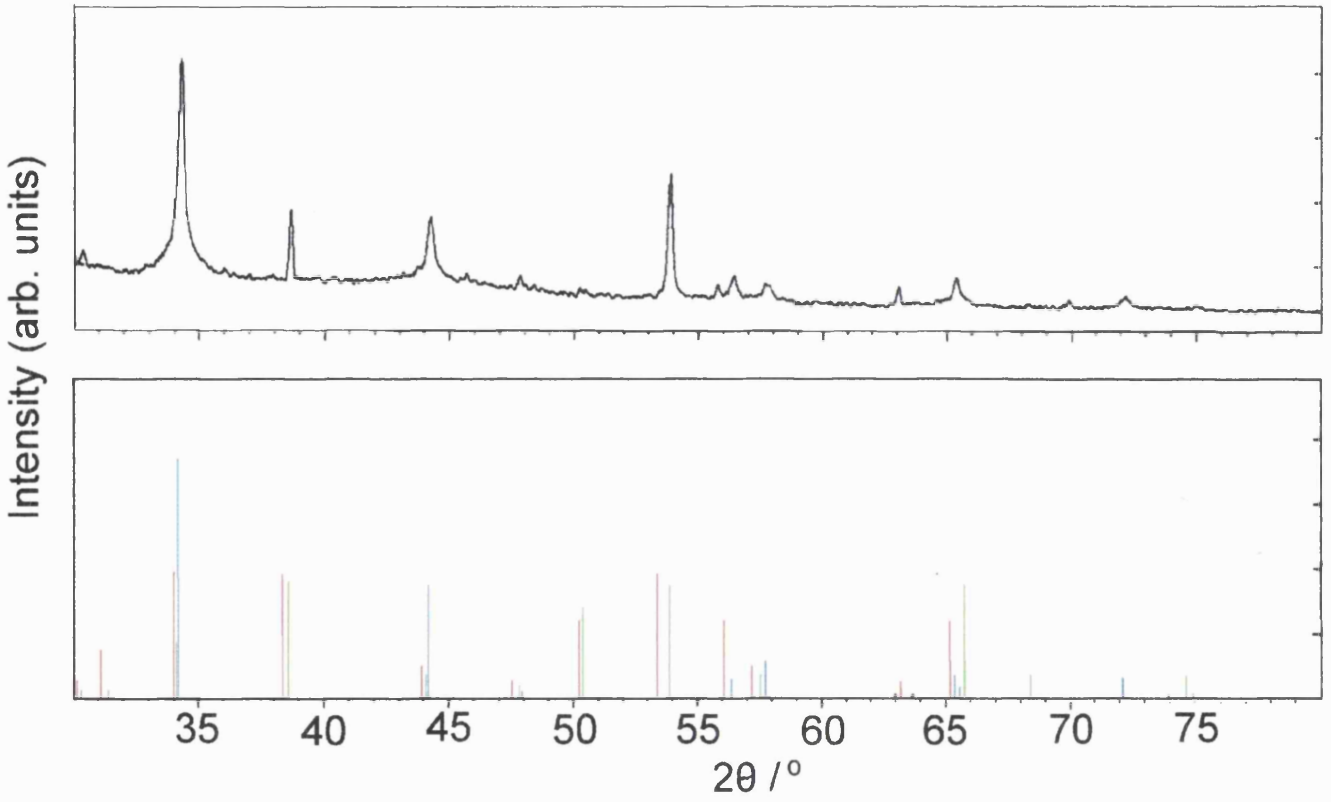

3.2.4 Annealing the precipitates under N_2 gas at 800 °C

In order to determine if the presence of H_2S was necessary for the precipitate to be converted to TiS_2, it was decided to anneal the precipitate under N_2. The precipitates from the thio "sol-gel" reaction were therefore heated under a flow of N_2 at 800 °C for 6 hours. This resulted in the formation of black solids for all of the samples used. Powder XRD of the materials[85] showed peaks corresponding to anatase. There was no evidence of crystalline TiS_2 in the spectra even after repetition of the reactions. Furthermore, the EDXA data showed a low sulfur content of the precipitates (less than 50%) suggesting that either oxidation or decomposition had occurred with the formation of TiO_2. It is possible that air got into the system during heating or that the precursor reacted with oxygen in the ceramic boats used to hold the samples. It seems likely, therefore, that H_2S gas is required to form TiS_2 under the annealing conditions used.

3.2.5 Annealing the thiolates under H_2S gas at 800 °C

It was then decided to eliminate the initial thio "sol-gel" step, in order to determine the influence this has on the nature of the product obtained. Consequently, the thiolate precursors $[Et_2NH_2][Ti_2(\mu\text{-}SCH_2Ph)_3(SCH_2Ph)_6]$ and $[Et_2NH_2][Ti(SC_6F_5)_4(NEt_2)]$ were heated under a constant flow of H_2S gas at 800 °C for 6 hours without the initial "sol-gel" reaction. A black precipitate was formed for $[Et_2NH_2][Ti(SC_6F_5)_4(NEt_2)]$ and for the thiolate $[Et_2NH_2][Ti_2(\mu\text{-}SCH_2Ph)_3(SCH_2Ph)_6]$ a black precipitate with a gold surface

resulted. Powder XRD of these materials[85] showed that a single phase of hexagonal TiS_2 had formed in both instances (Table 3.2) with a typical crystallite size from the X-ray broadening of 800 Å. Fig. 3.4 shows the powder XRD pattern of TiS_2 prepared from this route from $[Et_2NH_2][Ti(SC_6F_5)_4(NEt_2)]$. The X-ray powder patterns of the TiS_2 obtained were indexed and again gave exact matches to literature measurements.[86] Cell parameters for TiS_2 obtained from $[Et_2NH_2][Ti(SC_6F_5)_4(NEt_2)]$ gave a = 3.400(1) Å and c = 5.692(5) Å. TiS_2 obtained from $[Et_2NH_2][Ti_2(\mu\text{-}SCH_2Ph)_3(SCH_2Ph)_6]$ gave a = 3.4054(5) Å and c = 5.706(3) Å. The EDXA data showed a 1:2 ratio of Ti:S over a number of spots as expected.

The formation of crystalline TiS_2 by heating the thiolate precursors under H_2S at 800 °C suggests that the initial thio "sol-gel" step is not necessary. However, the material produced after the initial thio "sol-gel" step is much less air-sensitive than the thiolates themselves and are therefore easier to handle without decomposition occurring. The difference in air sensitivity of the two samples is attributed to a variation in porosity and surface area within the materials.[84]

Figure 3.4 X-ray diffraction pattern for product of annealing $[Et_2NH_2][Ti(SC_6F_5)_4(NEt_2)]$ under H_2S (top) and standard TiS_2 (bottom)

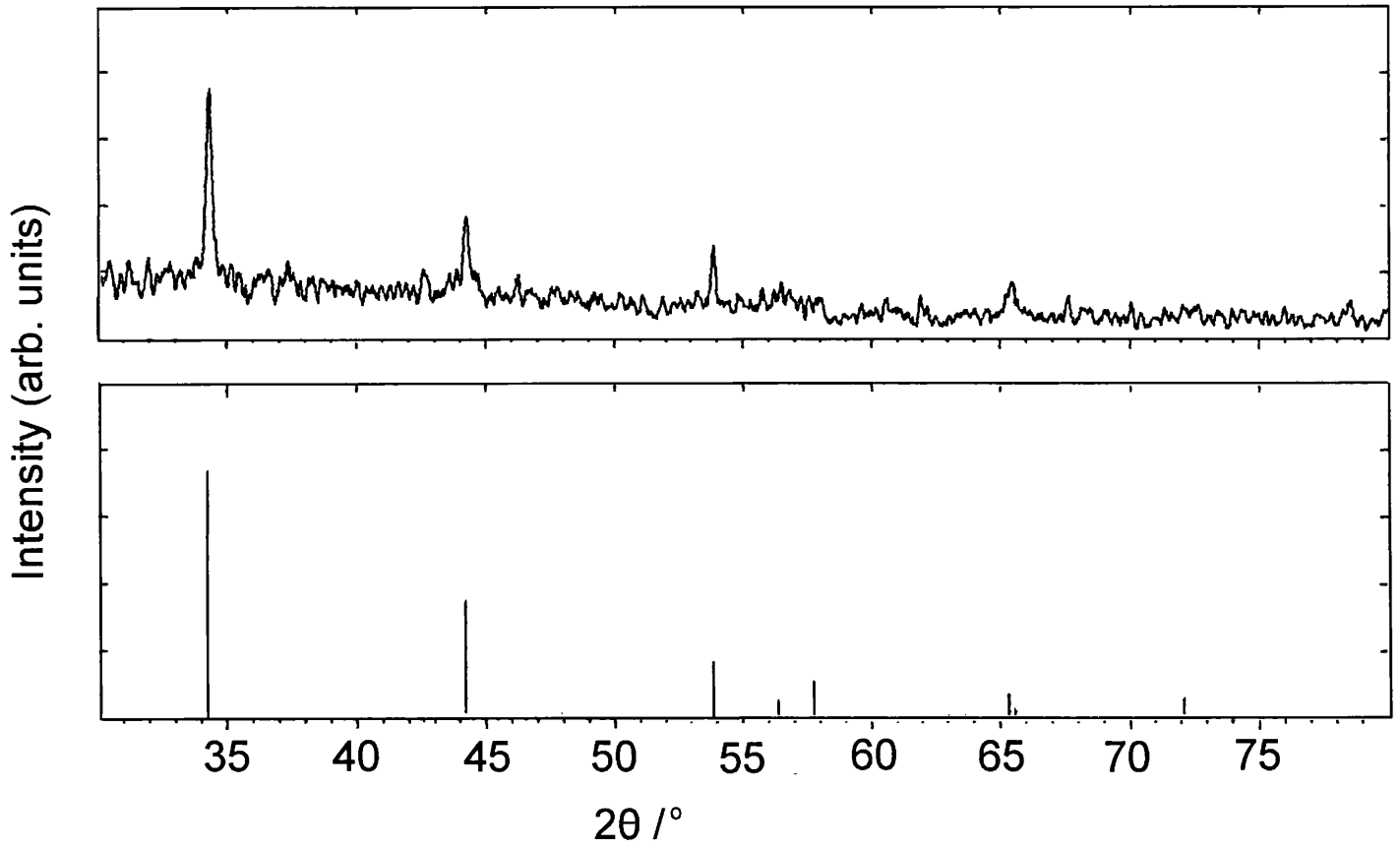

3.2.6 Annealing the precipitates under a vacuum

Finally it was decided to anneal the thiolate $[Et_2NH_2][Ti_2(\mu\text{-}SCH_2Ph)_3(SCH_2Ph)_6]$ under a vacuum at varying temperatures (500, 600, 800 and 1000 °C for three hours) to see if crystalline TiS_2 could be made without any use of H_2S gas. The ^1H NMR spectrum of the reaction byproducts, that were trapped in a cold trap during the experiment, showed the presence of Et_2NH and $(PhCH_2)_2S_2$. Powder XRD of the grey/black precipitate obtained after annealing the thiolate[85] showed that amorphous products were obtained at all temperatures used, except at 1000 °C, where nanocrystalline Ti_2S_3 was made. This result was unexpected, as it was anticipated that TiS_2 would be made from this method. However, EDXA data also showed a Ti:S ratio of 2:3 to be present which is in good agreement with Ti_2S_3. This confirms that pure, crystalline TiS_2 can not be made at this stage without the use of H_2S gas during the annealing process.

3.3 Thio "sol-gel" routes for obtaining disulfides of tantalum/niobium

Initial investigations showed this methodology to be successful in the making of titanium disulfide. It was decided to extend this route to the preparation of tantalum and niobium disulfides. Consequently, the thiolates $[Ta(S\text{-}2,6\text{-}Me_2C_6H_3)_4(NMe_2)]$ and $[Nb(S\text{-}2,6\text{-}Me_2C_6H_3)_5]$ were synthesised as described in chapter 2. The thio "sol-gel" step was carried out as described above and the black precipitates obtained were heated under H_2S gas for 6 hours at 800 °C.

3.4 Results and Discussion

The precipitates obtained from the thio "sol-gel" step (section 3.3) were annealed under H_2S gas at 800 °C as described earlier. This resulted in black precipitates for both [Ta(S-2,6-$Me_2C_6H_3$)$_4$(NMe_2)] and [Nb(S-2,6-$Me_2C_6H_3$)$_5$]. Powder XRD of the material[85] obtained from [Nb(S-2,6-$Me_2C_6H_3$)$_5$] showed that a single phase of crystalline NbS_2 had formed (Figure 3.5). A typical crystallite size of 970 Å was determined from the line broadening and the lattice parameters were found to be a = 3.334(8) Å and c = 17.88(1) Å which is in good agreement with literature values (where a = 3.335 Å and c = 17.86 Å).[87] EDXA data also confirmed that the Nb:S ratio was 1:2 over a number of spots. A Raman spectrum was taken and is shown in Figure 3.6. Peaks were found at 150, 192, 252, 381, 398 and 450 cm^{-1}. Unfortunately, a standard NbS_2 sample could not be found.

Analysis of the precipitate obtained from [Ta(S-2,6-$Me_2C_6H_3$)$_4$(NMe_2)] by powder XRD showed only the presence of Ta_2O_5 and not TaS_2 as was hoped, despite repeated attempts. This could be due to the sample being more sensitive to air and moisture than the niobium thiolate and therefore more readily oxidised or decomposed to the oxide. It is likely that more rigorous experimental methods are necessary to produce tantalum sulfides e.g. using aluminium/platinum boats instead of ceramic ones to hold the sample.

Nonetheless, the preparation of NbS_2 was successful and shows that the thio "sol-gel" method can be extended to the formation of other metal sulfides. Given more time it would also have been worth exploring this method at different temperatures and conditions.

Figure 3.5 X-ray diffraction pattern for NbS_2 prepared from thio "sol gel" treatment of [$Nb(S\text{-}2,6\text{-}Me_2C_6H_3)_5$] and standard NbS_2 (bottom)

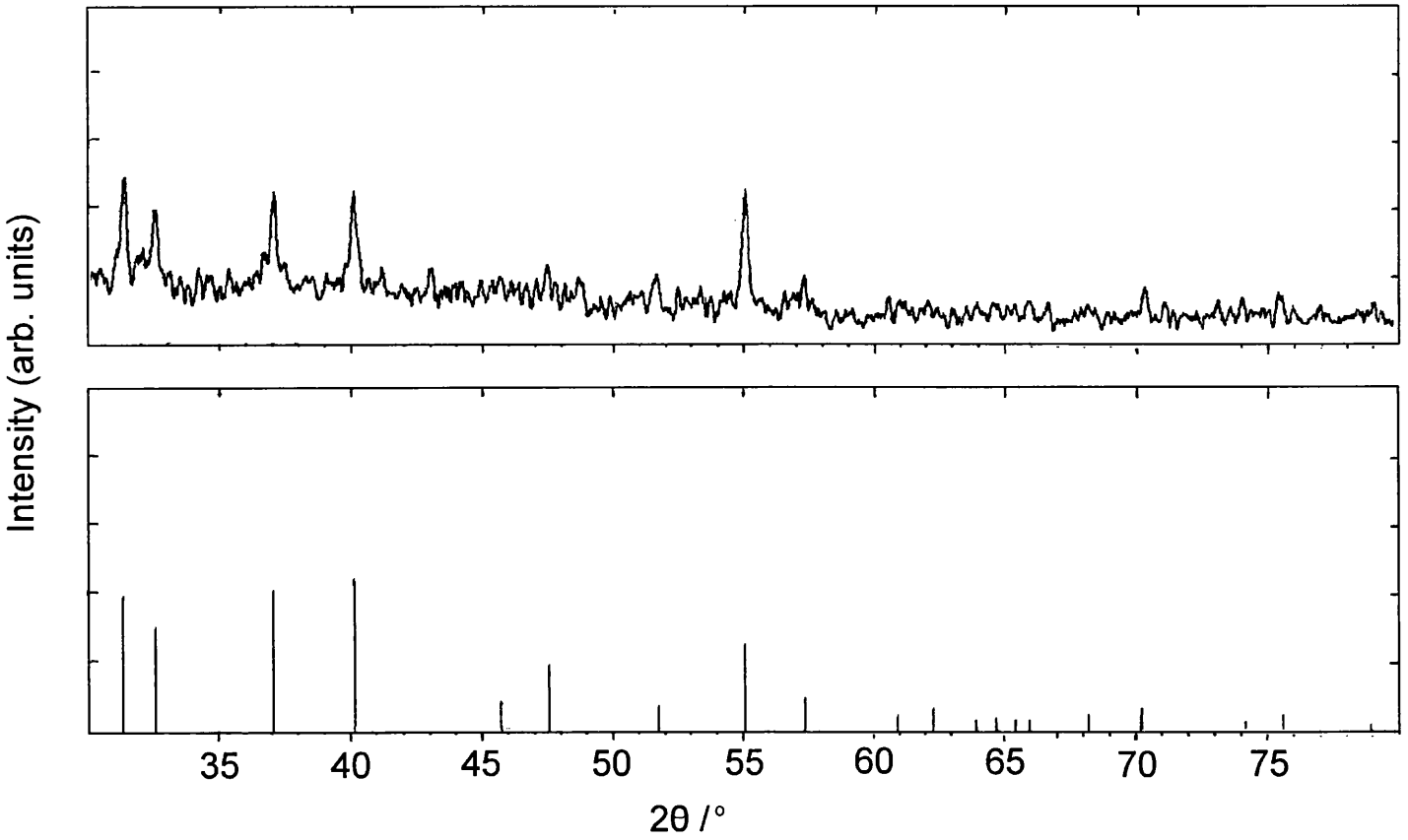

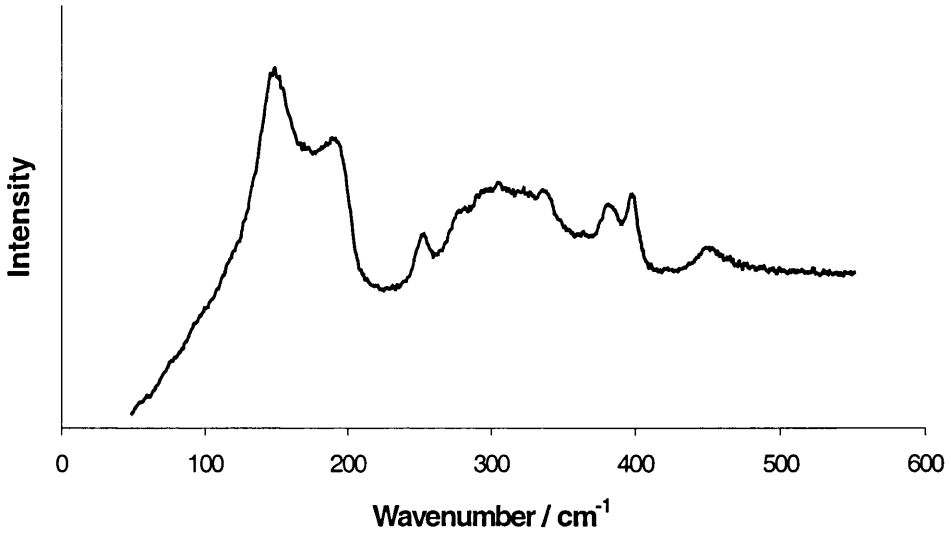

Figure 3.6 Raman spectrum for NbS_2 prepared from thio "sol gel" treatment of [Nb(S-2,6-$Me_2C_6H_3$)$_5$]

3.5 Use of hexamethyldisilathiane as a sulfur source

The second part of this chapter describes attempts to make metal disulfides from hexamethyldisilathiane (HMDST, $(Me_3Si)_2S$). It has already been shown that TiS_2 can be made from the reaction of $TiCl_4$ and HMDST followed by annealing of the precipitate at temperatures of 650 °C (see chapter 1).[59] By reacting HMDST with a transition metal halide, e.g. $NbCl_5$, it was hoped that an amorphous disulfide would be produced according to the proposed reaction (3.3).

$$NbCl_5 + 2.5\,(Me_3Si)_2S \longrightarrow NbS_2 + 5\,Me_3SiCl + 0.5\,S \qquad (3.3)$$

This method was also carried out for $TiCl_4$, $ZrCl_4$, $MoCl_5$, $NbCl_5$ and $TaCl_5$.

3.6 Results and Discussion

3.6.1 Reaction of $TiCl_4$ with HMDST

The reaction between $TiCl_4$ and 2 equivalents of HMDST in diethyl ether at room temperature resulted in the formation of a black precipitate. Powder XRD of the precipitate[85] showed that nanocrystalline TiS_2 had formed with a typical crystallite size from the X-ray broadening of 1000 Å (Figure 3.7).[88] However, the EDXA data showed incomplete formation of a titanium sulfide had occurred with the material being contaminated with chlorine. The EDXA data showed $TiS_{1.2}Cl_{0.5}$ over a number of spots.[88] Previous reports indicate that the reaction between $TiCl_4$ and excess HMDST in CH_2Cl_2, resulted in the isolation of an X-ray amorphous powder which was not analysed further.[59] However, heating of the powder to 650 °C resulted in the formation of either mixtures of TiS_2 and TiO_2, non-stiochiometric TiS_2 or crystalline TiS_2 depending on the precise conditions. It was therefore decided to anneal the amorphous powder described above in an attempt to form crystalline TiS_2. The amorphous powder was annealed at 800 °C under H_2S for 6 hours. These conditions were chosen to prevent the formation of TiO_2 or the formation of non-stoichiometric TiS_2 from the liberation of sulfur. The powder pattern of the annealed material showed that a single phase of hexagonal TiS_2 had formed with a typical crystallite size from the X-ray broadening of 800 Å (Figure 3.8). The X-ray powder pattern of the TiS_2 obtained was indexed and gave exact matches to literature measurements (Table 3.3).[85] However, the EDXA data showed a 2:3 ratio of Ti:S over a number of spots, suggesting that either an amorphous titanium sulfide (e.g. TiS) had

formed as well as the crystalline TiS_2 or that partial oxidation of the product had occurred. No evidence for the formation of a titanium oxide was seen from either powder XRD or Raman spectroscopy and so some amorphous material is likely to be present in the sample. Figure 3.9 shows an SEM image of the TiS_2 prepared from this method. The SEM showed agglomerates (dimension about 5 μm) of platelets of approximate size 2 μm.

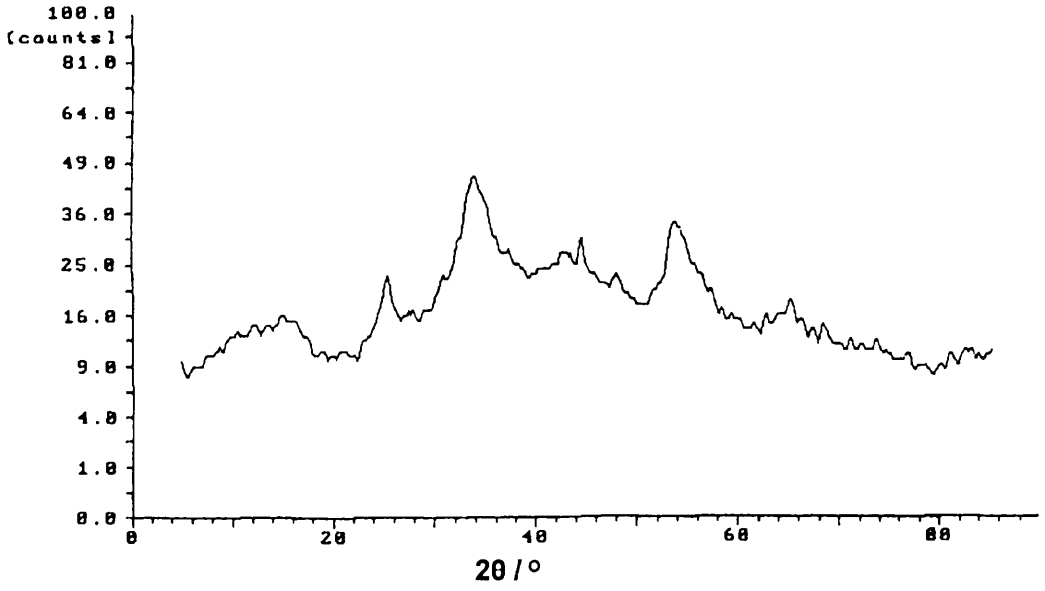

Figure 3.7 X-ray diffraction pattern for product obtained from the reaction of $TiCl_4$ with HMDST at room temperature[88]

Table 3.3 Lattice parameters obtained for MS_2 formed from the reaction of the transition metal chloride and HMDST

	Lattice parametres of MS_2[a,b]	
Metal chloride	*a*	*c*
$TiCl_4$ + HMDST	3.404(3)	5.71(1)
$NbCl_5$ + HMDST	3.337(1)	17.878(4)
$TaCl_5$ + HMDST	3.36(5)	5.78(9)
$NbCl_5/TaCl_5$ + HMDST*	3.374(1)	5.869(5)

[a]Unit cell dimensions *a, c* in Å

[b]Literature values - TiS_2: a = 3.4049; c = 5.6912[87], NbS_2: a = 3.335; c = 17.86,[88]

TaS_2: a = 3.385; c = 5.90.[90]

* adopts the hexagonal TaS_2 lattice

Figure 3.8 X-ray diffraction pattern for product of annealing precipitate of $TiCl_4$ and HMDST under H_2S (top) and standard TiS_2 (bottom)

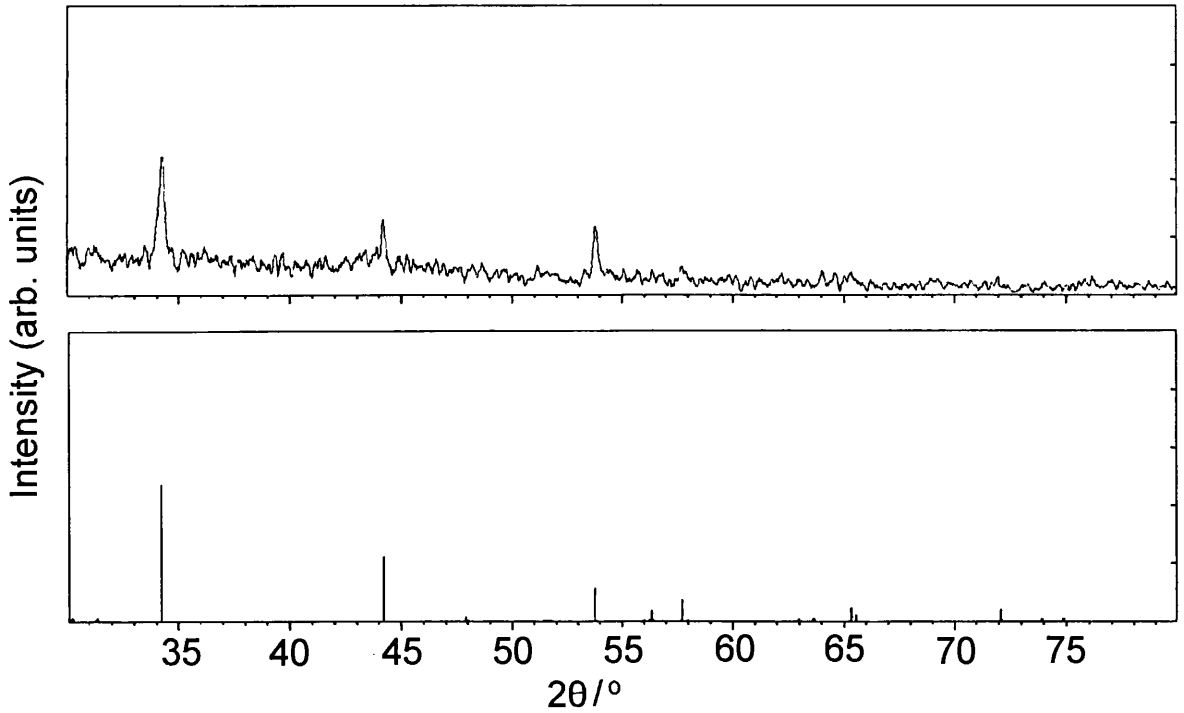

Figure 3.9 SEM profile of TiS_2 prepared from annealing the precipitate of $TiCl_4$ and HMDST

3.6.2 Reaction of $ZrCl_4$ with HMDST

The reaction between $ZrCl_4$ and HMDST resulted, after work-up, in the formation of a bright orange precipitate that was extremely air-sensitive and could not be analysed by EDXA as it oxidised before it could be successfully mounted onto the apparatus. It was again decided to anneal this precipitate under H_2S gas at 800 °C in an attempt to form the disulfide, ZrS_2. After repeated attempts at annealing under H_2S gas it was only possible to obtain nanocrystalline ZrO_2 from this precipitate, despite handling all reaction materials and products under an atmosphere of nitrogen. EDXA analysis on the black

precipitate obtained after annealing under H_2S gas showed the sulfur content to be very low (always less than 10%). It is possible that this material is exceptionally sensitive to air and moisture compared to the other materials used and so forms the oxide even under an H_2S environment.

3.6.3 Reaction of $NbCl_5$ with HMDST

The reaction between MCl_5 (where M = Nb, Ta, Mo) and 2.5 equivalents of HMDST at room temperature resulted, after work-up, in the formation of a black precipitate (Scheme 4, reactions (iii)–(v)). Powder XRD of the materials[85] revealed that they were all X-ray amorphous. EDXA and analytical data on the material showed that the incomplete formation of a metal sulfide had occurred. The EDXA data for the precipitate isolated from the reaction between $NbCl_5$ and HMDST showed $NbS_{1.2}Cl_{0.4}$ to have formed over a number of spots. Annealing of the precipitate at 800 °C under H_2S for 6 hours resulted in the isolation of crystalline NbS_2 (Table 3.3)[87] with a typical crystallite size from the X-ray broadening of 950 Å. Fig. 3.10 shows the powder XRD pattern of NbS_2 prepared from this route. The EDXA data showed good agreement with a 1:2 ratio of Nb:S over a number of spots. These results are similar to those described previously where either NbS_2 or $Nb_{1.12}S_2$ were isolated.[60] The SEM showed irregular platelets of approximately 1 μm diameter. The Raman spectrum of the NbS_2 prepared shows the presence of three bands at 140, 260 and 660 cm^{-1} (Figure 3.11). Unfortunately, we have been unable to find a NbS_2 standard or literature data for comparison. It is different to the spectrum obtained from the thio "sol-gel" route, which is surprising.

Figure 3.10 X-ray diffraction pattern for product of annealing precipitate of $NbCl_5$ and HMDST under H_2S (top) and standard NbS_2 (bottom)

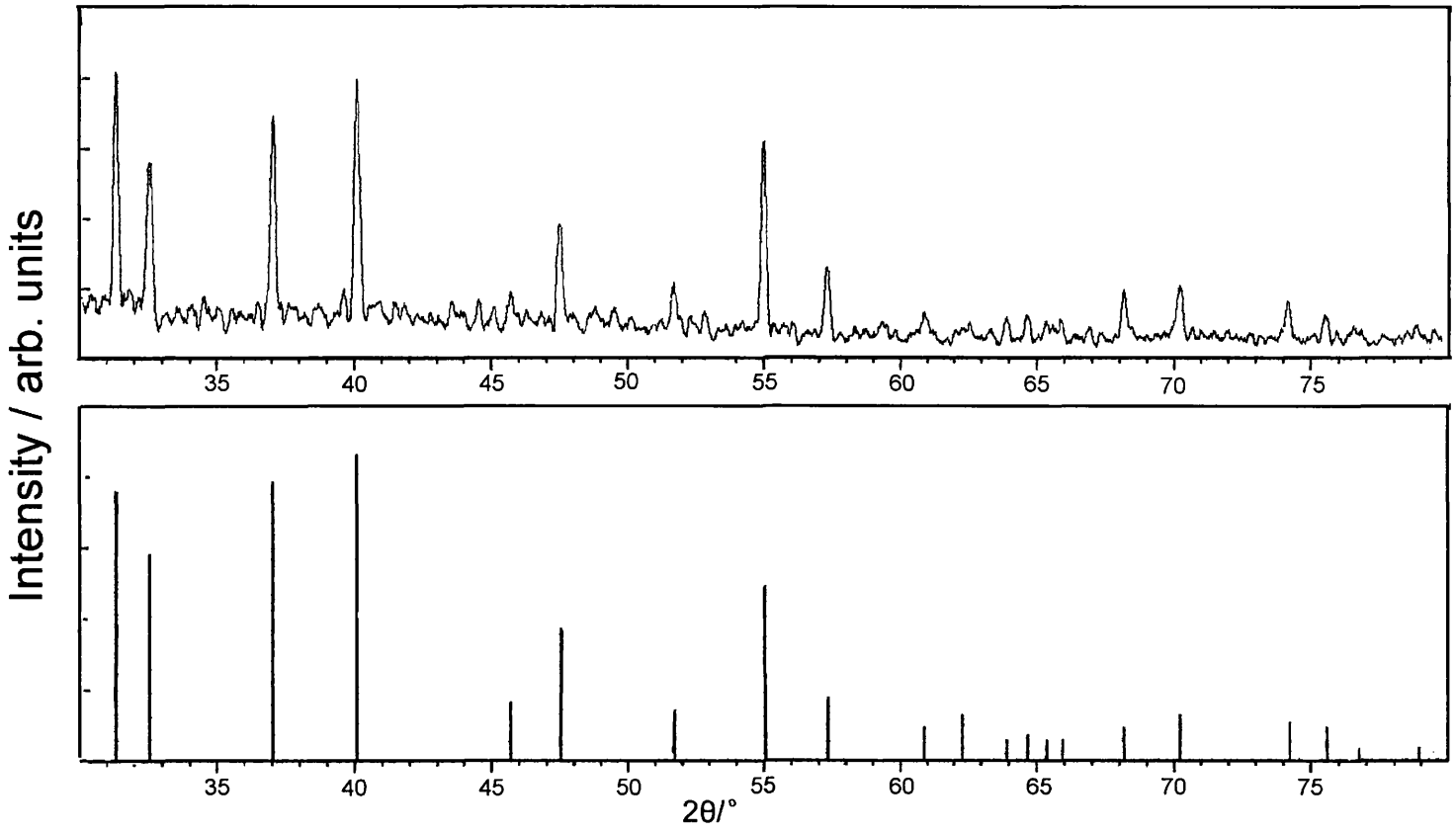

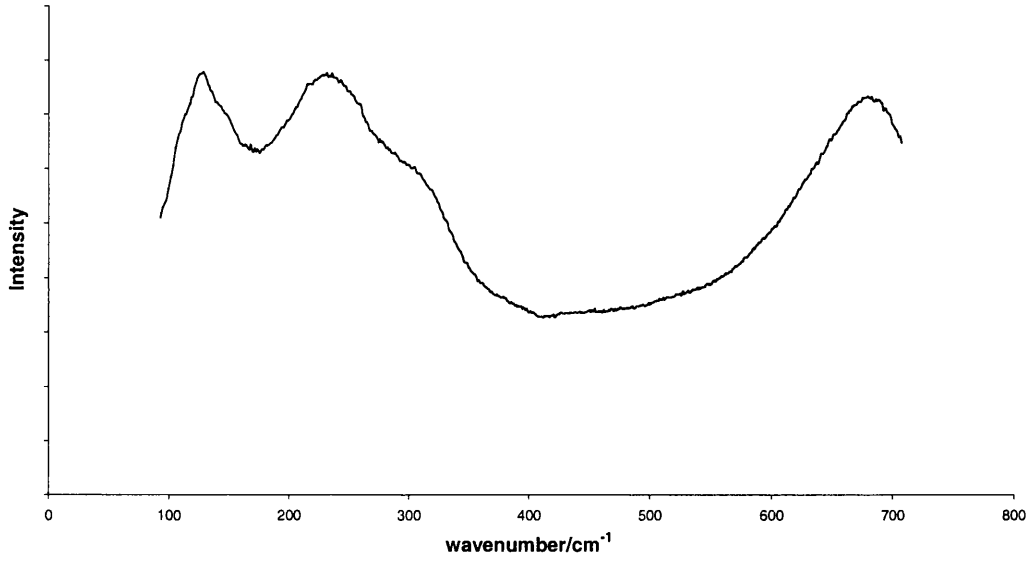

Figure 3.11 Raman spectrum of product of annealing precipitate of $NbCl_5$ and HMDST under H_2S

$$TiCl_4 + 2\,(Me_3Si)_2S \xrightarrow{Et_2O} TiS_{1.2}Cl_{0.5} \xrightarrow[800\ ^\circ C]{H_2S/6\ h} TiS_2 \qquad (i)$$

$$ZrCl_4 + 2\,(Me_3Si)_2S \xrightarrow{toluene} \text{not analysed} \xrightarrow[800\ ^\circ C]{H_2S/6\ h} ZrO_2 \qquad (ii)$$

$$MCl_5 + 2.5\,(Me_3Si)_2S \xrightarrow{toluene} \begin{cases} NbS_{1.2}Cl_{0.4} \xrightarrow[800\ ^\circ C]{H_2S/6\ h} NbS_2 & (iii) \\ TaSSi_3 \xrightarrow[800\ ^\circ C]{H_2S/6\ h} TaS_2 + TaO + TaSi_{0.4} & (iv) \\ MoS_{2.9}Cl \xrightarrow[800\ ^\circ C]{H_2S/6\ h} MoS_2 & (v) \end{cases}$$

Scheme 4 Reactions of transition metal chlorides and HMDST

3.6.4 Reaction of $TaCl_5$ with HMDST

The precipitate isolated from the reaction between $TaCl_5$ and HMDST was contaminated with large amounts of silicon but very little chlorine. This reaction was repeated and the presence of silicon was always observed. EDXA data showed $TaSSi_3$ to have formed over a number of spots and the analytical data revealed that a small amount of carbon and hydrogen was present in the material (C, 4.78%; H, 0.62%). The precipitate was again annealed under H_2S at 800 °C in an attempt to form TaS_2 and remove the silicon impurities. Analytical data for the annealed material showed that virtually no carbon and hydrogen remained in the material (C, 0.23%; H, 0.11%). However, the EDXA data on the annealed material showed the presence of $TaS_2Si_{0.5}$ over a number of spots suggesting that impure TaS_2 had formed. This was confirmed by the powder XRD of the material,[85] which showed the presence of crystalline TaS_2 (Table 3.3)[87] with a typical crystallite size from the X-ray broadening of 700 Å. However, peaks due to the presence of TaO and tantalum silicide ($TaSi_{0.40}$) were also detected as is shown in Figure 3.13. The SEM showed stacked hexagonal platelets of approximate diameter 2 μm and thickness 300 nm (Figure 3.12). Impurities can also be seen in the SEM and show that more than one material is present. The high levels of silicon present in the final material were not observed for any of the other transition metals used.

Figure 3.12 SEM profile of TaS_2 prepared from annealing the precipitate of $TaCl_5$ and HMDST

Figure 3.13 X-ray diffraction pattern for product of annealing precipitate of $TaCl_5$ and HMDST under H_2S (top) and standard TaS_2 (blue), TaO (red) and $TaSi_{0.4}$ (green)

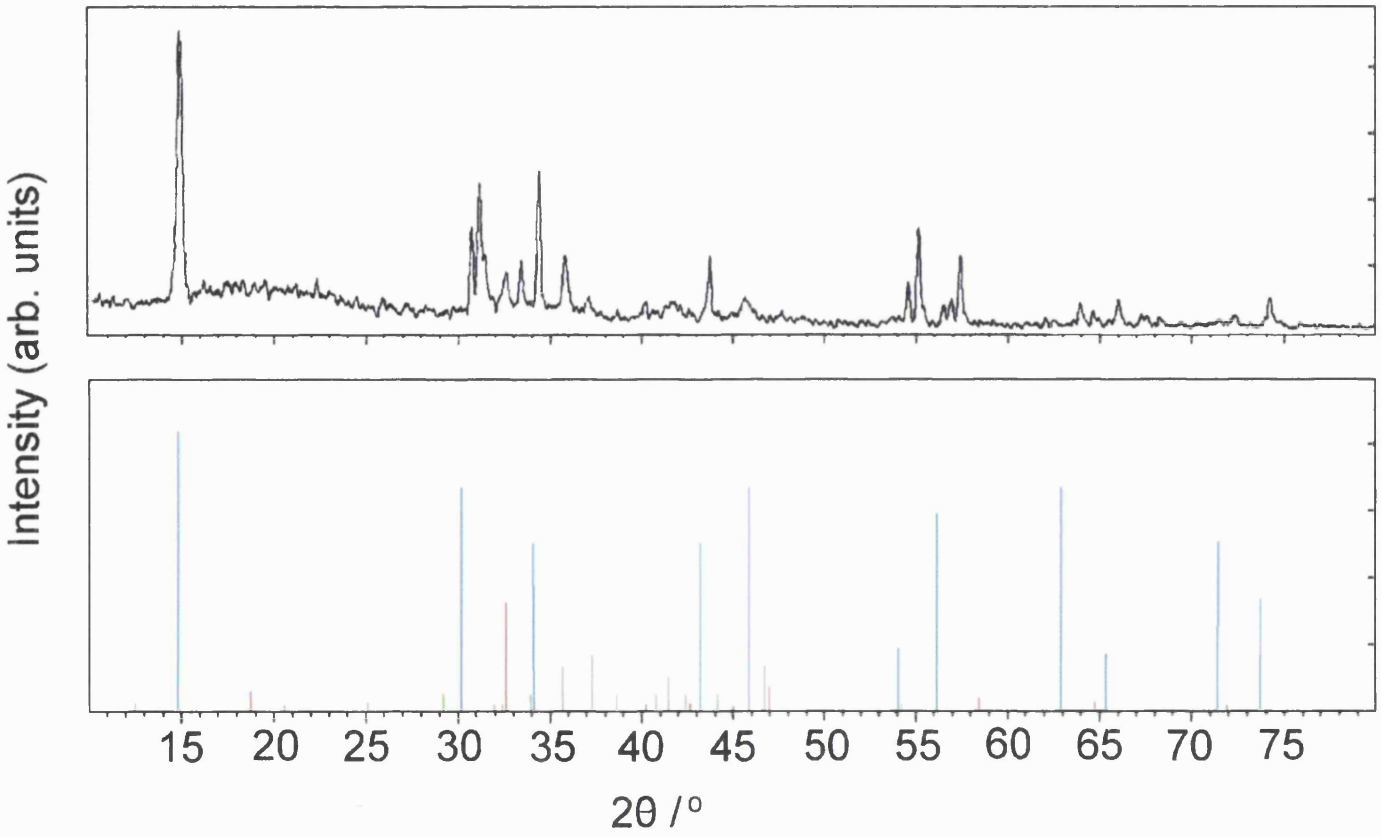

3.6.5 Reaction of $MoCl_5$ with HMDST

The black precipitate obtained from the reaction of $MoCl_5$ and 2.5 equivalents of HMDST was also X-ray amorphous. EDXA analysis showed the presence of $MoS_{2.9}Cl$ over a number of spots. The precipitate was again annealed at 800 °C under H_2S. Powder XRD of the annealed material[85] showed that nanocrystalline hexagonal MoS_2 had formed. The EDXA data showed good agreement with a 1:2 ratio of Mo:S over a number of spots. This is in contrast to previous reports where the reaction between $MoCl_5$ and excess HMDST in CH_2Cl_2 was reported to result in the formation of amorphous Mo_2S_5.[61] The SEM showed MoS_2 to consist of uniform spherical particles of approximately 100 nm diameter. These particles amalgamated into larger clumps of approximately 2 μm (Figure 3.14). The Raman spectrum of the annealed material is shown in Figure 3.15(a). This spectrum is similar to one obtained from a sample of standard MoS_2 purchased from Aldrich (Figure 3.15(b)). Although the two spectra are not identical, the peak positions do match.

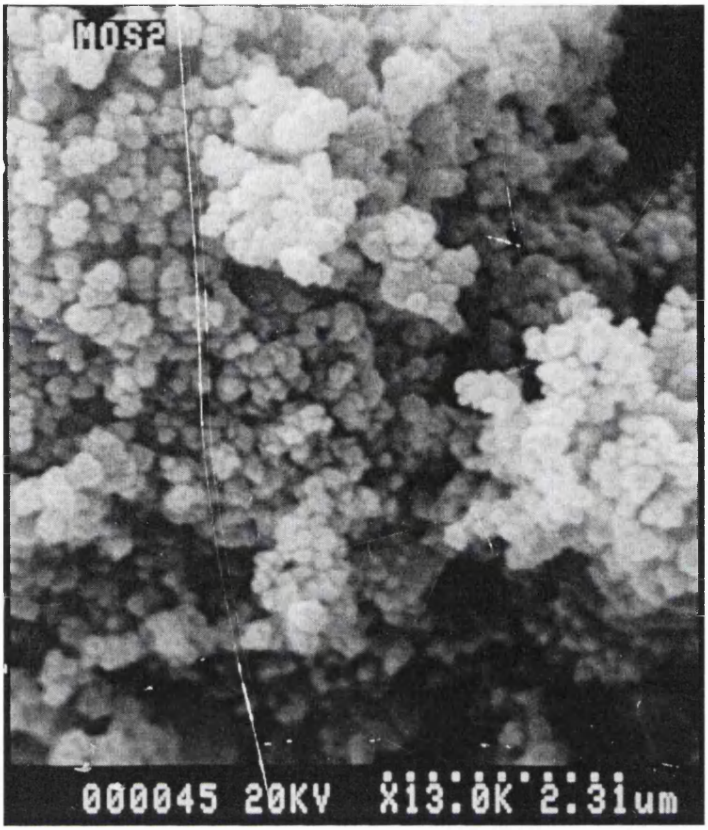

Figure 3.14 SEM profile of MoS_2 prepared from annealing the precipitate of $MoCl_5$ and HMDST

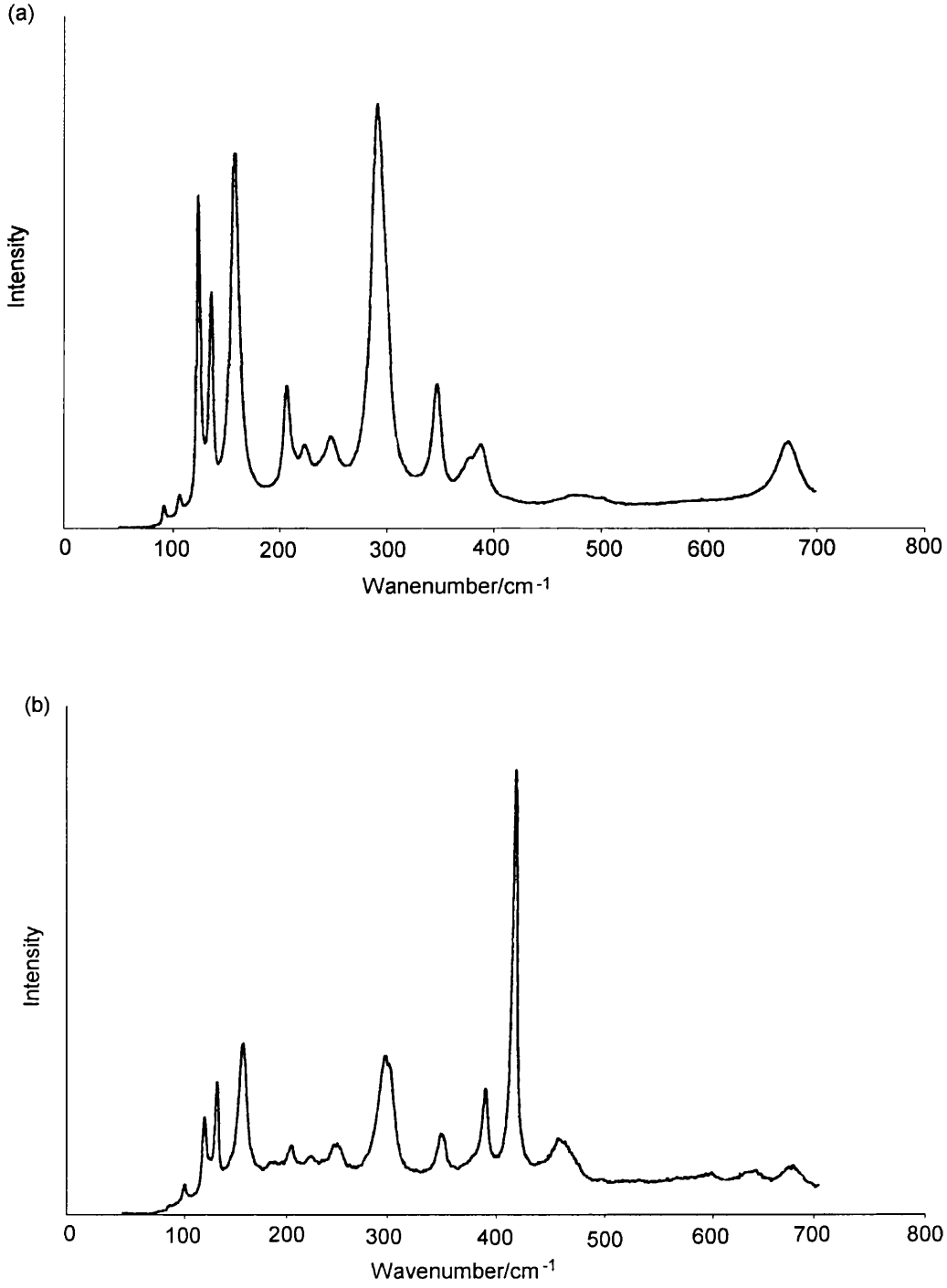

Figure 3.15 (a) Raman spectrum for product of annealing precipitate of $MoCl_5$ and HMDST under H_2S and (b) Standard sample of MoS_2

3.7 Preparation of mixed-metal disulfides

Given the success in preparing a range of crystalline transition metal sulfides, it was decided to attempt to make mixed-metal sulfides using $NbCl_5/TaCl_5$ and $TiCl_4/ZrCl_4$ and HMDST. It was hoped that the reaction would proceed according to the proposed equation 3.4.

$$NbCl_5 + TaCl_5 + 5\ (Me_3Si)_2S \longrightarrow 2\ Nb_{0.5}Ta_{0.5}S_2 + 10\ Me_3SiCl + 0.5\ S \quad (3.4)$$

3.8 Results and Discussion

3.8.1 Reaction of $NbCl_5$, $TaCl_5$ and HMDST

In order to attempt to synthesise a mixed-metal sulfide, the reaction between $NbCl_5$, $TaCl_5$ and 5 equivalents of HMDST was carried out in toluene. A black precipitate formed immediately on addition of HMDST. Powder XRD of the precipitate[85] revealed that it was X-ray amorphous. Analytical data showed that the precipitate was contaminated with small amounts of carbon and hydrogen (C 7.44% and H 0.77%). The precipitate was annealed at 800 °C under H_2S for 6 hours. EDXA analysis on the annealed powder showed good agreement with a 0.5:0.5:2 ratio of Nb:Ta:S over a number of spots suggesting the formation of $Nb_{0.5}Ta_{0.5}S_2$. The SEM showed an agglomeration of platelets of approximately 2 μm diameter. Powder XRD[85] of the material (Figure 3.16) revealed that the product $Nb_{0.5}Ta_{0.5}S_2$ adopted the hexagonal TaS_2 lattice with incorporation of Nb into the lattice.[89] A typical crystallite size was calculated

from the X-ray broadening and found to be 890 Å. It is interesting to note that the peaks obtained for the sample are also shifted to a slightly higher 2θ value when compared to the standard TaS_2 sample.

3.8.2 Reaction of $TiCl_4$, $ZrCl_4$ and HMDST

The reaction between $ZrCl_4$, $TiCl_4$ and 4 equivalents of HMDST was carried out in toluene. A black precipitate formed immediately on addition of HMDST. Powder XRD of the precipitate[85] revealed that it was X-ray amorphous. Analytical data showed that the precipitate was contaminated with small amounts of carbon and hydrogen (4.96 and 0.66% respectively). The precipitate was subsequently annealed at 800 °C under H_2S for 6 hours giving a black solid. EDXA analysis on the annealed powder showed that a Ti:Zr:S ratio of approximately 1:1:1 had formed although this was not always consistent over a number of spots. Powder XRD of the product showed only the presence of crystalline ZrO_2. It is likely that an amorphous titanium sulfide and ZrO_2 have actually been produced in this reaction, accounting for the Ti:Zr:S ratios found by EDXA. This is similar to the reaction where just $ZrCl_4$ was used and a sulfide could not be formed due to the sensitive nature of the material produced. It is also possible that the $ZrCl_4$ did not react with HMDST due to the much lower solubility of $ZrCl_4$ in toluene (compared to $TiCl_4$).

Finally, in order to establish if MS_2 could be formed directly without the annealing step, the reaction between $NbCl_5$ and HMDST was carried out in refluxing toluene.

Figure 3.16 X-ray diffraction pattern for product of annealing precipitate of $TaCl_5$ / $NbCl_5$ and HMDST under H_2S (top) and standard TaS_2 (bottom)

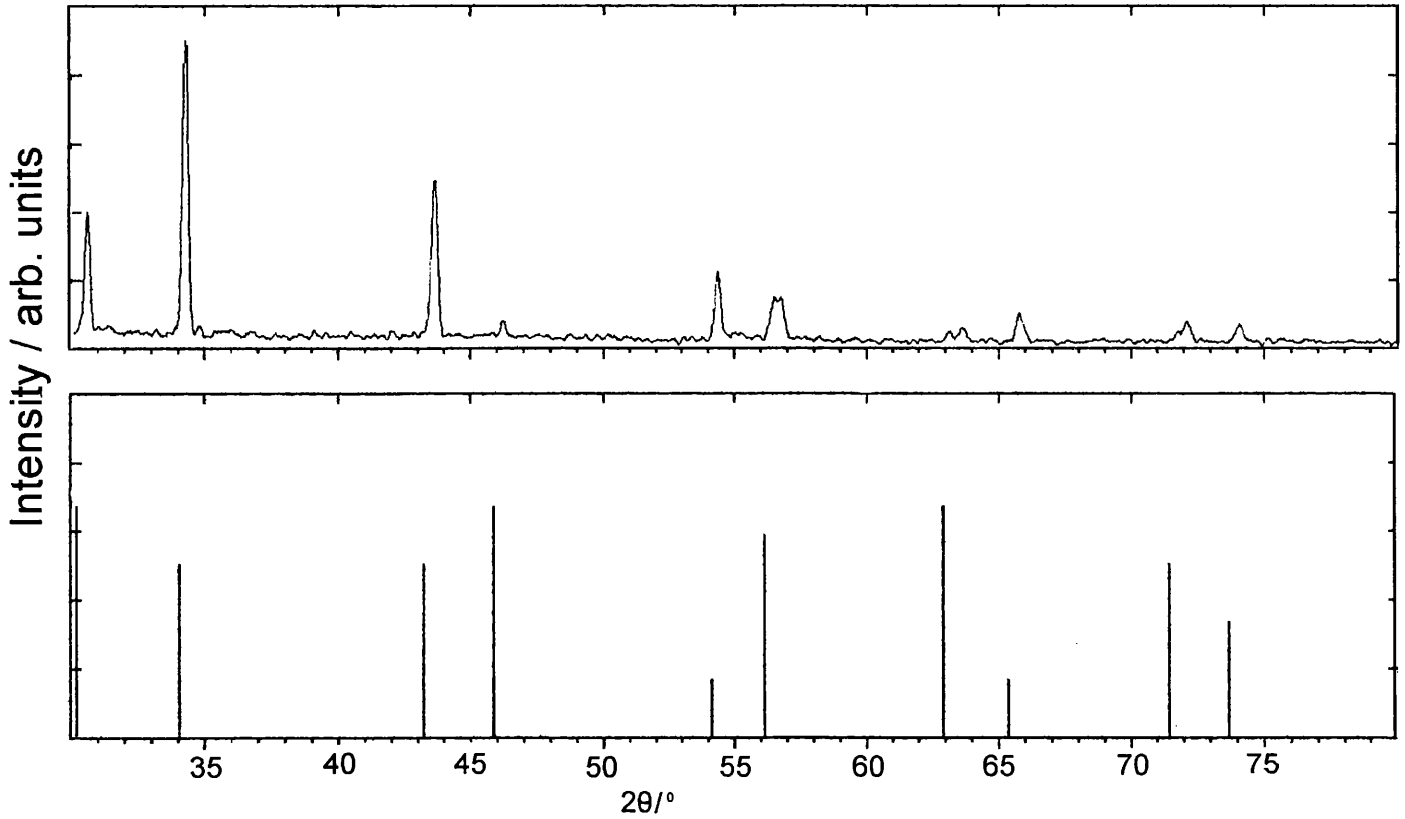

3.9 Reaction of $NbCl_5$ and HMDST under reflux

After refluxing $NbCl_5$ and 2.5 equivalents of HMDST for five hours, a black precipitate resulted. Powder XRD of this material[85] showed that it was X-ray amorphous. However, the EDXA data indicated that NbS_2 had formed with a 1:2 ratio of Nb:S over a number of spots. This is in contrast to the precipitate obtained from the same reaction at room temperature where the EDXA showed $NbS_{1.2}Cl_{0.4}$ to have formed. The Raman spectrum was similar to that shown in Fig. 3.9 for crystalline NbS_2 described above (Figure 3.17). This result indicates that amorphous NbS_2 can be prepared by the direct reaction of $NbCl_5$ and HMDST under refluxing conditions. In order to obtain crystalline NbS_2, however, it would be necessary to anneal the material.

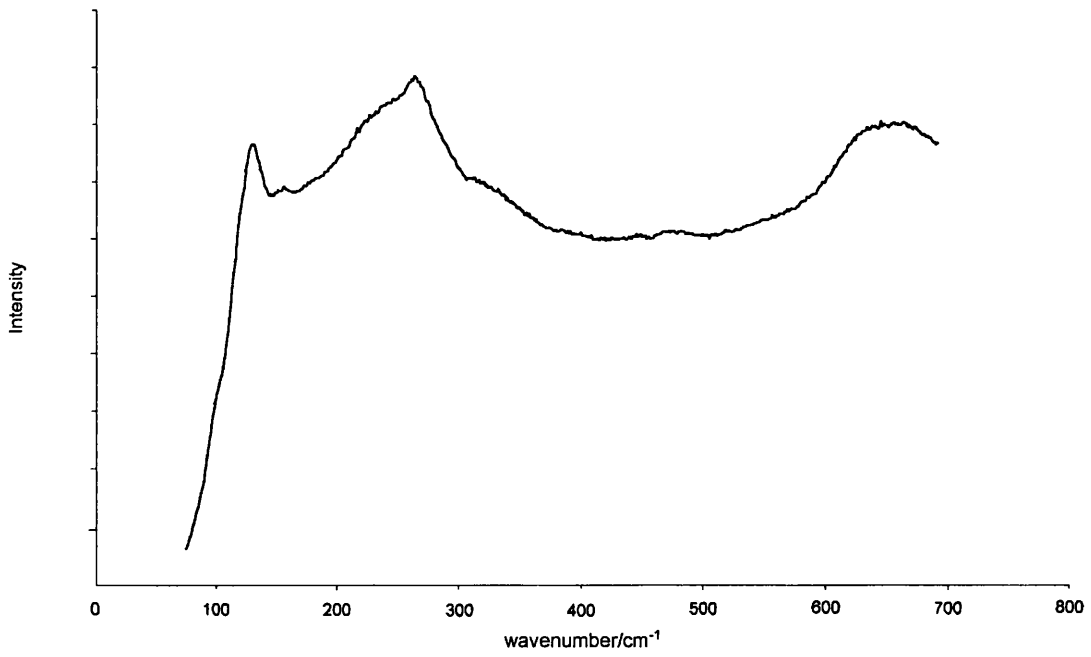

Figure 3.17 Raman spectrum for product of refluxing $NbCl_5$ and HMDST

3.10 Conclusions

The use of the thio "sol-gel" method was successful in obtaining crystalline TiS_2 and NbS_2 from thiolate starting materials. An analogous reaction using the tantalum thiolate, $[Ta(S\text{-}2,6\text{-}Me_2C_6H_3)_4(NMe_2)]$ as a starting material resulted in crystalline Ta_2O_5. Investigations into the formation of titanium sulfides using thiolate starting materials showed that crystalline TiS_2 could be made without the initial thio "sol-gel" reaction. It was also shown that metal sulfides could be made at 600 °C without any oxide impurities. In order to make pure TiS_2, however, higher annealing temperatures are required.

Reactions using HMDST and transition metal chlorides, and subsequent annealing of the precipitates obtained under H_2S gas resulted in the successful preparation of crystalline TiS_2, NbS_2 and $Nb_{0.5}Ta_{0.5}S_2$ as well as impure TaS_2 and nanocrystalline MoS_2. Sulfides of zirconium could not be made from this method owing to the sensitivity of these materials to air. Carrying out the reactions under refluxing conditions enabled an amorphous disulfide, NbS_2 to be produced without any annealing stage.

3.11 Experimental

All manipulations were performed under a dry, oxygen-free dinitrogen atmosphere using standard Schlenk techniques or in a Mbraun Unilab glove box. Owing to the toxic nature of H_2S all of the experiments were carried out in a well-ventilated fume cupboard. All solvents were distilled from appropriate drying agents prior to use (sodium and benzophenone for toluene and diethyl ether). All reagents were procured commercially from Aldrich and used without

further purification. Microanalytical data were obtained at University College London.

Physical measurements

^1H NMR spectra were recorded on Brüker AMX300 or DRX400 spectrometers. The NMR spectra are referenced to CD_2Cl_2 which was degassed and dried over molecular sieves prior to use; ^1H chemical shifts are reported relative to $SiMe_4$ (0.00 ppm). Raman spectra were acquired on a Renishaw Raman System 1000 using a helium-neon laser of wavelength 632.8 nm. The Raman system was calibrated against the emission lines of neon. Powder XRD measurements were recorded on a Siemens D5000 transmission diffractometer using germanium monochromated Cu-$K\alpha_1$ radiation (λ= 1.5406 Å) as thin films. SEM profiles and EDXA were performed on a Hitachi S570 instrument using the KEVEX system. Thermolysis studies were performed in a Carbolite tube furnace.

3.12 General Procedure for the thio "sol-gel" step using titanium thiolates

The titanium precursors, $[Et_2NH_2][Ti_2(\mu\text{-}SCH_2Ph)_3(SCH_2Ph)_6]$, $[Et_2NH_2]_3[Ti(SC_6F_5)_5][SC_6F_5]_2$, $[Et_2NH_2][Ti(SC_6F_5)_4(NEt_2)]$ and $[Ti(S^tBu)_4]$/ $[Ti(S^tBu)_3(NEt_2)]$ were synthesised as described in Chapter 2 and used as starting materials. In a typical experiment, a sample of one of the aforementioned thiolates (0.30 g) was dissolved in toluene (40 cm^3) to give a dark red solution. H_2S gas was bubbled through the solution at room temperature and a brown/black precipitate formed immediately. The H_2S gas was allowed to bubble through the mixture for 10 min, after which the solid was allowed to settle. The solvent was

removed by syringe and the residue was washed twice with 20 cm^3 of fresh toluene. The washings from the toluene were analysed by ^1H NMR spectroscopy in order to ascertain any byproducts formed during the reaction. The solid was dried *in vacuo* (10^{-3} mmHg) for 2 hours resulting in a black/brown precipitate. This was then analysed by powder XRD and elemental analysis. The black/brown precipitates were annealed in two different ways, under H_2S or under N_2, the details of which are described below for a typical experiment. ^1H NMR of byproducts for $[Et_2NH_2][Ti_2(\mu\text{-}SCH_2Ph)_3(SCH_2Ph)_6]$ ($CDCl_3$): δ 1.65 (t, 2H, $HSCH_2Ph$), 3.50 (s, 2H, $SCH_2C_6H_5$), 3.62 (d, 4H, $HSCH_2Ph$), 7.12-7.24 (m, 15H, $SCH_2C_6H_5$ and $HSCH_2C_6H_5$). ^1H NMR of byproducts for $[Et_2NH_2]_3[Ti(SC_6F_5)_5][SC_6F_5]_2$ ($CDCl_3$): δ 1.29 (q, 6H, NCH_2CH_3), 2.96 (t, 4H, NCH_2CH_3), 9.14 (s, 2H, H_2NEt_2). ^1H NMR of byproducts for $[Et_2NH_2]_3[Ti(SC_6F_5)_4(NEt_2)]$ ($CDCl_3$): δ 1.34 (q, 6H, NCH_2CH_3), 3.04 (t, 4H, NCH_2CH_3), 9.26 (s, 2H, H_2NEt_2). ^1H NMR of byproducts for $[Ti(S^tBu)_4]/[Ti(S^tBu)_3(NEt_2)]$ ($CDCl_3$): δ 0.80, 1.18, 1.21, 1.30 (four singlets in a 1:1:2:1 ratio, $SC(CH_3)_3$) .

3.13 Annealing the precipitate under H_2S

A sample of the precipitate was placed in a ceramic boat and heated under a constant stream of H_2S gas at 800 °C for 6 hours in a quartz tube using a furnace. A black solid resulted (black with a gold surface formed from the precipitate obtained from $[Et_2NH_2][Ti_2(\mu\text{-}SCH_2Ph)_3(SCH_2Ph)_6]$) which was reanalysed by powder XRD, EDXA/SEM and Raman spectroscopy. The precipitates were also annealed under H_2S at a temperature of 600 °C for 6 hours

in order to compare the reaction products obtained at lower temperatures. Powder XRD and EDXA/SEM results were obtained on the resulting solids.

3.14 Annealing the precipitate under N_2 (no H_2S present)

A sample of the precipitate was placed in a ceramic boat and heated under a constant stream of N_2 at 800 °C for 6 hours using a furnace. A black solid resulted which was analysed by powder XRD, and EDXA/SEM.

3.15 Reaction of the titanium thiolates with H_2S (no thio "sol-gel" step)

A sample of the thiolate (0.30 g) was placed in a ceramic boat that was placed in a quartz tube. The thiolate was heated under a constant stream of H_2S gas at 800 °C for 6 hours using a furnace. A black solid resulted (black with a gold surface formed from the precipitate obtained from $[Et_2NH_2][Ti_2(\mu\text{-}SCH_2Ph)_3(SCH_2Ph)_6]$) which was analysed by powder XRD, EDXA/SEM and Raman spectroscopy.

3.16 Annealing the precipitate under vacuum

A sample of $[Et_2NH_2][Ti_2(\mu\text{-}SCH_2Ph)_3(SCH_2Ph)_6]]$ (0.30 g) was placed in a quartz tube and heated under vacuum at temperatures of 500, 600, 800 and 1000 °C for three hours. The vacuum line was fitted with liquid N_2 trap in order to isolate any volatile, liquid byproducts produced in the reaction. The reaction byproducts were analysed by ^1H NMR spectroscopy. The resulting grey / black solid was analysed by Powder XRD and EDAX. ^1H NMR of byproducts ($CDCl_3$): δ 1.05 (t, 3H, NCH_2CH_3), 2.64 (q, 2H, NCH_2CH_3), 3.73 (s, 2H, $SCH_2C_6H_5$), 7.20-7.30 (m, 5H, $SCH_2C_6H_5$).

3.17 Thio "sol-gel" reactions for niobium and tantalum

A standard sample of the thiolate (0.3 g of $[Ta(S\text{-}2,6\text{-}Me_2C_6H_3)_4(NMe_2)]$ or $[Nb(S\text{-}2,6\text{-}Me_2C_6H_3)_5]$) was dissolved in toluene and H_2S gas was bubbled through the solution for a period of 10 minutes. In both instances a black precipitate was formed immediately. This was allowed to settle and washed twice with toluene. The solid was dried *in vacuo* (10^{-3} mmHg) for 2 hours resulting in a black/brown precipitate. The precipitate was then analysed by powder XRD. The powder was then annealed under H_2S gas for 6 hours at 800 °C and the resulting black solids were reanalysed by Powder XRD and EDXA/SEM and Raman spectroscopy.

3.18 Reaction of $TiCl_4$ and HMDST[88]

$TiCl_4$ (4.74 mmol) was added dropwise to a stirred solution of HMDST (2 cm^3, 9.48 mmol) in diethyl ether (40 cm^3). The solution turned red immediately on addition of $TiCl_4$. After one minute the reaction mixture turned dark brown and the mixture was stirred for 15 h at room temperature. The resulting black precipitate was allowed to settle and the colourless liquid was syringed off and the remaining solid was dried *in vacuo* (0.81 g). The precipitate was characterised by powder XRD and EDXA/SEM. The precipitate was annealed as described below for a typical experiment.

3.19 Annealing the precipitate under H_2S

A sample of the precipitate was placed in a ceramic boat and heated under a constant stream of H_2S gas at 800 °C for 6 hours using a furnace. The resulting black solid was analysed by powder XRD, EDXA/SEM and Raman spectroscopy.

3.20 Reaction of $ZrCl_4$ and HMDST

$ZrCl_4$ (0.583 g, 2.50 mmol) was added to a stirred mixture of HMDST (1.05 cm^3, 5.00 mmol) and toluene (20 cm^3). The solution turned to a cream colour immediately on addition of $ZrCl_4$. After stirring for 15 hours a bright orange precipitate formed (0.31 g). The precipitate was characterised by powder XRD and EDXA/SEM. The precipitate was annealed and reanalysed as described above.

3.21 Reaction of $MoCl_5$ and HMDST[88]

HMDST (2 cm^3, 9.48 mmol) was added dropwise to a stirred red solution of $MoCl_5$ (1.04 g, 3.792 mmol) in diethyl ether (35 cm^3). A black/brown precipitate formed immediately and the mixture was stirred for 15 h at room temperature. The resulting black precipitate was allowed to settle and the colourless liquid was syringed off and the remaining solid was dried *in vacuo* (0.78 g). The precipitate was characterised by powder XRD and EDXA/SEM. The black precipitate was annealed and reanalysed using the procedure described above.

3.22 Reaction of MCl_5 (M = Nb, Ta) and HMDST

HMDST (1.32 cm^3, 6.25 mmol) was added dropwise to a stirred slurry of MCl_5 (2.5 mmol) in toluene (20 cm^3). The formation of a black precipitate (black/green for $NbCl_5$) was observed immediately on addition of HMDST. The reaction mixture was stirred for 15 h at room temperature. The resulting black precipitate was allowed to settle and the colourless liquid was syringed off and the remaining solid was dried *in vacuo* (0.325 g (Nb); 0.625 g (Ta)). The precipitates were analysed by powder XRD and EDXA/SEM. The black precipitate was annealed and reanalysed as described above.

3.23 Analytical data for precipitates

Precipitate from $ZrCl_4$ + HMDST: Found C, 6.47; H, 0.83. Precipitate from $TaCl_5$ + HMDST: Found C, 4.78; H, 0.62. Precipitate from $NbCl_5$ + HMDST (room temperature): Found C, 7.28; H, 1.00.

3.24 Reaction of $NbCl_5$, $TaCl_5$ and HMDST

HMDST (1.32 cm^3, 6.25 mmol) was added dropwise to a stirred slurry of a mixture of $NbCl_5$ (0.34 g, 1.25 mmol) and $TaCl_5$ (0.45 g, 1.25 mmol) in toluene (20 cm^3). Formation of a black precipitate was observed immediately on addition of HMDST. The reaction mixture was stirred for 12 h at room temperature. The resulting blue/black precipitate was allowed to settle and the colourless liquid was syringed off and the remaining solid was dried *in vacuo* (0.49 g).

Analytical data for the precipitate: Found C, 7.44; H, 0.77. The precipitate was also characterised by powder XRD and EDXA/SEM. The blue/black precipitate was annealed as described earlier.

3.25 Reaction of $TiCl_4$, $ZrCl_4$ and HMDST

HMDST (1.05 cm^3, 5.00 mmol) was added dropwise to a stirred slurry of a mixture of $TiCl_4$ (1.25 cm^3 1M in toluene, 1.25 mmol) and $ZrCl_4$ (0.29 g, 1.25 mmol) in toluene (20 cm^3). Formation of a black precipitate was observed immediately on addition of HMDST. The reaction mixture was stirred for 12 h at room temperature. The resulting black precipitate was allowed to settle and the colourless liquid was syringed off and the remaining solid was dried *in vacuo* (0.24 g).

Analytical data for the precipitate: Found C, 4.96; H, 0.66. The precipitate was also characterised by powder XRD and EDXA/SEM. The black precipitate was annealed as described earlier.

3.26 Reaction of $NbCl_5$ and HMDST under reflux

The procedure was similar to above, however, after the addition of HMDST the mixture was refluxed for 5 h. The resulting black precipitate was allowed to settle and the colourless liquid was syringed off. The remaining solid was washed twice with fresh toluene, dried *in vacuo* and isolated (0.305 g). The precipitate was then analysed by EDXA, Raman Spectroscopy and Powder XRD.

Analytical data for the precipitate: Found C, 9.49; H, 1.04. The precipitates were also characterised by powder XRD and EDXA/SEM.

Chapter 4 Transition metal thiolates as precursors to metal sulfides

In this chapter, the potential of early transition metal thiolates as precursors to thin-films of metal sulfides is explored. The decomposition pathways of the thiolate precursors, $[Et_2NH_2][Ti_2(\mu\text{-}SCH_2Ph)_3(SCH_2Ph)_6]$, $[Ti(S^tBu)_4]/[Ti(S^tBu)_3(NEt_2)]$, $[Ta(S\text{-}2,6\text{-}Me_2C_6H_3)_4(NMe_2)]$ and $[Nb(S\text{-}2,6\text{-}Me_2C_6H_3)_5]$ were explored by Thermal Gravimetric Analysis (TGA). Vapour-phase deposition studies of these compounds were carried out in order to assess the ability of the materials to produce thin-films as well as analysing the films produced. Finally, chemical vapour deposition (CVD) was carried out on the thiolate compounds at low pressure (LPCVD) and at atmospheric pressure using an aerosol-assisted technique (AACVD).

4.1 Thermal Gravimetric Analysis

Initial investigations into the suitability of the thiolates synthesised earlier as precursors to metal sulfides involved TGA of the compounds. Typically, a known amount (approximately 10 mg) of the sample was heated to a temperature of 500 °C in an aluminium boat. By measuring the weight loss upon heating the samples at a uniform rate the decomposition pathways were studied. The TGA results of $[Et_2NH_2][Ti_2(\mu\text{-}SCH_2Ph)_3(SCH_2Ph)_6]$, $[Ti(S^tBu)_4]/[Ti(S^tBu)_3(NEt_2)]$, $[Ta(S\text{-}2,6\text{-}Me_2C_6H_3)_4(NMe_2)]$ and $[Nb(S\text{-}2,6\text{-}Me_2C_6H_3)_5]$ at a heating rate of 10 °C/min from 20 to 500 °C, under N_2, are shown in Figures 4.1, 4.2, 4.3 and 4.4 respectively.

The decomposition of $[Et_2NH_2][Ti_2(\mu\text{-}SCH_2Ph)_3(SCH_2Ph)_6]$ is clean and shows a total weight loss of 73% starting at 65 °C and finishing at 400 °C (Figure 4.1). This does not indicate that decomposition to TiS_2 has occurred (where the % weight loss would be 91.2%), but that another species has formed. It is therefore unlikely that $[Et_2NH_2][Ti_2(\mu\text{-}SCH_2Ph)_3(SCH_2Ph)_6]$ will make a good precursor to thin-films of TiS_2 using thermal decomposition methods such as CVD.

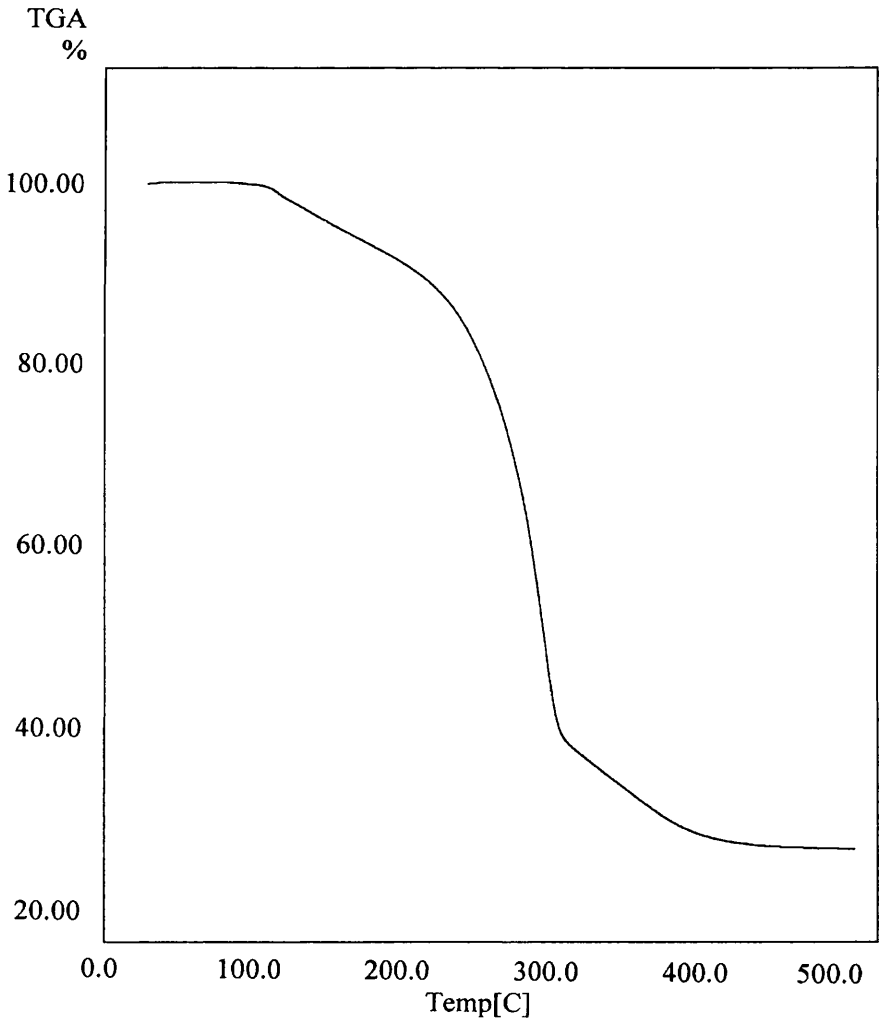

Figure 4.1 TGA of $[Et_2NH_2][Ti_2(\mu\text{-}SCH_2Ph)_3(SCH_2Ph)_6]$

The decomposition of $[Ti(S^tBu)_4]/[Ti(S^tBu)_3(NEt_2)]$ is clean and shows a weight loss of 67% starting at 75 °C and finishing at 350 °C (Figure 4.2). $[Ti(S^tBu)_4]$ decomposing to TiS_2 would result in a 72% mass loss and $[Ti(S^tBu)_3(NEt_2)]$ decomposing to TiS_2 would result in a 68.6% mass loss. Given the accuracy of the TGA used (*ca.* 2%) this behaviour indicates a good decomposition to TiS_2 up to 500 °C. However, since the material is a mixture of ill-defined proportions, an accurate interpretation of the TGA results is not possible.

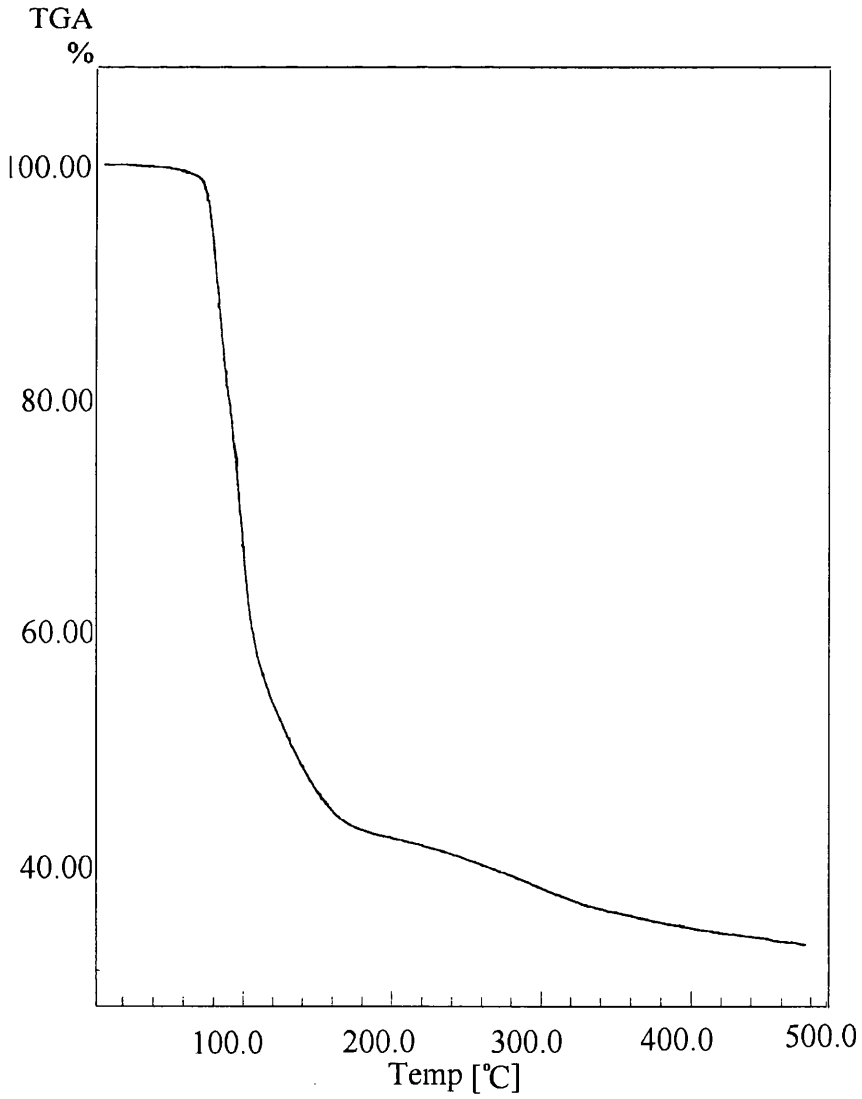

Figure 4.2 TGA of $[Ti(S^tBu)_4]/[Ti(S^tBu)_3(NEt_2)]$

The decomposition of [Ta(S-2,6-$Me_2C_6H_3)_4(NMe_2)$] has an onset temperature of 230 °C and is completed at 310 °C (Figure 4.3). The TGA shows a total weight loss of 67%. This is in good agreement with the calculated value of 68% for the formation of TaS_2 from this compound.

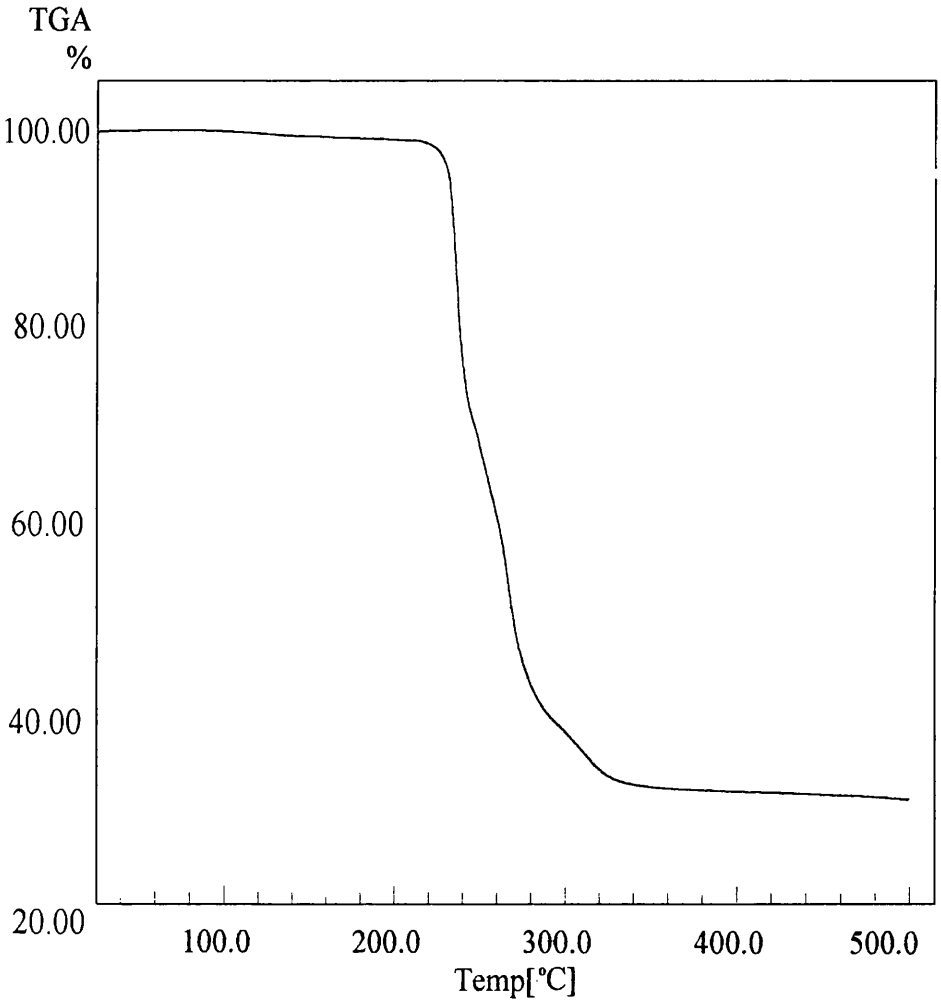

Figure 4.3 TGA of [Ta(S-2,6-$Me_2C_6H_3)_4(NEt_2)$]

The decomposition of [Nb(S-2,6-$Me_2C_6H_3)_5$] shows an onset temperature of 90 °C and is completed at 367 °C (Figure 4.4). The TGA shows a total weight loss of 72%, which is less than the calculated value of 79.8% for the formation of

NbS_2. This behaviour indicates an incomplete decomposition to NbS_2 at 500 °C has occurred.

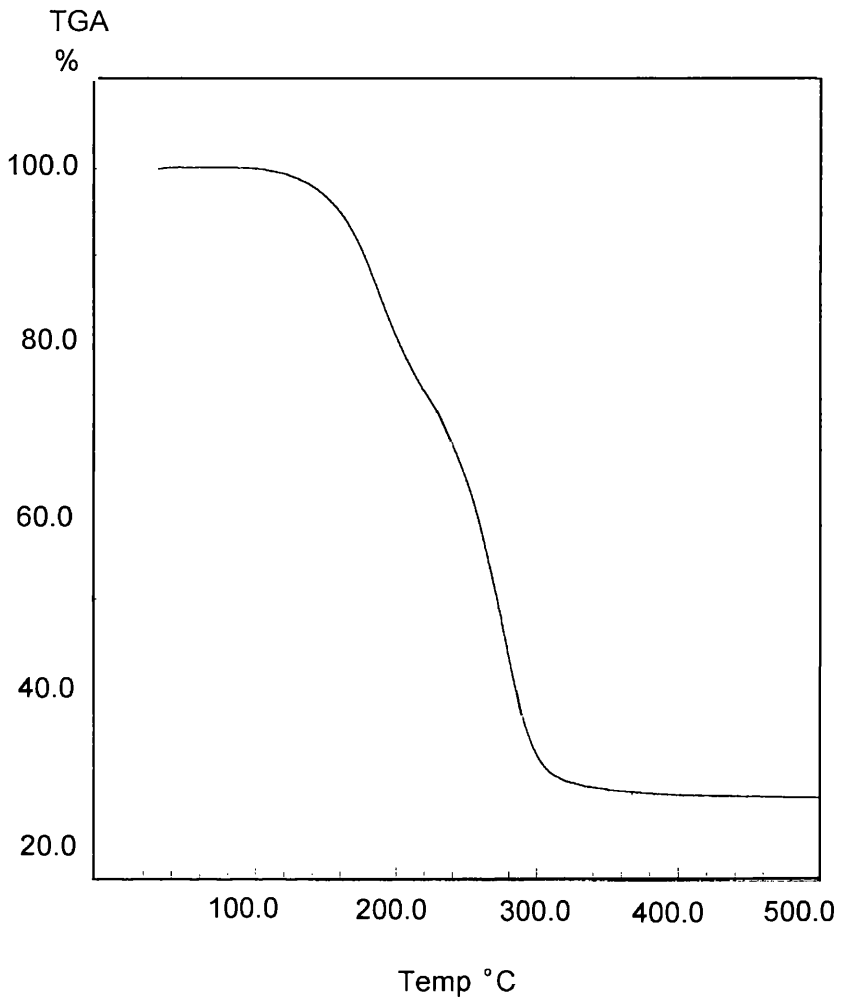

Figure 4.4 TGA of [Nb(S-2,6-$Me_2C_6H_3$)$_5$]

4.2 Vapour-phase thin-film studies

Given the results obtained from TGA, tube furnace reactions were carried out on all three of the neutral thiolates obtained ([Ti(S^{t}Bu)$_4$]/[Ti(S^{t}Bu)$_3$(NEt$_2$)], [Ta(S-2,6-$Me_2C_6H_3$)$_4$(NMe$_2$)] and [Nb(S-2,6-$Me_2C_6H_3$)$_5$]) in order to assess whether thin-films of metal sulfides could be made at low pressure. The

apparatus used is shown in Figure 4.5 and the experimental procedure is described at the end of the chapter.

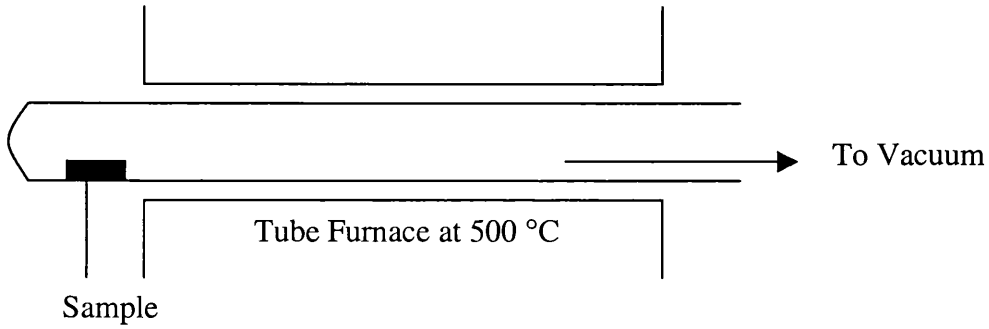

Figure 4.5 Tube furnace apparatus for vapour-phase deposition studies

In all instances a film was deposited on the inside of the hot wall glass tube. The EDXA data for the film deposited from $[Ti(S^tBu)_4]/[Ti(S^tBu)_3(NEt_2)]$ showed a 1:2 ratio of Ti:S, over a number of spots, which is in good agreement with the formation of TiS_2. The Raman spectrum of the TiS_2 film prepared here was very similar to that obtained for bulk TiS_2 with bands at 338 and 372 cm^{-1}. A UV-Vis spectrum was taken of the film. This showed that the TiS_2 film had a direct band gap of 1.9 eV (Figure 4.6). This compares well with a previous report that gave a band gap of 1.9 eV.[90] By Scanning Electron Microscopy (SEM) the TiS_2 film shows a 'crazy paving' island-growth mechanism with an island size of 0.2 μm (Fig. 4.7).

Two reports on the decomposition of $[Ti(S^tBu)_4]$ have been previously published, as described in chapter 1.[22,23] The results obtained from the vapour-phase deposition studies described above suggest the formation of TiS_2 from the

mixture $[Ti(S^tBu)_4]/[Ti(S^tBu)_3(NEt_2)]$ rather than TiS. The use of compound $[Ti(S^tBu)_3(NEt_2)]$ as the precursor has little effect on the end material obtained.

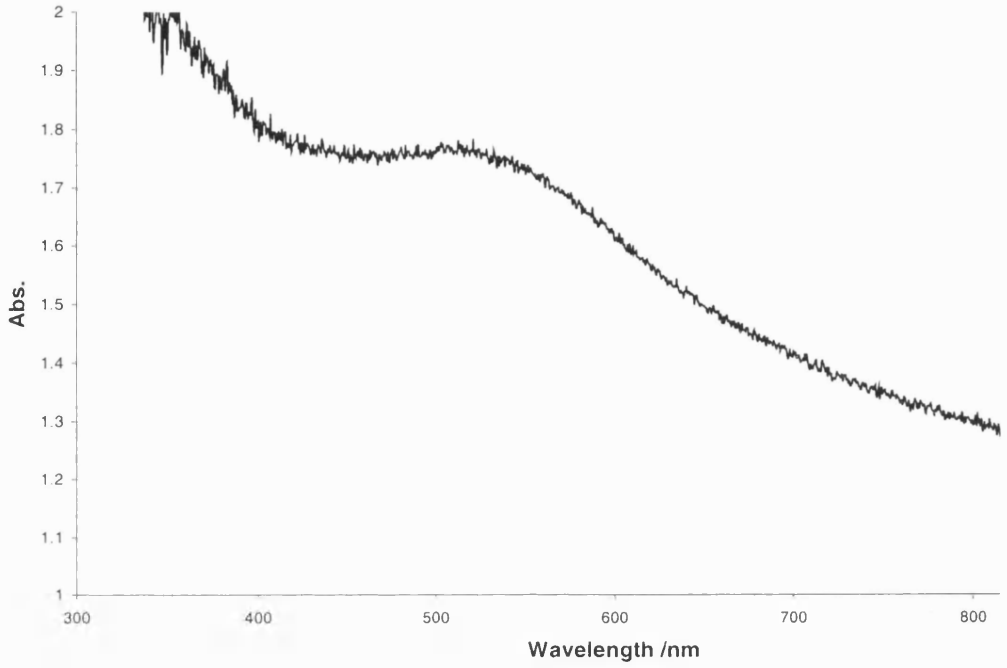

Figure 4.6 UV/Vis spectrum for TiS_2 obtained from deposition of $[Ti(S^tBu)_4]/[Ti(S^tBu)_3(NEt_2)]$

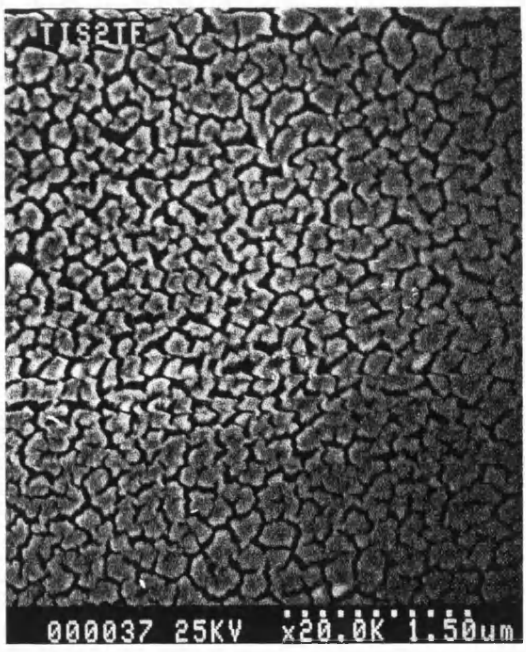

Figure 4.7 SEM of the thin-film obtained from the tube furnace reaction of $[Ti(S^tBu)_4]/[Ti(S^tBu)_3(NEt_2)]$

The EDXA data for the film deposited from [Ta(S-2,6-$Me_2C_6H_3)_4(NMe_2)$] showed a 2.5:1 ratio of Ta:S over a number of spots. This data suggests that TaS_2 has not been isolated, which is in contrast to the TGA results. It is possible that hydrolysis or oxidation of the films has occurred either during or after deposition. However, significant breakthrough of the excitation volume through the coating to the underlying glass meant that accurate quantitative analysis was difficult. The tantalum sulfide film grown showed a finer grain microstructure, by SEM, with a 0.1 μm island growth (Figure 4.8).

Figure 4.8 SEM of the thin-film obtained from the tube furnace reaction of [Ta(S-2,6-$Me_2C_6H_3)_4(NMe_2)$]

The EDXA data for the film deposited from $[Nb(S\text{-}2,6\text{-}Me_2C_6H_3)_5]$ showed a 1:1 ratio of Nb:S over a number of spots suggesting the formation of NbS. This is in contrast to the TGA results that suggest a species of larger molecular mass than NbS_2 is formed after thermal decomposition. SEM results showed an island growth of approximtely 0.2 μm (Figure 4.9).

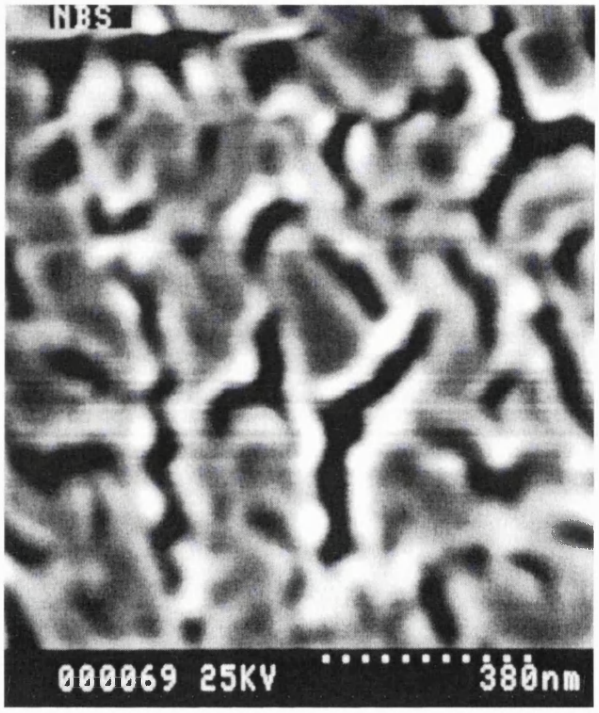

Figure 4.9 SEM of the thin-film obtained from the tube furnace reaction of $[Nb(S\text{-}2,6\text{-}Me_2C_6H_3)_5]$

It was then decided to undertake CVD studies of these compounds in order to see if sulfides could be deposited onto substrates. The first method used was LPCVD.

4.3 Low-pressure chemical vapour deposition studies

Initial efforts into LPCVD studies focussed on the design of a suitable apparatus. One of the earliest problems encountered during the design of a rig was in keeping all parts of the apparatus warm. This is important in preventing any vapour formed during the reaction from condensing before it reaches the substrate. This is a particular problem when conducting studies at low pressures. Hence, the apparatus needed to have a small width and be wrapped in heater tape to enable heating of the precursor, the substrate and also the intermediate area (along which the vapour transports). A schematic of the final apparatus used is shown below (Figure 4.10). Another problem encountered during preliminary invesigations into LPCVD was in forming thin-films on the nozzle of the apparatus due to it becoming too hot (from the graphite block). Hence, the position of the graphite block, the nozzle and the temperature of the substrate had to be carefully measured.

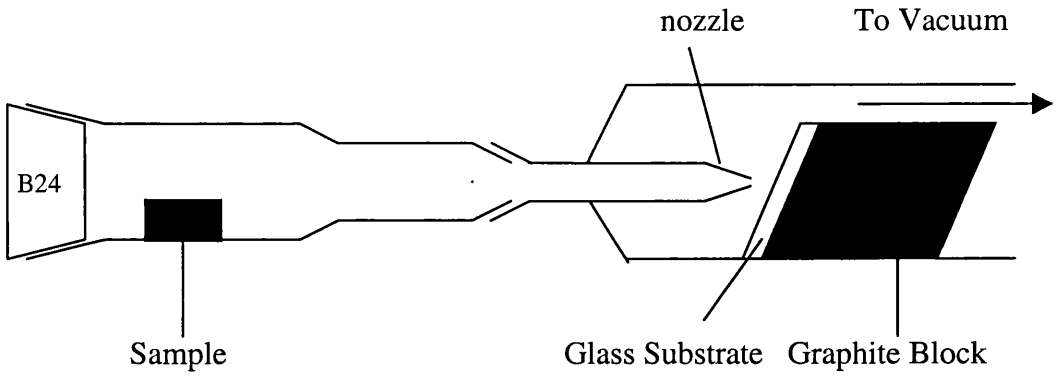

Figure 4.10 Schematic of the LPCVD rig

4.4 Results and Discussion

Depositions carried out using the precursors [Nb(S-2,6-$Me_2C_6H_3)_5$] and [Ta(S-2,6-$Me_2C_6H_3)_4(NMe_2)$] proved disappointing. Thin-films were not obtained using a variety of temperatures. Decomposition of the precursor occurred without any appreciable vapour transport occurring. One explanation for this is that the precursors were not volatile enough to produce the required vapour under the low-pressure conditions used. This is not surprising, considering the high melting points of these compounds (as described in Chapter 2). The TGA result obtained for [Ta(S-2,6-$Me_2C_6H_3)_4(NMe_2)$] also showed that the onset temperature for decomposition was 230 °C, which is high.

Studies carried out on [$Ti(S^tBu)_4$]/[$Ti(S^tBu)_3(NEt_2)$] were more successful. Thin films of a red/brown colour were produced on SnO_2-coated glass substrates at a temperature of 200 °C. The precursor was heated to a temperature of 45 °C before an appreciable vapour formed. EDXA data on the films suggested a Ti:S ratio that varied from 1:1 to 1:2 across the substrate which is in contrast to the vapour-phase studies (where TiS_2 was formed). Subsequent analysis using electron probe showed that TiS was the only phase obtained. This is similar to the previous results studied by Bochmann *et al.*[22] It is possible, however, that TiS_2 and either TiO_2 or amorphous phases of titanium sulfides have formed, e.g. by decomposition or oxidation. Raman peaks were broad and difficult to interpret. Nonetheless, the results were promising and show that [$Ti(S^tBu)_4$]/[$Ti(S^tBu)_3(NEt_2)$] can be used as a precursor to thin-films of titanium sulfides.

Finally, studies into the potential of these compounds as precursors to sulfides using aerosol-assisted CVD (AACVD) were explored.

4.5 Aerosol-assisted chemical vapour deposition studies

Deposition studies using aerosol-assisted CVD were carried out. Unfortunately this method did not produce any significant coatings, despite using a number of precursors, substrates, temperatures, flow rates and even solvents. Results using H_2S gas in the system were also unsuccessful. Possible explanations for this were that the precursors decomposed before reaching the substrate, or that pyrolysis did not occur on the substrate, for example, due to flow rates of the carrier gas being too high. It is likely that modifications to the apparatus would produce more promising results, but time constraints did not allow this.

4.6 Conclusions

Thermal Gravimetric Analysis studies showed that [Ta(S-2,6-$Me_2C_6H_3)_4(NMe_2)$] decomposes to give TaS_2. Vapour-phase deposition studies were successful in producing thin-films of TiS_2. Thin-films of NbS and Ta_2S were also made from this method.

Low-pressure chemical vapour deposition studies were successful in making thin-films of TiS from $[Ti(S^tBu)_4)]/[Ti(S^tBu)_3(NEt_2)]$. [Ta(S-2,6-$Me_2C_6H_3)_4(NMe_2)$] and [Nb(S-2,6-$Me_2C_6H_3)_5$] were not suitably volatile to give any deposition using this method. AACVD studies were

unsuccessful and modifications in the apparatus and experimental method used are probably required to produce significant results.

4.7 Experimental

4.8 Vapour-phase studies

Typically, a sample of the precursor (0.30 g) was loaded into a glass ampoule (40 cm length x 9 mm diameter) in the glovebox. The ampoule was then placed in a furnace such that 30 cm was inside the furnace and the end containing the sample protruded by 4 cm (Figure 4.5).

The ampoule was heated to a temperature of 450 °C under dynamic vacuum. The ampoule was slowly drawn into the furnace over a period of a few minutes until the sample started to melt. Once the compound had decomposed the furnace was allowed to cool to room temperature. A film resulted on the inside wall of the ampoule where the tube was in the furnace (black for $[Ta(S\text{-}2,6\text{-}Me_2C_6H_3)_4(NMe_2)]$ and $[Nb(S\text{-}2,6\text{-}Me_2C_6H_3)_5]$, purple for $[Ti(S^tBu)_4]$/$[Ti(S^tBu)_3(NEt_2)]$). The films were analysed by EDXA/SEM, Raman spectroscopy and UV/Vis.

4.9 LPCVD experiments

The sample (typically 0.1 - 0.3g) was placed in the tube as shown in Figure 4.10. The sample tube was wrapped in heater tape and a thermocouple was used in order to heat the precursor and the intermediate glassware. The tube was then attached to another tube that contained the glass substrate and the graphite heating block. A thermocouple was again used to regulate the

temperature of the graphite block and the substrate. The apparatus was sealed at one end using a B24 stopper and the other end was connected to a vacuum line. The apparatus was purged with nitrogen before adding the precursor and then evacuated to a pressure of 10^{-2} atm. The substrate was heated to a set temperature. After allowing the substrate to reach the required temperature the precursor was finally heated slowly until a vapour formed. Experiments were carried out using $[Ti(S^tBu)_4]/[Ti(S^tBu)_3(NEt_2)]$, $[Ta(S\text{-}2,6\text{-}Me_2C_6H_3)_4(NMe_2)]$ and $[Nb(S\text{-}2,6\text{-}Me_2C_6H_3)_5]$. Red/brown thin-films were obtained for $[Ti(S^tBu)_4]/[Ti(S^tBu)_3(NEt_2)]$ and were analysed by EDXA, electron probe and Raman spectroscopy. It is interesting to note that purple films of TiS[22] and grey-blue films of TiS_2[23] were made previously using this method.

4.10 AACVD experiments

Typically a sample (0.1 - 0.3 g) of the precursor was weighed out and dissolved in 50 cm^3 of CH_2Cl_2 into a specially adapted round-bottomed flask. The bottom of this flask was "thinned" in order to allow a mist to be produced. A humidifier was then placed under the flask and turned on, producing a fine mist of the solvent with the dissolved precursor. This spray was then transported *via* a flow of nitrogen gas onto the preheated glass substrate.

References

1. A. Wold and K. Dwight, Solid State Chemistry: Synthesis, Structure and Properties of Selected Oxides and Sulfides, Chapman & Hall, New York, 1993.
2. R. H. Friend and A. D. Yoffe, *Adv. Phys.*, 1987, **36**, 1.
3. Cotton and Wilkinson, Advanced Inorganic Chemistry, 4th Ed. 1980, 696.
4. G. M. Nazri, D. M. MacArthur and J. F. Ogara, *Chem. Mater.*, 1989, **1**, 370 and references therein.
5. T. S. Lewkebandara and C. H. Winter, *Adv. Mater.*, 1994, **6**, 237.
6. M. S. Wittingham, *Prog. Solid State Chem.*, 1978, **12**, 41.
7. R.C. Bill, *Wear*, 1985, **106**, 283.
8. I. L. Singer, *Mater. Res. Soc. Symp. Proc.*, 1989, **140**. 215.
9. H. Hahn and P. Ness, *Z. Anorg. Allg. Chem.*, 1959, **302**, 17.
10. G. Meunieier, R. Doromoy and A. Levasseur, *Mater. Sci. Eng.*, 1989, **B3**, 19.
11. P. J. McKarns, M. J. Heeg and C. H. Winter, *Inorg. Chem.* 1998, **37**, 4743.
12. D. Zehnder, C. Deshpandey, B. Dunn and R. F. Bunshah, *Solid State Ionics*, 1986, **18/19**, 813.
13. M. L. Hitchman and K. F. Jensen, Chemical Vapour Deposition, Principles and Applications, 1993.
14. A. Paul and J. A. Odriozola, *Mater. Sci. Eng.*, 2001, **A300**, 22.
15. T. Kodas and M. Hampden-Smith, The Chemistry of Metal CVD, VCH publishers, 1994.
16. S. Kikkawa, M. Miyazaki and M. Koizumi, *J. Mater. Res.*, 1990, **5**, 2894.

17. W. S. Rees, Jr., CVD of Nonmetals, VCH publishers, Weinheim, 1996.

18. T. S. Lewkebandara, C. H. Winter, J. W. Proscia and A. R. Rheingold, *Inorg. Chem.*, 1993, **32**, 3807.

19. A. C. Jones and P. O'Brien, CVD of Compound Semiconductors, Precursor Synthesis, Development and Applications, VCH publishers, Weinheim, 1996.

20. M. Bochmann, *Chem. Vap. Deposition.*, 1996, **2**, 85.

21. A. C. Jones, *Chem. Soc. Rev.*, 1997, 101.

22. M. Bochmann, I. Hawkins and L. M. Wilson, *Chem. Commun.*, 1988, 344.

23. J. Cheon, J. E. Gozum and G. S. Girolami, *Chem. Mater.*, 1997, **9**, 1847.

24. D. W. Stephan and T. T. Nadasdi, *Coord. Chem. Rev.*, 1996, **147**, 147

25. D. C. Bradley and P. A. Hammersley, *J. Chem. Soc. A*, 1967, 1894.

26. R. J. H. Clarke and D. Kaminaris, *Inorg. Chim. Acta.*, 1974, **11**, L7.

27. J. R. Dorfman, C. Pulla Rao and R. H. Holm, *Inorg. Chem.*,1985, **24**, 453.

28. G. A. Sigel and P. P. Power, *Inorg. Chem.*, 1987, **26**, 2819.

29. D. T. Corwin, J. F. Corning, S. A. Koch, M. Millar, *Inorg. Chim. Acta.*, 1995, **229**, 335.

30. W. Stuer, K. Kirschbaum and D. M. Giolando, *Angew. Chem. Int. Ed, Eng.*, 1994, **33**, 1981.

31. C. Puke, K. Schmengler, K. Kirschbaum, O. Conrad and G. M. Giolando, *Acta. Cryst.*, 2000, **C56**, e542.

32. J. T. Kim, J. W. Park and S. M. Koo, *Polyhedron*, 2000, **19**, 1139.

33. F. Senocq, N. Viguier and A. Gleizes, Eur. J. Solid State Inorg. Chem., 1996, **33**, 1185.

34. H. Fung and M. Hesselbarth, *Z. Chem.*, 1966, **6**, 227.

35. D. Coucouvanis, A. Hadjikyriacou, R. Lester and M. G. Kanatzidis, *Inorg. Chem.*, 1994, **33**, 3645.

36. M. Cowie and M. J. Bennett, *Inorg. Chem.,* 1976, **15**, 1595.

37. H. Kawaguchi, K. Tatsumi and R. E. Kramer, *Inorg. Chem.*, 1996, **35**, 4391.

38. C. P. Gerlach, V. Christou and J. Arnold, *Inorg. Chem.*, 1996, **35**, 2758.

39. K. Tatsumi, I. Matsubara, Y. Sekiguchi, A. Nakamura and C. Mealli, *Inorg. Chem.*, 1989, **28**, 773.

40. K. Tatsumi, Y. Sekiguchi and A. Nakamura, *J. Am. Chem. Soc.*, 1986, **108**, 1358.

41. S. M. Koo, R. Bergero, A. Saligoglou and D. Coucouvanis, *Inorg. Chem.*, 1990, **29**, 4844.

42. R. Fandos, C. Hernandez, I. Lopez-Solera, A. Otero, A. Rodriguez and M. J. Ruiz, *Organometallics*, 2000, **19**, 5318.

43. J. Curnow, M. Curtis, A. Rheingold and B. Haggerty, *Inorg. Chem.*, 1991, **30**, 4043.

44. K. Tatsumi, Y. Sekiguchi, A. Nakamura, R. E. Cramer and J. J. Rupp, *Angew. Chem., Int. Edn. Engl.*, 1986, **25**, 86.

45. P. R. Bonneau, R. F. Jarvis, R. B. Kaner, *Nature*, 1991, **349**, 510.

46. L. E. Conroy, *Inorg. Synth.*, 1970, **12**, 158.

47. R. R. Chianelli, M. B. Dines, *Inorg. Chem.*, 1978, **17**, 2758.

48. X. Chen and R. Fan, *Chem. Mater.*, 2001, **13**, 802.

49. H. Liao, Y. Wang, S. Zhang and Y. Qian, *Chem. Mater.*, 2001, **13**, 6.

50. D. C. Bradley, *Chem. Rev.*, 1989, **89**, 1317.

51. L. L. Hench and J. K. West, *Chem. Rev.*, 1990, **90**, 33.

52. M. A. Sriram and P. N. Kumta, *J. Am. Ceram. Soc.*, 1994, **77**, 1381.

53. P. N. Kumta, and M. A. Sriram, *J. Mater. Chem.*, 1994, **29**, 1135.

54. V. Stanic, T. H. Etsell, A. C. Pierre and R. J. Mikula, *J. Mater. Chem.* 1997, **7**, 105.

55. M. A. Sriram and P. N. Kumta, *J. Mater. Chem.*, 1998, **8**, 2441.

56. M. A. Sriram and P. N. Kumta, *J. Mater. Chem.*, 1998, **8**, 2453.

57. L. S. Jenkins and G. R. Willey, *J. Chem. Soc., Dalton Trans*, 1979, 1697.

58. M. J. Martin, G. -H. Qiang and D. M. Schleich, *Inorg. Chem.*, 1988, **27**, 2804.

59. A. Bensalem and D. M. Schleich, *Mat. Res. Bull.*, 1988, **23**, 857.

60. A. Bensalem and D. M. Schleich, *Mat. Res. Bull.*, 1990, **25**, 349.

61. D. M. Schleich and M. J. Martin, *J. Solid State Chemistry*, 1986, **64**, 359.

62. A. Bensalem and D. M. Schleich, *Inorg. Chem.*, 1991, **30**, 2052.

63. C. D. Chandler, C. Roger and M. J. Hampden-Smith, *Chem. Rev.*, 1993, **93**, 1205.

64. K. G. Caulton and L. G. Hubert-Pfalzgraf, *Chem. Rev.*, 1990, **90**, 969.

65. D. W. Stephan, *Coor. Chem. Rev.*, 1989, **95**, 41.

66. D. C. Bradley and I. M. Thomas, *J. Chem. Soc. A*, 1960, **82**, 3857.

67. W. Clegg, M. R. J. Elsegood, L. J. Farrugia, F. J. Lawlor, N. C. Norman and A. J. Scott, *Chem. Soc., Dalton Trans.*, 1995, 2129.

68. C. J. Carmalt, C. W. Dinnage, I. P. Parkin, A. J. P. White and D. J. Williams, *J. Chem. Soc., Dalton Trans.*, 2000, 3500.

69. R. A. Jones, S. T. Schwab and B. R. Whittlesey, *Polyhedron*, 1984, **3**, 505.

70. C. J. Carmalt, C. W. Dinnage, I. P. Parkin and J. W. Steed, *Inorg. Chem.*, 2000, **39**, 2693.

71. E. Delgado, E. Hernandez, A. Hedayat, J. Tornero and R. Torres, *J. Organomet. Chem.*, 1994, **466**, 119.

72. For an overview of interactions involving an acceptor C_6F_5 group see I. Alkorta, I. Rozas and J. Elguero, *J. Org. Chem.*, 1997, **62**, 4687.

73. I. A. Guzei, L. M. Liable-Sands, A. L. Rheingold and C. H. Winter, *Polyhedron*, 1997, **16**, 4017.

74. S. Suh, J. H. Hardesty, T. A. Albright and D. M. Hoffman, *Inorg. Chem.*, 1999, **38**, 1627.

75. C. J. Carmalt, C. W. Dinnage, I. P. Parkin, A. J. P. White and D. J. Williams, *J. Chem. Soc., Dalton Trans.*, 2001, 2558.

76. A. R. Dias, A. M. Galvao, A. C. Galvao and M. S. Salema, *J. Chem. Soc., Dalton Trans.*, 1997, 1055.

77. R. A. Jones, J. G. Hefner and T. C. Wright, *Polyhedron*, 1984, **3**, 1121.

78. D. C. Bradley and I. M. Thomas, *Can. J. Chem.*, 1962, **40**, 1355.

79. D. C. Bradley and I. M. Thomas, *Can. J. Chem.*, 1962, **40**, 449.

80. K. C. Wallace, W. M. Davis and R. R. Schrock, *Inorg. Chem.*, 1990, **29**, 1104.

81. R. R. Schrock, M. Wesolek, A. H. Liu, K. C. Wallace and J. C. Dewan, *Inorg. Chem.*, 1988, **27**, 2050.

82. D. C. Bradley, M. B. Hursthouse, A. J. Howes, A. N. de M. Jelfs, J. D. Runnacles and M. Thornton-Pett, *J. Chem. Soc., Dalton Trans.*, 1991, 841.

83. U. Zucchini, E. Albizzati and U. Giannini, *J. Organometal. Chem.*, 1971, **26**, 357.

84. C. J. Carmalt, C. W. Dinnage and I. P. Parkin, *J. Mater. Chem.*, 2000, **10**, 2823.

85. PDF –2 database 1990, International Center for Diffraction Data, Swarthmore, PA, 19081, 1990.

86. Y. Jeannin, J. Bernard and C.R. Seances, *Acad. Sci. (Paris)*, 1959, **248**, 2875.

87. D. Powell and D. Jacobson, *J. Solid State Chem.*, **37**, 140.

88. Novel Low Temperature Synthesis of Metal Sulfides, M. A. Colucci, Private Communication, University of Bath.

89. Blitz, Kocher, *Z. Anorg. Allg. Chem.*, 1938, **85**, 238.

90. R. B. Murray and A. D. Yoffe, *J. Phys.*, **C5**, 3038, 1972.

91. PDF-2 database, 1990, International Center for Diffraction Data, Swarthmore, PA, 19081,1980.

92. Z. Otwinowski and W. Minor, in Methods in Enzymology, C. Carter and R. M. Sweet, Eds., Academic Press, New York, 1996.

93. G. M. Sheldrick, SHELX-97, University of Gottingen, 1997.

List of Publications

1. C. J. Carmalt, C. W. Dinnage, I. P. Parkin and J. W. Steed, Synthesis and characterisation of a homoleptic thiolate complex of titanium (IV), *Inorg. Chem.*, 2000, **39**, 269.

2. C. J. Carmalt, C. W. Dinnage, I. P. Parkin, A. J. P. White and D. J. Williams. Synthesis and structural characterisation of titanium (IV) thiolate compounds, *J. Chem. Soc., Dalton Trans.*, 2000, 3500.

3. C. J. Carmalt, C. W. Dinnage and I. P. Parkin, Thio sol-gel synthesis of titanium sulfide from titanium thiolates, *J. Mater. Chem.*, 2000, **10**, 2823.

4. C. J. Carmalt, C. W. Dinnage, I. P. Parkin, A. J. P. White and D. J. Williams, Thiolate derivatives of titanium (IV) and tantalum (V) as precursors to metal sulfides, *J. Chem. Soc., Dalton Trans.*, 2001, 2558.

5. C. J. Carmalt, C. W. Dinnage, I. P. Parkin, M. A. Colucci, T. G. Hibbert and K. C. Molloy. The use of hexamethyldisilathiane for the synthesis of transition metal sulfides, submitted for publication, July 2001.

6. C. J. Carmalt, C. W. Dinnage, I. P. Parkin, A. J. P. White and D. J. Williams, Synthesis of a homoleptic niobium (V) thiolate complex and the preparation of

niobium sulfide via thio "sol-gel" and vapour phase thin-film experiments, to be submitted for publication.

Appendix

Table 1. Crystal data and structure refinement for anion of **1**.

Empirical formula	C68 H75 S9 Ti2	
Formula weight	1276.62	
Temperature	100(2) K	
Wavelength	0.71070 Å	
Crystal system	Monoclinic	
Space group	P21/c	
Unit cell dimensions	a = 21.573(4) Å	α = 90 °
	b = 17.224(3) Å	β = 97.29(3)°
	c = 17.577(4) Å	χ = 90 °
Volume	6479(2) $Å^3$	
Z	4	
Density (calculated)	1.309 Mg/m^3	
Absorption coefficient	0.576 mm^{-1}	
F(000)	2684	
Crystal size	0.3 x 0.1 x 0.1 mm^3	
Theta range for data collection	2.55 to 27.50 °	
Index ranges	-26<=h<=28, -22<=k<=22, -22<=l<=20	
Reflections collected	55504	
Independent reflections	14854 [R(int) = 0.064]	
Completeness to theta = 27.50 °	99.8 %	
Absorption correction	Scalepack	
Refinement method	Full-matrix least-squares on F^2	
Data / restraints / parameters	14854 / 0 / 660	
Goodness-of-fit on F^2	1.037	
Final R indices [I>2sigma(I)]	R1 = 0.0521, wR2 = 0.1162	
R indices (all data)	R1 = 0.0834, wR2 = 0.1303	
Extinction coefficient	0.00030(17)	
Largest diff. peak and hole	1.281 and -1.330 e.$Å^{-3}$	

Table 2. Atomic coordinates (x 10^4) and equivalent isotropic displacement parameters ($Å^2$ x 10^3) for anion of **1**. U(eq) is defined as one third of the trace of the orthogonalized U^{ij} tensor.

	x	y	z	U(eq)
Ti(1)	2584(1)	357(1)	4325(1)	14(1)
S(1)	1708(1)	-379(1)	4870(1)	16(1)
C(1)	1284(1)	-1052(2)	4171(2)	24(1)
Ti(2)	2564(1)	-1054(1)	5727(1)	16(1)
S(2)	2934(1)	337(1)	5760(1)	15(1)
C(2)	686(1)	-1346(2)	4428(2)	21(1)
S(3)	3138(1)	-936(1)	4563(1)	16(1)
C(3)	656(1)	-2094(2)	4729(2)	26(1)
S(4)	1888(1)	1395(1)	4289(1)	17(1)
C(4)	96(1)	-2377(2)	4933(2)	29(1)
S(5)	3447(1)	1021(1)	3998(1)	20(1)
C(5)	-435(1)	-1921(2)	4851(2)	26(1)
S(6)	2326(1)	-118(1)	3067(1)	19(1)
C(6)	-407(1)	-1171(2)	4572(2)	27(1)
S(7)	1985(1)	-981(1)	6762(1)	20(1)
C(7)	151(1)	-886(2)	4355(2)	26(1)
S(8)	2373(1)	-2400(1)	5405(1)	21(1)
C(8)	2417(1)	905(2)	6313(2)	18(1)
S(9)	3406(1)	-1438(1)	6627(1)	22(1)
C(9)	2657(1)	1714(2)	6486(2)	18(1)
C(10)	3129(1)	1845(2)	7094(2)	25(1)
C(11)	3327(2)	2594(2)	7280(2)	33(1)
C(12)	3058(2)	3220(2)	6864(2)	34(1)
C(13)	2591(2)	3097(2)	6262(2)	32(1)
C(14)	2387(2)	2342(2)	6079(2)	26(1)
C(15)	3978(1)	-777(2)	4893(2)	22(1)
C(16)	4384(1)	-1079(2)	4323(2)	20(1)
C(17)	4729(2)	-588(2)	3925(2)	37(1)
C(18)	5127(2)	-884(2)	3428(2)	48(1)
C(19)	5176(2)	-1664(2)	3320(2)	37(1)
C(20)	4830(2)	-2163(2)	3706(2)	34(1)
C(21)	4442(2)	-1876(2)	4211(2)	30(1)
C(22)	2246(1)	2281(2)	3947(2)	27(1)
C(23)	1758(1)	2855(2)	3626(2)	22(1)
C(24)	1479(2)	3347(2)	4103(2)	31(1)
C(25)	1030(2)	3872(2)	3811(3)	47(1)
C(26)	844(2)	3907(2)	3031(3)	49(1)
C(27)	1125(2)	3432(2)	2545(2)	42(1)
C(28)	1583(2)	2902(2)	2841(2)	30(1)
C(29)	3812(1)	1644(2)	4780(2)	25(1)
C(30)	4147(1)	2304(2)	4437(2)	21(1)
C(31)	3925(2)	3056(2)	4437(2)	29(1)
C(32)	4227(2)	3653(2)	4093(2)	36(1)
C(33)	4755(2)	3502(2)	3753(2)	35(1)
C(34)	4981(2)	2752(2)	3744(2)	35(1)
C(35)	4678(1)	2160(2)	4077(2)	28(1)

C(36)	1778(2)	558(2)	2522(2)	25(1)
C(37)	1484(1)	197(2)	1783(2)	23(1)
C(38)	842(2)	120(2)	1640(2)	38(1)
C(39)	569(2)	-199(3)	952(2)	52(1)
C(40)	931(2)	-457(2)	412(2)	44(1)
C(41)	1569(2)	-388(2)	550(2)	31(1)
C(42)	1844(2)	-58(2)	1228(2)	24(1)
C(43)	1212(1)	-515(2)	6635(2)	25(1)
C(44)	763(1)	-952(2)	7068(2)	20(1)
C(45)	868(1)	-1039(2)	7862(2)	24(1)
C(46)	466(2)	-1470(2)	8244(2)	28(1)
C(47)	-56(2)	-1814(2)	7841(2)	35(1)
C(48)	-175(2)	-1715(2)	7060(2)	38(1)
C(49)	233(2)	-1286(2)	6674(2)	29(1)
C(50)	3019(2)	-2814(2)	4938(2)	30(1)
C(51)	2921(1)	-3654(2)	4733(2)	26(1)
C(52)	2557(2)	-3875(2)	4061(2)	27(1)
C(53)	2478(2)	-4654(2)	3853(2)	30(1)
C(54)	2762(2)	-5221(2)	4335(2)	32(1)
C(55)	3124(2)	-5014(2)	5008(2)	31(1)
C(56)	3207(2)	-4238(2)	5201(2)	30(1)
C(57)	3604(1)	-657(2)	7318(2)	27(1)
C(58)	4225(1)	-772(2)	7806(2)	24(1)
C(59)	4764(2)	-891(2)	7463(2)	38(1)
C(60)	5340(2)	-926(2)	7898(3)	58(1)
C(61)	5387(2)	-862(3)	8680(3)	66(2)
C(62)	4853(2)	-763(2)	9042(3)	58(1)
C(63)	4268(2)	-720(2)	8596(2)	35(1)
C(3S)	2395(2)	-1797(2)	2154(2)	35(1)
C(4S)	1840(4)	-2129(2)	2491(3)	82(2)
C(1S)	3502(2)	-1494(3)	2283(3)	79(2)
C(2S)	2998(3)	-1890(3)	2638(2)	79(2)
C(5S)	1252(3)	-2019(3)	1970(4)	80(2)

Table 3. Bond lengths [Å] and angles [°] for anion of **1**.

Ti(1)-S(5)	2.3183(9)	C(32)-C(33)	1.377(5)
Ti(1)-S(4)	2.3308(9)	C(33)-C(34)	1.381(5)
Ti(1)-S(6)	2.3582(10)	C(34)-C(35)	1.381(5)
Ti(1)-S(3)	2.5364(9)	C(36)-C(37)	1.505(4)
Ti(1)-S(2)	2.5395(10)	C(37)-C(38)	1.383(4)
Ti(1)-S(1)	2.5609(9)	C(37)-C(42)	1.392(4)
S(1)-C(1)	1.847(3)	C(38)-C(39)	1.390(5)
S(1)-Ti(2)	2.5132(10)	C(39)-C(40)	1.379(5)
C(1)-C(2)	1.508(4)	C(40)-C(41)	1.372(5)
Ti(2)-S(7)	2.3366(11)	C(41)-C(42)	1.384(4)
Ti(2)-S(9)	2.3484(11)	C(43)-C(44)	1.509(4)
Ti(2)-S(8)	2.4090(10)	C(44)-C(49)	1.383(4)
Ti(2)-S(2)	2.5249(9)	C(44)-C(45)	1.393(4)
Ti(2)-S(3)	2.5295(10)	C(45)-C(46)	1.379(4)
S(2)-C(8)	1.850(3)	C(46)-C(47)	1.385(5)
C(2)-C(7)	1.391(4)	C(47)-C(48)	1.376(5)
C(2)-C(3)	1.398(4)	C(48)-C(49)	1.389(5)
S(3)-C(15)	1.853(3)	C(50)-C(51)	1.499(4)
C(3)-C(4)	1.391(4)	C(51)-C(52)	1.387(5)
S(4)-C(22)	1.846(3)	C(51)-C(56)	1.394(4)
C(4)-C(5)	1.382(4)	C(52)-C(53)	1.395(4)
S(5)-C(29)	1.841(3)	C(53)-C(54)	1.383(5)
C(5)-C(6)	1.385(5)	C(54)-C(55)	1.379(5)
S(6)-C(36)	1.839(3)	C(55)-C(56)	1.384(5)
C(6)-C(7)	1.397(4)	C(57)-C(58)	1.509(4)
S(7)-C(43)	1.838(3)	C(58)-C(63)	1.383(5)
S(8)-C(50)	1.848(3)	C(58)-C(59)	1.391(4)
C(8)-C(9)	1.503(4)	C(59)-C(60)	1.375(5)
S(9)-C(57)	1.827(3)	C(60)-C(61)	1.370(7)
C(9)-C(14)	1.384(4)	C(61)-C(62)	1.394(7)
C(9)-C(10)	1.398(4)	C(62)-C(63)	1.401(5)
C(10)-C(11)	1.385(4)	C(3S)-C(2S)	1.470(6)
C(11)-C(12)	1.388(5)	C(3S)-C(4S)	1.513(7)
C(12)-C(13)	1.381(5)	C(4S)-C(5S)	1.479(8)
C(13)-C(14)	1.397(4)	C(1S)-C(2S)	1.486(8)
C(15)-C(16)	1.504(4)		
C(16)-C(17)	1.376(4)	S(5)-Ti(1)-S(4)	98.64(3)
C(16)-C(21)	1.394(4)	S(5)-Ti(1)-S(6)	92.27(4)
C(17)-C(18)	1.396(5)	S(4)-Ti(1)-S(6)	99.54(4)
C(18)-C(19)	1.364(5)	S(5)-Ti(1)-S(3)	95.66(3)
C(19)-C(20)	1.373(5)	S(4)-Ti(1)-S(3)	165.02(3)
C(20)-C(21)	1.387(4)	S(6)-Ti(1)-S(3)	84.26(3)
C(22)-C(23)	1.503(4)	S(5)-Ti(1)-S(2)	96.14(4)
C(23)-C(24)	1.383(4)	S(4)-Ti(1)-S(2)	98.44(3)
C(23)-C(28)	1.385(5)	S(6)-Ti(1)-S(2)	158.75(3)
C(24)-C(25)	1.374(5)	S(3)-Ti(1)-S(2)	75.53(3)
C(25)-C(26)	1.380(6)	S(5)-Ti(1)-S(1)	172.34(3)
C(26)-C(27)	1.379(6)	S(4)-Ti(1)-S(1)	83.45(3)
C(27)-C(28)	1.395(5)	S(6)-Ti(1)-S(1)	94.65(3)
C(29)-C(30)	1.512(4)	S(3)-Ti(1)-S(1)	81.79(3)
C(30)-C(31)	1.382(4)	S(2)-Ti(1)-S(1)	76.23(3)
C(30)-C(35)	1.398(4)	C(1)-S(1)-Ti(2)	111.91(11)
C(31)-C(32)	1.396(5)	C(1)-S(1)-Ti(1)	112.91(10)
		Ti(2)-S(1)-Ti(1)	86.14(3)

C(2)-C(1)-S(1)	112.5(2)	C(24)-C(23)-C(22)	120.9(3)
S(7)-Ti(2)-S(9)	86.26(3)	C(28)-C(23)-C(22)	120.2(3)
S(7)-Ti(2)-S(8)	98.20(3)	C(25)-C(24)-C(23)	121.1(3)
S(9)-Ti(2)-S(8)	88.96(3)	C(24)-C(25)-C(26)	120.2(4)
S(7)-Ti(2)-S(1)	91.00(3)	C(27)-C(26)-C(25)	119.6(3)
S(9)-Ti(2)-S(1)	168.63(3)	C(26)-C(27)-C(28)	120.2(4)
S(8)-Ti(2)-S(1)	102.35(3)	C(23)-C(28)-C(27)	120.0(3)
S(7)-Ti(2)-S(2)	97.41(3)	C(30)-C(29)-S(5)	108.8(2)
S(9)-Ti(2)-S(2)	92.05(3)	C(31)-C(30)-C(35)	118.0(3)
S(8)-Ti(2)-S(2)	164.39(3)	C(31)-C(30)-C(29)	121.4(3)
S(1)-Ti(2)-S(2)	77.35(3)	C(35)-C(30)-C(29)	120.5(3)
S(7)-Ti(2)-S(3)	171.75(3)	C(30)-C(31)-C(32)	120.7(3)
S(9)-Ti(2)-S(3)	98.68(3)	C(33)-C(32)-C(31)	120.4(3)
S(8)-Ti(2)-S(3)	88.53(3)	C(32)-C(33)-C(34)	119.7(3)
S(1)-Ti(2)-S(3)	82.87(3)	C(33)-C(34)-C(35)	119.9(3)
S(2)-Ti(2)-S(3)	75.91(3)	C(34)-C(35)-C(30)	121.4(3)
C(8)-S(2)-Ti(2)	107.71(9)	C(37)-C(36)-S(6)	111.2(2)
C(8)-S(2)-Ti(1)	113.06(10)	C(38)-C(37)-C(42)	118.5(3)
Ti(2)-S(2)-Ti(1)	86.35(3)	C(38)-C(37)-C(36)	120.0(3)
C(7)-C(2)-C(3)	118.8(3)	C(42)-C(37)-C(36)	121.5(3)
C(7)-C(2)-C(1)	120.8(3)	C(37)-C(38)-C(39)	120.0(3)
C(3)-C(2)-C(1)	120.3(3)	C(40)-C(39)-C(38)	120.8(3)
C(15)-S(3)-Ti(2)	108.62(10)	C(41)-C(40)-C(39)	119.6(3)
C(15)-S(3)-Ti(1)	110.07(10)	C(40)-C(41)-C(42)	119.9(3)
Ti(2)-S(3)-Ti(1)	86.32(3)	C(41)-C(42)-C(37)	121.1(3)
C(4)-C(3)-C(2)	120.3(3)	C(44)-C(43)-S(7)	110.6(2)
C(22)-S(4)-Ti(1)	110.32(10)	C(49)-C(44)-C(45)	118.4(3)
C(5)-C(4)-C(3)	120.6(3)	C(49)-C(44)-C(43)	119.9(3)
C(29)-S(5)-Ti(1)	112.52(10)	C(45)-C(44)-C(43)	121.7(3)
C(4)-C(5)-C(6)	119.6(3)	C(46)-C(45)-C(44)	120.8(3)
C(36)-S(6)-Ti(1)	109.21(10)	C(45)-C(46)-C(47)	120.2(3)
C(5)-C(6)-C(7)	120.2(3)	C(48)-C(47)-C(46)	119.5(3)
C(43)-S(7)-Ti(2)	119.64(10)	C(47)-C(48)-C(49)	120.3(3)
C(2)-C(7)-C(6)	120.5(3)	C(44)-C(49)-C(48)	120.7(3)
C(50)-S(8)-Ti(2)	111.09(10)	C(51)-C(50)-S(8)	112.8(2)
C(9)-C(8)-S(2)	112.41(18)	C(52)-C(51)-C(56)	117.8(3)
C(57)-S(9)-Ti(2)	109.66(10)	C(52)-C(51)-C(50)	121.1(3)
C(14)-C(9)-C(10)	119.1(3)	C(56)-C(51)-C(50)	121.1(3)
C(14)-C(9)-C(8)	120.5(3)	C(51)-C(52)-C(53)	121.5(3)
C(10)-C(9)-C(8)	120.2(3)	C(54)-C(53)-C(52)	119.3(3)
C(11)-C(10)-C(9)	120.3(3)	C(55)-C(54)-C(53)	120.1(3)
C(10)-C(11)-C(12)	120.2(3)	C(54)-C(55)-C(56)	120.0(3)
C(13)-C(12)-C(11)	120.0(3)	C(55)-C(56)-C(51)	121.2(3)
C(12)-C(13)-C(14)	119.8(3)	C(58)-C(57)-S(9)	113.4(2)
C(9)-C(14)-C(13)	120.6(3)	C(63)-C(58)-C(59)	119.4(3)
C(16)-C(15)-S(3)	111.7(2)	C(63)-C(58)-C(57)	120.3(3)
C(17)-C(16)-C(21)	118.0(3)	C(59)-C(58)-C(57)	120.2(3)
C(17)-C(16)-C(15)	121.6(3)	C(60)-C(59)-C(58)	120.8(4)
C(21)-C(16)-C(15)	120.3(3)	C(61)-C(60)-C(59)	120.0(4)
C(16)-C(17)-C(18)	120.6(3)	C(60)-C(61)-C(62)	120.5(4)
C(19)-C(18)-C(17)	120.8(3)	C(61)-C(62)-C(63)	119.3(4)
C(18)-C(19)-C(20)	119.5(3)	C(58)-C(63)-C(62)	119.9(4)
C(19)-C(20)-C(21)	120.2(3)	C(2S)-C(3S)-C(4S)	114.7(4)
C(20)-C(21)-C(16)	121.0(3)	C(5S)-C(4S)-C(3S)	111.5(4)
C(23)-C(22)-S(4)	111.3(2)	C(3S)-C(2S)-C(1S)	110.4(4)
C(24)-C(23)-C(28)	118.9(3)		

Symmetry transformations used to generate equivalent atoms:

Table 4. Anisotropic displacement parameters ($Å^2 \times 10^3$) for anion of **1**. The anisotropic displacement factor exponent takes the form: $-2\pi^2[h^2a^{*2}U^{11} + ... + 2\ hka^*b^*U^{12}]$

	U^{11}	U^{22}	U^{33}	U^{23}	U^{13}	U^{12}
C(1)	22(1)	31(2)	18(2)	-4(1)	3(1)	-6(1)
C(2)	20(1)	25(2)	19(2)	-7(1)	3(1)	-7(1)
C(3)	24(2)	21(2)	36(2)	-8(1)	9(1)	0(1)
C(4)	28(2)	22(2)	38(2)	-5(1)	9(1)	-5(1)
C(5)	20(1)	33(2)	26(2)	-7(1)	6(1)	-9(1)
C(6)	20(1)	34(2)	25(2)	-2(1)	-1(1)	2(1)
C(7)	28(2)	26(2)	22(2)	4(1)	-3(1)	-2(1)
C(8)	21(1)	18(1)	16(1)	-2(1)	8(1)	0(1)
C(9)	20(1)	15(1)	19(2)	-6(1)	7(1)	-1(1)
C(10)	24(2)	23(2)	29(2)	-9(1)	0(1)	3(1)
C(11)	23(2)	33(2)	40(2)	-16(2)	-2(1)	2(1)
C(12)	33(2)	23(2)	47(2)	-12(2)	7(2)	-7(1)
C(13)	45(2)	18(2)	34(2)	-2(1)	5(2)	1(2)
C(14)	32(2)	21(2)	23(2)	-5(1)	0(1)	-2(1)
C(15)	20(1)	24(2)	22(2)	-3(1)	1(1)	2(1)
C(16)	17(1)	24(2)	20(2)	3(1)	2(1)	2(1)
C(17)	30(2)	28(2)	57(2)	9(2)	20(2)	4(2)
C(18)	41(2)	46(2)	63(3)	20(2)	33(2)	7(2)
C(19)	27(2)	53(2)	32(2)	0(2)	12(1)	12(2)
C(20)	30(2)	31(2)	41(2)	-11(2)	7(2)	2(2)
C(21)	29(2)	25(2)	38(2)	0(1)	14(1)	-2(1)
C(22)	21(1)	19(1)	41(2)	9(1)	8(1)	1(1)
C(23)	23(1)	14(1)	30(2)	4(1)	5(1)	-2(1)
C(24)	33(2)	26(2)	34(2)	-4(1)	2(1)	2(1)
C(25)	43(2)	27(2)	69(3)	-5(2)	7(2)	13(2)
C(26)	35(2)	27(2)	81(3)	19(2)	-5(2)	8(2)
C(27)	47(2)	37(2)	37(2)	21(2)	-11(2)	-15(2)
C(28)	38(2)	24(2)	30(2)	5(1)	7(1)	-7(1)
C(29)	28(2)	26(2)	21(2)	1(1)	3(1)	-5(1)
C(30)	22(1)	22(2)	19(2)	2(1)	-1(1)	-1(1)
C(31)	27(2)	27(2)	34(2)	-2(1)	8(1)	-2(1)
C(32)	39(2)	22(2)	46(2)	1(2)	4(2)	-5(2)
C(33)	42(2)	32(2)	33(2)	3(2)	7(2)	-16(2)
C(34)	26(2)	45(2)	37(2)	4(2)	10(2)	-6(2)
C(35)	23(2)	28(2)	34(2)	3(1)	5(1)	-1(1)
C(36)	32(2)	21(2)	21(2)	-3(1)	-3(1)	9(1)
C(37)	31(2)	19(1)	18(2)	1(1)	0(1)	3(1)
C(38)	28(2)	56(2)	30(2)	-4(2)	3(1)	3(2)
C(39)	27(2)	83(3)	44(2)	-8(2)	-4(2)	-6(2)
C(40)	47(2)	58(2)	25(2)	-11(2)	-7(2)	-11(2)
C(41)	43(2)	28(2)	21(2)	-3(1)	6(1)	1(2)
C(42)	30(2)	20(1)	22(2)	1(1)	4(1)	-2(1)
C(43)	27(2)	21(2)	29(2)	6(1)	11(1)	6(1)

C(44)	21(1)	19(1)	21(2)	1(1)	7(1)	4(1)
C(45)	26(2)	25(2)	23(2)	-1(1)	5(1)	-1(1)
C(46)	34(2)	33(2)	20(2)	4(1)	10(1)	2(2)
C(47)	31(2)	38(2)	38(2)	1(2)	14(2)	-11(2)
C(48)	29(2)	46(2)	39(2)	-4(2)	1(2)	-14(2)
C(49)	31(2)	35(2)	20(2)	-2(1)	-1(1)	0(1)
C(50)	34(2)	19(2)	42(2)	-3(1)	19(2)	0(1)
C(51)	30(2)	18(2)	31(2)	-3(1)	15(1)	0(1)
C(52)	31(2)	23(2)	29(2)	6(1)	10(1)	7(1)
C(53)	27(2)	35(2)	29(2)	-7(1)	6(1)	2(2)
C(54)	29(2)	21(2)	48(2)	-8(2)	7(2)	0(1)
C(55)	32(2)	20(2)	41(2)	9(1)	0(2)	6(1)
C(56)	34(2)	28(2)	27(2)	1(1)	1(1)	3(1)
C(57)	27(2)	31(2)	21(2)	-2(1)	1(1)	7(1)
C(58)	25(2)	20(1)	24(2)	3(1)	-3(1)	0(1)
C(59)	28(2)	38(2)	49(2)	15(2)	8(2)	4(2)
C(60)	21(2)	46(2)	105(4)	22(3)	-2(2)	-1(2)
C(61)	38(2)	48(3)	101(4)	-6(3)	-38(3)	3(2)
C(62)	73(3)	46(2)	46(3)	-12(2)	-32(2)	14(2)
C(63)	40(2)	28(2)	33(2)	-6(2)	-6(2)	8(2)
C(3S)	82(3)	13(1)	12(2)	-1(1)	11(2)	17(2)
C(4S)	196(7)	18(2)	44(3)	-8(2)	68(4)	-9(3)
C(1S)	76(3)	96(4)	53(3)	-40(3)	-34(3)	59(3)
C(2S)	144(5)	67(3)	24(2)	-12(2)	0(3)	70(4)
C(5S)	121(5)	32(2)	105(5)	-3(3)	79(4)	-16(3)

Table 5. Hydrogen coordinates (x 10^4) and isotropic displacement parameters ($Å^2$x 10^3) for anion of **1**.

	x	y	z	U(eq)
H(1A)	1185	-783	3672	28
H(1B)	1557	-1500	4092	28
H(3)	1019	-2411	4794	32
H(4)	79	-2889	5131	35
H(5)	-817	-2120	4985	32
H(6)	-767	-850	4528	32
H(7)	166	-374	4157	31
H(8A)	1995	935	6018	22
H(8B)	2378	633	6801	22
H(10)	3316	1419	7380	30
H(11)	3647	2680	7694	39
H(12)	3194	3733	6993	41
H(13)	2409	3524	5973	39
H(14)	2060	2259	5672	31
H(15A)	4056	-215	4972	26
H(15B)	4091	-1042	5391	26
H(17)	4696	-42	3988	44
H(18)	5367	-537	3163	57
H(19)	5448	-1861	2981	44
H(20)	4857	-2707	3628	40
H(21)	4211	-2226	4484	35
H(22A)	2519	2522	4378	32
H(22B)	2509	2140	3546	32
H(24)	1599	3323	4641	38
H(25)	849	4211	4147	56
H(26)	524	4257	2831	58
H(27)	1007	3464	2007	50
H(28)	1774	2574	2505	36
H(29A)	3489	1853	5076	30
H(29B)	4113	1338	5132	30
H(31)	3563	3168	4674	35
H(32)	4067	4167	4093	43
H(33)	4963	3911	3526	42
H(34)	5345	2644	3509	42
H(35)	4833	1645	4061	34
H(36A)	1447	705	2836	30
H(36B)	2004	1035	2407	30
H(38)	587	285	2013	45
H(39)	126	-240	854	62
H(40)	740	-681	-54	53
H(41)	1822	-566	181	37
H(42)	2285	-4	1316	29
H(43A)	1251	27	6823	30
H(43B)	1049	-502	6083	30
H(45)	1221	-798	8144	29
H(46)	547	-1530	8784	34
H(47)	-330	-2117	8103	42

H(48)	-537	-1940	6782	45
H(49)	147	-1220	6135	35
H(50A)	3061	-2515	4466	36
H(50B)	3414	-2759	5287	36
H(52)	2356	-3486	3733	33
H(53)	2232	-4793	3386	36
H(54)	2707	-5753	4202	39
H(55)	3316	-5404	5340	38
H(56)	3464	-4102	5661	36
H(57A)	3614	-159	7037	32
H(57B)	3272	-618	7657	32
H(59)	4734	-949	6922	46
H(60)	5706	-994	7656	70
H(61)	5786	-886	8978	80
H(62)	4887	-724	9584	70
H(63)	3901	-655	8837	42
H(3S1)	2421	-2051	1653	42
H(3S2)	2321	-1237	2055	42
H(4S1)	1908	-2691	2589	98
H(4S2)	1804	-1873	2987	98
H(1S1)	3541	-1730	1784	118
H(1S2)	3899	-1548	2619	118
H(1S3)	3400	-942	2213	118
H(2S1)	3097	-2450	2701	95
H(2S2)	2971	-1667	3151	95
H(5S1)	1184	-1464	1870	121
H(5S2)	902	-2230	2209	121
H(5S3)	1281	-2289	1485	121

Table 1. Crystal data and structure refinement for **2**.

Empirical formula	[C30 F25 S5 Ti][C6 F5S]2[Et2 NH2]3
Formula weight	1664.18
Temperature	183(2) K
Diffractometer Used	Siemens P4/RA
Wavelength	1.54178 Å
Crystal system	Monoclinic
Space group	P21/c
Unit cell dimensions	a = 9.9531(9) Å α = 90 °
	b = 31.429(2) Å β = 91.577(8) °
	c = 21.014(2) Å χ = 90 °
Volume	6571.2(10) $Å^3$
Z	4
Density (calculated)	1.682 Mg/m^{-1}
Absorption coefficient	4.475 mm^{-1}
F(000)	3320
Crystal colour/morphology	Deep red platy needles
Crystal size	0.57 x 0.21 x 0.06 mm^3
Theta range for data collection	2.53 to 60.01 °
Limiting indices	-8<=h<=11, -27<=k<=35,
	-23<=l<=14
Scan type	ω-scans
Reflections collected	10236
Independent reflections	9610 (R(int) = 0.0313)
Observed reflections [F>4sigma(F)]	6536
Absorption correction	Empirical
Max. and min. transmission	0.7312 and 0.2859
Structure solution method	Direct
Refinement method	Full-matrix least-squares on F^2
Data / restraints / parameters	8670 / 0 / 902
Goodness-of-fit on F^2	1.041
Final R indices [F>4sigma(F)]	R1 = 0.0536, wR2 = 0.1227
R indices (all data)	R1 = 0.0933, wR2 = 0.1477
Extinction coefficient	0.00007(3)
Largest diff. peak and hole	0.557 and -0.320 $eÅ^{-3}$
Mean and maximum shift/error	0.000 and -0.001

Table 2. Atomic coordinates [x 10^4], equivalent isotropic displacement parameters [$Å^2$ x 10^3] and site occupancy factors for **2**. U(eq) is defined as one third of the trace of the orthogonalized U^{ij} tensor.

	x	y	z	U(eq)	sof
Ti	2500(1)	7228(1)	8523(1)	35(1)	1
S(1)	2997(1)	7220(1)	7419(1)	37(1)	1
S(2)	1721(1)	7204(1)	9596(1)	45(1)	1
S(3)	212(1)	7174(1)	8229(1)	56(1)	1
S(4)	3620(1)	6577(1)	8705(1)	45(1)	1
S(5)	3662(1)	7854(1)	8817(1)	50(1)	1
C(1)	1801(5)	7908(2)	6817(2)	41(1)	1
F(1)	2756(4)	8156(1)	7096(2)	63(1)	1
C(2)	904(6)	8104(2)	6394(2)	53(2)	1
F(2)	1005(5)	8523(1)	6273(2)	80(1)	1
C(3)	-74(6)	7868(2)	6085(2)	53(2)	1
F(3)	-933(4)	8056(2)	5680(2)	78(1)	1
C(4)	-131(6)	7446(2)	6199(2)	57(2)	1
F(4)	-1074(4)	7206(2)	5898(2)	84(1)	1
C(5)	781(5)	7251(2)	6617(2)	46(1)	1
F(5)	692(4)	6830(1)	6697(2)	70(1)	1
C(6)	1776(5)	7482(2)	6941(2)	33(1)	1
C(7)	3907(5)	7149(2)	10427(2)	42(1)	1
F(7)	4016(4)	6740(1)	10266(2)	74(1)	1
C(8)	4829(5)	7309(2)	10867(2)	52(2)	1
F(8)	5803(4)	7057(2)	11115(2)	90(1)	1
C(9)	4804(6)	7722(2)	11031(2)	61(2)	1
F(9)	5735(4)	7885(2)	11435(2)	97(2)	1
C(10)	3830(8)	7981(2)	10778(3)	63(2)	1
F(10)	3754(7)	8391(1)	10934(2)	112(2)	1
C(11)	2883(6)	7817(2)	10352(2)	46(1)	1
F(11)	1892(5)	8069(1)	10133(2)	82(1)	1
C(12)	2923(5)	7403(2)	10150(2)	35(1)	1
C(13)	-722(6)	7939(2)	8681(3)	54(1)	1
F(13)	143(5)	8128(2)	8292(2)	94(1)	1
C(14)	-1538(7)	8194(2)	9030(3)	70(2)	1
F(14)	-1475(6)	8619(2)	8979(3)	116(2)	1
C(15)	-2429(7)	8013(3)	9433(3)	71(2)	1
F(15)	-3241(5)	8253(2)	9779(2)	122(2)	1
C(16)	-2509(6)	7576(3)	9477(3)	61(2)	1
F(16)	-3372(4)	7395(2)	9862(2)	106(2)	1
C(17)	-1679(5)	7328(2)	9110(2)	48(1)	1
F(17)	-1793(4)	6908(1)	9167(2)	75(1)	1
C(18)	-760(5)	7503(2)	8712(2)	41(1)	1
C(19)	2946(6)	6179(2)	7575(3)	50(1)	1
F(19)	1665(3)	6220(1)	7746(2)	57(1)	1
C(20)	3178(7)	5988(2)	7004(3)	59(2)	1
F(20)	2162(5)	5849(1)	6632(2)	85(1)	1
C(21)	4453(8)	5941(2)	6805(3)	68(2)	1
F(21)	4725(6)	5764(1)	6247(2)	102(2)	1
C(22)	5498(7)	6088(2)	7187(3)	70(2)	1
F(22)	6776(5)	6047(2)	7000(2)	108(2)	1
C(23)	5259(6)	6280(2)	7763(3)	54(1)	1
F(23)	6306(4)	6414(2)	8126(2)	78(1)	1
C(24)	3963(5)	6337(2)	7975(2)	42(1)	1
C(25)	5783(5)	7722(2)	7994(2)	40(1)	1
F(25)	5764(3)	7307(1)	8162(1)	51(1)	1
C(26)	6754(5)	7848(2)	7582(2)	45(1)	1

F(26)	7606(3)	7567(1)	7346(2)	64(1)	1
C(27)	6832(6)	8271(2)	7420(2)	57(2)	1
F(27)	7784(4)	8396(1)	7017(2)	77(1)	1
C(28)	5972(7)	8556(2)	7674(3)	58(2)	1
F(28)	6059(5)	8970(1)	7516(2)	92(1)	1
C(29)	4991(6)	8422(2)	8072(2)	52(1)	1
F(29)	4146(5)	8716(1)	8294(2)	80(1)	1
C(30)	4872(5)	8000(2)	8260(2)	41(1)	1
S(6)	426(1)	4811(1)	8989(1)	43(1)	1
C(41)	2942(6)	5090(2)	8693(2)	46(1)	1
F(41)	2410(3)	5480(1)	8609(2)	57(1)	1
C(42)	4310(6)	5050(2)	8606(2)	53(1)	1
F(42)	5042(4)	5387(1)	8440(2)	71(1)	1
C(43)	4897(6)	4659(2)	8675(3)	60(2)	1
F(43)	6232(4)	4617(2)	8570(2)	85(1)	1
C(44)	4149(7)	4314(2)	8836(3)	61(2)	1
F(44)	4727(5)	3933(1)	8898(2)	87(1)	1
C(45)	2794(7)	4360(2)	8929(2)	53(1)	1
F(45)	2092(4)	4017(1)	9092(2)	64(1)	1
C(46)	2144(5)	4751(2)	8867(2)	40(1)	1
S(7)	549(1)	4856(1)	6078(1)	39(1)	1
C(51)	3034(5)	4858(2)	6697(2)	38(1)	1
F(51)	2402(3)	4958(1)	7236(1)	55(1)	1
C(52)	4418(5)	4830(2)	6737(2)	43(1)	1
F(52)	5094(3)	4904(1)	7281(1)	63(1)	1
C(53)	5114(5)	4725(2)	6204(2)	46(1)	1
F(53)	6471(3)	4709(1)	6234(2)	70(1)	1
C(54)	4430(6)	4650(2)	5644(3)	54(1)	1
F(54)	5101(4)	4551(2)	5116(2)	81(1)	1
C(55)	3058(5)	4694(2)	5616(2)	48(1)	1
F(55)	2440(3)	4638(1)	5042(1)	70(1)	1
C(56)	2297(5)	4798(2)	6133(2)	36(1)	1
N(60)	431(4)	5726(1)	5201(2)	41(1)	1
C(61)	1807(5)	5758(2)	4943(3)	54(1)	1
C(62)	1849(7)	6048(2)	4377(3)	71(2)	1
C(63)	-48(6)	6127(2)	5500(3)	51(1)	1
C(64)	-1294(7)	6065(2)	5870(3)	69(2)	1
N(70)	-602(4)	4804(1)	7517(2)	41(1)	1
C(71)	-1287(6)	4384(2)	7465(3)	55(1)	1
C(72)	-279(9)	4035(2)	7452(3)	77(2)	1
C(73)	-1495(5)	5184(2)	7525(3)	51(1)	1
C(74)	-664(7)	5576(2)	7621(3)	65(2)	1
N(80)	54(6)	5740(2)	9715(2)	57(1)	1
C(81)	1274(9)	6011(2)	9805(3)	85(3)	1
C(82)	2390(9)	5770(3)	10123(4)	92(3)	1
C(83)	-1138(9)	5967(2)	9439(3)	83(3)	1
C(84)	-2314(9)	5681(3)	9334(4)	100(3)	1

Table 3. Bond lengths [Å] and angles [°] for **2**.

Ti-S(1)	2.3860(13)	C(27)-F(27)	1.345(6)
Ti-S(2)	2.4058(13)	C(27)-C(28)	1.359(9)
Ti-S(3)	2.350(2)	C(28)-F(28)	1.344(7)
Ti-S(4)	2.356(2)	C(28)-C(29)	1.370(8)
Ti-S(5)	2.357(2)	C(29)-F(29)	1.344(7)
S(1)-C(6)	1.760(5)	C(29)-C(30)	1.388(8)
S(2)-C(12)	1.762(5)	S(6)-C(46)	1.746(6)
S(3)-C(18)	1.757(5)	C(41)-F(41)	1.344(6)
S(4)-C(24)	1.751(5)	C(41)-C(42)	1.385(8)
S(5)-C(30)	1.763(5)	C(41)-C(46)	1.385(8)
C(1)-F(1)	1.351(6)	C(42)-F(42)	1.337(7)
C(1)-C(6)	1.364(7)	C(42)-C(43)	1.366(9)
C(1)-C(2)	1.386(7)	C(43)-F(43)	1.359(7)
C(2)-F(2)	1.345(7)	C(43)-C(44)	1.362(10)
C(2)-C(3)	1.372(9)	C(44)-F(44)	1.333(7)
C(3)-F(3)	1.328(6)	C(44)-C(45)	1.375(9)
C(3)-C(4)	1.348(10)	C(45)-F(45)	1.334(7)
C(4)-F(4)	1.349(7)	C(45)-C(46)	1.394(8)
C(4)-C(5)	1.388(8)	S(7)-C(56)	1.751(5)
C(5)-F(5)	1.336(7)	C(51)-F(51)	1.348(5)
C(5)-C(6)	1.392(7)	C(51)-C(52)	1.380(7)
C(7)-F(7)	1.334(6)	C(51)-C(56)	1.389(7)
C(7)-C(8)	1.380(8)	C(52)-F(52)	1.331(6)
C(7)-C(12)	1.381(7)	C(52)-C(53)	1.373(7)
C(8)-F(8)	1.345(7)	C(53)-F(53)	1.352(6)
C(8)-C(9)	1.344(10)	C(53)-C(54)	1.363(8)
C(9)-F(9)	1.341(7)	C(54)-F(54)	1.347(6)
C(9)-C(10)	1.363(10)	C(54)-C(55)	1.373(8)
C(10)-F(10)	1.332(8)	C(55)-F(55)	1.350(6)
C(10)-C(11)	1.381(9)	C(55)-C(56)	1.381(7)
C(11)-F(11)	1.336(6)	N(60)-C(61)	1.491(6)
C(11)-C(12)	1.369(8)	N(60)-C(63)	1.491(7)
C(13)-F(13)	1.343(7)	C(61)-C(62)	1.499(9)
C(13)-C(14)	1.368(10)	C(63)-C(64)	1.495(8)
C(13)-C(18)	1.371(8)	N(70)-C(71)	1.487(7)
C(14)-F(14)	1.344(9)	N(70)-C(73)	1.488(7)
C(14)-C(15)	1.368(11)	C(71)-C(72)	1.489(9)
C(15)-F(15)	1.337(7)	C(73)-C(74)	1.496(9)
C(15)-C(16)	1.378(11)	N(80)-C(83)	1.489(9)
C(16)-F(16)	1.325(7)	N(80)-C(81)	1.492(9)
C(16)-C(17)	1.386(9)	C(81)-C(82)	1.487(12)
C(17)-F(17)	1.329(7)	C(83)-C(84)	1.488(13)
C(17)-C(18)	1.373(7)		
C(19)-F(19)	1.341(7)	S(3)-Ti-S(4)	115.52(7)
C(19)-C(20)	1.367(8)	S(3)-Ti-S(5)	126.47(7)
C(19)-C(24)	1.391(8)	S(4)-Ti-S(5)	117.14(6)
C(20)-F(20)	1.333(8)	S(3)-Ti-S(1)	88.22(5)
C(20)-C(21)	1.355(10)	S(4)-Ti-S(1)	92.24(5)
C(21)-F(21)	1.333(7)	S(5)-Ti-S(1)	98.65(5)
C(21)-C(22)	1.375(11)	S(3)-Ti-S(2)	84.76(5)
C(22)-F(22)	1.348(7)	S(4)-Ti-S(2)	89.10(5)
C(22)-C(23)	1.379(10)	S(5)-Ti-S(2)	87.07(5)
C(23)-F(23)	1.343(7)	S(1)-Ti-S(2)	172.73(6)
C(23)-C(24)	1.389(8)	C(6)-S(1)-Ti	113.05(14)
C(25)-F(25)	1.352(6)	C(12)-S(2)-Ti	112.21(14)
C(25)-C(26)	1.374(7)	C(18)-S(3)-Ti	110.5(2)
C(25)-C(30)	1.388(8)	C(24)-S(4)-Ti	109.6(2)
C(26)-F(26)	1.330(6)	C(30)-S(5)-Ti	112.5(2)
C(26)-C(27)	1.375(9)	F(1)-C(1)-C(6)	119.9(4)

F(1)-C(1)-C(2)	117.2(5)	C(20)-C(21)-C(22)	119.0(6)
C(6)-C(1)-C(2)	122.9(5)	F(22)-C(22)-C(21)	120.2(7)
F(2)-C(2)-C(3)	119.7(5)	F(22)-C(22)-C(23)	118.9(8)
F(2)-C(2)-C(1)	120.3(6)	C(21)-C(22)-C(23)	120.8(6)
C(3)-C(2)-C(1)	119.9(5)	F(23)-C(23)-C(22)	119.2(6)
F(3)-C(3)-C(4)	121.4(6)	F(23)-C(23)-C(24)	119.3(5)
F(3)-C(3)-C(2)	119.9(6)	C(22)-C(23)-C(24)	121.6(6)
C(4)-C(3)-C(2)	118.7(5)	C(23)-C(24)-C(19)	115.2(5)
C(3)-C(4)-F(4)	120.0(5)	C(23)-C(24)-S(4)	122.9(4)
C(3)-C(4)-C(5)	121.1(6)	C(19)-C(24)-S(4)	121.9(4)
F(4)-C(4)-C(5)	118.9(6)	F(25)-C(25)-C(26)	117.2(5)
F(5)-C(5)-C(4)	118.2(5)	F(25)-C(25)-C(30)	119.3(4)
F(5)-C(5)-C(6)	120.3(4)	C(26)-C(25)-C(30)	123.4(5)
C(4)-C(5)-C(6)	121.6(6)	F(26)-C(26)-C(25)	120.7(5)
C(1)-C(6)-C(5)	115.8(4)	F(26)-C(26)-C(27)	120.6(5)
C(1)-C(6)-S(1)	123.6(4)	C(25)-C(26)-C(27)	118.7(5)
C(5)-C(6)-S(1)	120.4(4)	F(27)-C(27)-C(28)	121.1(6)
F(7)-C(7)-C(8)	117.7(5)	F(27)-C(27)-C(26)	118.9(6)
F(7)-C(7)-C(12)	120.9(5)	C(28)-C(27)-C(26)	120.0(5)
C(8)-C(7)-C(12)	121.5(5)	F(28)-C(28)-C(27)	119.7(5)
F(8)-C(8)-C(9)	119.2(6)	F(28)-C(28)-C(29)	120.0(6)
F(8)-C(8)-C(7)	120.2(6)	C(27)-C(28)-C(29)	120.3(6)
C(9)-C(8)-C(7)	120.5(5)	F(29)-C(29)-C(28)	117.6(5)
F(9)-C(9)-C(8)	120.9(7)	F(29)-C(29)-C(30)	120.0(5)
F(9)-C(9)-C(10)	119.4(7)	C(28)-C(29)-C(30)	122.4(6)
C(8)-C(9)-C(10)	119.6(5)	C(29)-C(30)-C(25)	115.1(5)
F(10)-C(10)-C(9)	121.7(6)	C(29)-C(30)-S(5)	120.2(4)
F(10)-C(10)-C(11)	118.6(7)	C(25)-C(30)-S(5)	124.7(4)
C(9)-C(10)-C(11)	119.7(6)	F(41)-C(41)-C(42)	116.8(5)
F(11)-C(11)-C(12)	118.8(5)	F(41)-C(41)-C(46)	120.6(5)
F(11)-C(11)-C(10)	119.2(5)	C(42)-C(41)-C(46)	122.5(5)
C(12)-C(11)-C(10	122.0(5)	F(42)-C(42)-C(43)	120.4(5)
C(11)-C(12)-C(7)	116.5(5)	F(42)-C(42)-C(41)	120.4(5)
C(11)-C(12)-S(2)	121.2(4)	C(43)-C(42)-C(41)	119.2(6)
C(7)-C(12)-S(2)	122.2(4)	F(43)-C(43)-C(44)	120.5(6)
F(13)-C(13)-C(14)	117.8(6)	F(43)-C(43)-C(42)	119.1(6)
F(13)-C(13)-C(18)	119.3(6)	C(44)-C(43)-C(42)	120.4(6)
C(14)-C(13)-C(18)	122.9(6)	F(44)-C(44)-C(43)	120.1(6)
F(14)-C(14)-C(13)	120.7(7)	F(44)-C(44)-C(45)	120.1(6)
F(14)-C(14)-C(15)	119.8(7)	C(43)-C(44)-C(45)	119.8(6)
C(13)-C(14)-C(15)	119.5(7)	F(45)-C(45)-C(44)	118.4(5)
F(15)-C(15)-C(14)	121.0(8)	F(45)-C(45)-C(46)	119.4(5)
F(15)-C(15)-C(16)	119.3(8)	C(44)-C(45)-C(46)	122.2(6)
C(14)-C(15)-C(16)	119.7(6)	C(41)-C(46)-C(45)	115.8(5)
F(16)-C(16)-C(15)	120.6(6)	C(41)-C(46)-S(6)	121.7(4)
F(16)-C(16)-C(17)	120.2(7)	C(45)-C(46)-S(6)	122.4(4)
C(15)-C(16)-C(17)	119.1(6)	F(51)-C(51)-C(52)	116.9(4)
F(17)-C(17)-C(18)	120.9(5)	F(51)-C(51)-C(56)	120.0(4)
F(17)-C(17)-C(16)	117.1(5)	C(52)-C(51)-C(56)	123.1(4)
C(18)-C(17)-C(16)	122.0(6)	F(52)-C(52)-C(53)	119.3(5)
C(13)-C(18)-C(17)	116.7(5)	F(52)-C(52)-C(51)	121.4(4)
C(13)-C(18)-S(3)	123.0(4)	C(53)-C(52)-C(51)	119.4(4)
C(17)-C(18)-S(3)	120.2(5)	F(53)-C(53)-C(54)	120.6(4)
F(19)-C(19)-C(20)	117.6(6)	F(53)-C(53)-C(52)	119.8(5)
F(19)-C(19)-C(24)	119.0(5)	C(54)-C(53)-C(52)	119.6(5)
C(20)-C(19)-C(24)	123.4(6)	F(54)-C(54)-C(53)	120.2(5)
F(20)-C(20)-C(21)	119.1(6)	F(54)-C(54)-C(55)	120.2(5)
F(20)-C(20)-C(19)	120.9(6)	C(53)-C(54)-C(55)	119.5(5)
C(21)-C(20)-C(19)	120.0(7)	F(55)-C(55)-C(54)	117.0(4)
F(21)-C(21)-C(20)	122.1(8)	F(55)-C(55)-C(56)	119.2(5)
F(21)-C(21)-C(22)	118.9(7)	C(54)-C(55)-C(56)	123.8(5)

C(55)-C(56)-C(51)	114.6(4)	C(71)-N(70)-C(73)	116.1(4)
C(55)-C(56)-S(7)	122.5(4)	N(70)-C(71)-C(72)	110.4(5)
C(51)-C(56)-S(7)	122.9(4)	N(70)-C(73)-C(74)	109.6(5)
C(61)-N(60)-C(63)	113.9(4)	C(83)-N(80)-C(81)	114.3(6)
N(60)-C(61)-C(62)	112.0(5)	C(82)-C(81)-N(80)	111.2(6)
N(60)-C(63)-C(64)	112.8(5)	C(84)-C(83)-N(80)	112.6(6)

Table 4. Anisotropic displacement parameters [$Å^2$ x 10^3] for **2**. The anisotropic displacement factor exponent takes the form: $-2\pi^2$ [$(ha^*)^2U11 + ... + 2hka^*b^*U12$]

	U11	U22	U33	U23	U13	U12
Ti	33(1)	40(1)	33(1)	3(1)	1(1)	-3(1)
S(1)	38(1)	41(1)	33(1)	2(1)	-1(1)	4(1)
S(2)	37(1)	63(1)	34(1)	3(1)	1(1)	-8(1)
S(3)	35(1)	85(1)	47(1)	-15(1)	-3(1)	3(1)
S(4)	51(1)	39(1)	44(1)	7(1)	-1(1)	2(1)
S(5)	59(1)	50(1)	41(1)	-9(1)	11(1)	-15(1)
C(1)	46(3)	40(3)	35(2)	0(2)	-6(2)	2(2)
F(1)	81(2)	42(2)	66(2)	6(1)	-18(2)	-13(2)
C(2)	73(4)	48(3)	39(2)	10(2)	7(3)	22(3)
F(2)	119(3)	50(2)	71(2)	14(2)	-8(2)	21(2)
C(3)	51(3)	68(4)	40(2)	3(2)	-1(2)	27(3)
F(3)	71(2)	106(3)	57(2)	10(2)	-13(2)	41(2)
C(4)	44(3)	78(5)	48(3)	-8(3)	-9(2)	3(3)
F(4)	65(2)	107(3)	78(2)	0(2)	-36(2)	-14(2)
C(5)	44(3)	49(3)	43(2)	0(2)	-4(2)	0(3)
F(5)	81(2)	48(2)	78(2)	3(2)	-29(2)	-14(2)
C(6)	33(2)	36(3)	30(2)	-1(2)	-1(2)	2(2)
C(7)	47(3)	39(3)	42(2)	2(2)	1(2)	1(2)
F(7)	109(3)	43(2)	69(2)	2(2)	-20(2)	23(2)
C(8)	40(3)	77(5)	38(2)	6(3)	-2(2)	9(3)
F(8)	70(2)	133(4)	66(2)	9(2)	-20(2)	38(3)
C(9)	55(3)	91(5)	36(2)	-13(3)	3(2)	-23(4)
F(9)	77(3)	155(5)	58(2)	-29(2)	-6(2)	-52(3)
C(10)	103(5)	42(3)	45(3)	-13(2)	12(3)	-10(4)
F(10)	200(6)	59(3)	76(2)	-31(2)	3(3)	-17(3)
C(11)	63(3)	39(3)	37(2)	4(2)	0(2)	18(3)
F(11)	122(3)	64(2)	61(2)	-5(2)	-3(2)	50(3)
C(12)	35(2)	43(3)	28(2)	6(2)	3(2)	5(2)
C(13)	50(3)	55(4)	57(3)	10(3)	-3(3)	-10(3)
F(13)	88(3)	84(3)	109(3)	29(2)	14(2)	-31(3)
C(14)	69(4)	52(4)	86(4)	-13(3)	-24(4)	-2(3)
F(14)	126(4)	55(3)	166(5)	-20(3)	-30(4)	5(3)
C(15)	49(4)	94(6)	68(4)	-34(4)	-13(3)	22(4)
F(15)	81(3)	164(6)	119(4)	-76(4)	-9(3)	48(3)
C(16)	39(3)	96(6)	48(3)	2(3)	10(2)	0(3)
F(16)	64(2)	171(5)	84(3)	24(3)	37(2)	-2(3)
C(17)	38(3)	56(4)	48(3)	11(2)	-4(2)	0(3)
F(17)	65(2)	61(2)	98(3)	29(2)	4(2)	-7(2)
C(18)	29(2)	53(3)	40(2)	3(2)	-2(2)	-4(2)
C(19)	62(4)	30(3)	57(3)	5(2)	6(3)	2(3)
F(19)	48(2)	49(2)	74(2)	-3(2)	2(2)	-9(2)
C(20)	91(5)	30(3)	55(3)	-1(2)	-2(3)	4(3)
F(20)	132(4)	52(2)	70(2)	-10(2)	-15(2)	-12(2)

C(21)	104(6)	42(4)	58(3)	13(3)	15(4)	22(4)
F(21)	181(5)	61(3)	67(2)	1(2)	43(3)	37(3)
C(22)	70(4)	62(4)	80(4)	30(3)	38(4)	38(4)
F(22)	87(3)	122(4)	117(3)	39(3)	50(3)	55(3)
C(23)	41(3)	57(4)	63(3)	24(3)	-1(3)	11(3)
F(23)	45(2)	87(3)	103(3)	25(2)	0(2)	13(2)
C(24)	45(3)	30(3)	50(2)	10(2)	4(2)	5(2)
C(25)	39(3)	39(3)	42(2)	3(2)	-11(2)	-9(2)
F(25)	50(2)	41(2)	61(2)	8(1)	-6(1)	0(1)
C(26)	34(3)	60(4)	42(2)	-3(2)	-5(2)	-3(3)
F(26)	42(2)	82(3)	67(2)	-7(2)	3(1)	6(2)
C(27)	56(3)	72(4)	44(3)	-1(3)	6(2)	-29(3)
F(27)	76(2)	92(3)	64(2)	-2(2)	21(2)	-38(2)
C(28)	82(4)	40(3)	53(3)	-4(2)	4(3)	-20(3)
F(28)	147(4)	46(2)	83(2)	6(2)	25(3)	-30(2)
C(29)	69(4)	42(3)	46(3)	-6(2)	6(3)	-7(3)
F(29)	117(3)	44(2)	80(2)	-6(2)	33(2)	9(2)
C(30)	44(3)	39(3)	39(2)	-2(2)	-4(2)	-14(2)
S(6)	51(1)	40(1)	39(1)	4(1)	0(1)	-2(1)
C(41)	58(3)	40(3)	41(2)	4(2)	0(2)	4(3)
F(41)	67(2)	33(2)	71(2)	10(1)	10(2)	2(2)
C(42)	56(4)	53(4)	49(3)	10(2)	4(2)	-2(3)
F(42)	66(2)	61(2)	87(2)	17(2)	10(2)	-16(2)
C(43)	50(4)	72(4)	60(3)	9(3)	13(3)	10(3)
F(43)	58(2)	98(3)	98(3)	24(2)	18(2)	21(2)
C(44)	73(4)	48(4)	61(3)	12(3)	7(3)	29(3)
F(44)	90(3)	60(3)	112(3)	20(2)	16(2)	32(2)
C(45)	75(4)	35(3)	50(3)	1(2)	8(3)	4(3)
F(45)	86(2)	32(2)	74(2)	7(1)	12(2)	-1(2)
C(46)	57(3)	31(3)	33(2)	5(2)	0(2)	2(2)
S(7)	33(1)	46(1)	39(1)	0(1)	1(1)	-4(1)
C(51)	39(3)	36(3)	39(2)	1(2)	3(2)	2(2)
F(51)	47(2)	81(2)	37(1)	-5(1)	3(1)	3(2)
C(52)	42(3)	43(3)	44(2)	2(2)	-5(2)	-1(2)
F(52)	43(2)	97(3)	49(2)	-5(2)	-13(1)	2(2)
C(53)	36(3)	51(3)	51(3)	-2(2)	-1(2)	8(2)
F(53)	33(2)	99(3)	77(2)	-9(2)	-1(1)	9(2)
C(54)	44(3)	67(4)	52(3)	-17(3)	10(2)	1(3)
F(54)	51(2)	130(4)	63(2)	-30(2)	14(2)	9(2)
C(55)	42(3)	60(4)	42(2)	-11(2)	2(2)	1(3)
F(55)	50(2)	116(3)	45(2)	-28(2)	0(1)	-2(2)
C(56)	33(2)	35(3)	39(2)	-1(2)	-1(2)	-1(2)
N(60)	35(2)	44(3)	42(2)	0(2)	0(2)	-5(2)
C(61)	39(3)	59(4)	65(3)	-10(3)	11(2)	-8(3)
C(62)	88(5)	54(4)	73(4)	-14(3)	41(3)	-21(4)
C(63)	55(3)	42(3)	56(3)	-7(2)	11(2)	-3(3)
C(64)	65(4)	58(4)	85(4)	-14(3)	34(3)	-2(3)
N(70)	34(2)	50(3)	38(2)	1(2)	5(2)	2(2)
C(71)	59(4)	49(3)	56(3)	-5(2)	6(3)	-8(3)
C(72)	111(6)	48(4)	73(4)	1(3)	15(4)	6(4)
C(73)	40(3)	57(4)	57(3)	-7(3)	-5(2)	6(3)
C(74)	72(4)	52(4)	69(3)	2(3)	-15(3)	0(3)
N(80)	92(4)	39(3)	42(2)	6(2)	14(2)	0(3)
C(81)	136(7)	45(4)	74(4)	-11(3)	30(5)	-43(5)
C(82)	95(6)	105(7)	75(4)	-13(4)	-2(4)	-50(6)
C(83)	133(7)	67(5)	49(3)	15(3)	9(4)	46(5)
C(84)	94(6)	125(8)	79(5)	-7(5)	-19(4)	48(6)

Table 5. Hydrogen coordinates (x 10^4), isotropic displacement parameters ($Å^2$ x 10^3) and site occupancy factors for **2**.

	x	y	z	U(eq)	sof
H(60A)	423(4)	5517(1)	5493(2)	49	1
H(60B)	-148(4)	5654(1)	4883(2)	49	1
H(61A)	2113(5)	5470(2)	4818(3)	65	1
H(61B)	2434(5)	5865(2)	5280(3)	65	1
H(62A)	2767(7)	6060(2)	4222(3)	106	1
H(62B)	1563(7)	6334(2)	4501(3)	106	1
H(62C)	1243(7)	5939(2)	4039(3)	106	1
H(63A)	-226(6)	6341(2)	5163(3)	61	1
H(63B)	671(6)	6240(2)	5788(3)	61	1
H(64A)	-1565(7)	6336(2)	6055(3)	103	1
H(64B)	-1119(7)	5857(2)	6211(3)	103	1
H(64C)	-2017(7)	5959(2)	5586(3)	103	1
H(70A)	-49(4)	4830(1)	7187(2)	49	1
H(70B)	-88(4)	4805(1)	7876(2)	49	1
H(71A)	-1856(6)	4376(2)	7071(3)	66	1
H(71B)	-1876(6)	4345(2)	7833(3)	66	1
H(72A)	-744(9)	3760(2)	7418(3)	115	1
H(72B)	276(9)	4041(2)	7845(3)	115	1
H(72C)	296(9)	4072(2)	7085(3)	115	1
H(73A)	-2139(5)	5156(2)	7873(3)	62	1
H(73B)	-2014(5)	5203(2)	7117(3)	62	1
H(74A)	-1253(7)	5826(2)	7626(3)	97	1
H(74B)	-35(7)	5603(2)	7272(3)	97	1
H(74C)	-160(7)	5557(2)	8027(3)	97	1
H(80A)	255(6)	5521(2)	9458(2)	69	1
H(80B)	-163(6)	5630(2)	10094(2)	69	1
H(81A)	1565(9)	6115(2)	9386(3)	101	1
H(81B)	1050(9)	6262(2)	10067(3)	101	1
H(82A)	3177(9)	5956(3)	10176(4)	137	1
H(82B)	2622(9)	5525(3)	9860(4)	137	1
H(82C)	2108(9)	5672(3)	10541(4)	137	1
H(83A)	-1390(9)	6200(2)	9730(3)	99	1
H(83B)	-897(9)	6096(2)	9028(3)	99	1
H(84A)	-3071(9)	5844(3)	9153(4)	150	1
H(84B)	-2570(9)	5556(3)	9741(4)	150	1
H(84C)	-2077(9)	5453(3)	9039(4)	150	1

Table 1. Crystal data and structure refinement for **3**.

Empirical formula	[C28 H10 N F20 S4 Ti][C4 H12 N]
Formula weight	990.66
Temperature	193(2) K
Diffractometer Used	Siemens P4/RA
Wavelength	1.54178 Å
Crystal system	Monoclinic
Space group	C2/c
Unit cell dimensions	a = 15.2002(12) Å α = 90 °
	b = 17.6154(12) Å β = 91.179(12) °
	c = 14.117(2) Å χ = 90 °
Volume	3779.1(7) $Å^3$
Z	4
Density (calculated)	1.741 Mg/m^3
Absorption coefficient	5.184 mm^{-1}
F(000)	1976
Crystal colour/morphology	Deep red blocks
Crystal size	0.43 x 0.37 x 0.23 mm^3
Theta range for data collection	3.84 to 63.59 °
Limiting indices	-14<=h<=17, -15<=k<=20,
	-12<=l<=16
Scan type	ω-scans
Reflections collected	3219
Independent reflections	3093 (R(int) = 0.0494)
Observed reflections [F>4sigma(F)]	2598
Absorption correction	Ellipsoidal
Max. and min. transmission	0.2352 and 0.0844
Structure solution method	Direct
Refinement method	Full-matrix least-squares on F^2
Data/restraints/parameters	2979 / 6 / 291
Goodness-of-fit on F^2	1.061
Final R indices [F>4sigma(F)]	R1 = 0.0552, wR2 = 0.1427
R indices (all data)	R1 = 0.0684, wR2 = 0.1595
Extinction coefficient	0.00018(11)
Largest diff. peak and hole	0.598 and -0.378 $e.Å^{-3}$
Mean and maximum shift/error	0.000 and 0.004

Table 2. Atomic coordinates [x 10^4], equivalent isotropic displacement parameters [$Å^2$ x 10^3] and site occupancy factors for **3**. U(eq) is defined as one third of the trace of the orthogonalized U^{ij} tensor.

	x	y	z	U(eq)	sof
Ti	0	2665(1)	7500	40(1)	1
S(1)	677(1)	3348(1)	8808(1)	50(1)	1
S(2)	1318(1)	3042(1)	6680(1)	48(1)	1
N	0	1615(2)	7500	54(1)	1
C(1)	1836(2)	3362(2)	8813(2)	48(1)	1
C(2)	2282(2)	4047(2)	8845(3)	53(1)	1
F(2)	1826(2)	4703(2)	8793(2)	71(1)	1
C(3)	3187(2)	4092(3)	8909(3)	58(1)	1
F(3)	3596(2)	4767(2)	8901(2)	82(1)	1
C(4)	3675(2)	3437(3)	8937(3)	59(1)	1
F(4)	4554(2)	3480(2)	8990(2)	85(1)	1
C(5)	3264(3)	2746(3)	8905(3)	57(1)	1
F(5)	3736(2)	2108(2)	8926(2)	77(1)	1
C(6)	2359(3)	2713(2)	8849(3)	52(1)	1
F(6)	1980(2)	2032(1)	8822(2)	67(1)	1
C(7)	1378(2)	2511(2)	5630(3)	48(1)	1
C(8)	1754(2)	1784(2)	5616(3)	49(1)	1
F(8)	2061(2)	1475(1)	6418(2)	62(1)	1
C(9)	1831(2)	1374(2)	4781(3)	56(1)	1
F(9)	2212(2)	690(2)	4795(2)	77(1)	1
C(10)	1537(2)	1676(3)	3947(3)	58(1)	1
F(10)	1585(2)	1272(2)	3145(2)	77(1)	1
C(11)	1194(2)	2398(3)	3924(3)	58(1)	1
F(11)	916(2)	2703(2)	3101(2)	78(1)	1
C(12)	1127(2)	2806(2)	4753(3)	52(1)	1
F(12)	819(2)	3519(2)	4686(2)	68(1)	1
C(13)	166(3)	1183(2)	8371(3)	57(1)	1
C(14)	900(3)	600(3)	8295(4)	74(1)	1
N(20)	-80(17)	4920(5)	7684(16)	99(6)	0.50
C(21)	-579(12)	5198(18)	8488(14)	166(15)	0.50
C(22)	-1529(10)	5347(9)	8333(13)	113(5)	0.50
C(23)	334(14)	5506(6)	7101(11)	138(8)	0.50
C(24)	863(13)	5184(11)	6301(13)	99(5)	0.50

Table 3. Bond lengths [Å] and angles [°] for **3**.

Ti-N	1.849(4)	C(1)-S(1)-Ti	114.83(12)
Ti-S(1)	2.4166(9)	C(7)-S(2)-Ti	108.31(11)
Ti-S(1)#1	2.4166(9)	C(13)#1-N-C(13)	117.3(4)
Ti-S(2)#1	2.4273(8)	C(13)#1-N-Ti	121.3(2)
Ti-S(2)	2.4273(8)	C(13)-N-Ti	121.3(2)
S(1)-C(1)	1.761(3)	C(2)-C(1)-C(6)	115.8(3)
S(2)-C(7)	1.758(4)	C(2)-C(1)-S(1)	120.1(3)
N-C(13)#1	1.463(5)	C(6)-C(1)-S(1)	124.0(3)
N-C(13)	1.463(5)	F(2)-C(2)-C(3)	117.7(4)
C(1)-C(2)	1.384(5)	F(2)-C(2)-C(1)	119.7(3)
C(1)-C(6)	1.392(5)	C(3)-C(2)-C(1)	122.7(4)
C(2)-F(2)	1.349(5)	F(3)-C(3)-C(4)	119.7(3)
C(2)-C(3)	1.380(5)	F(3)-C(3)-C(2)	120.8(4)
C(3)-F(3)	1.342(5)	C(4)-C(3)-C(2)	119.4(4)
C(3)-C(4)	1.372(6)	F(4)-C(4)-C(5)	120.5(4)
C(4)-F(4)	1.338(4)	F(4)-C(4)-C(3)	119.4(4)
C(4)-C(5)	1.368(6)	C(5)-C(4)-C(3)	120.1(3)
C(5)-F(5)	1.332(5)	F(5)-C(5)-C(4)	120.3(4)
C(5)-C(6)	1.378(6)	F(5)-C(5)-C(6)	120.2(4)
C(6)-F(6)	1.332(5)	C(4)-C(5)-C(6)	119.5(4)
C(7)-C(12)	1.388(5)	F(6)-C(6)-C(5)	118.0(4)
C(7)-C(8)	1.403(5)	F(6)-C(6)-C(1)	119.5(3)
C(8)-F(8)	1.332(5)	C(5)-C(6)-C(1)	122.5(4)
C(8)-C(9)	1.389(5)	C(12)-C(7)-C(8)	115.7(3)
C(9)-F(9)	1.337(5)	C(12)-C(7)-S(2)	122.3(3)
C(9)-C(10)	1.360(6)	C(8)-C(7)-S(2)	121.7(3)
C(10)-F(10)	1.340(5)	F(8)-C(8)-C(9)	118.3(4)
C(10)-C(11)	1.376(7)	F(8)-C(8)-C(7)	119.8(3)
C(11)-F(11)	1.340(5)	C(9)-C(8)-C(7)	121.9(4)
C(11)-C(12)	1.379(6)	F(9)-C(9)-C(10)	120.0(4)
C(12)-F(12)	1.342(5)	F(9)-C(9)-C(8)	120.1(4)
C(13)-C(14)	1.522(6)	C(10)-C(9)-C(8)	120.0(4)
		F(10)-C(10)-C(9)	120.1(4)
N-Ti-S(1)	119.86(3)	F(10)-C(10)-C(11)	119.9(4)
N-Ti-S(1)#1	119.86(3)	C(9)-C(10)-C(11)	120.0(4)
S(1)-Ti-S(1)#1	120.27(6)	F(11)-C(11)-C(10)	120.2(4)
N-Ti-S(2)#1	105.90(3)	F(11)-C(11)-C(12)	120.0(4)
S(1)-Ti-S(2)#1	80.92(3)	C(10)-C(11)-C(12)	119.8(4)
S(1)#1-Ti-S(2)#1	83.39(3)	F(12)-C(12)-C(11)	117.3(4)
N-Ti-S(2)	105.90(3)	F(12)-C(12)-C(7)	120.1(3)
S(1)-Ti-S(2)	83.39(3)	C(11)-C(12)-C(7)	122.6(4)
S(1)#1-Ti-S(2)	80.92(3)	N-C(13)-C(14)	114.0(3)
S(2)#1-Ti-S(2)	148.20(5)		

Symmetry transformations used to generate equivalent atoms:

Table 4. Anisotropic displacement parameters [$Å^2$ x 10^3] for **3**. The anisotropic displacement factor exponent takes the form: $-2\pi^2$ [$(ha^*)^2U11 + ... + 2hka^*b^*U12$]

	U11	U22	U33	U23	U13	U12
Ti	30(1)	43(1)	47(1)	0	7(1)	0
S(1)	34(1)	64(1)	53(1)	-9(1)	7(1)	-1(1)
S(2)	34(1)	59(1)	51(1)	-2(1)	11(1)	-7(1)
N	40(2)	44(2)	77(3)	0	18(2)	0
C(1)	34(2)	60(2)	48(2)	-6(1)	5(1)	3(1)
C(2)	40(2)	58(2)	62(2)	-7(2)	11(1)	3(1)
F(2)	50(1)	59(1)	105(2)	-9(1)	9(1)	5(1)
C(3)	42(2)	70(2)	63(2)	-8(2)	10(2)	-11(2)
F(3)	54(1)	77(2)	115(2)	-16(2)	21(1)	-19(1)
C(4)	32(2)	86(3)	58(2)	-3(2)	6(1)	3(2)
F(4)	33(1)	118(2)	103(2)	-8(2)	8(1)	2(1)
C(5)	45(2)	73(2)	52(2)	4(2)	7(1)	14(2)
F(5)	63(2)	86(2)	82(2)	12(1)	5(1)	29(1)
C(6)	48(2)	61(2)	48(2)	0(1)	5(1)	1(2)
F(6)	64(1)	55(1)	81(2)	2(1)	7(1)	-1(1)
C(7)	31(1)	61(2)	53(2)	1(1)	12(1)	-9(1)
C(8)	37(2)	60(2)	51(2)	2(1)	12(1)	-7(1)
F(8)	59(1)	67(1)	60(1)	6(1)	11(1)	5(1)
C(9)	46(2)	57(2)	65(2)	-5(2)	20(2)	-11(2)
F(9)	84(2)	60(1)	87(2)	-7(1)	27(1)	1(1)
C(10)	46(2)	77(2)	52(2)	-13(2)	15(1)	-20(2)
F(10)	75(2)	97(2)	61(1)	-24(1)	18(1)	-26(1)
C(11)	40(2)	83(3)	50(2)	4(2)	5(1)	-16(2)
F(11)	69(2)	113(2)	51(1)	9(1)	2(1)	-2(1)
C(12)	36(2)	68(2)	53(2)	4(2)	9(1)	-4(1)
F(12)	61(1)	76(2)	67(1)	15(1)	13(1)	8(1)
C(13)	50(2)	53(2)	70(2)	2(2)	15(2)	3(2)
C(14)	69(3)	64(2)	88(3)	7(2)	5(2)	14(2)
N(20)	95(10)	83(5)	120(19)	2(6)	-24(10)	20(7)
C(21)	109(14)	91(14)	301(43)	-40(20)	63(19)	3(12)
C(22)	120(12)	87(8)	132(12)	-5(8)	26(10)	-9(8)
C(23)	223(25)	38(5)	154(16)	7(6)	-30(14)	18(8)
C(24)	127(15)	58(7)	112(10)	-11(7)	0(10)	-4(9)

Table 5. Hydrogen coordinates (x 10^4), isotropic displacement parameters ($Å^2$ x 10^3) and site occupancy factors for **3**.

	x	y	z	U(eq)	sof
H(13A)	-382(3)	919(2)	8545(3)	69	1
H(13B)	319(3)	1542(2)	8888(3)	69	1
H(14A)	974(3)	334(3)	8901(4)	110	1
H(14B)	1450(3)	857(3)	8140(4)	110	1
H(14C)	748(3)	233(3)	7796(4)	110	1
H(20A)	-452(17)	4638(5)	7300(16)	119	0.50
H(20B)	354(17)	4599(5)	7910(16)	119	0.50
H(21A)	-300(12)	5674(18)	8713(14)	199	0.50
H(21B)	-516(12)	4822(18)	9007(14)	199	0.50
H(22A)	-1784(10)	5530(9)	8923(13)	169	0.50
H(22B)	-1825(10)	4877(9)	8135(13)	169	0.50
H(22C)	-1609(10)	5732(9)	7838(13)	169	0.50
H(23A)	725(14)	5820(6)	7511(11)	166	0.50
H(23B)	-130(14)	5842(6)	6833(11)	166	0.50
H(24A)	1121(13)	5601(11)	5940(13)	148	0.50
H(24B)	477(13)	4883(11)	5882(13)	148	0.50
H(24C)	1333(13)	4861(11)	6561(13)	148	0.50

Table 1. Crystal data and structure refinement for **5**.

Empirical formula	C16 H37 N S3 Ti
Formula weight	387.55
Temperature	183(2) K
Diffractometer Used	Siemens P4/RA
Wavelength	1.54178 Å
Crystal system	Orthorhombic
Space group	Pbca
Unit cell dimensions	a = 10.1445(8) Å α = 90 °
	b = 15.861(4) Å β = 90 °
	c = 28.332(2) Å χ = 90 °
Volume	4558.6(12) $Å^3$,
Z	8
Density (calculated)	1.129 Mg/m^3
Absorption coefficient	5.694 mm^{-1}
F(000)	1680
Crystal colour/morphology	Red blocks
Crystal size	0.50 x 0.47 x 0.33 mm^3
Theta range for data collection	3.12 to 60.00 °
Limiting indices	0<=h<=11, 0<=k<=17,
	-31<=l<=0
Scan type	ω-scans
Reflections collected	3351
Independent reflections	3351 (R(int) = 0.0000)
Observed reflections [F>4sigma(F)]	2199
Absorption correction	Semi-empirical from psi-scans
Max. and min. transmission	0.7677 and 0.3474
Structure solution method	Direct
Refinement method	Full-matrix least-squares on F^2
Data / restraints / parameters	2984 / 0 / 191
Goodness-of-fit on F^2	1.039
Final R indices [F>4sigma(F)]	R1 = 0.0566, wR2 = 0.1368
R indices (all data)	R1 = 0.1062, wR2 = 0.1979
Extinction coefficient	0.00017(8)
Largest diff. peak and hole	0.296 and -0.364 $e.Å^{-3}$
Mean and maximum shift/error	0.000 and 0.000

Table 2. Atomic coordinates [x 10^4], equivalent isotropic displacement parameters [$Å^2$ x 10^3] and site occupancy factors for **5**. U(eq) is defined as one third of the trace of the orthogonalized U^{ij} tensor.

	x	y	z	U(eq)	sof
Ti	1854(1)	5873(1)	1307(1)	35(1)	1
S(1)	353(1)	5777(1)	703(1)	43(1)	1
S(2)	1392(1)	6960(1)	1819(1)	45(1)	1
S(3)	3904(2)	6246(1)	1049(1)	55(1)	1
N	1752(5)	4847(3)	1620(1)	40(1)	1
C(1)	613(6)	6594(4)	238(2)	49(1)	1
C(2)	1041(8)	7420(4)	449(2)	60(2)	1
C(3)	1646(7)	6256(5)	-106(2)	62(2)	1
C(4)	-702(7)	6671(6)	-14(3)	71(2)	1
C(5)	-362(6)	7028(4)	2004(2)	48(1)	1
C(6)	-1090(8)	7564(7)	1656(4)	101(4)	1
C(7)	-1009(6)	6161(5)	2030(3)	65(2)	1
C(8)	-328(8)	7421(6)	2495(3)	87(3)	1
C(9)	5267(6)	5462(5)	1022(2)	53(2)	1
C(10)	5748(11)	5315(9)	1518(3)	117(4)	1
C(11)	6365(9)	5906(7)	751(4)	115(4)	1
C(12)	4802(11)	4657(7)	799(5)	119(4)	1
C(13)	1557(7)	4066(4)	1344(2)	55(2)	1
C(14)	152(9)	3737(5)	1369(2)	72(2)	1
C(15)	1707(6)	4713(4)	2134(2)	45(1)	1
C(16)	2871(6)	4236(4)	2326(2)	54(2)	1

Table 3. Bond lengths [Å] and angles [°] for **5**.

Ti-N	1.856(5)
Ti-S(3)	2.283(2)
Ti-S(1)	2.295(2)
Ti-S(2)	2.302(2)
S(1)-C(1)	1.866(6)
S(2)-C(5)	1.858(6)
S(3)-C(9)	1.861(7)
N-C(15)	1.472(6)
N-C(13)	1.480(7)
C(1)-C(2)	1.504(10)
C(1)-C(4)	1.518(9)
C(1)-C(3)	1.528(9)
C(5)-C(6)	1.496(10)
C(5)-C(7)	1.525(9)
C(5)-C(8)	1.526(10)
C(9)-C(12)	1.502(12)
C(9)-C(10)	1.507(11)
C(9)-C(11)	1.524(10)
C(13)-C(14)	1.519(10)
C(15)-C(16)	1.504(8)

N-Ti-S(3)	115.5(2)
N-Ti-S(1)	105.2(2)
S(3)-Ti-S(1)	112.52(7)
N-Ti-S(2)	110.06(14)
S(3)-Ti-S(2)	101.16(7)
S(1)-Ti-S(2)	112.62(7)
C(1)-S(1)-Ti	112.7(2)
C(5)-S(2)-Ti	114.6(2)
C(9)-S(3)-Ti	121.2(2)
C(15)-N-C(13)	113.5(4)
C(15)-N-Ti	127.0(4)
C(13)-N-Ti	119.2(3)
C(2)-C(1)-C(4)	111.7(6)
C(2)-C(1)-C(3)	111.2(6)
C(4)-C(1)-C(3)	109.3(5)
C(2)-C(1)-S(1)	111.5(4)
C(4)-C(1)-S(1)	105.3(4)
C(3)-C(1)-S(1)	107.7(5)
C(6)-C(5)-C(7)	109.4(7)
C(6)-C(5)-C(8)	112.3(8)
C(7)-C(5)-C(8)	109.4(6)
C(6)-C(5)-S(2)	108.7(5)
C(7)-C(5)-S(2)	111.9(4)
C(8)-C(5)-S(2)	105.0(5)
C(12)-C(9)-C(10)	111.2(9)
C(12)-C(9)-C(11)	114.3(8)
C(10)-C(9)-C(11)	107.7(8)
C(12)-C(9)-S(3)	110.6(6)
C(10)-C(9)-S(3)	107.8(6)
C(11)-C(9)-S(3)	104.8(5)
N-C(13)-C(14)	112.8(5)
N-C(15)-C(16)	113.9(5)

Table 4. Anisotropic displacement parameters [$Å^2$ x 10^3] for **5**.
The anisotropic displacement factor exponent takes the form:
$-2\pi^2[(ha^*)^2U11 + ... + 2hka^*b^*U12]$

	U11	U22	U33	U23	U13	U12
Ti	36(1)	36(1)	33(1)	-1(1)	-1(1)	0(1)
S(1)	48(1)	45(1)	37(1)	6(1)	-7(1)	-6(1)
S(2)	42(1)	42(1)	50(1)	-11(1)	5(1)	-3(1)
S(3)	40(1)	52(1)	72(1)	5(1)	9(1)	-2(1)
N	47(2)	46(3)	28(2)	2(2)	-1(2)	5(2)
C(1)	58(3)	53(3)	35(3)	10(3)	4(3)	-2(3)
C(2)	82(4)	52(4)	46(3)	12(3)	9(3)	0(4)
C(3)	64(4)	83(5)	40(3)	9(3)	11(3)	0(4)
C(4)	64(4)	95(6)	54(4)	28(4)	-8(3)	4(4)
C(5)	41(3)	47(3)	55(3)	3(3)	7(3)	1(3)
C(6)	58(4)	114(8)	131(8)	63(7)	33(5)	41(5)
C(7)	44(3)	63(4)	87(5)	-4(4)	10(3)	-9(3)
C(8)	83(5)	100(6)	78(5)	-36(5)	40(5)	-29(5)
C(9)	43(3)	61(4)	57(3)	7(3)	6(3)	7(3)
C(10)	87(6)	180(13)	86(6)	31(8)	-17(6)	23(8)
C(11)	71(5)	110(8)	164(10)	68(8)	65(6)	25(6)
C(12)	98(7)	86(7)	174(12)	-43(8)	17(8)	18(6)
C(13)	85(4)	44(3)	36(3)	-4(3)	-8(3)	9(3)
C(14)	116(7)	55(4)	46(3)	3(3)	-8(4)	-26(5)
C(15)	66(4)	43(3)	28(2)	0(2)	-1(3)	8(3)
C(16)	64(4)	56(4)	43(3)	3(3)	-16(3)	3(3)

Table 5. Hydrogen coordinates (x 10^4), isotropic displacement parameters ($Å^2$ x 10^3) and site occupancy factors for **5**.

	x	y	z	U(eq)	sof
H(2A)	1891(8)	7346(4)	609(2)	90	1
H(2B)	380(8)	7610(4)	678(2)	90	1
H(2C)	1131(8)	7841(4)	198(2)	90	1
H(3A)	1343(7)	5719(5)	-238(2)	93	1
H(3B)	2481(7)	6169(5)	62(2)	93	1
H(3C)	1777(7)	6663(5)	-362(2)	93	1
H(4A)	-949(7)	6122(6)	-146(3)	107	1
H(4B)	-628(7)	7086(6)	-269(3)	107	1
H(4C)	-1378(7)	6854(6)	211(3)	107	1
H(6A)	-675(8)	8121(7)	1639(4)	151	1
H(6B)	-2009(8)	7625(7)	1757(4)	151	1
H(6C)	-1063(8)	7297(7)	1345(4)	151	1
H(7A)	-533(6)	5810(5)	2258(3)	97	1
H(7B)	-982(6)	5894(5)	1718(3)	97	1
H(7C)	-1928(6)	6223(5)	2131(3)	97	1
H(8A)	157(8)	7049(6)	2710(3)	131	1
H(8B)	-1231(8)	7495(6)	2611(3)	131	1
H(8C)	111(8)	7970(6)	2480(3)	131	1
H(10A)	6045(11)	5850(9)	1654(3)	176	1
H(10B)	6483(11)	4914(9)	1513(3)	176	1
H(10C)	5028(11)	5085(9)	1709(3)	176	1
H(11A)	6614(9)	6424(7)	917(4)	173	1
H(11B)	6055(9)	6047(7)	433(4)	173	1
H(11C)	7132(9)	5532(7)	729(4)	173	1
H(12A)	4496(11)	4771(7)	477(5)	179	1
H(12B)	4076(11)	4422(7)	985(5)	179	1
H(12C)	5531(11)	4251(7)	789(5)	179	1
H(13A)	2163(7)	3626(4)	1463(2)	66	1
H(13B)	1786(7)	4176(4)	1010(2)	66	1
H(14A)	77(9)	3222(5)	1180(2)	109	1
H(14B)	-453(9)	4165(5)	1245(2)	109	1
H(14C)	-75(9)	3614(5)	1698(2)	109	1
H(15A)	891(6)	4400(4)	2213(2)	55	1
H(15B)	1659(6)	5268(4)	2293(2)	55	1
H(16A)	2776(6)	4170(4)	2668(2)	81	1
H(16B)	3682(6)	4548(4)	2257(2)	81	1
H(16C)	2913(6)	3678(4)	2177(2)	81	1

Table 1. Crystal data and structure refinement for **7**.

Empirical formula	C34 H42 N S4 Ta
Formula weight	773.88
Temperature	203(2) K
Diffractometer Used Siemens	P4/PC
Wavelength	0.71073 Å
Crystal system	Tetragonal
Space group	I41/a
Unit cell dimensions	a = 32.088(7) Å α = 90 °
	b = 32.088(7) Å β = 90 °
	c = 13.126(3) Å χ = 90 °
Volume	13515(6) $Å^3$
Z	16
Density (calculated)	1.521 Mg/m^3
Absorption coefficient	3.524 mm^{-1}
F(000)	6240
Crystal colour/morphology	Orange/red blocks
Crystal size	0.80 x 0.67 x 0.60 mm^3
Theta range for data collection	1.80 to 25.00 °
Limiting indices	0<=h<=38, 0<=k<=38,
	0<=l<=15
Scan type	ω-scans
Reflections collected	6188
Independent reflections	5949 (R(int) = 0.0330)
Observed reflections [F>4sigma(F)]	4529
Absorption correction	Ellipsoidal
Max. and min. transmission	0.2165 and 0.1883
Structure solution method	Patterson
Refinement method	Full-matrix least-squares on F^2
Data / restraints / parameters	5561 / 0 / 362
Goodness-of-fit on F^2	1.013
Final R indices [F>4sigma(F)]	R1 = 0.0373, wR2 = 0.0694
R indices (all data)	R1 = 0.0605, wR2 = 0.0800
Extinction coefficient	0.000046(8)
Largest diff. peak and hole	0.537 and -0.498 $eÅ^{-3}$
Mean and maximum shift/error	0.000 and 0.008

Table 2. Atomic coordinates [x 10^4], equivalent isotropic displacement parameters [$Å^2$ x 10^3] and site occupancy factors for **7**. U(eq) is defined as one third of the trace of the orthogonalized U^{ij} tensor.

	x	y	z	U(eq)	sof
Ta	11042(1)	5936(1)	7297(1)	26(1)	1
S(1)	11339(1)	5816(1)	8972(1)	36(1)	1
S(2)	10586(1)	5956(1)	5823(1)	39(1)	1
S(3)	10415(1)	6178(1)	8094(1)	33(1)	1
S(4)	11160(1)	5203(1)	7158(1)	36(1)	1
N	11454(2)	6317(2)	6786(4)	33(1)	1
C(1)	11846(2)	6174(3)	6344(6)	51(2)	1
C(2)	11413(2)	6767(2)	6735(6)	49(2)	1
C(3)	11863(2)	6007(2)	8938(5)	32(1)	1
C(4)	12189(2)	5732(2)	8766(5)	36(1)	1
C(5)	12594(2)	5891(2)	8769(6)	47(2)	1
C(6)	12665(2)	6309(3)	8963(6)	53(2)	1
C(7)	12336(2)	6575(2)	9151(6)	46(2)	1
C(8)	11928(2)	6430(2)	9147(5)	36(1)	1
C(9)	12123(2)	5277(2)	8578(6)	48(2)	1
C(10)	11581(2)	6726(2)	9392(6)	46(2)	1
C(11)	10759(2)	6362(2)	4968(5)	34(1)	1
C(12)	11044(2)	6269(2)	4214(6)	49(2)	1
C(13)	11169(3)	6584(3)	3565(7)	62(2)	1
C(14)	11016(3)	6981(3)	3663(7)	67(2)	1
C(15)	10718(3)	7064(2)	4393(6)	53(2)	1
C(16)	10583(2)	6761(2)	5058(6)	44(2)	1
C(17)	11217(3)	5832(3)	4057(7)	72(3)	1
C(18)	10267(3)	6865(3)	5868(7)	57(2)	1
C(19)	10422(2)	6191(2)	9458(5)	34(1)	1
C(20)	10446(2)	6574(2)	9961(5)	42(2)	1
C(21)	10416(3)	6574(3)	11010(6)	57(2)	1
C(22)	10367(3)	6211(3)	11574(6)	61(2)	1
C(23)	10338(2)	5841(3)	11064(6)	49(2)	1
C(24)	10368(2)	5817(2)	10010(5)	39(2)	1
C(25)	10487(2)	6981(2)	9409(6)	51(2)	1
C(26)	10339(2)	5408(2)	9487(6)	50(2)	1
C(27)	10953(2)	4956(2)	6046(5)	35(1)	1
C(28)	10529(2)	4842(2)	6031(6)	41(2)	1
C(29)	10384(3)	4631(2)	5182(7)	53(2)	1
C(30)	10647(3)	4534(3)	4384(7)	65(2)	1
C(31)	11056(3)	4636(3)	4423(7)	66(2)	1
C(32)	11228(2)	4848(2)	5259(6)	49(2)	1
C(33)	10243(2)	4932(2)	6898(6)	47(2)	1
C(34)	11689(3)	4935(3)	5282(9)	73(3)	1

Table 3. Bond lengths [Å] and angles [°] for **7**.

Ta-N	1.921(5)	C(11)-S(2)-Ta	109.2(2)
Ta-S(4)	2.389(2)	C(19)-S(3)-Ta	115.7(2)
Ta-S(3)	2.398(2)	C(27)-S(4)-Ta	116.1(2)
Ta-S(1)	2.427(2)	C(2)-N-C(1)	111.9(6)
Ta-S(2)	2.428(2)	C(2)-N-Ta	125.9(5)
S(1)-C(3)	1.788(6)	C(1)-N-Ta	122.1(5)
S(2)-C(11)	1.807(6)	C(4)-C(3)-C(8)	122.3(6)
S(3)-C(19)	1.791(7)	C(4)-C(3)-S(1)	119.6(5)
S(4)-C(27)	1.789(6)	C(8)-C(3)-S(1)	118.0(5)
N-C(2)	1.450(8)	C(3)-C(4)-C(5)	118.0(6)
N-C(1)	1.458(8)	C(3)-C(4)-C(9)	122.7(6)
C(3)-C(4)	1.387(9)	C(5)-C(4)-C(9)	119.3(6)
C(3)-C(8)	1.400(9)	C(6)-C(5)-C(4)	120.5(7)
C(4)-C(5)	1.397(9)	C(7)-C(6)-C(5)	120.4(7)
C(4)-C(9)	1.496(9)	C(6)-C(7)-C(8)	121.0(7)
C(5)-C(6)	1.384(11)	C(7)-C(8)-C(3)	117.8(6)
C(6)-C(7)	1.378(11)	C(7)-C(8)-C(10)	119.3(6)
C(7)-C(8)	1.389(9)	C(3)-C(8)-C(10)	122.9(6)
C(8)-C(10)	1.499(9)	C(12)-C(11)-C(16)	121.6(6)
C(11)-C(12)	1.380(10)	C(12)-C(11)-S(2)	119.5(5)
C(11)-C(16)	1.403(9)	C(16)-C(11)-S(2)	118.8(5)
C(12)-C(13)	1.380(11)	C(11)-C(12)-C(13)	118.4(7)
C(12)-C(17)	1.521(11)	C(11)-C(12)-C(17)	122.6(7)
C(13)-C(14)	1.372(13)	C(13)-C(12)-C(17)	118.9(8)
C(14)-C(15)	1.378(13)	C(14)-C(13)-C(12)	121.2(8)
C(15)-C(16)	1.377(10)	C(13)-C(14)-C(15)	119.5(8)
C(16)-C(18)	1.507(11)	C(16)-C(15)-C(14)	121.5(8)
C(19)-C(20)	1.397(9)	C(15)-C(16)-C(11)	117.7(7)
C(19)-C(24)	1.412(9)	C(15)-C(16)-C(18)	120.2(7)
C(20)-C(21)	1.379(11)	C(11)-C(16)-C(18)	122.2(7)
C(20)-C(25)	1.500(10)	C(20)-C(19)-C(24)	120.8(6)
C(21)-C(22)	1.389(13)	C(20)-C(19)-S(3)	119.5(5)
C(22)-C(23)	1.364(13)	C(24)-C(19)-S(3)	119.5(5)
C(23)-C(24)	1.389(10)	C(21)-C(20)-C(19)	117.9(7)
C(24)-C(26)	1.483(11)	C(21)-C(20)-C(25)	119.2(7)
C(27)-C(32)	1.402(11)	C(19)-C(20)-C(25)	122.8(6)
C(27)-C(28)	1.408(9)	C(20)-C(21)-C(22)	122.7(8)
C(28)-C(29)	1.384(10)	C(23)-C(22)-C(21)	118.3(8)
C(28)-C(33)	1.492(10)	C(22)-C(23)-C(24)	122.2(7)
C(29)-C(30)	1.383(13)	C(23)-C(24)-C(19)	118.1(7)
C(30)-C(31)	1.353(14)	C(23)-C(24)-C(26)	120.4(7)
C(31)-C(32)	1.404(12)	C(19)-C(24)-C(26)	121.4(6)
C(32)-C(34)	1.506(11)	C(32)-C(27)-C(28)	122.2(6)
		C(32)-C(27)-S(4)	118.5(5)
N-Ta-S(4)	119.4(2)	C(28)-C(27)-S(4)	119.0(5)
N-Ta-S(3)	121.6(2)	C(29)-C(28)-C(27)	117.7(7)
S(4)-Ta-S(3)	119.04(6)	C(29)-C(28)-C(33)	120.0(7)
N-Ta-S(1)	98.5(2)	C(27)-C(28)-C(33)	122.3(6)
S(4)-Ta-S(1)	81.40(6)	C(30)-C(29)-C(28)	120.9(8)
S(3)-Ta-S(1)	89.17(6)	C(31)-C(30)-C(29)	120.7(8)
N-Ta-S(2)	96.9(2)	C(30)-C(31)-C(32)	121.8(9)
S(4)-Ta-S(2)	93.49(6)	C(27)-C(32)-C(31)	116.6(7)
S(3)-Ta-S(2)	80.37(6)	C(27)-C(32)-C(34)	123.9(7)
S(1)-Ta-S(2)	164.37(5)	C(31)-C(32)-C(34)	119.4(8)
C(3)-S(1)-Ta	106.9(2)		

Table 4. Anisotropic displacement parameters [$Å^2$ x 10^3] for **7**.The anisotropic displacement factor exponent takes the form: $-2\pi^2$ [$(ha^*)^2U11 + ... + 2hka^*b^*U12$]

C

	U11	U22	U33	U23	U13	U12
Ta	25(1)	25(1)	28(1)	1(1)	-1(1)	-4(1)
S(1)	29(1)	49(1)	31(1)	5(1)	-5(1)	-9(1)
S(2)	43(1)	38(1)	36(1)	5(1)	-10(1)	-12(1)
S(3)	27(1)	38(1)	32(1)	4(1)	-1(1)	1(1)
S(4)	38(1)	27(1)	44(1)	-1(1)	-10(1)	0(1)
N	29(2)	39(3)	32(3)	2(2)	-4(2)	-8(2)
C(1)	35(4)	59(5)	58(5)	3(4)	12(3)	-1(3)
C(2)	57(4)	30(3)	60(5)	10(3)	-6(4)	-11(3)
C(3)	30(3)	40(3)	25(3)	-1(2)	-5(2)	-4(2)
C(4)	37(3)	35(3)	36(3)	4(3)	-8(3)	-1(3)
C(5)	35(3)	58(4)	48(4)	10(3)	-3(3)	5(3)
C(6)	36(4)	66(5)	55(5)	9(4)	-4(3)	-18(3)
C(7)	45(4)	44(4)	48(4)	-3(3)	-8(3)	-13(3)
C(8)	36(3)	44(4)	29(3)	2(3)	-5(3)	-6(3)
C(9)	47(4)	38(4)	58(5)	0(3)	-11(3)	3(3)
C(10)	49(4)	42(4)	48(4)	-15(3)	-15(3)	8(3)
C(11)	41(3)	31(3)	29(3)	5(2)	-13(3)	-8(2)
C(12)	53(4)	53(4)	41(4)	1(3)	3(3)	-2(3)
C(13)	58(5)	82(6)	47(5)	15(4)	10(4)	0(4)
C(14)	90(7)	59(5)	52(5)	24(4)	-10(5)	-9(5)
C(15)	68(5)	36(4)	54(5)	11(3)	-13(4)	-7(3)
C(16)	44(4)	46(4)	42(4)	7(3)	-11(3)	2(3)
C(17)	89(7)	78(6)	49(5)	-4(5)	10(5)	29(5)
C(18)	57(5)	54(4)	60(5)	-7(4)	-4(4)	14(4)
C(19)	28(3)	38(3)	34(3)	1(3)	2(2)	-1(2)
C(20)	35(3)	52(4)	39(4)	-5(3)	0(3)	3(3)
C(21)	59(5)	63(5)	49(5)	-14(4)	-5(4)	16(4)
C(22)	56(5)	91(7)	37(4)	5(4)	9(4)	26(4)
C(23)	37(4)	67(5)	43(4)	20(4)	11(3)	12(3)
C(24)	22(3)	53(4)	43(4)	9(3)	3(3)	1(2)
C(25)	54(4)	42(4)	57(5)	-5(3)	-1(4)	0(3)
C(26)	49(4)	50(4)	52(5)	18(3)	-2(3)	-11(3)
C(27)	41(3)	27(3)	37(3)	-4(3)	-8(3)	0(3)
C(28)	50(4)	28(3)	46(4)	-2(3)	-10(3)	-2(3)
C(29)	64(5)	39(4)	55(4)	-7(4)	-21(4)	4(3)
C(30)	94(7)	48(4)	53(5)	-20(4)	-29(5)	13(4)
C(31)	81(6)	60(5)	58(5)	-19(4)	0(5)	19(5)
C(32)	58(4)	33(3)	55(4)	-5(3)	-7(4)	10(3)
C(33)	43(4)	48(4)	49(4)	0(3)	-9(3)	-10(3)
C(34)	51(5)	76(6)	91(7)	-17(6)	18(5)	7(4)

Table 5. Hydrogen coordinates (x 10^4), isotropic displacement parameters ($Å^2$ x 10^3) and site occupancy factors for **7**.

	x	y	z	U(eq)	sof
H(1A)	11856(2)	6251(3)	5630(6)	76	1
H(1B)	11864(2)	5873(3)	6406(6)	76	1
H(1C)	12077(2)	6302(3)	6702(6)	76	1
H(2A)	11146(2)	6849(2)	7014(6)	73	1
H(2B)	11432(2)	6856(2)	6031(6)	73	1
H(2C)	11635(2)	6896(2)	7126(6)	73	1
H(5A)	12820(2)	5713(2)	8637(6)	56	1
H(6A)	12939(2)	6412(3)	8968(6)	63	1
H(7A)	12389(2)	6858(2)	9284(6)	55	1
H(9A)	11896(2)	5178(2)	9003(6)	72	1
H(9B)	12375(2)	5126(2)	8744(6)	72	1
H(9C)	12053(2)	5233(2)	7867(6)	72	1
H(10A)	11382(2)	6728(2)	8836(6)	70	1
H(10B)	11693(2)	7004(2)	9486(6)	70	1
H(10C)	11443(2)	6637(2)	10012(6)	70	1
H(13A)	11362(3)	6525(3)	3046(7)	75	1
H(14A)	11113(3)	7195(3)	3235(7)	81	1
H(15A)	10605(3)	7333(2)	4438(6)	63	1
H(17A)	11388(3)	5756(3)	4638(7)	108	1
H(17B)	11385(3)	5827(3)	3443(7)	108	1
H(17C)	10989(3)	5636(3)	3991(7)	108	1
H(18A)	10404(3)	6878(3)	6526(7)	85	1
H(18B)	10053(3)	6651(3)	5882(7)	85	1
H(18C)	10141(3)	7132(3)	5716(7)	85	1
H(21A)	10428(3)	6830(3)	11356(6)	68	1
H(22A)	10354(3)	6219(3)	12289(6)	74	1
H(23A)	10296(2)	5595(3)	11438(6)	59	1
H(25A)	10555(2)	6929(2)	8701(6)	76	1
H(25B)	10705(2)	7145(2)	9721(6)	76	1
H(25C)	10225(2)	7131(2)	9448(6)	76	1
H(26A)	10610(2)	5334(2)	9212(6)	75	1
H(26B)	10138(2)	5427(2)	8936(6)	75	1
H(26C)	10250(2)	5197(2)	9969(6)	75	1
H(29A)	10102(3)	4553(2)	5149(7)	63	1
H(30A)	10542(3)	4396(3)	3808(7)	78	1
H(31A)	11230(3)	4563(3)	3875(7)	79	1
H(33A)	10208(2)	5231(2)	6966(6)	70	1
H(33B)	10360(2)	4820(2)	7522(6)	70	1
H(33C)	9974(2)	4804(2)	6770(6)	70	1
H(34A)	11821(3)	4803(3)	4701(9)	109	1
H(34B)	11808(3)	4824(3)	5906(9)	109	1
H(34C)	11736(3)	5234(3)	5254(9)	109	1

Table 1. Crystal data and structure refinement for **8**.

Empirical formula	C40 H45 S5 Nb
Formula weight	778.97
Temperature	203(2) K
Diffractometer Used	Siemens P4/RA
Wavelength	1.54178 Å
Crystal system	Triclinic
Space group	P-B1
Unit cell dimensions	a = 10.6085(4) Å α = 81.733(4) °
	b = 10.7974(4) Å β = 82.984(4)°
	c = 19.0869(11) Å χ = 61.955(3)°
Volume	1905.8(2) $Å^3$
Z	2
Density (calculated)	1.357 Mg/m^3
Absorption coefficient	5.329 mm^{-1}
F(000)	812
Crystal colour/morphology	Very dark red platy needles
Crystal size	0.57 x 0.40 x 0.10 mm^3
Theta range for data collection	2.34 to 59.99°
Limiting indices	-11<=h<=0, -12<=k<=10,
	-21<=l<=21
Scan type	ω-scans
Reflections collected	5998
Independent reflections	5644 (R(int) = 0.0369)
Observed reflections[F>4sigma(F)]	5206
Absorption correction	Empirical
Max. and min. transmission	6686 and 1999
Structure solution method	Direct
Refinement method	Full-matrix least-squares on F^2
Data/restraints/parameters	5565 / 0 / 416
Goodness-of-fit on F^2	1.050
Final R indices [F>4sigma(F)]	R1 = 0.0368, wR2 = 0.0905
R indices (all data)	R1 = 0.0401, wR2 = 0.0965
Extinction coefficient	0.00068(11)
Largest diff. peak and hole	0.742 and -0.685 $eÅ^{-3}$
Mean and maximum shift/error	0.000 and 0.000

Table 2. Atomic coordinates [x 10^4], equivalent isotropic displacement parameters [$Å^2$ x 10^3] and site occupancy factors for **8**. U(eq) is defined as one third of the trace of the orthogonalized U^{ij} tensor.

	x	y	z	U(eq)	sof
Nb	6051(1)	6506(1)	2514(1)	21(1)	1
S(1)	3827(1)	7188(1)	2011(1)	28(1)	1
S(2)	8309(1)	6433(1)	2557(1)	32(1)	1
S(3)	6169(1)	8013(1)	1459(1)	33(1)	1
S(4)	5249(1)	7237(1)	3663(1)	33(1)	1
S(5)	6676(1)	4077(1)	2585(1)	31(1)	1
C(1)	2978(3)	6265(4)	2545(2)	26(1)	1
C(2)	2033(4)	6878(4)	3122(2)	31(1)	1
C(3)	1368(4)	6129(5)	3522(2)	43(1)	1
C(4)	1586(4)	4856(5)	3344(2)	48(1)	1
C(5)	2443(4)	4309(4)	2745(2)	43(1)	1
C(6)	3132(4)	5006(4)	2331(2)	31(1)	1
C(7)	1665(4)	8321(4)	3298(2)	42(1)	1
C(8)	3968(4)	4411(5)	1661(2)	46(1)	1
C(9)	9155(4)	7200(4)	1907(2)	37(1)	1
C(10)	9940(4)	6478(5)	1326(2)	46(1)	1
C(11)	10684(5)	7084(6)	863(3)	66(2)	1
C(12)	10657(5)	8314(7)	987(3)	71(2)	1
C(13)	9855(5)	9019(6)	1563(3)	62(1)	1
C(14)	9069(5)	8490(5)	2033(2)	48(1)	1
C(15)	10033(5)	5109(5)	1186(2)	61(1)	1
C(16)	8159(5)	9301(5)	2627(3)	59(1)	1
C(17)	4827(4)	8613(4)	844(2)	35(1)	1
C(18)	4991(4)	7762(5)	314(2)	44(1)	1
C(19)	3995(5)	8316(6)	-203(2)	59(1)	1
C(20)	2897(5)	9661(7)	-201(3)	65(2)	1
C(21)	2731(5)	10483(5)	320(3)	57(1)	1
C(22)	3678(4)	9985(4)	852(2)	44(1)	1
C(23)	6210(6)	6286(6)	297(3)	69(2)	1
C(24)	3473(5)	10881(5)	1428(3)	62(1)	1
C(25)	6125(4)	8043(4)	4022(2)	29(1)	1
C(26)	5522(4)	9511(4)	3944(2)	42(1)	1
C(27)	6174(5)	10123(4)	4271(3)	56(1)	1
C(28)	7341(5)	9313(4)	4661(3)	54(1)	1
C(29)	7902(4)	7872(4)	4737(2)	39(1)	1
C(30)	7310(4)	7204(4)	4420(2)	29(1)	1
C(31)	4245(6)	10424(5)	3521(3)	66(1)	1
C(32)	7967(4)	5627(4)	4516(2)	34(1)	1
C(33)	7570(4)	3268(3)	3388(2)	27(1)	1
C(34)	9068(4)	2541(3)	3361(2)	29(1)	1
C(35)	9731(4)	1874(4)	3992(2)	35(1)	1
C(36)	8950(4)	1906(4)	4625(2)	39(1)	1
C(37)	7473(4)	2579(4)	4638(2)	38(1)	1
C(38)	6753(4)	3258(3)	4027(2)	30(1)	1
C(39)	9961(4)	2457(4)	2683(2)	45(1)	1
C(40)	5146(4)	3949(4)	4075(2)	47(1)	1

Table 3. Bond lengths [Å] and angles [°] for **8**.

Nb-S(4)	2.3609(9)	S(2)-Nb-S(3)	77.08(3)
Nb-S(5)	2.3707(8)	S(1)-Nb-S(3)	78.12(3)
Nb-S(2)	2.3708(9)	C(1)-S(1)-Nb	107.28(11)
Nb-S(1)	2.3961(8)	C(9)-S(2)-Nb	127.27(12)
Nb-S(3)	2.4289(8)	C(17)-S(3)-Nb	118.53(11)
S(1)-C(1)	1.780(3)	C(25)-S(4)-Nb	117.20(11)
S(2)-C(9)	1.778(3)	C(33)-S(5)-Nb	106.88(10)
S(3)-C(17)	1.773(4)	C(6)-C(1)-C(2)	120.6(3)
S(4)-C(25)	1.782(3)	C(6)-C(1)-S(1)	119.1(3)
S(5)-C(33)	1.790(3)	C(2)-C(1)-S(1)	119.9(3)
C(1)-C(6)	1.405(5)	C(3)-C(2)-C(1)	118.2(4)
C(1)-C(2)	1.405(5)	C(3)-C(2)-C(7)	119.4(3)
C(2)-C(3)	1.401(5)	C(1)-C(2)-C(7)	122.3(3)
C(2)-C(7)	1.496(5)	C(4)-C(3)-C(2)	121.3(4)
C(3)-C(4)	1.369(6)	C(3)-C(4)-C(5)	119.8(4)
C(4)-C(5)	1.385(6)	C(4)-C(5)-C(6)	121.2(4)
C(5)-C(6)	1.390(5)	C(5)-C(6)-C(1)	118.5(4)
C(6)-C(8)	1.501(5)	C(5)-C(6)-C(8)	118.7(4)
C(9)-C(10)	1.394(6)	C(1)-C(6)-C(8)	122.8(3)
C(9)-C(14)	1.406(6)	C(10)-C(9)-C(14)	122.8(4)
C(10)-C(11)	1.408(6)	C(10)-C(9)-S(2)	119.7(3)
C(10)-C(15)	1.495(7)	C(14)-C(9)-S(2)	117.3(3)
C(11)-C(12)	1.369(8)	C(9)-C(10)-C(11)	117.0(5)
C(12)-C(13)	1.384(8)	C(9)-C(10)-C(15)	123.2(4)
C(13)-C(14)	1.394(6)	C(11)-C(10)-C(15)	119.8(4)
C(14)-C(16)	1.486(7)	C(12)-C(11)-C(10)	121.3(5)
C(17)-C(18)	1.405(6)	C(11)-C(12)-C(13)	120.5(4)
C(17)-C(22)	1.408(6)	C(12)-C(13)-C(14)	121.0(5)
C(18)-C(19)	1.392(6)	C(13)-C(14)-C(9)	117.4(5)
C(18)-C(23)	1.510(7)	C(13)-C(14)-C(16)	120.0(5)
C(19)-C(20)	1.370(8)	C(9)-C(14)-C(16)	122.6(4)
C(20)-C(21)	1.367(8)	C(18)-C(17)-C(22)	120.6(4)
C(21)-C(22)	1.383(6)	C(18)-C(17)-S(3)	119.4(3)
C(22)-C(24)	1.498(7)	C(22)-C(17)-S(3)	119.7(3)
C(25)-C(30)	1.395(5)	C(19)-C(18)-C(17)	118.2(4)
C(25)-C(26)	1.395(5)	C(19)-C(18)-C(23)	120.3(4)
C(26)-C(27)	1.399(6)	C(17)-C(18)-C(23)	121.5(4)
C(26)-C(31)	1.498(6)	C(20)-C(19)-C(18)	120.9(5)
C(27)-C(28)	1.368(6)	C(21)-C(20)-C(19)	120.8(4)
C(28)-C(29)	1.372(6)	C(20)-C(21)-C(22)	120.9(5)
C(29)-C(30)	1.387(5)	C(21)-C(22)-C(17)	118.6(4)
C(30)-C(32)	1.498(5)	C(21)-C(22)-C(24)	120.6(4)
C(33)-C(34)	1.402(5)	C(17)-C(22)-C(24)	120.8(4)
C(33)-C(38)	1.409(5)	C(30)-C(25)-C(26)	122.0(3)
C(34)-C(35)	1.395(5)	C(30)-C(25)-S(4)	119.3(3)
C(34)-C(39)	1.495(5)	C(26)-C(25)-S(4)	118.4(3)
C(35)-C(36)	1.373(6)	C(25)-C(26)-C(27)	117.3(4)
C(36)-C(37)	1.382(6)	C(25)-C(26)-C(31)	122.6(4)
C(37)-C(38)	1.387(5)	C(27)-C(26)-C(31)	120.1(4)
C(38)-C(40)	1.502(5)	C(28)-C(27)-C(26)	121.2(4)
		C(27)-C(28)-C(29)	120.3(4)
S(4)-Nb-S(5)	107.57(3)	C(28)-C(29)-C(30)	121.1(4)
S(4)-Nb-S(2)	93.91(3)	C(29)-C(30)-C(25)	117.9(3)
S(5)-Nb-S(2)	101.87(3)	C(29)-C(30)-C(32)	119.1(3)
S(4)-Nb-S(1)	101.16(3)	C(25)-C(30)-C(32)	123.0(3)
S(5)-Nb-S(1)	92.31(3)	C(34)-C(33)-C(38)	120.9(3)
S(2)-Nb-S(1)	155.18(3)	C(34)-C(33)-S(5)	119.5(3)
S(4)-Nb-S(3)	125.32(3)	C(38)-C(33)-S(5)	119.3(3)
S(5)-Nb-S(3)	127.11(3)	C(35)-C(34)-C(33)	118.2(3)

C(35)-C(34)-C(39)	119.7(3)	C(37)-C(38)-C(33)	118.2(3)
C(33)-C(34)-C(39)	122.2(3)	C(37)-C(38)-C(40)	118.8(3)
C(36)-C(35)-C(34)	121.5(3)	C(33)-C(38)-C(40)	123.0(3)
C(35)-C(36)-C(37)	119.6(4)		
C(36)-C(37)-C(38)	121.5(4)		

Table 4. Anisotropic displacement parameters [$Å^2$ x 10^3]
for **8**.The anisotropic displacement factor exponent takes the form:
$-2\pi^2$ [$(ha^*)^2U11 + ... + 2hka^*b^*U12$]

	U11	U22	U33	U23	U13	U12
Nb	22(1)	21(1)	19(1)	0(1)	-1(1)	-10(1)
S(1)	27(1)	32(1)	26(1)	4(1)	-5(1)	-17(1)
S(2)	28(1)	41(1)	29(1)	8(1)	-5(1)	-19(1)
S(3)	30(1)	41(1)	26(1)	11(1)	-6(1)	-19(1)
S(4)	34(1)	48(1)	26(1)	-12(1)	4(1)	-25(1)
S(5)	37(1)	24(1)	34(1)	-1(1)	-11(1)	-13(1)
C(1)	23(2)	30(2)	24(2)	4(1)	-4(1)	-11(1)
C(2)	22(2)	39(2)	28(2)	2(2)	-3(1)	-10(2)
C(3)	28(2)	57(3)	32(2)	10(2)	1(2)	-15(2)
C(4)	36(2)	54(3)	53(3)	20(2)	-8(2)	-26(2)
C(5)	38(2)	35(2)	60(3)	8(2)	-17(2)	-23(2)
C(6)	27(2)	31(2)	35(2)	1(2)	-9(1)	-13(2)
C(7)	34(2)	46(2)	43(2)	-14(2)	3(2)	-13(2)
C(8)	46(2)	51(2)	48(2)	-22(2)	-4(2)	-24(2)
C(9)	25(2)	48(2)	35(2)	16(2)	-8(2)	-20(2)
C(10)	29(2)	58(3)	36(2)	16(2)	-2(2)	-13(2)
C(11)	33(2)	91(4)	49(3)	25(3)	2(2)	-18(2)
C(12)	48(3)	93(4)	70(4)	43(3)	-14(3)	-44(3)
C(13)	53(3)	74(3)	69(3)	33(3)	-25(3)	-44(3)
C(14)	42(2)	62(3)	48(2)	23(2)	-20(2)	-35(2)
C(15)	51(3)	67(3)	44(3)	-8(2)	13(2)	-13(2)
C(16)	66(3)	54(3)	68(3)	1(2)	-15(2)	-37(2)
C(17)	33(2)	50(2)	23(2)	13(2)	-3(1)	-24(2)
C(18)	41(2)	70(3)	24(2)	1(2)	3(2)	-31(2)
C(19)	64(3)	107(4)	26(2)	0(2)	0(2)	-57(3)
C(20)	48(3)	106(4)	45(3)	34(3)	-17(2)	-47(3)
C(21)	37(2)	62(3)	63(3)	31(2)	-11(2)	-23(2)
C(22)	35(2)	43(2)	48(2)	21(2)	-7(2)	-21(2)
C(23)	69(3)	84(4)	44(3)	-29(3)	4(2)	-23(3)
C(24)	58(3)	41(2)	76(3)	-1(2)	-3(2)	-17(2)
C(25)	33(2)	26(2)	27(2)	-9(1)	0(1)	-13(2)
C(26)	46(2)	27(2)	44(2)	-7(2)	-12(2)	-8(2)
C(27)	70(3)	23(2)	77(3)	-11(2)	-19(3)	-17(2)
C(28)	65(3)	38(2)	67(3)	-15(2)	-21(2)	-24(2)
C(29)	41(2)	37(2)	42(2)	-8(2)	-13(2)	-17(2)
C(30)	28(2)	27(2)	28(2)	-4(1)	1(1)	-11(1)
C(31)	63(3)	38(2)	77(4)	-5(2)	-28(3)	-2(2)
C(32)	41(2)	28(2)	30(2)	0(1)	-7(2)	-12(2)
C(33)	29(2)	16(2)	36(2)	0(1)	-6(1)	-9(1)
C(34)	29(2)	19(2)	38(2)	-5(1)	-2(2)	-9(1)
C(35)	31(2)	23(2)	48(2)	-3(2)	-11(2)	-9(1)
C(36)	48(2)	27(2)	39(2)	5(2)	-16(2)	-15(2)
C(37)	51(2)	28(2)	34(2)	2(2)	-2(2)	-18(2)
C(38)	29(2)	22(2)	39(2)	0(1)	-3(2)	-12(1)
C(39)	39(2)	37(2)	46(2)	-3(2)	6(2)	-8(2)
C(40)	34(2)	38(2)	61(3)	6(2)	4(2)	-15(2)

Table 5. Hydrogen coordinates (x 10^4), isotropic displacement parameters ($Å^2$ x 10^3) and site occupancy factors for **8**.

	x	y	z	U(eq)	sof
H(3A)	760(4)	6507(5)	3921(2)	51	1
H(4A)	1154(4)	4355(5)	3628(2)	57	1
H(5A)	2561(4)	3450(4)	2617(2)	51	1
H(7A)	850(4)	8633(4)	3641(2)	64	1
H(7B)	1430(4)	8970(4)	2870(2)	64	1
H(7C)	2477(4)	8294(4)	3497(2)	64	1
H(8A)	4977(4)	3879(5)	1748(2)	68	1
H(8B)	3825(4)	5176(5)	1293(2)	68	1
H(8C)	3641(4)	3795(5)	1511(2)	68	1
H(11A)	11210(5)	6634(6)	461(3)	79	1
H(12A)	11187(5)	8682(7)	678(3)	85	1
H(13A)	9840(5)	9868(6)	1638(3)	74	1
H(15A)	10604(5)	4368(5)	1535(2)	91	1
H(15B)	10475(5)	4883(5)	715(2)	91	1
H(15C)	9078(5)	5188(5)	1218(2)	91	1
H(16A)	8447(5)	8722(5)	3073(3)	88	1
H(16B)	7165(5)	9568(5)	2569(3)	88	1
H(16C)	8271(5)	10143(5)	2626(3)	88	1
H(19A)	4077(5)	7759(6)	-558(2)	71	1
H(20A)	2251(5)	10024(7)	-562(3)	78	1
H(21A)	1963(5)	11398(5)	316(3)	69	1
H(23A)	7113(6)	6324(6)	234(3)	104	1
H(23B)	6122(6)	5854(6)	-94(3)	104	1
H(23C)	6179(6)	5731(6)	740(3)	104	1
H(24A)	4321(5)	11004(5)	1434(3)	92	1
H(24B)	3315(5)	10426(5)	1882(3)	92	1
H(24C)	2651(5)	11795(5)	1341(3)	92	1
H(27A)	5804(5)	11109(4)	4221(3)	68	1
H(28A)	7760(5)	9746(4)	4877(3)	64	1
H(29A)	8701(4)	7328(4)	5009(2)	46	1
H(31A)	3976(6)	11408(5)	3550(3)	98	1
H(31B)	3454(6)	10236(5)	3709(3)	98	1
H(31C)	4477(6)	10221(5)	3029(3)	98	1
H(32A)	8337(4)	5259(4)	4060(2)	52	1
H(32B)	7247(4)	5343(4)	4719(2)	52	1
H(32C)	8741(4)	5258(4)	4832(2)	52	1
H(35A)	10736(4)	1392(4)	3985(2)	42	1
H(36A)	9417(4)	1473(4)	5046(2)	46	1
H(37A)	6944(4)	2577(4)	5070(2)	45	1
H(39A)	10939(4)	1743(4)	2754(2)	68	1
H(39B)	9943(4)	3363(4)	2536(2)	68	1
H(39C)	9582(4)	2209(4)	2319(2)	68	1
H(40A)	4817(4)	3760(4)	3670(2)	70	1
H(40B)	4772(4)	4959(4)	4078(2)	70	1
H(40C)	4811(4)	3574(4)	4508(2)	70	1